DOTTORATO DI RICERCA IN SCIENZE CHIMICHE

CICLO XXXII

COORDINATORE Prof. PIERO BAGLIONI

STUDYING MULTIVALENT IMINOSUGAR GLYCOMIMETICS TO TARGET ENZYMES FOR HEALTHCARE APPLICATIONS

Settore Scientifico Disciplinare CHIM/06

Dottorando
Dott. Costanza Vanni

Tutore
Prof. Francesca Cardona

Coordinatore
Prof. Piero Baglioni

_____

Anni 2016/2019

Summary

Home is behind
The world ahead
And there are many paths to tread
Through shadow
To the edge of night
Until the stars are all alight

Mist and shadow
Cloud and shade
All shall fade

(*J.R.R. Tolkien*, The Lord of the Rings)

Preface

The main focus of this PhD thesis is the study of iminosugars as potential glycosidases inhibitors. Two main classes of these carbohydrates mimics have been taken into consideration, namely polyhydroxylated pyrrolidines and piperidines, which were treated from different point of view, in particular in terms of *Multivalency*, one of the main issues studied in this work. If iminosugars is the pivotal class of molecules under deep examination, different types of glycosidases target have been screened, accordingly to the azasugar nature and to the final application consequently.

Since the key role played in nature by chemical process of recognition between carbohydrates and glycosidases is known, several efforts have been done in the field of carbohydrate chemistry. Glycosidases indeed are key hydrolytic enzymes involved in many physiological functions, such as intestinal digestion, post-translational processing of the sugar chain of glycoproteins, quality-control systems in the endoplasmic reticulum (ER) and ER-associated degradation mechanism and the lysosomal catabolism of glycoconjugates. For this reason, the inhibition of those enzymes could be very important in several, not only biomedical, but also industrial applications. A branch of glycoscience concerns in fact the synthesis of carbohydrates mimics, such as iminosugars, a class of natural compounds in which a nitrogen atom replaces the endocyclic oxygen of sugars. They are demonstrated to be excellent glycosidases inhibitors because of their structural resemblance to the terminal sugar moiety in the natural substrates (the non-reducing end of polysaccharides). Starting from this point is possible to design new iminosugar-based drugs for the treatment of different pathologies by employing themselves as bioactive moiety or as 'carbohydrate targeting-probe', but also in the crop protection field as novel insecticides and fungicides.

More recently, a new revaluation of iminosugars application to glycosidases inhibition arose following the possibility to create *multivalent* structures in which more than one unit of bioactive moiety are linked together onto a common scaffold. Since the first decade of 2000's indeed, the multivalency has been predominantly exploited for the study of the interaction between multivalent ligands and lectins. Nowadays it can be applied to increase the biological response towards enzymes with a deep enzyme cavity.

Chapter 1 gives an overview of iminosugars, ranging from their natural occurrence and their classification to the synthetic methodologies and their application. In the 1970's their

biological activity as potent glycosidases inhibitors became known, and this opened up a great interest towards a deep investigation about the mechanisms involved. However, large amounts of starting material are required for biological studies and the need to find new ways to synthesize them grew, being still now a hot topic in this branch of glycoscience. Lot of efforts were done in the total synthesis of iminosugars, since it is an important tool both for the structural confirmation of the natural compounds and to furnish new synthetic analogs with increased biological activity. Moreover, biological iminosugars' target is a wide range of glycosidase enzymes, depending on the molecule's structure, and consequently they could be used as drugs in the treatment of different kind of pathologies.

Chapter 2 moves to a different application of iminosugar glycomimetics, having the synthesis of new potent and selective insecticides the final goal: the synthesis of new pseudodisaccharide mimetics based on pyrrolidine iminosugars as inhibitors of trehalases. These enzymes are retaining α- glucosidases that cleave the glycosidic bond converting trehalose in two units of glucose. This disaccharide has several functions in different organisms such as fungi, mycobacteria, and insects.

The synthesis of new pseudodisaccharide mimetics using a stereoselective α-glucosylation is presented, and allowed the preparation of a small library of new α,β-mixtures and β-pseudodisaccharides. Their biological evaluation towards insect trehalase of midge larvae of *C. riparius* and porcine kidney trehalase was also reported.

Chapter 3 has the *multivalency* as the key concept and illustrates the synthetic strategies developed in our group at the University of Florence to build up new multivalent architectures exploiting different types of scaffolds, from gold nanoparticles to dendrimeric scaffolds. Starting from commercially available carbohydrates precursors, azido key intermediate structures were synthesized, from enantiopure cyclic nitrones and were then anchored onto different platforms. With those intermediates a small library of multivalent structures based on pyrrolidine and piperidine iminosugars have been obtained exploring Copper (I) catalyzed Azide-Alkyne Cycloaddition (CuAAC) with propargylated scaffolds characterized by different structure and valency. Moreover, a novel copper-free route consisting of subsequently repeated 1,3-dipolar cycloadditions was explored, in order to avoid all the drawbacks related to the possible presence of copper in the biological environment.

Chapter 4 deals with the synthesis of new monovalent and multivalent systems based on sugars and on iminosugar glycomimetics, in order to identify a new class of inhibitors/activators with a selectivity profile with respect to the different isozymes of carbonic anhydrases (CAs). The most potent CAs inhibitors are sulphonamides that could be functionalized with structures able to interact with prostetic group and providing so an adequate selectivity towards the different CAs families. Here the possibility to differentiate different CAs families exploiting different sugar or iminosugar 'tails' is reported. While the importance of the sugar component is already known, the effect of an iminosugar on the enzyme has never been studied. Moreover, also the concept of multivalency applied to those class of metalloenzymes is explored. For this reason, the synthesis of a small library of monovalent compounds that contain sugar or iminosugar moiety bound with different linkers to the sulphonamide moiety is here reported.

Part of this PhD thesis has been the object of publications and communications at conferences.

PAPERS:

1. Matassini C., D'Adamio G., Vanni C., Goti A., Cardona F. "Studies for the Multimerization of DAB-1-Based Iminosugars through Iteration of the Nitrone Cycloaddition/Ring-Opening/Allylation Sequence", *Eur. J. Org. Chem.*, **2019**, *30*, 4897-4905.
2. D'Adamio G., Forcella M., Fusi P., Matassini C., Ferhati X., Vanni C., Cardona F. "Probing the Influence of Linker Length and Flexibility in the Design and Synthesis of New Trehalase Inhibitors", *Molecules*, **2018**, *23*, 436.
3. Matassini C., Vanni C., Goti A., Morrone A., Marradi M., Cardona F. "Multimerization of DAB-1 onto Au GNPs affords new potent and selective N-acetylgalactosamine-6-sulfatase (GALNS) inhibitors", *Org. Biomol. Chem.*, **2018**, *16*, 8604-8612.

CONGRESSES:

1. **C. Vanni**, C. Matassini, A. Goti, F. Cardona, M. Marradi, A. Bodlenner, P. Compain. Poster Comunication: "Multimeric deoxynojirimycin derivatives to investigate glycosidases inhibition exploiting gold glyconanoparticles". XX European Carbohydrate Symposium EUROCARB, Leiden, Netherlands, June 30- July 5 2019. N° abstract: PC-231.
2. **C. Vanni**, C. Matassini, F. Cardona, A. Goti, M. Marradi, A. Bodlenner, P. Compain. Oral Comunication: "Iminosugars derivatives grafted onto gold glyconanoparticles: a new class of multivalent glycosidases inhibitors". XLIV "A. Corbella" International Summer School on Organic Synthesis, Gargnano (BS), Italy, June 9-13 2019. N° abstract: OC- 17.
3. **C. Vanni**, C. Matassini, F. Cardona, A. Angeli, F. Carta, C. T. Supuran, A. Goti. Oral Comunication: "Mono- and multivalent sugars and iminosugars as modulators in Carbonic Anhydrase inhibition". X PhD day, Sesto Fiorentino (FI), Italy, May 23 2019. N° abstract: OC-52.
4. **C. Vanni**, C. Matassini, A. Goti, F. Cardona.

Oral Comunication: "Multivalent glycomimetics: anchoring iminosugars on dendrimeric and globular scaffolds". Merck-Elsevier Young Chemist Symposium-MEYCS, Rimini (RN), Italy, November 19-21 2018. N° abstract: OC-19.

5. **C. Vanni**, C. Matassini, A. Goti, F. Cardona.
Oral Comunication: "Multivalent architectures to anchor pyrrolidine and piperidine iminosugars: a new generation of glycomimetics". XXXVI Convegno Interregionale TUMA, Pisa (PI), Italy, October 4-5 2018. N° abstract: OC-20.

6. **C. Vanni**, C. Matassini, A. Goti, F. Cardona.
Poster Comunication: "Multivalent iminosugars grafted onto different scaffolds as new glycomimetics for biological applications". 22nd International Conference in Organic Synthesis-22nd ICOS, Firenze (FI), Italy, September 16-21 2018. N° abstract: PC-474.

7. **C. Vanni**, G. D'Adamio, M. Forcella, P. Fusi, C. Matassini, X. Ferhati, F. Cardona
Oral Comunication: "Iminosugar-based trehalase inhibitors: the key role of linker lenght and flexibility". XVI Convegno-Scuola sulla Chimica dei Carboidrati, Pontignano (SI), Italy, June 17-20 2018. N° abstract: OC-17.

8. **C. Vanni**, C. Matassini, F. Cardona, A. Goti, P. Compain, A. Bodlenner, A. Morrone
Poster Comunication: "How to address therapeutically relevant enzymes using iminosugars grafted onto gold glyconanoparticles". XLIII "A. Corbella" International Summer School on Organic Synthesis, Gargnano (BS), Italy, June 10-14 2018. N° abstract: PC- 44.

9. **C. Vanni**, C. Matassini, F. Cardona, A. Goti
Oral Comunication: "Multimerization of iminosugars onto gold nanoparticles: new glyconanoinhibitors". IX PhD day, Sesto Fiorentino (FI), Italy, May 31 2018. N° abstract: OC-9.

10. **C. Vanni**, C. Matassini, F. Cardona, A. Goti, P. Compain, A. Bodlenner
Poster Comunication: "Gold glyconanoparticles decorated with bioactive iminosugars: new multivalent tools to target glycosidases". XIX European Carbohydrate Symposium EUROCARB, Barcellona, Spain, July 2-6 2017. N° abstract: PC-190.

11. C. Vanni, C. Matassini, F. Cardona, A. Goti
Poster Comunication: "Gold glyconanoparticles decorated with bioactive iminosugars: new multivalent tools to target glycosidases". IIX PhD day, Sesto Fiorentino (FI), Italy, May 24 2017. N° abstract: PC-5.

OTHER COMMUNICATIONS AS CO-AUTHOR:

1. C. Matassini, C. Vanni, M. Marradi, F. Cardona, A. Goti "Copper-free methodologies for the multimerization of bioactive iminosugars". XXXIX Convegno Nazionale della Divisione di Chimica Organica della Società Chimica Italiana (CDCO19), Torino, Italy, September 8-12 2019. N° abstract: OC-106.

Chapter 1

Iminosugars as glycosidases inhibitors
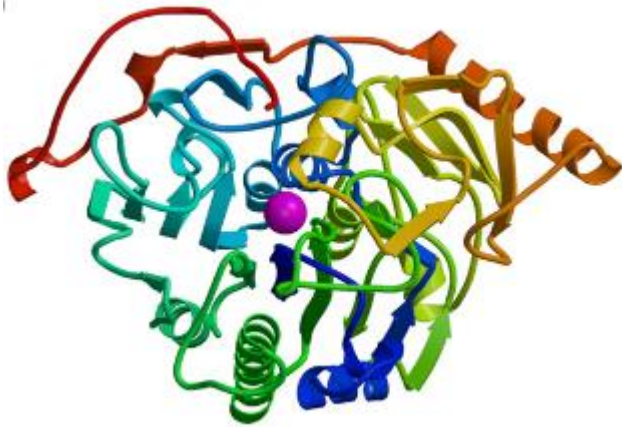
1.1 Iminosugars: natural glycomimetics

In the wide glycomimetics world, a significant role is held by iminosugars, sugar mimics in which a nitrogen atom with basic properties replaces the endocyclic oxygen (Figure 1.1).
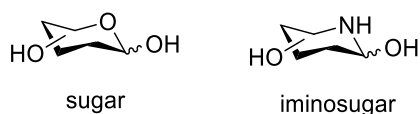

sugar   iminosugar

Figure 1.1: General carbohydrate structure compared with general iminosugar structure.

Many iminosugars are present in nature. Isolated from plants and microorganisms, iminosugars, or polyhydroxylated alkaloids, can be classified considering different aspects of their nature; the most common manner is to divide them into five classes, depending on the structure of their carbon skeleton: piperidine, pyrrolidine, indolizidine, pyrrolizidines and nortropanes. In figure 1.2 some examples of iminosugars well known in the literature, divided by the kind of structure are shown.

Piperidine   **Pyrrolidine**

1   **2**   **3**   **4**

1-Deoxyinojirimicin   Isofagomine   1,4-dideoxy-1,4-imino-D-arabinitol   2,5-dideoxy-2,5-imino-D-mannitol
(DNJ)   (DAB-1)   (DMDP)

Indolizidine   **Pyrrolizidine**   **Nortropanes**

5   **6**   **7**
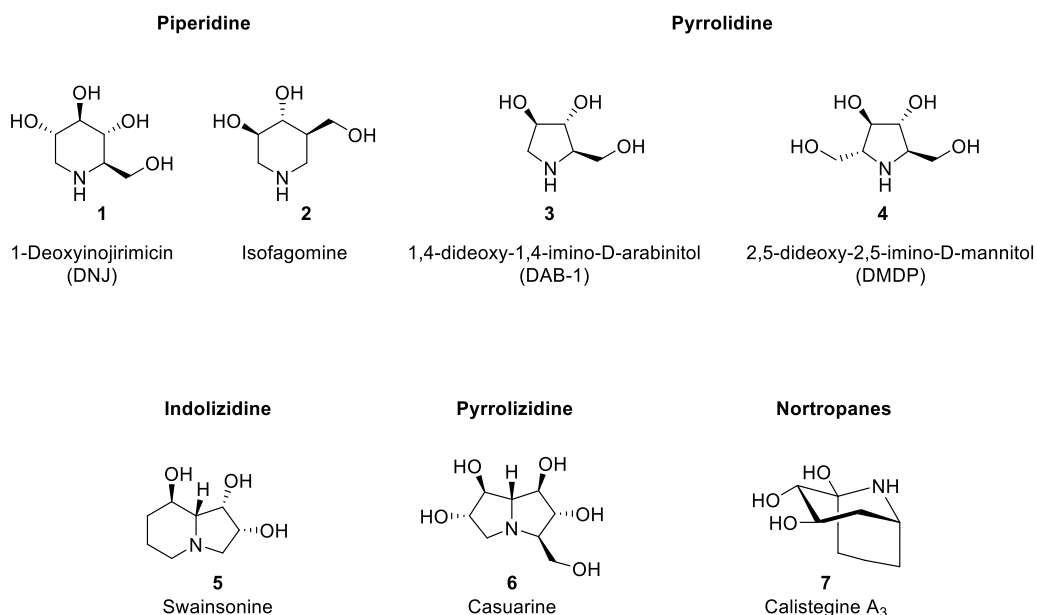Swainsonine   Casuarine   Calistegine A$_3$

Figure 1.2: Structure-based classification of iminosugars and some examples.

Considering the natural hydrolytic process catalysed by glycosidases in many important biological processes and its transition state, it is easy to understand how iminosugars became, since their discovery in 1960s, one of the most privileged class of glycosidases

inhibitors. Indeed their structural resemblance to the terminal sugar moiety in the natural substrates (polysaccharides) makes them able to interact with human glycosidases, other proteins and sugar receptors.[1] The key of their potency is that at physiological pH the nitrogen atom of the iminosugar results protonated and the cationic species formed are able to perfectly mimic the oxocarbenium ion involved in the transition state of the hydrolysis catalysed by glycosidase enzymes (Figure 1.3).
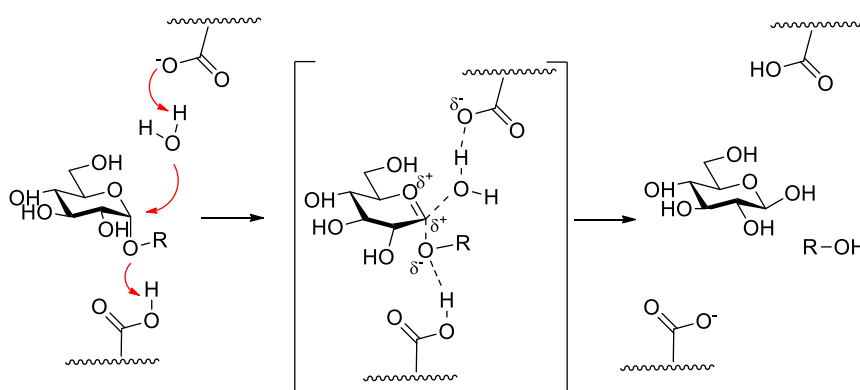

Figure 1.3: Example of an inverting glycosidase mechanism: an oxocarbenium ion like transition state is always involved in the hydrolytic process.

Their therapeutic applications go back a long time ago, starting from the traditional Chinese medicine in which iminosugars were used in the treatment of diseases such as diabetes and bacterial infections, to the 17th century when a similar drug based on iminosugars was produced in industrial scale.[2] However, we can fix the begin of scientific story of iminosugar in the 1960s, when the first synthesis of 1-deoxynojirimycin (DNJ, **1**, Figure 1.4) was reported by Paulsen and coworkers[3] and almost simultaneously the group of Prof. Inouye discovered the antibiotic properties of nojirimycin (NJ, **8**, Figure 1.4) by isolating it from *Streptomyces* bacteria.[4] Hence the interest towards this class of compounds could only increase, especially after that the inhibitory activity against an α-glucosidase of DNJ was for the first time announced: it was the starting point for the discovery of hundreds of polyhydroxylated alkaloids, known also as iminosugars.[5]

[1] Compain P., Martin O. R., *Iminosugars: from synthesis to therapeutic applications*, Wiley-VCH, Weinheim, **2007.**

[2] Aerts J. M. F. G., *Proc. European Working Group for the Study of Gaucher Disease*, **2006**.

[3] Paulsen H., *Angew. Chem. Int. Ed. Engl*., **1966**, *5*, 495-511.

[4] Inouye S., Tsurouka T., Niida T*., J. Antibiot. Ser*., **1966**, *A19*, 288–292.

[5] Stütz A. E., *Iminosugars as Glycosidase Inhibitors. Nojirimycin and Beyond*, Wiley-VCH, Weinheim, Germany, **1999**.
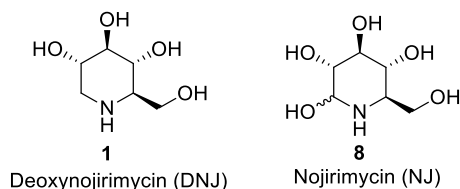
Figure 1.4: Deoxynojirimycin, **DNJ** and nojirimycin, **NJ**.

One of the biggest challenges in this field is the efficient isolation of enantiomeric pure compounds, since a large amount of material is necessary to perform biological studies. Indeed the complexity of iminosugars structures, characterized on one hand by lot of hydroxyl groups and on the other by the basic nature of the endocyclic nitrogen atom, makes the synthesis not a trivial task.

The glycosidases inhibition field offers such a wide range of topics, considering that according to the different structures of iminosugar, different type of glycosidases can be inhibited, and different therapeutic and industrial applications are possible.[6]

1.2 Glycosidases and therapeutic glycomimetics

1.2.1 Glycosidase enzymes

Why is inhibiting glycosidases so important?
Since glycosidases are involved in different processes, their inhibition represents a powerful tool both to clarify the biological mechanisms and to develop treatments for different types of diseases. As mentioned before, iminosugars represent excellent glycosidases inhibitors, due to their ability to mimic the oxocarbenium ion like transition state. Great efforts have been made in recent years to design and synthesize inhibitors of glycosidases. Given their multitude of roles *in vivo* indeed, inhibition of these enzymes is extremely attractive in the developing of new potential drugs to be used in the treatment of viral infections,[7] diabetes[8] and lysosomal storage disorders.[9]

---

[6] For a recent review see: Compain P., *Chem. Rec.* **2019**, *19*, 1–14.

[7] Mehta A., Zitzmann N., Rudd P. M., Block T. M., Dwek R. A., *FEBS Lett.*, **1998**, *430*, 17–22.

[8] Krentz A. J., Bailey C. J., *Drugs*, **2005**, *65*, 385–411.

[9] Fan J.-Q., Ishii S., Asano N., Suzuki Y., *Nat. Med.*, **1999**, *5*, 112–115. b) Sawkar A. R., Cheng W.-C., Beutler E., Wong C.-H., Balch W. E., Kelly J. W., *Proc. Natl. Acad. Sci. U. S. A.*, **2002**, *99*, 15428–15433.

Glycoside hydrolases (GHs; EC 3.2.1.-), well known as glycosidases, are enzymes responsible for the hydrolysis of the glycosidic linkage in carbohydrate compounds such as di-, oligo- and polysaccharides essential to life.[1,10] In order to understand the significance of those enzymes we can just think to the variety of biological processes in which they are involved, such as catabolism of glycoconjugates (particular emphasis in this thesis will be given to the lysosomal one), intestinal digestion, post-translational processing of the sugar chain of glycoproteins, quality-control systems in the endoplasmic reticulum (ER) and ER-associated degradation mechanisms. All these processes rely at the basis of life in organisms such as humans, animals and plants. Regarding the structural diversity of carbohydrates and the extreme stability of the glycosidic bond, glycosidases have been considered the most specific and proficient of catalysts, indeed they could enhance the reaction rate until 10^{17} fold over the uncatalysed reaction.[11] They are part of the so-called "carbohydrate-active enzymes" (CAZymes) and represent from 1 to 3% of the proteins encoded by the genomes of most organisms.[12] This classification is based on amino acid sequence similarity and to date 156 sequence-distinct families of glycosidases are present, and they are constantly increasing (they can be found on the online database http://www.cazy.org). Enzymes within a sequence-related family catalyze the cleavage of the glycosidic bond by the same mechanism and share a similar overall structural fold.[13] The reaction catalyzed by glycosidases is formally a nucleophilic substitution at the saturated carbon of the anomeric position and can take place with either retention or inversion of the anomeric stereochemistry (Figure 1.5), giving so two basic types of glycosyl-transferring enzymes: "retaining" and "inverting".[14]

_____

[10] a) Gloster T. M. and Davies G. J., *Org. Biomol. Chem.* **2010**, *8*, 305–320; b) Stütz A. E. and Wrodnigg T. M., *Adv. Carbohydr. Chem. Biochem.* **2011**, *66*, 187-298.

[11] Wolfenden R., Lu X. D., Young G., *J. Am. Chem. Soc.* **1998**, *120*, 6814–6815.

[12] Davies G. J., Gloster T. M., Henrissat B., *Curr. Opin. Struct. Biol.*, **2005**, *15*, 637-645.

[13] Cantarel B. L., Coutinho P. M., Rancurel C., Bernard T., Lombard V., Henrissat B., *Nucleic Acids Res.*, **2008**, *37*, D233-238.

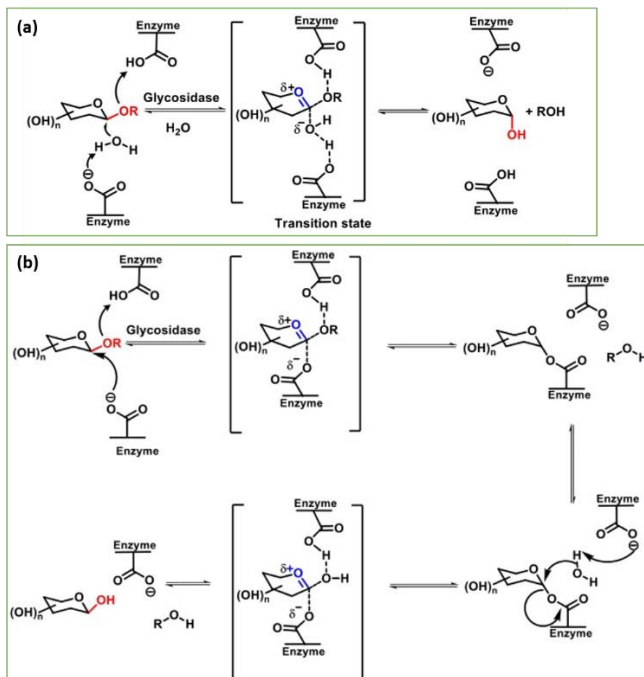[14] Rempel B. P., Withers S. G., *Glycobiology*, **2008**, *18*, 570–586.

Figure 1.5: (a) Mechanism for an inverting β-glucosidase. (b) Mechanism for a retaining β-glucosidase.

The bond cleavage performed by GHs is catalysed by the action of two acidic residues in the enzymatic active site. In "inverting glycosidases" the nucleophilic attack on the anomeric position is done by the water molecule, deprotonated by one of the acids that works as a base. At this point the removal of the -OR group is catalysed by the other carboxylic acid. The steps of breaking-formation of the glycosidic bonds occur through a concerted oxocarbenium ion-like transition state, in which the positive charge is partially stabilized by the ring oxygen. In inverting glycosidases, the product has the opposite configuration at anomeric position with respect to the starting substrate. For the "retaining glycosidases" instead, the mechanism differs from the first one by the formation of a covalently bound glycosyl-enzyme intermediate, and hence proceeds through two oxocarbenium ion-like transition states. It is important to note that the proton delivered during general acid catalysis is delivered in either a syn- or anti-fashion, depending on the specific enzyme. Moreover, glycosidases can be further divided according to whether the sugar is in a five-membered (furanose) or a six-membered (pyranose) ring (Figure 1.6). In the case of pyranosyl-transferring enzymes it is also useful to distinguish whether, in the preferred conformation, the leaving group is equatorial or axial. [15]

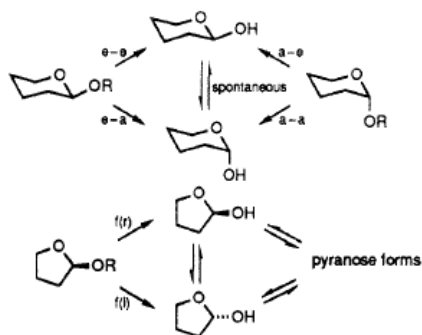[15] Sinnott ML., *Chem Rev.*, **1990**, *90*, 1171–1202.

_____

Figure 1.6: Example of pyranosyl and furanosyl-transferring hydrolases mechanism.

Carbohydrates represent one of the most abundant family of natural compounds, with different type of linkages. Since the mode of action of glycosidases involves the cleavage of glycosidic bonds between sugar molecules, individual glycosidases show specificity for certain sugar molecules and for a specific anomeric configuration of that sugar. In that sense sometimes, it can be useful talk about α- or β-glycosidases. Polyhydroxylated alkaloids can be extremely potent and specific inhibitors of glycosidases by mimicking the pyranosyl or furanosyl moiety of their natural substrates.

As structural and mechanistic studies have become more sophisticated, it is possible to acquire more and more information about different mode of actions and mechanisms and the study of the interactions substrate-enzyme complexes become easier. For example, other mechanisms have been proposed for small subsets of glycoside hydrolases that are substantially different from the inverting/retaining glycosidases, and this information help the inhibitor designing for these enzymes. Several families containing glycosidases which hydrolyse substrates containing *N*-acetylhexosamine with retention of configuration (which are classified into families GH18, GH20, GH56, GH84, GH85, and is likely for GH25)[16] have been shown to lack a conventional catalytic nucleophile, but instead use a substrate-assisted catalytic mechanism (Figure 1.7). The acetamido group at the C-2 position of the substrate acts as a nucleophile to attack the anomeric carbon to create an enzyme-stabilized oxazoline intermediate. The intermediate is hydrolysed by a water molecule, which is activated by a residue acting as a general base. In most cases, a second carboxylate-containing residue orients and polarizes the 2-acetamido group to increase its nucleophilicity.

_____

[16] a) Macauley M. S., Whitworth G. E., Debowski A.W., Chin D., Vocadlo D. J., *J. Biol. Chem.*, **2005**, *280*, 25313-25322; b) Umekawa M., Huang W., Li B., Fujita K., Ashida H., Wang L., Yamamoto K. *J., Biol. Chem.*, **2008**, *283*, 4469-4479.
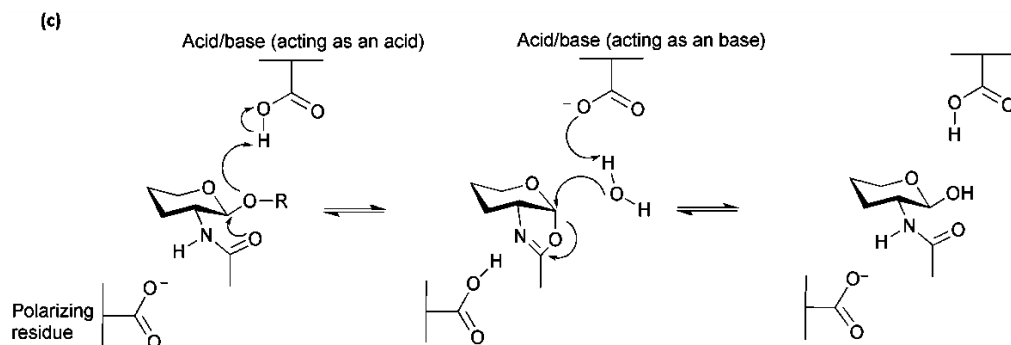
Figure 1.7: Substrate-assisted mechanism proposed for families 18, 20, 56, 84, 85 and possibly 25.

Glycosidases are synthesized in the endoplasmic reticulum where they adopt their native conformations and are transported into the lysosomes through the Golgi apparatus.[17] If a mutation in genes encoding for enzymes (such as integral membrane proteins and transport proteins, all with lysosomal localization) is present, a defect of one or more of the different functions of lysosomes can take place. For example, a protein may not be synthesized, or it can be synthesized with a defect, being in that way recognized as altered by the quality control systems of the cell and for this reason degraded. The consequence is the inability to metabolize a specific substrate (sphingolipids, glycosaminoglycans, glycoproteins and glycogen), which accumulates in lysosomes, provoking after a series of events, cell death and tissue and organ damage. When this series of event occurs, we have the so-called Lysosomal Storage Disorders.

1.2.1 Lysosomal Storage Disorders

Lysosomal Storage Disorders (LSDs) are a group of about 70 hereditary metabolic diseases caused by mutations in genes that code for enzymes, integral proteins of membrane and transport proteins with lysosomal localization. The mutation prevents the enzyme to overcome the efficient quality control of the endoplasmic reticulum, causing a reduced lysosomal activity, and therefore an abnormal accumulation of not metabolised substrate in the lysosomes. [18] Thus, the wide range of symptoms in LSDs may be explained by the activation of several deleterious processes, such as the release of acid hydrolases into the cytoplasm causing cellular damage, the dysregulation of apoptosis or the abnormal

---

[17] Parenti G., Andria G., Ballabio A., *Annu. Rev. Med*., **2015**, *66*, 471-486.

[18] Ortolano S., Viéitez I., Navarro C., Spuch C., *Pat. Endocr. Metab. Immune Drug. Discov.*, **2014**, 8, 9-25.

accumulation of lipids causing defective transport of substrates into and out of the lysosomes (Figure 1.8).[19]
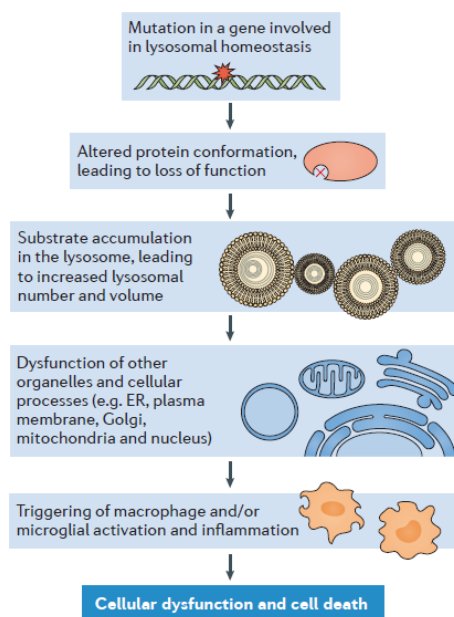

Figure 1.8: The pathogenic cascade in lysosomal storage disorders (LSDs).

Their symptomatology depends on the stored substrate and organs affected by this accumulation. LSDs can be classified on the base of the involved enzymes and consequently on the abnormally accumulated substrate (Figure 1.9).

Although individually very rare, the incidence of LSDs as a group is estimated to be as high as 1 in 4000 in some countries,[20] even if the exact prevalence is difficult to estimate, considering the clinical heterogeneity of LSDs, which may lead to missed diagnoses. According to Medical Genetics Service of the Hospital de Clínicas de Porto Alegre data, the investigation of high-risk subjects led to 3,512 LSD diagnoses in Brazil from 1982 to 2017.[21] Most of LSDs are neuronopathic, with Central Nervous System (CNS) involvement, progressive neurodegeneration and cognitive impairment. The most severe forms occur in infants with onset in utero (i.e. Sialidosis, Galactosialidosis, GM1 gangliosidosis, Gaucher type II, MPSIVA) or within 6 months and outcome in the second year of life, while in the

---

[19] Platt F.M., *Nat. Rev. Drug Discov.*, **2018**, 17, 133–150.

[20] Giugliani R., Federhen A., Michelin-Tirelli K., Riegel M., Burin M., *Genet. Mol. Biol.*, **2017**, *40*, 31-39.

[21] Poswar F. O., Vairo F., Burin M., Michelin-Tirelli K., Brusius-Facchin A. C., Kubaski F., Fischinger C., Souza M., Baldo G., Giugliani R., *Genet. Mol. Biol.*, **2019**, *42*, 165-177.

less severe forms, clinical symptoms eventually appear during adulthood and are the cause of reduced life expectation.

DISEASE	GENE	ENZYME	STORAGE PRODUCT
Tay-Sachs	HEX A	β-Hexosaminidase A	GM2, Condroitin sulfate
Sandhoff	HEX B	β-Hexosaminidase A/B	GL4, GA2 GM2
Fabry	GLA	α-Galactosidase A	Gb3 LysoGb3
Gaucher	GBA	β-Glucosidase	Glucocerebroside
GM1 Gangliosidosis	GLB1	β- Galactosidase	GM1
Krabbe	GALC	Galactosylcerebrosidase	GalCer, Psychosine
Pompe	GAA	α-Glucosidase	Glycogen
MPS I	IDUA	Iduronidase	Dermatin sulfate, Heparin sulfate
MPS II	IDS	Iduronate sulfatase	Dermatin sulfate, Heparin sulfate
MPS III A	SGSH	*N*-Sulfoglucosamine sulfohydrolase	Heparan sulfate
MPS III B	NAGLU	α-*N*-Acetylglucosaminidase	Heparan sulfate
MPS III C	HGSNAT	Heparan-α-glucosaminide *N*-acetyltransferase	Heparan sulfate
MPS III D	GNS	Glucosamine (*N*-acetyl)-6-sulfatase	Heparan sulfate
MPS IV A	GALNS	*N*-Acetylglucosamine 6 sulfatase	Keratan sulfate, Chontroitin sulfate, Keratin sulfate
MPS IV B	GALB1	β- Galactosidase	GM1-ganglioside and Keratan sulfate
MPS VI	ARSB	*N*-Acetylgalactosamine 4-sulfatase	Dermatan sulfate
MPS VII	GUSB	β- Glucoronidase	Chondroitin sulfate
Niemann-Pick A-B	SMPD1	Acid sphingomyelin phosphodiesterase 1	Sphingomyelin
Niemann-Pick C	NPC1-2	NPC-1 and NPC-2	Cholesterol, lipids
Infantile NCL (CLN1)	CLN1(PPT1)	Palmitoyl-protein thioesterase 1	Lipopigments
Late Infantile NCL (CLN2)	CLN2(PPT1)	Tripetiyl-peptidase 1	Lipopigments
MLD	ARSA	Arylsulfatase A	Sulfatides

Figure 1.9: Molecular basis of frequent lysosomal storage diseases.

The first therapeutic strategies directed towards the treatment of these diseases were introduced in the early 1990s, and since then several new approaches have become available or tested in preclinical studies. The first approach raised from the simplest intuition based on the subministration (or the restoring) of the deficient enzyme activity, the so-called Enzyme replacement therapy (ERT). Available since 1996, until now ERT is approved for the treatment of 7 kind of LSDs and under clinical trial for other seven.[17] It consists in an infusion of a recombinant enzyme (similar to the natural one), which is taken up into the cell through membrane receptors (typically mannose-6-phosphate receptors) and replaces the catalytic action of the missing or non-functional lysosomal enzyme.[22] However, this approach is limited by several disadvantages: first recombinant enzymes are

---

[22] Brady R. O., *Annu. Rev. Med*., **2006**, *57*, 283-96.

very expensive. It requires lifelong, repeated infusions of large quantities of the respective exogenous enzyme and not all patients may benefit from them. Furthermore, ERT relies on active transport to eventually enter the cell and then the lysosome. These are likely rate-limiting steps; thus, despite massive infusions of recombinant enzyme, only a small proportion may actually make it into the lysosome. Moreover, following a continuous infusion of an 'external' system in to the body, the risk of an immune response against the administered enzyme is high.[21] To finish, the biggest limitation of this therapy is that the infused enzyme is unable to cross the blood brain barrier. For this reason, ERT is useful only in diseases without neuropathic involvement.

Other alternative treatments are present to date, the Substrate Reducing Therapy (SRT) and the Gene Therapy. The first one inhibits specific steps in the biosynthetic pathways of substrates to restore the equilibrium between the synthesis of substrates and their degradation by lysosomal enzymes,[23] using small-molecule enzyme inhibitors that are involved in substrate biosynthesis. The Gene Therapy instead, is directed toward increasing or restoring defective enzyme activity in patients' cells and tissues by delivering a wild-type copy of the defective gene.[24] Unfortunately they both have disadvantages, most of whom similar to those already seen for ERT.

The development of new strategies to effectively target the brain and bone is of primary importance to guarantee a better quality of life for patients affected by LSDs.
In that sense a promising frontier is the emergent active-site-specific chaperone (ASSC) therapy, or pharmacological chaperone therapy (PCT).[25] PC is a small molecule with high affinity for the active site of the target protein that reach the mutated enzyme specifically binding itself to the protein and acting as a folding template. Certain mutations in LSDs cause the synthesis of improperly folded proteins that are retarded in endoplasmic reticulum (ER) and degraded by "quality control" mechanism, called ER-associated degradation (ERAD). At subinhibitory concentrations, a small molecule able to act as potent competitive inhibitor, catalyzes the restoring of native-like conformation, avoiding or decelerating in this way the degradation of the enzyme by ERAD in the cell. The enzyme is so able to retain full or partial activity being correctly folded, and it can reach its normal site of action. The most attractive aspects in this type of therapy, are that those ASSCs can be administrated orally and presumably can gain access to most cell types and CNS (central nervous system).

_____

[23] Platt F.M., Jeyakumar M., *Acta Paediatr*., **2008**, *97*, 88–93.

[24] Sands M.S., Davidson B.L., *Mol. Ther*., **2006**, *13*, 839–49.

[25] Fan J.-Q., *Trends Pharmacol. Sci.* **2003**, *24*, 355–360. b) Desnick R. J., Schuchman E. H., *Nat. Rev. Genet*, **2002**, *3*, 954–966.
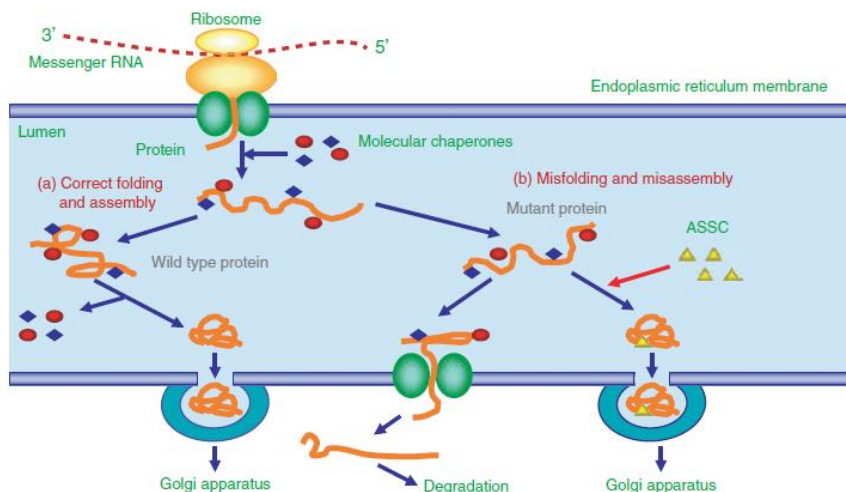
Figure 1.10: Endoplasmic reticulum (ER) quality-control system and active-site-specific chaperone (ASSC) therapy.[1]

Compounds called to act as chaperones are those that show high affinity to target protein, and who better than reversible enzymatic inhibitors? Once the enzyme/substrate complex is formed and goes out of the ER, the inhibitor at subinhibitory concentrations can be easily replaced by the natural substrate that is nearby in high level of concentration, because it results still not metabolized (Figure 1.10). According to what has been reported until now, iminosugars represent the ideal candidates to be used as pharmacological chaperones. As we will deepen later, also SRT based-drugs already approved for the treatment of lysosomal storage disorders have iminosugars as fundament.

1.2.2 β-Glucosidase – Gaucher Disease

One of the most diffuse LSD is Gaucher Disease, related to β-glucosidase, a glycoside hydrolase enzyme (EC 3.2.1.45). Also known as glucocerobrosidase or GCase, β-glucosidase, it is a peripheral membrane protein that catalyses the hydrolysis of glucoceramide (GlcCer, **9**, Figure 1.11) to β-glucose (**10**) and ceramide (**11**) in presence of the modulator protein saposin C and lipid (Figure 1.11).[26]

---

[26] Lieberman R.L.,Wustman B.A., Huertas P., Powe A.C. Jr., Pine C.W., Khanna R., Schlossmacher M.G., Ringe D., Petsko G. A., *Nat. Chem. Biol*., **2007**, *3*, 101–107.
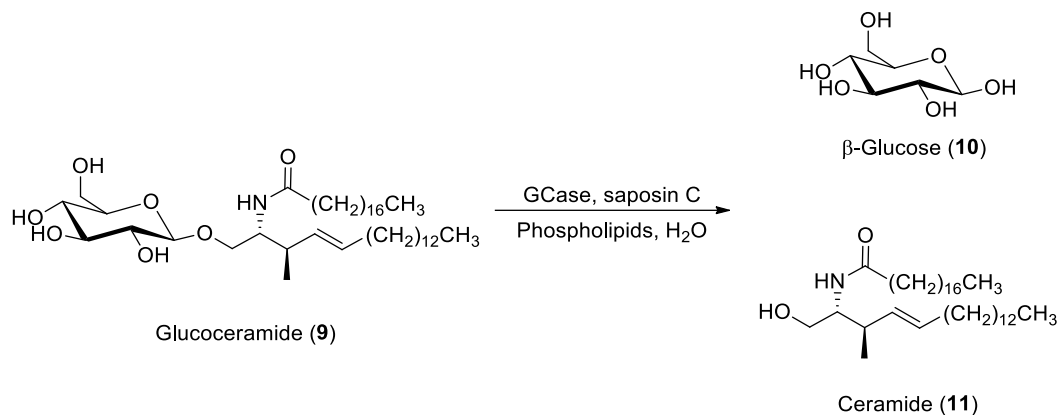
Figure 1.11: Scheme of the reaction performed by GCase.

Total or partial GCase enzyme deficiency leads to an abnormal accumulation of GlcCer (**9**) inside microphages lysosomes, with serious consequences that are symptoms of the LSDs called Gaucher Disease (GD). GD is a systemic disorder that presents with a various degree of systemic and neurological manifestations; to date, more than 400 mutations have been identified in the GBA1 gene and all of these cause the total or partial absence of enzymatic activity of the GCase protein. In this situation GCase is not properly folded and accumulates in the endoplasmic reticulum (ER), where it is degraded by the proteasome: GCase is not transported to the lysosome and, consequently, an accumulation of glucosylceramide is found there. Gaucher disease can be divided into 3 phenotypes based on the presence or absence of neurological manifestations and on the rate of its progression. In type 1 (GD1), the mildest and most common of the three clinical forms of Gaucher's disease (90-95% of cases), patients suffer from bone pain, skeletal lesions, anaemia and liver or spleen damage without any neuronal involvement. Type 2 Gaucher (<5% of cases) is characterized by severe and early neurological involvement that develops in newborns starting at 3-6 months of age. Splenomegaly and hepatosplenomegaly are almost always present while growth retardation may be the first sign of the disease. Also called subacute neurological GD, the type 3 Gaucher form (5% of cases) shows the visceral manifestations described in GD1, usually combined with neurologic-oculomotor involvement. Among all the LSDs, the Gaucher possesses the broader alternative therapies, counting at least two approved therapies based on different approaches (ERT and SRT) on the market, and one on clinical trial based on the use of PC (Figure 1.12).
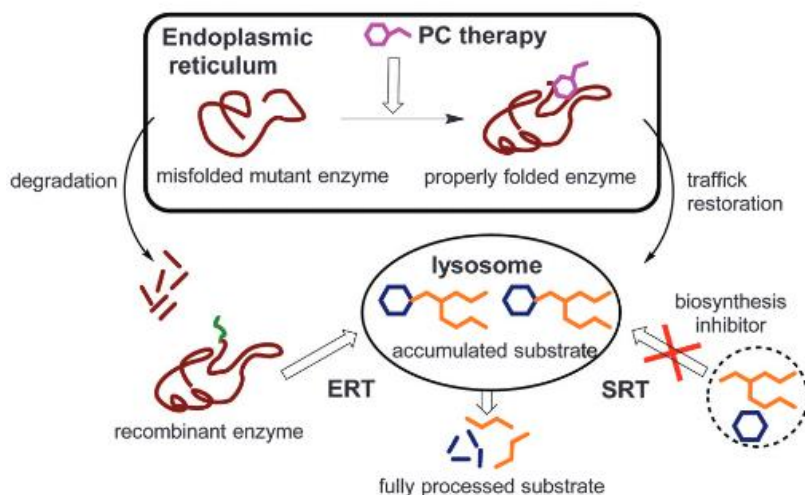
Figure 1.12: The major sites of action of the current lysosomal storage disorder therapeutics.

Indeed, Gaucher disease is the first lysosomal storage for which the recombinant human β-glucocerebrosidase enzyme was developed and approved by the FDA in 1991 (Imiglucerase, Cerezyme®).[27] Moreover, other two drugs based on ERT are now on the market: Taliglucerase alfa (Elelyso®) and Velaglucerase (Vpriv®).[20] The other main therapeutic approach for treating GD and currently available is to reduce the amount of substrate entering the lysosome, thereby compensating for the catabolic defect. This approach (SRT) is now in clinical practice for the treatment of mild-to-moderate type 1 Gaucher disease, and it is based on the use of *N*-butyldeoxynojirimycin (*N*B-DNJ **12**, Miglustat, Zavesca®, figure 1.13). It inhibits GlcCer synthase (K_i, 7.4 μM) if the *N*-alkyl chain is at least three carbon atoms in length[28] and is a competitive inhibitor for ceramide able to lower the rates of synthesis of all GlcCer-based glycolipids, thus reducing glycolipid accumulation.[29]

---

[27] Barton N.W., Brady R.O., Dambrosia J.M., Di Bisceglie A.M., Doppelt S.H., Hill S.C., Mankin H.J., Murray G.J., Parker R.I., Argoff C.E., *N. Engl. J. Med*., **1991**, *324*, 1464-1470.

[28] Platt F.M., Neises G.R., Dwek R.A., Butters T.D., *J. Biol. Chem*., **1994**, *269*, 8362–8365.

[29] Lachmann R.H., *Curr. Opin. Investig. Drugs.*, **2003**, *4*, 472–479.
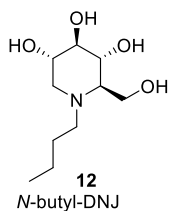
Figure 1.13: NB-DNJ.

An approach that has recently attracted much interest in the treatment of Gaucher Disease is the one that uses PCs. The chaperoning activity of an iminosugar already known as potent β-glucocerebrosidase inhibitor, *N*-nonyl-deoxynojirimycin (*N*N-DNJ, figure 1.13), was demonstrated for the firs time in 2002 by Sawkar and co-workers. Indeed, if subministrated at subinhibitory concentrations, it enhanced about two-fold the residual activity in mutated N370S enzyme (the most frequent mutation involved in Gaucher Disease).[30] From this starting point, other groups discovered other iminosugars able to act as ASSCs, paving the way for the research in this field. In Figure 1.14 are reported some examples of potential chaperones iminosugar-based for GD.
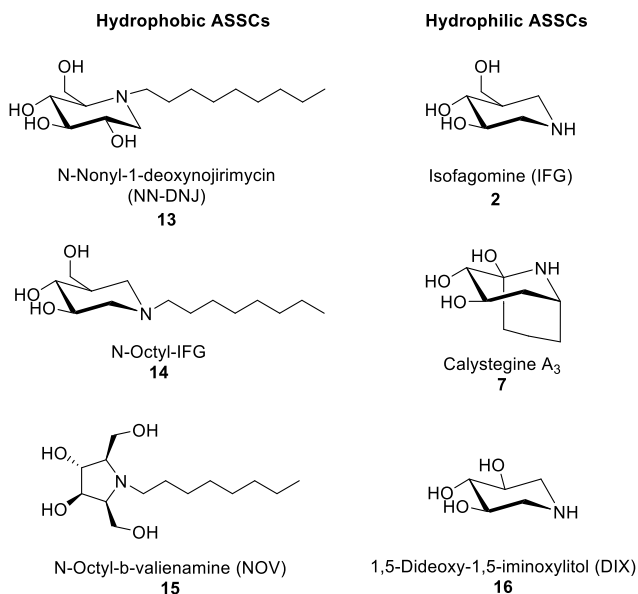

Figure 1.14: Structures of some potential ASSCs in GD treatment.

_____

[30] Sewkar A.R, Cheng W.C, Beutler E., Wong C.H., Balch W.E, Kelly J.W., *Proc. Natl. Acad. Sci USA*, **2002**, *99*, 15428-15433.

For example, the synthetic 1-*N*-iminosugar isofagomine (IFG, **2**), underwent a clinical trial against GD under the name of Plicera™.[31]

Following the pioneering work on *N*B-DNJ and *N*N-DNJ, several examples of *N*-alkylated iminosugar frameworks have been proposed as pharmacological chaperones for GD, again following the common concept to conjugate an iminosugar with a lipophilic moiety: the former may mimic the sugar part or the transition state towards glycosidic cleavage and the latter may mimic the ceramide aglycone of the natural substrate, glucosylceramide (**9**, Figure 1.11). An example is another *N*-alkylated piperidine iminosugar synthetized in our research group in 2015. It showed measurable chaperone activity with human fibroblasts derived from Gaucher patients bearing the N370/RecNcil mutation (**17**, Figure 1.15) and it can increase 1.25-fold GCase activity at 100μM concentration.[32]
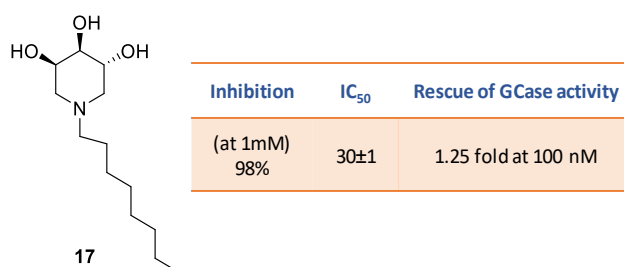

Inhibition	IC$_{50}$	Rescue of GCase activity
(at 1mM) 98%	30±1	1.25 fold at 100 nM

Figure 1.15: Inhibition, IC$_{50}$ and chaperoning activity for compound **17**.

Just for mentioning, structure–activity relationship studies indicated that a simple 1,2-shift of the alkyl chain from the endocyclic nitrogen to the "anomeric" carbon could lead to more potent glucosidase inhibitors.[33] Indeed, relevant examples have been reported for two *C*-alkylated analogues of IFG (**2**), compounds **18** and **19** (Figure 1.16), for which a 1.50-fold[34] and a remarkable 1.80-fold[35] GCase activity enhancements at 10 nM in N370S GD fibroblasts were observed, respectively. Interestingly, compounds **18** and **19** have the opposite configuration of the alkylated carbon atom, showing that both configurations are able to achieve the biological activity.

[31] Steet R.A., Chung S., Wustman B., Powe A., Do H., Kornfeld S.A., *Proc. Natl. Acad. Sci. USA*, **2006**, *103*, 3813–13818.

[32] Parmeggiani C., Catarzi S., Matassini C., D'Adamio G., Morrone A., Goti A., Paoli P., Cardona F., *Chem. Bio. Chem.*, **2015**, *16*, 2054–2064.

[33] Godin G., Compain P., Martin O. R., Ikeda K., Yu L., Asano N., *Bioorg. Med. Chem. Lett*. **2004**, *14*, 5991 –5995.

[34] T. Hill, M. B. Tropak, D. Mahuran, S. G. Withers, *ChemBioChem* **2011**, *12*, 2152-2154.

[35] P. Compain, O. R. Martin, C. Boucheron, G. Godin, L. Yu, K. Ikeda, N. Asano, *ChemBioChem* **2006**, *7*, 1356-1359.
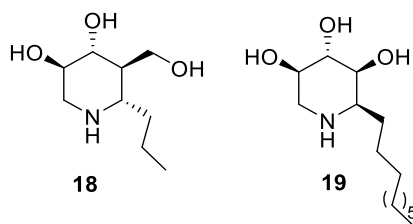
_____

Figure 1.16: Two examples of *C*-alkylated chaperones.

Moreover recently, a series of *C*-alkylated iminosugars varying the alkyl chain length was reported in our research group (Figure 1.17), giving interesting chaperoning activity.[36]
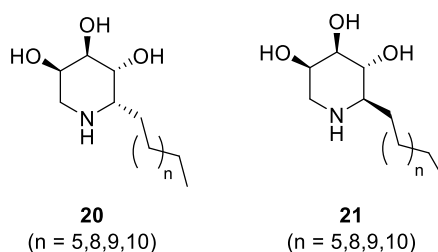

20
(n = 5,8,9,10)

21
(n = 5,8,9,10)

Figure 1.17: New *C*-alkylated chaperones.

1.2.4 Sulfatases – Mucopolysaccharidosis II and IV A

Another class of glycosidases of our interest are sulfatases, enzymes which catalyse the hydrolysis of sulfuric acid esters from a wide variety of substrates, including glycosaminoglycans (GAGs, mucopolysaccharides), glycolipids and steroids. Eleven different mammalian sulfatases have been identified; eight in lysosomes and three associated with microsomal membranes. Anyway, the residues of the active site are highly conserved thus indicating that they all have common structures. This similarity is guaranteed by the presence of a cysteine residue that is first post-traslationally modified into a formyglycine and then hydroxylated into an activated hydroxylformyglycine, necessary for sulfatase activity of the enzyme (Figure 1.18).[37]

_____

[36] Clemente F., Matassini C., Goti A., Morrone A., Paoli P., Cardona F., *ACS Med. Chem. Lett*., **2019**, *10*, 621–626.
[37] Schmidt B., Selmer T., Ingendoh A., von Figura.K., *Cell*, **1995**, *82*, 271–278.
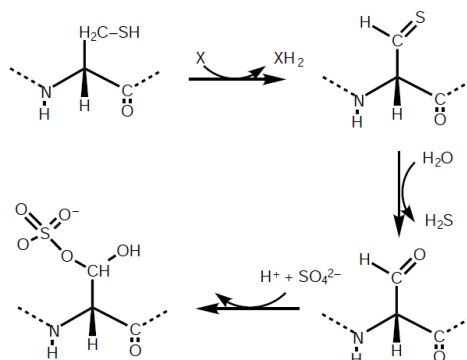
Figure 1.18: Scheme for the post-translational modification of the essential active-site cysteine residue.[38]

When this process does not occur, because of a deficiency of a specific lysosomal sulfatase, the degradation of substrates is not possible and leads in this way to rare inherited clinical disorders called mucopolysaccharidoses (MPS) belonging to LSDs.

Clinical manifestations of the mucopolysaccharidoses depend on the specific enzyme deficiency, the end organ affected, and the accumulation of glycosaminoglycans in the affected organs. For example brain can be affected, minimizing in this case other somatic manifestations, whereas in diseases in which the brain is not involved, there is no mental retardation. MPS disorders share many common clinical features to variable degrees. These include coarse facial features, short stature, skeletal dysplasia (dysostosis multiplex), joint stiffness, organomegaly, cardiac valve disease, corneal clouding, hearing loss, airway obstruction, and respiratory infections.[39]

Specific degradative lysosomal enzyme deficiencies have been identified for all the mucopolysaccharidoses (Figure 1.19). The glycosaminoglycans that are stored and excreted in the urine of the various mucopolysaccharidoses are dermatan sulfate, heparan sulfate, keratan sulfate, and chondroitin 4/6 sulfates.[40]

---

[38] Bond C.S., Clements P.R., Ashby S.J., Collyer C.A., Harrop S.J., Hopwood J.J., Guss J.M., *Struct*ure, **1997**, *5*, 277-289.

[39] Neufeld E., Muenzer J., *The Mucopolysaccharidoses*, McGraw-Hill, **2014**.

[40] Yu C., *Lysosomal storage disorders: Mucopolysaccharidoses*, Elsevier, **2017**, 191-209.
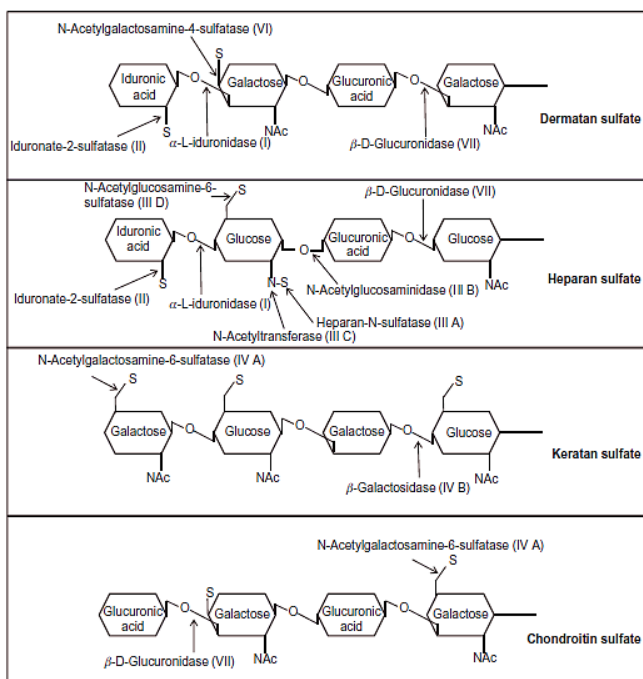
Figure 1.19: The catabolism of GAGs. Enzyme deficiencies in different MPS types are shown in parentheses.

Nondegraded or partially degraded fragments of GAGs are excreted in the urine, which can be used for screening and diagnosis of MPS disorders. Various enzyme replacement therapies (ERTs) have been developed or are under investigation for treatment of MPS.

Mucopolisaccharidose IV A (Morquio A syndrome): it is caused by a deficiency in the enzyme *N*-acetylgalactosamine-6-sulfatase (GALNS) that cleaves the C-6 sulfate group from the N-acetylgalactosamine-6-sulfate residue of chondroitin-6-sulfate (Figure 1.19). It is estimated that incidence for this disease ranges from one to 76,000 births in Northern Ireland and one to 640,000 births in Western Australia.[41] The disease presents two phenotypes depending on its severity: a mild form, which generally allows the patient a full life span, and a severe form, which often results in death before the second decade of life.[42] There is no definitive cure for Morquio syndrome, indeed the current standard of care is medical and surgical management of the involved systems with the goal of palliation, prevention, and slowing of the progression of complications.[43] Currently in the treatment of Morquio A syndrome an ERT therapy based on elosulfase alfa (Vimizim®, BioMarin) is used, recently

---

[41] Solanki G. A., Martin K. W., Theroux M. C., Lampe C., White K. K., Shediac R., Lampe C. G., Beck M., Mackenzie W. G., Hendriksz C. J., Harmatz P. R., J. *Inherited Metab. Dis.*, **2013**, 36, 339.

[42] Northover H., Cowie R. A., Wraith J. E., *J. Inherited Metab. Dis.*, **1996**, *19*, 357–365.

[43] Davison J.E., Kearney S., Horton J., Foster K., Peet A.C., Hendriksz C.J., *J. Inherit. Metab. Dis. Epub.*, **2012**.

approved by the FDA (Food and Drug Administration) and by the EMA (European Medicines Agency). Not being effective for CNS involvement, again there is a need for the identification of compounds which can act as PCs for this orphan disease. Recently Garman and co-workers determined the three-dimensional structure of the enzyme acetylgalactosamine-6-sulphatase (GALNS) and demonstrated its dimeric nature.[44] With this structural information in hands, we contributed to the field by synthetizing pyrrolidine-based inhibitors (deeply discussed in Chapter 3).[45]

Mucopolisaccharidose II A (Hunter syndrome): it is caused by a deficiency of iduronate-2-sulfatase (IDS), which cleaves the C-2 sulfate from L-iduronic acid residues at the nonreducing ends (NREs) of heparin, heparan sulfate, and dermatan sulfate (Figure 1.19). More than 500 mutations have been identified to date, approximately 40% of which are deletions, duplications, insertions, indels, or complex rearrangements mechanisms (Human Gene Mutation Database (HGMD)).[40] It is chronicle and progressive and patients with MPS II are often classified as severe MPS II or a more mild attenuated form (attenuated MPS II). The most severe form of MPS II is characterized by progressive cognitive impairment, progressive airway disease, and heart disease. Death usually occurs in the first, second, or third decades of life. Those with an attenuated form of MPS II typically have no-to-minimal cognitive involvement, living well into adulthood. It is probably an underestimated incidence of 1.3 per 100,000 newborn males[46] and the most common symptoms are problems with internal organs such as liver and heart, hearing loss, motor difficulties and skeletal deformations. Idursulfase based ERT therapy (Elaprase®, Shire Human Genetic Therapy, Inc., Cambridge, MA), which has been on the market since 2006, is now available in more than 40 countries.

To date still little investigated, these two pathologies constitute an interesting test bench for the development of PCs that can be used as such or in combination with ERT therapy, already available for both. It has been shown that the combined use of a PC with ERT therapy is able to increase the life time of the conformationally stable form of the enzyme, reducing the need to undergo enzymatic administration therapy. Also for this reason it is necessary to research and develop new PCs.

Considering these concepts and considering also our interest in the synthesis of nitrogenating glycomimetics, our research group contributed to the field with a preliminary investigation of the potential inhibitory activity of some multivalent pyrrolidine-based

[44] Rivera Colón Y., Schutsky E. K., Zita A. K., Garman S. C., *J. Mol. Biol.*, **2012**, *423*, 736-751.
[45] (a) Matassini C., Parmeggiani C., Cardona F., Goti A., *Tetrahedron Lett.* **2016**, *57*, 5407. (b) Matassini C., Vanni C., Goti A., Morrone A., Marradi M., Cardona F., *Org. Biom. Chem.*, **2018**, *16*, 8604.
[46] Beck M., Wijburg F. A., Gal A., *Eur. J. Hum. Genet.*, **2012**, *20*.

iminosugars to be tested against these two types of sulfatases.[47] The aspect of multivalency will be deeply discussed in Chapter 3, entirely devoted to this topic, the most studied in this PhD thesis.

1.2.5 Golgi α-Mannosidase – Anticancer applications

α-Mannosidases hydrolyze terminal α-mannosidic linkages from glycan moieties of various glycoconjugates. In eukaryotes, they are involved in the processing and degradation of *N*-glycans by hydrolyzing the terminal α1–2-, α1–3- and α1–6-linked mannose residues from high-mannose, hybrid and complex type N-glycans present in glycoproteins. Initially, the α-mannosidases were classified into three groups: acidic/lysosomal, intermediate/Golgi and neutral/cytosolic. A more recent classification categorizes those enzymes into two classes based on inhibition and sequence similarity: Class I α-mannosidase of glycosyl hydrolase (GH) family 47 present in the endoplasmic reticulum (ER α-man), and the Golgi apparatus (GM I) that hydrolyzes specifically α1–2-mannosidic linkages involved in maturation of N-glycans. These are classified as Class II α-mannosidases of GH family 38. In eukaryotic cells the N-glycosylation pathway is responsible for proper processing of proteins as they are synthesized in the endoplasmic reticulum (ER) and Golgi apparatus. It follows a well-defined series of steps and involves a considerable number of enzymes responsible for both the extension (glycosyl transferases) and trimming (glycosyl hydrolases) at various steps of the assembly process. The pathway begins with the assembly and transfer of αGlc3Man9GlcNAc2 (where Glc is glucose, Man is mannose and GlcNAc is N-acetyl-glucosamine) oligo-saccharide precursor onto a newly formed polypeptide chain. Initial processing involves a series of trimming events by ER-resident glycosidases. As the pathway progresses through the Golgi, the trimming steps are followed by the action of some transferases and mannosidases, resulting in the mature glycosylation structure on the nascent protein destine for the cell surface, the lysosomes or secretion.[48] Any kind of alterations are generally associated in cancer growth. New drugs aimed at the key enzymes involved in this pathway using sugar or iminosugars have opened up a new approach for anticancer therapies.[49]

_____

[47] D'Adamio G., Matassini C., Parmeggiani C., Catarzi S., Morrone A., Goti A., Paoli P., Cardona F., *RSC Adv.*, **2016**, *6*, 64847-64851.

[48] van den Elsen J.M., Kuntz D.A., Rose D.R., *EMBO J.*, **2001**, *20(12)*, 3008–3017.

[49] Wrodnigg T.M., Steiner A.J., Ueberbacher B.J., *Curr. Med. Chem. Anti-Cancer Agents*, **2008**, *8*, 77-85.
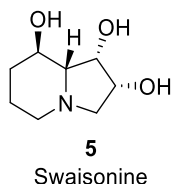
5
Swaisonine

Figure 1.20: Swaisonine, α-mannosidase inhibitor.

Jack bean α-mannosidase (JBM) is a commercially available exo-glycosidase, widely used as a tool for glycan analysis that exhibits activity toward several different substrate, cleaving α1–2-, α1–3- and α1–6-linked mannose residues from various glycoprotein preparations.[50] Due to its properties similar to those of Golgi α-mannosidase II (an important therapeutic target), JBM serves as a model enzyme for structural and mechanistic studies for inhibitors. Until the first resolution of crystal structure of the apo structures of JBα-man reported by Compain in 2018,[51] interactions with inhibitors have been studied using indirect methods such as atomic force microscopy, dynamic light scattering, NMR or mass spectroscopy. These studies have led to a number of competing hypotheses and binding models involving large aggregates, additional interactions with enzyme subsites or formation of discrete cross-linked complexes, all of whom involving multivalent inhibitors (see Chapter 3).[45a]

An example of GMII inhibitor is swaisonine (**5**, SW, figure 1.20),[52] an indolizidine iminosugar. However, SW presents a problem of selectivity: it results a potent inhibitor also of lysosomal α-mannosidase (LManII) and it can lead to many undesirable side effects (the symptoms of mannosidosis disease).[53] In that sense, once again the concept of multivalency can help us (Chapter 3).

1.2.6 Trehalase

Glycosidase enzymes are ubiquitous in nature, in a wide range of organisms. For example, in different organisms such as fungi, mycobacteria and insects, trehalases [EC 3.2.1.28] are present. These glycosidases are responsible for the hydrolysis of ingested trehalose (α-D-glucopyranosyl α-D-glucopyranoside, **22** in figure 1.21), a disaccharide with a multifunctional physiological role in various organisms. Trehalose is particularly

---

[50] Li Y.T., *J. Biol. Chem.*, **1996**, *241*, 1010–1012.

[51] Howard E., Cousido-Siah A., Lepage M. L., Schneider J. P., Bodlenner A., Mitschler A., Meli A., Izzo I., Alvarez H. A., Podjarny A., Compain P., *Angew. Chem. Int. Ed.*, **2018**, *57*, 8002.

[52] Daniel P.F., Winchester B., Warren C.D., *Glycobiology*, **1994**, *4*, 551–566.

[53] Dantas A. F. M., Riet-Correa F., Gardner D. R., Medeiros R. M. T., Barros S. S., Anjos B. L., Lucena R. B., *Toxicon*, **2007**, *49*, 111–116.

important for insects (it constitutes their major blood sugar)[54] as it is hydrolysed into glucose, which is vital for insect flight.
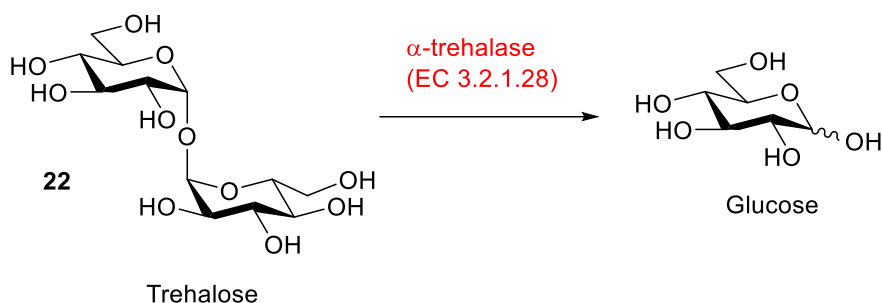

Figure 1.21: Hydrolysis of trehalose catalysed by α-trehalase.

Trehalose is not found in mammalian cells, although humans do possess a trehalase enzymes in intestinal villi and kidney brush border cells, probably to handle ingested trehalose. The absence of trehalose in the metabolism of mammals, together with the physiological relevance of trehalose hydrolysis in insects, makes insect trehalase inhibition a relevant target for the development of selective insecticides that are potentially non-toxic to mammals.[55] Compounds able to inhibit insect trehalase, without affecting the human one, are excellent candidates for insecticides not toxic for humans (green insecticides). Among the most powerful inhibitors of trehalases there are some natural pseudodisaccharides and analogues, such as validoxylamine A (**23**), trehazolin (**24**) and casuarine-6-*O*-α-D-glucoside (**25**) in which a glucose unit is bounded to a glycomimetic (Figure 1.22).[56]
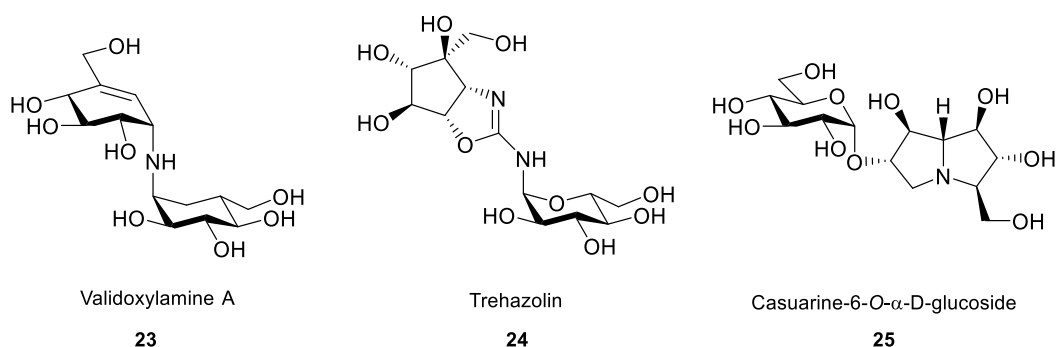

Figure 1.22: Some natural and non-natural trehalase inhibitors.

[54] Becker A., Schlöder P., Steele J. E., Wegener G., *Experientia*, **1996**, *52*, 433–439.

[55] Bini D., Cardona F., Gabrielli L., Russo L., Cipolla L., *Carbohydr. Chem*., **2012**, *37*, 259.

[56] Kato A., Kano E., Adachi I., Molyneux R. J., Watson A. A., Nash R. J., Fleet G. W. J., Wormald M. W., Kizu H., Ikeda K., Asano N., *Tetrahedron: Asymmetry*, **2003**, *14*, 325–331.

Inhibition studies revealed that these compounds are able to specifically block trehalase activity in a micromolar or submicromolar range. The extremely high affinity of the pseudodisaccharide inhibitors derives from the synergistic interactions of an alkaloid unit and a sugar moiety with two enzyme's subsites. Indeed, the active site of trehalase contains two different substructures, one for catalysis and one for recognition; this hypothesis was confirmed in 2007 when Davies and co-workers solved the first three-dimensional structure of a bacterial trehalase.[57] These findings allowed us to understand how casuarine-based inhibitors place themselves inside the catalytic site in order to better mimic the natural configuration. Isolation and purification of these trehalose mimetics from natural sources are very difficult and expensive and afford only minute amount of compounds. In order to overcome these problems and generate highly potent trehalase inhibitors with potential insecticidal activity, several synthetic efforts have been done. In our research group the first total synthesis of casuarine-6-*O*-α-D-glucoside (**25**) was achieved,[58] and casuarine glucoside derivatives bearing modifications at C-7 were synthesized (**26** and **27**, figure 1.23).
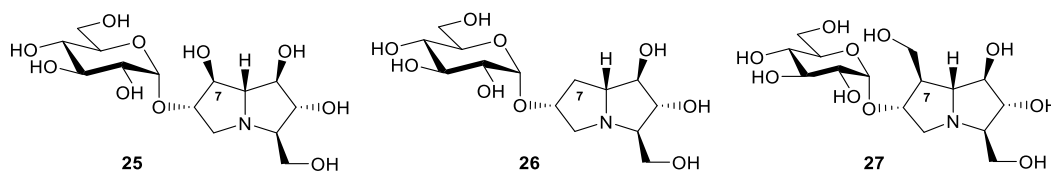

Figure 1.23: 6-*O*-α-D-glucopyranosyl casuarine derivatives.

Upon biological assays of the synthetized compounds, we found different biological activities, thus showing how slight modifications of C-7 of the B ring (OH, H, CH₂OH) were able to influence both the potency and specificity of inhibition.[59] From those results we were able to project and synthesize new selective trehalase inhibitors (See Chapter 2).

1.2.7 Multivalency

Recently it has been demonstrated that the simultaneous introduction of several iminosugar units onto a common scaffold leads to a remarkable increase of the inhibitory activity towards some glycosidases. This phenomenon, known as the multivalent effect,

---

[57] Gibson R. P., Gloster T. M., Roberts S., Warren R. A. J., de Gracia S., García Á., Chiara J. L., Davies G. J., *Angew. Chem. Int. Ed.* **2007**, *46*, 4115-4119.

[58] Cardona F., Parmeggiani C., Faggi E., Bonaccini C., Gratteri P., Sim L., Gloster T. M., Roberts S., Davies G. J., Rose D. R., Goti A., *Chem. Eur. J.* **2009**, *15*, 1627-1636.

[59] Cardona F., Goti A., Parmeggiani C., Parenti P., Forcella M., Fusi P., Cipolla L., Roberts S. M., Davies G. J., Gloster T. M., *Chem.Commun.*, **2010**, *46*, 2629-2631.

_____

has been extensively studied for carbohydrate-lectin interactions, but only in recent years has it acquired increasing interest with regards to the inhibition of glycosidase.[6,45(a),60] The multivalent effect (*Multivalent Effect*, MVE) is defined as the increasing in the biological response of compounds having multiple bioactive units linked together on a common scaffold, compared to the activity of the same unit in monomeric form. Since in biological processes the recognition of a substrate by an enzyme takes place through a very fast association/dissociation equilibrium, an increasing in the local concentration of the ligand in proximity of the active site, consequently increases the chances to form such a bond.
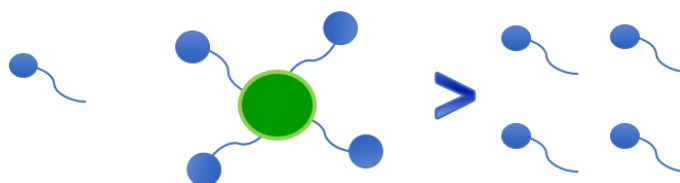

Figure 1.24: Representation of the multivalent effect: increased activity towards the target enzyme when the epitops are covalently linked.

However, if the concentration of the single monomer unit is increased, the same effect is not observed. This shows that the cluster of single units linked together in a multivalent structure is the one responsible to increases the relative power (relative potency, *rp*) of the structure. Here relies the key to understand the MVE. The MVE indeed, is defined positive when the ratio rp/n is greater than 1, where n represents the number of biological units grafted on the scaffold.

This concept was deeply investigated in the field of lectins, where the presence of several carbohydrate-binding sites on the protein's surface has inspired the design of a variety of glycoclusters with impressive binding affinity.[61] On the contrary, the use of multivalent-based strategy has been less explored in glycosidase inhibition, due to the monomeric nature of many of these carbohydrate-processing enzymes. Surprisingly, in the last decade it was demonstrated that also for enzymes with a single active site presentation affinity enhancement can occurs, since the high local concentration of the active moiety on the multivalent scaffold, close to the recognition site, may favor a mechanism of recapture, called "statistical rebinding".[45a] From here, a variety of different scaffolds onto which multimerize different type of bioactive iminosugars are reported in literature, and also our research group contributed to the field designing different multivalent architectures, such

---

[60] (a) Gouin S. G., *Chem. Eur. J*. **2014**, *20*, 11616-11628; (b) Compain P., Bodlenner A., *ChemBioChem*., **2014**, *15*, 1239-1251; (c) Zelli R., Longevial J.-F., Dumy P., Marra A., *New J. Chem*., **2015**, *39*, 5050-5074.

[61] Martinez A., Ortiz Mellet C., García Fernández J. M., *Chem. Soc. Rev*. **2013**, *42*, 4746-4773.

as dendrimers,[32] gold glyconanoparticles[45,b] and resorcinarenes[62] exploiting different synthetic methodologies (see Chapter 3).

1.3 Aim of the work

The principal aim of this PhD thesis is the study of multivalent iminosugar glycomimetics to target enzymes for healthcare applications. The MVE has been studied by multimerizing iminosugar belonging to two classes (piperidines and pyrrolidines) onto different kind of scaffolds, to get an overview of the multivalent effect applied to different glycosidases involved in some Lysosomal Storage Disorders. We also compared the activity of some of the synthesized compounds with other non-lysosomal glycosidases, interesting for anticancer applications. The main strategy used to achieve multivalent compounds is the *click chemistry* reaction CuAAC (copper-mediated azide-alkyne cycloaddition),[63] one of the most common method reported in literature to date in this field. Indeed, it is a very versatile and ultra-fast synthetic procedure that allows to easily obtain multimeric compounds with a high valency degree. On the other hand, it is associated with a general drawback, consisting in the possibility of complexation of copper that could occur by the several triazole moieties presents in dendrimers, producing a cytotoxicity of final products if traces of copper remain as impurities. For this reason, also alternative strategies were considered in the synthesis of final multimeric iminosugars. In particular, two different methodologies were investigated in this PhD thesis, the first one involving in the synthesis of Au glyconanoparticles, polyvalent nanoclusters based on self-assembled monolayers of thyol glycoconjugates attached to gold nanoparticles by Au-S ligation. The second, exploiting a sequence of 1,3-dipolar cycloaddition with a high stereo and regioselectivity.

Moving to a different application and changing the glycosidase target, I have dealt with the synthesis of selective trehalase inhibitors. The common thread are iminosugars, used in this case conjugated with a glucose unit in order to get a pseudodisaccharide able to mimic trehalose to be used as green insecticide. We combined the inhibition potency of some compounds with the selectivity of a similar derivatives that contained an inverted stereochemistry in a specific position (previously obtained results), getting new more potent and more selective pseudodisaccharides.

Again, interested in the study of iminosugar potentiality and in better understanding MVE, we started a project aimed at the synthesis of Carbonic Anhydrase

[62] Cardona F., Isoldi G., Sansone F., Casnati A., Goti A., *J. Org. Chem.,* **2012**, *77*, 6980-6988.
[63] (a) Kolb H. C., Finn M. G., Sharpless K. B., *Angew. Chem.*, *Int. Ed.*, **2001**, *40*, 2004–2021; (b) Rostovtsev V. C., Green L. G., Fokin V. V., Sharpless K. B., *Angew. Chem.*, *Int. Ed.*, **2002**, *41*, 2596–2599; (c) Tornøe C. W., Christensen C., Meldal M., *J. Org. Chem.*, **2002**, *67*, 3057–3064.

(CAs) modulators. CAs enzymes are strongly inhibited by compounds bearing a pharmacophoric arylsulfonamide moiety. Even if in literature several examples of sulfonamide-sugars are reported, there are no data about some possible conjugation of the sulfonamide moiety with iminosugar derivatives. Moreover, the multivalent effect against CAs has been investigated just with reference to the sulfonamide function, without considering the hypothesis of multimerize the sugar 'scaffold' necessary to give the right selectivity towards some specific human isoforms to fill this gap. We synthesized a small library of monovalent compounds that contain sugar or iminosugar moiety bound with different linkers to the sulfonamide pharmacophore, and a preliminary example of multivalent sulfonamide-sugar conjugate.

Chapter 2

Iminosugars as agrochemicals: Pseudodisaccharides as trehalase inhibitors
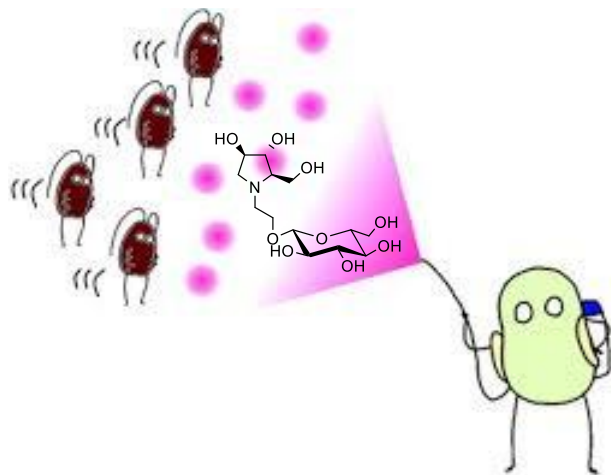
2.1 Introduction

Trehalose (α-D-glucopyranosyl α-D-glucopyranoside, **22**, Figure 2.1) is a disaccharide with a multifunctional physiological role in various organisms (e.g. bacteria, fungi, invertebrates and higher plants).[64]
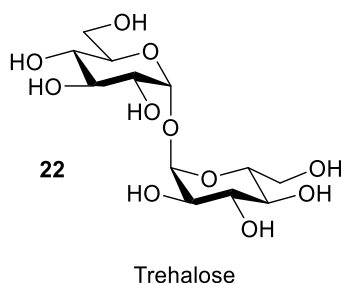

22

Trehalose
Figure 2.1: Trehalose structure.

In order to use trehalose, insect tissues have the enzyme α,α-trehalase (EC 3.2.1.28), which promotes the irreversible hydrolysis of trehalose into two molecules of D-glucose with inversion at the anomeric configuration.[65] Although insects possess two distinct forms of trehalases, a soluble one (localized in haemolymph) and a membrane-bound trehalase (localized in tissues), very little is known about this latter and the difference in function about soluble and membrane-bound trehalases.[66] While trehalose is not present in mammalian cells, humans do possess the enzyme trehalase, only at intestinal level, probably to hydrolyze occasionally ingested trehalose. Indeed, intolerance to fungi has been correlated with the absence or deficit of trehalases in mammals.[64] For the important role of trehalose-derived glucose in larvae survival and development, trehalase inhibitors have been considered in recent years an interesting target for the identification of novel insecticides and fungicides. However, due to the presence of trehalase also in mammals, specificity towards insect trehalase is crucial for the development of drugs that are safe for plants and mammals, and possibly also for insects that are of benefit in nature.[67]

As mentioned in the introduction, the most powerful inhibitors of trehalases are some natural pseudodisaccharides and analogs shown in Figure 2.2, such as validoxylamine (**23**), trehazolin (**24**) and some inhibitors containing iminosugar moieties, such as casuarine-6-*O*-D-glucoside (**25**), a casuarine (**6**) derivative and its non-natural analogues **26** and **27**. Casuarine and casuarine-6-*O*-D-glucoside were isolated for the first time in 1996 from *the leaves of Eugenia jambolana Lam. (Myrtaceae)* and from the bark of Casuarina equisetifolia

[64] Elbein A. D., Pan Y. T., Pastuszak I., Carroll D., *Glycobiology*, **2003**, *13*, 17R-27R.
[65] Defaye J., Driguez H., Henrissat B., *Carbohydr. Res.*, **1983**, *124*, 265-273.
[66] Tang B., Chen X., Liu Y., Tian H., Liu J., Hu J., Xu W., Zhang W., *BMC Mol. Biol.*, **2008**, *9*, 51-57.
[67] Bini D., Cardona F., Gabrielli L., Russo L., Cipolla L., *Carbohydrate Chem.,* **2012**, *37*, 259-302.

L. (Casuarinaceae), two plants well known for their therapeutic action against diarrhoea, breast cancer, diabetes and bacterial infections.[68]

They are well known inhibitors of the fungal glucoamylase from *Aspergillus niger*. Moreover, they are also known to inhibit porcine kidney trehalase (IC_{50}=12 and 0.34 µm, respectively).

validoxylamine A (**23**)

Trehazolin **24**

25 R = OH
26 R = H
27 R = CH$_2$OH

Casuarine (**6**)

(−)-Uniflorine A (**28**)
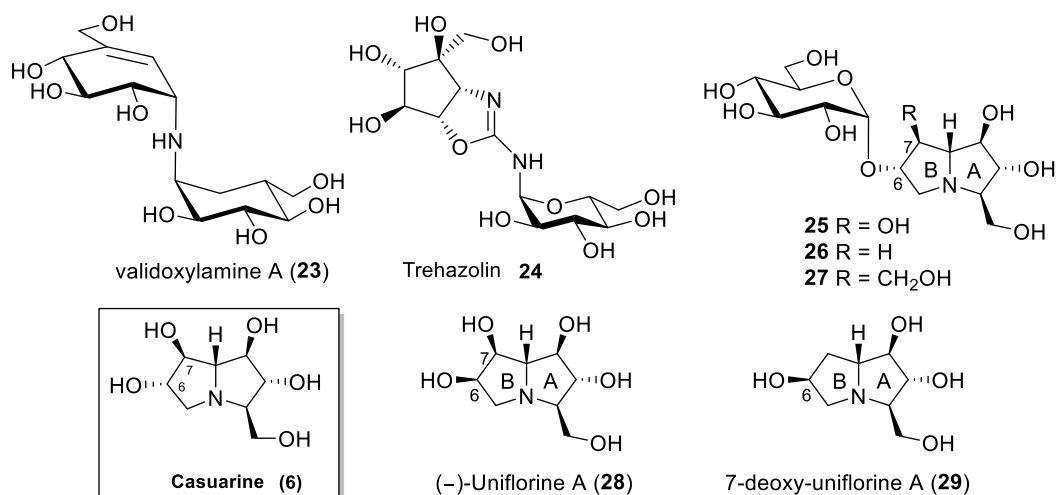
7-deoxy-uniflorine A (**29**)

Figure 2.2: Most potent trehalase inhibitors.

The first investigated trehalase three-dimensional structure was the family 37 periplasmic enzyme from *Escherichia coli* (Tre37A), which was solved in complex with **23**,[57] with casuarine-6-*O*-D-glucoside **25**[58] and with non-natural analogue **27** (Figure 2.3).[59] These findings were achieved in collaboration with Prof. Davies in 2007[58] and the presence of two enzymatic subsites was confirmed, showing that those compounds mimic the natural glucose configuration placing the A ring of pyrrolizidine nucleus in the primary catalytic site (figure 2.3).

_____

[68] Wormald M. R., Nash R. J., Watson A. A., Bhadoria B. K., Langford R., Sims A., Fleet G. W. J., *Carbohydr. Lett.,* **1996**, *2*, 169 – 174.
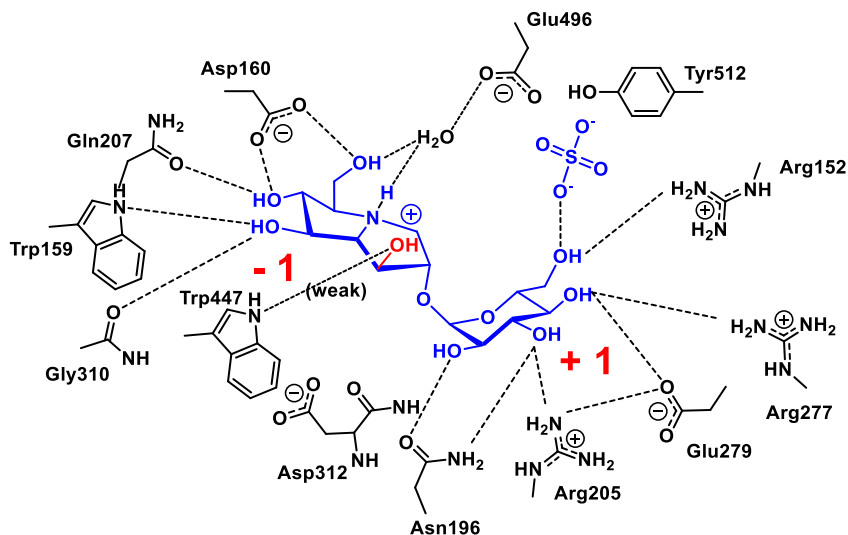
Figure 2.3: **25** and Tre37A (E496 is the catalytic base, D312 the catalytic acid).

It is worth remembering that the isolation from natural sources of those compounds is not a trivial task, and also when it is possible, the isolate amounts are so small that is much better to find a synthetic methodology to obtain them in order to perform more reliable biological tests. In those cases, the reasons of such complexity can be ascribed to the presence of highly complex and challenging structure of casuarine, but also to the fact that it is the most highly hydroxylated pyrrolizidine alkaloid and possesses six contiguous carbon stereocenters. An additional problematic issue in the synthesis of casuarine 6-*O*-α-glucoside lies in the selectivity of glucosylation of the hydroxy group at C-6. Our focus was therefore to find an efficient and selective synthetic pathway. The first synthesis of pseudodisaccharide **25** was achieved in our research group in 2009, and started with nitrone **30**, available in multigram scale from 2,3,5-tri-*O*-benzylarabinofuranose, and exploited the sequence of a selective 1,3-dipolar cycloaddition, a reductive cleavage of the N-O bond[69] with Zn in acetic acid followed by spontaneous *N*-cyclization and a Tamao-Fleming oxidation. The compound was then obtained with a glucosylation reaction (Scheme 2.1).[58] Moreover, following the same strategy, also casuarine glucoside derivatives bearing modifications on C-7, **26** and **27**, were synthesized: they have a hydrogen atom and a hydroxymethyl group instead of hydroxyl moiety respectively.

---

[69] Cardona F., Faggi E., Liguori F., Cacciarini M., Goti A., *Tetrahedron Lett*., **2003**, *44*, 2315 –2318.
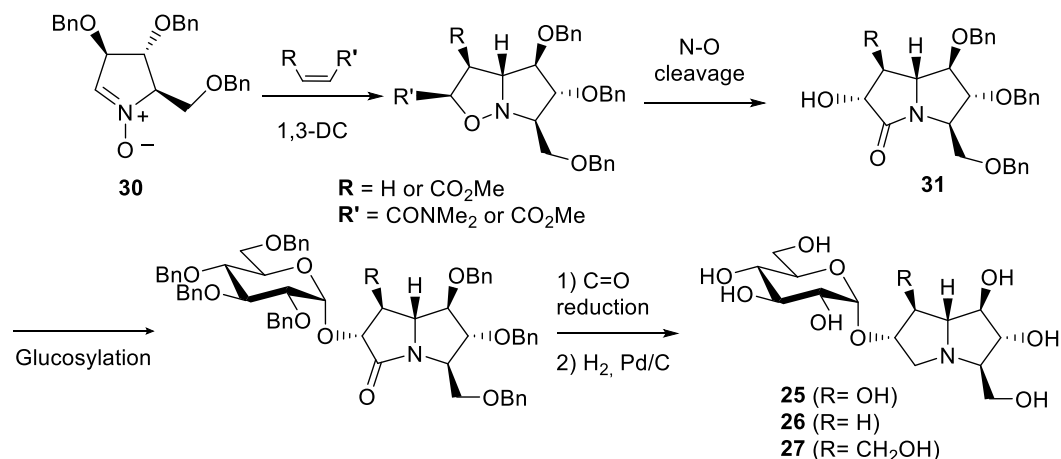
Scheme 2.1: General procedure for the syntheses of pseudodisaccharides **25**, **26** and **27**.

Compounds **25-27** were tested against trehalases from commercial porcine kidney, *E. coli* (Tre37A) and *C. riparius* and biological tests showed that the best inhibitor was casuarine glucoside **25**, with a K_i in the nanomolar range. However, the most selective compound was 7-homocasuarine glucoside **27**; even if was less potent than compound **25**, it was much more selective towards *C. riparius* with respect to porcine kidney trehalase that can be taken as a model for the human one (Table 2.1). Those results showed how slight modifications of C-7 of the B ring (OH, H, CH₂OH) were able to influence both the potency and specificity of inhibition.

Compound	Tre 37A K_i	*C. riparius* K_i	Porcine Kidney K_i
Casuarine (6)	17 μM	0.12 μM	
Casuarine-6-O-α-D-glucoside (25)	12 nM	0.66 nM	11 nM
7-deoxycasuarine-6-O-α-D-glucoside (26)	86 nM	22 nM	138 nM
7-homocasuarine-6-O-α-D-glucoside (27)	2.8 μM	157 nM	>10 μM
(−)-uniflorine A (28)	n.d	177 nM	>1 mM
7-deoxy-uniflorine A (29)	n.d	175 nM	>1 mM

Table 2.1: Inhibition towards different trehalases (taken from ref 59). n.d. stands for not determined.

We reasoned that in the same way also modification on different positions of the pyrrolizidine nucleus could somehow influence the biological activity towards trehalases.

In order to verify this hypothesis simpler natural (−)-uniflorine A (**28**) and non-natural analogue 7-deoxy-uniflorine A (**29**) were synthesized (figure 2.2). They both bear the opposite configuration in B ring at C-6 position with respect to casuarine, obtained with a Mitsunobu reaction.[59] They actually showed an excellent inhibitory profile, being completely selective towards the insect trehalase (Table 2.1), much more with respect to compounds **25**-**27**. Those results demonstrated that stereochemistry at C-6 has actually a key role in the specificity against insect trehalases.

Following our interest in the identification of new more potent and selective trehalase inhibitors, we wanted to understand if by inverting the configuration at C-6 in the disaccharide **26**, we could combine the high inhibition potency typical of pseudodisaccharide compounds **25**-**27** to the best selectivity obtained with uniflorine derivatives **28**-**29**. For this reason, we designed the synthesis of the pseudodisaccharide **32** (7-deoxyuniflorine A glucoside, figure 2.4), that possesses both the pseudodisaccharide structure and the same configuration at C-6 of uniflorine. Moreover, in order to reduce the overall number of synthetic steps required for the synthesis of disaccharides bearing the pyrrolizidine nucleus such as compounds **25**-**27** and **32** itself, we also thought about simplifying these structures by affording simpler pseudodisaccharide inhibitors **33**-**35** (Figure 2.4), that bear the glucose unit linked to the pyrrolidine DAB-1 instead of the pyrrolizidine nucleus. Indeed DAB-1 possesses the same structure of ring A of the pyrrolizidine nucleus (Figure 2.4). Additionally, we had previously verified that DAB-1 is able to mimic glucose by imparting trehalase inhibition in pseudodisaccharide mimetics.[70]
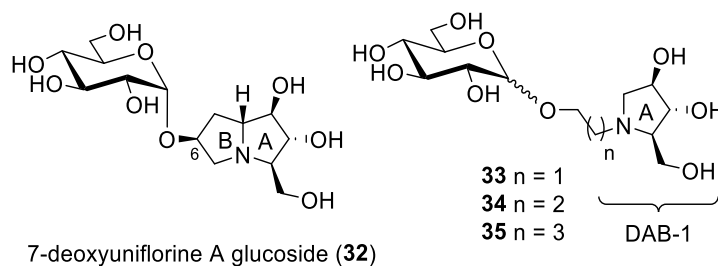

7-deoxyuniflorine A glucoside (**32**)

33 n = 1
34 n = 2
35 n = 3

DAB-1

Figure 2.4: This thesis: synthesis of a new pseudodisaccharide mimetic **32** and of a series of more flexible disaccharide mimics **33**-**35** bearing the DAB-1 nucleus instead of the pyrrolizidine moiety.

The choice to synthetize three different tether lengths (compounds **33**-**35**) arose from the need to understand which was the most appropriate distance between the glucosyl moiety and the DAB-1 portion necessary to obtain the best flexibility of the pseudodisaccharide.

[70] Bini D., Cardona F., Forcella M., Parmeggiani C., Parenti P., Nicotra F., Cipolla. L., *Beilstein J. Org. Chem.,* **2012**, *8*, 514–521.

_____

2.2 Results and discussion

      Part of the work described below was the object of previous works achieved in my research group. The key intermediate of the synthesis of both pyrrolizidine-based (**32**) and pyrrolidine-based (**33**-**35**) pseudodisaccharides is the enantiopure nitrone **30,** readily available from D-arabinose in 5 steps (Scheme 2.2).[71] However, while on one hand further 5 steps are necessary to access the pyrrolizidine glucosyl acceptor (lactam **36**),[69] the hydroxypyrrolidine glucosyl acceptors **38-40** are in principle readily available from amine **37**.[72] Pyrrolidine **37**, recently synthesized by some of us in a one-pot 2-steps sequence from nitrone **30** (Scheme 2.2),[47] has the same stereochemical pattern of the hydroxyl groups of ring A in lactam **36**, which is responsible for the key interactions within the enzyme active site of the final compounds.[58,58] Therefore, compound **37** is in principle able to mimic the more complex pyrrolizidine skeleton of lactam **36**. We also reasoned that pyrrolidine **37** could be easily functionalized at the endocyclic nitrogen atom to afford the desired glucosyl acceptors **38**-**40**, allowing to probe different spatial lengths between the sugar and the iminosugar unit of the target pseudodisaccharides.
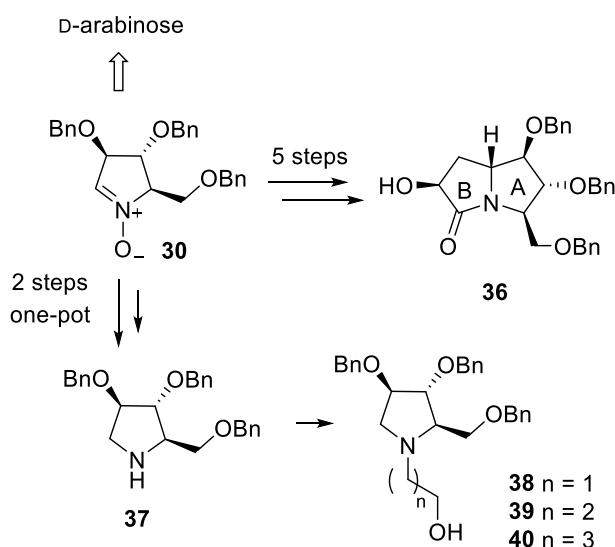

Scheme 2.2: Synthetic steps to access pyrrolizidine lactam **36** and hydroxypyrrolidines **38**-**40** from nitrone **30** through the key intermediate **37**.

---

[71] (a) Cardona F., Faggi E., Liguori F., Cacciarini M., Goti A., *Tetrahedron Lett.,* **2003**, *44*, 2315–2318. (b) Martella D., D'Adamio G., Parmeggiani C., Cardona F., Moreno-Clavijo E., Robina I., Goti A., *Eur. J. Org. Chem*., **2016**, 1588-1598.

[72] (a) Overkleeft H.S., van Wiltenburg J., Pandit U.K.,*Tetrahedron* **1994**, *50*, 4215–4224. (b) Zhou X., Liu W.-J., Ye J.-L., Huang P.-Q., *Tetrahedron,* **2007**, *63*, 6346–6357.

The synthesis of compound **36** was achieved in a previous work in our research group[73] following the scheme below (Scheme 2.3).
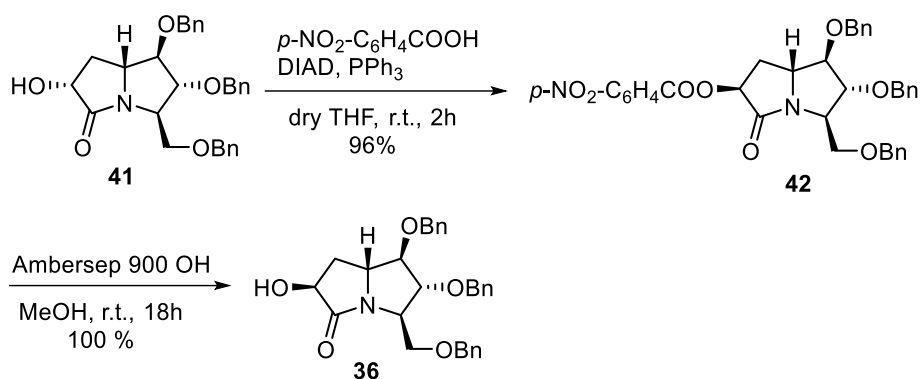

Scheme 2.3: Synthesis of lactam **36**.

 The OH group at C-6 was therefore employed as the acceptor in the glucosylation reaction with the benzyl protected glucopyranosyl trichloroacetimidate **43**. The reaction, performed in diethyl ether at -20 °C, was highly selective in favour of the α-anomer, as reported before for the casuarine derivatives,[58,59] and afforded the α glucoside **44α** as the major product (86% yield). Small amounts (4% yield) of the β-anomer **44β** were isolated and characterized. Reduction of the C=O bond in **44α** with LiAlH4 in refluxing THF afforded compound **45** in excellent yield (90%). The final catalytic hydrogenation, followed by treatment with the ion exchange resin 50WX8-200 gave 7-deoxy-uniflorine A glucoside **32** in 93% yield over two steps (Scheme 2.4). The α -configuration of the glucose moiety was confirmed by ^{1}H NMR.

[73] D'Adamio G., Sgambato A., Forcella M., Caccia S., Parmeggiani C., Casartelli M., Parenti P., Bini D., Cipolla L. Fusi P., Cardona F., *Org. Biomol. Chem.*, **2015**, *13*, 886-892.
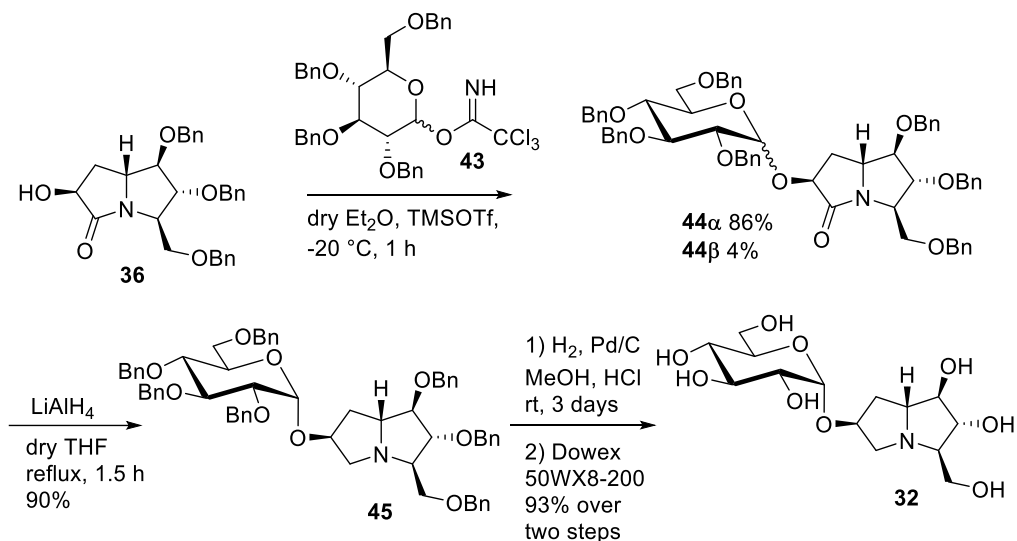
Scheme 2.4: Synthesis of the pseudodisaccharide 7-deoxyuniflorine A glucoside (**32**).

In order to reduce the overall number of synthetic steps necessary to access the glucosyl acceptor in the final glucosylation with trichloroacetimidate **43**, a series of pseudodisaccharide derivatives were prepared containing a DAB-1 nucleus and a remaining D-glucose unit linked through a 2, 3 or 4-carbon atoms spacer. The starting point was nitrone intermediate **30**, that was reduced using NaBH$_4$ followed by a N-O cleavage performed in Zn in acetic acid, to give pyrrolidine **37** in 98% overall yield. It was then *N*-alkylated with an excess of 2-bromo-1-ethanol, 3-bromo-1-propanol and 4-bromo-1-butanol in THF using Et$_3$N as the base at room temperature, affording in this way alcohols **38** (92% yield),[72,b] **39** (94% yield) and **40** (88% yield), that bear a free hydroxyl group at the end of the aliphatic chain, thus allowing selective glucosylation at this position (Scheme 2.5).
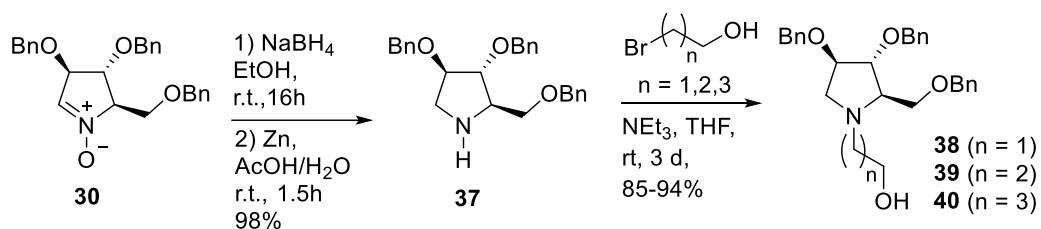
Scheme 2.5: Synthesis of the alcohols **38**-**40**.

Using the glucosyl donor **43**[74], protected with benzyl groups, we obtained a mixture of the two α:β anomers, and only a small amount of a product was recovered (scheme 2.6). The corresponding mixture of deprotected α,β isomers **49-51** were obtained with a catalytic hydrogenation in acidic MeOH and Pd/C as hydrochloride salts, that were passed onto an ion exchange resin (DOWEX 50WX8-200) eluting successively with MeOH, H_2O and 6% aqueous ammonia. The final elution with ammonia afforded pure glucosyl derivatives **49-51** as a mixture of α and β anomers, in 32-40% yields as (**49**α,β, α:β 2:1; **50**α,β, α:β 1:1; **51**α,β, α:β 1.2:1 as determined by ^{1}H NMR analysis).[75]
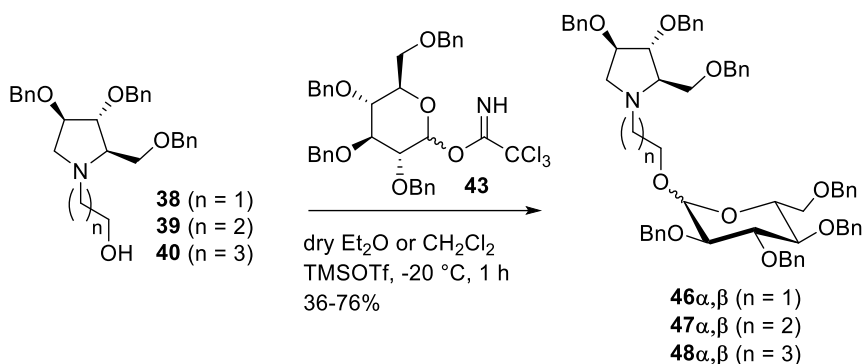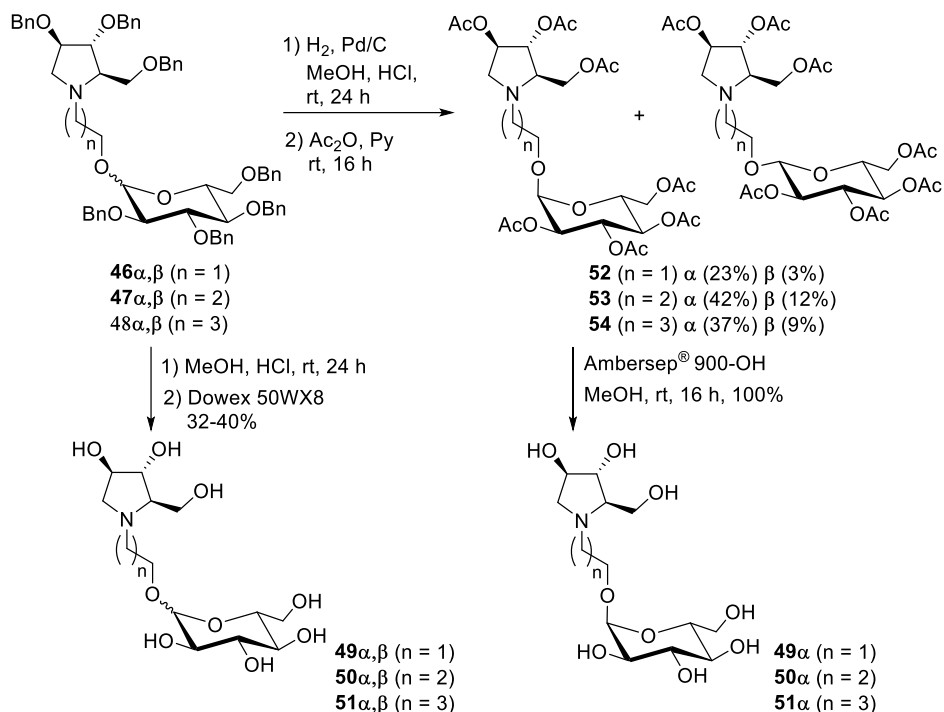

Scheme 2.6: Glucosylation reaction to afford pseudodisaccharides **46-48**.

Due to the impossibility to separate the α and β isomers both with benzylated and free hydroxyl groups, we decided to directly react the crude obtained by catalytic hydrogenation of **46–48α,β** with an excess of acetic anhydride in pyridine affording the corresponding peracetylated compounds **52–54** as α,β mixtures. As expected, in all cases, the two isomers were separated by flash column chromatography, affording pure compounds **52α**, **53α** and **54α** in 23%, 42% and 37% yields over two steps and β-isomers (**52β**, **53β** and **54β** in 3%, 12% and 9% yield) impure of some traces of the corresponding α-isomers (Scheme 3). The α-isomers **52–54α** were subsequently treated with strongly basic Ambersep 900 OH resin in MeOH, leading to pure polyhydroxylated α-pseudodisaccharides **49–51**α in quantitative yield.

[74] Stick R.V., Williams S.J., *Eds. Elsevier*, **2009**, 1133–1202.

[75] D'Adamio G., Forcella M., Fusi P., Matassini C., Ferhati X., Vanni C., Cardona F., *Molecules*, **2018**, *23*, 436.

46α,β (n = 1)
47α,β (n = 2)
48α,β (n = 3)

52 (n = 1) α (23%) β (3%)
53 (n = 2) α (42%) β (12%)
54 (n = 3) α (37%) β (9%)

49α,β (n = 1)
50α,β (n = 2)
51α,β (n = 3)

49α (n = 1)
50α (n = 2)
51α (n = 3)

Scheme 2.7: Synthesis of pseudodisaccharides **49-51α**.

Synthesized compounds **32**, **49α**, **50α**, **51α** and the α/β mixture of compounds **49**, **50** and **51** were tested for their inhibitory activity against insect (*C. riparius*) and porcine kidney trehalases and the results are shown in Table 2.2, together with the previously published data on compounds **26**, **28** and **29**.

Compound	*C. riparius* trehalase (IC$_{50}$)	Porcine Trehalase (IC$_{50}$)	Selectivity[2]
26	44 ± 1 nM	479 ± 45 nM	10
28	177 ± 18 nM	>1 mM	>5649
29	175 ± 12 nM	>1 mM	>5714
32	29.49 ± 7.26 μM	190.60± 34.15 μM	6
49α,β	2.30 ± 0.13 μM	7.67 ± 3.91 μM	3
49α	9.36 ± 1.49 μM	27.64 ± 5.35 μM	3
49β	0.784 ± 0.059 μM	5.84 ± 0.26 μM	
50α,β	>1000 μM	n.d.[3]	-
50α	>1000 μM	n.d.[3]	-
51α,β	>1000 μM	n.d.[3]	-
51α	>1000 μM	n.d.[3]	-

Table 2.2: Biological activity (IC$_{50}$) towards *C. riparius* and porcine trehalases. [2]Selectivity is the ratio between IC$_{50}$ value against porcine trehalase and the IC$_{50}$ value against *C. riparius* trehalase. [3]n.d.= not determined.

The biological data reported in table 2.2 show that compound **32** was active only in the μM range, even if a rather good selectivity was still observed with respect to porcine trehalase. We argue that the with such configuration at C-6, the pseudodisaccharide is not able to place the glucosyl moiety in the active catalytic site with favorable interactions. Among the pyrrolidinic series on the contrary, only compound **49** seems to possess the right distance between the glucosyl moiety and the iminosugar ring, while compounds with a longer linker chain completely lost their inhibitory properties (**50-51**). Thus, considering only the compounds **49α,β** and **49α**, only the mixture of two anomers gave a good inhibitory and selectivity profile, suggesting us that probably the major contribution to inhibition towards *C. riparius* trehalase is given by the isolated β anomer. The data reported above are the object of previous work done in the research group. My contribution to this work inserts in this context, and it consists in finding a strategy to synthesize the pseudodisaccharide **49β** selectively, in order to verify our hypothesis in which we attribute the merit of the selectivity to the β anomer. Because of the impossibility to obtain the isolate β anomer applying the synthetic strategy used before (scheme 2.6), we decided to exploit the differentiation achievable by changing the protecting groups of the glucosyl donor.

We employed the *O*-acetyl protected 1-α-trichloroacetimidate **57** (Scheme 2.8), which would in principle favor the formation of β-pseudodisaccharide **58** in the following glycosylation reaction through the orthoester procedure (1,2-trans glycosylation)[74]. Selective deprotection of **55** with ethylendiamine in acetic acid following the procedure reported by Sun et al.[76] afforded in 86% yield compound **56**, that was treated with trichloroacetonitrile to obtain **57** in 85% yield. Glycosylation reaction with **38** at 0 °C in dry CH$_2$Cl$_2$ in the presence of TMSOTF (1.5 equiv) afforded 39% yield of the β-glucoside **58** as the major compound, although impure of a partially deacetylated isomer. The ^{1}H-NMR spectrum of compound **58** showed a dd at 5.05 ppm for H-2' signal (appearing as a *pseudo* triplet), with coupling constants of 9.6 and 9.8 Hz. This indicates an *axial-axial* relationship with both H-1' and H-3', and therefore confirms the β-configuration of the glucose moiety. Deprotection of the benzyl groups by catalytic hydrogenation and of the acetyl groups by treatment with Ambersep 900-OH, allowed to isolate pure disaccharide **49β** in 43% yield over 2 steps (Scheme 2.8).

---

[76] Sun Q., Yang Q., Gong S., Fu Q., Xiao Q., *Bioorg. Med. Chem*. **2013**, *21*, 6778–6787.
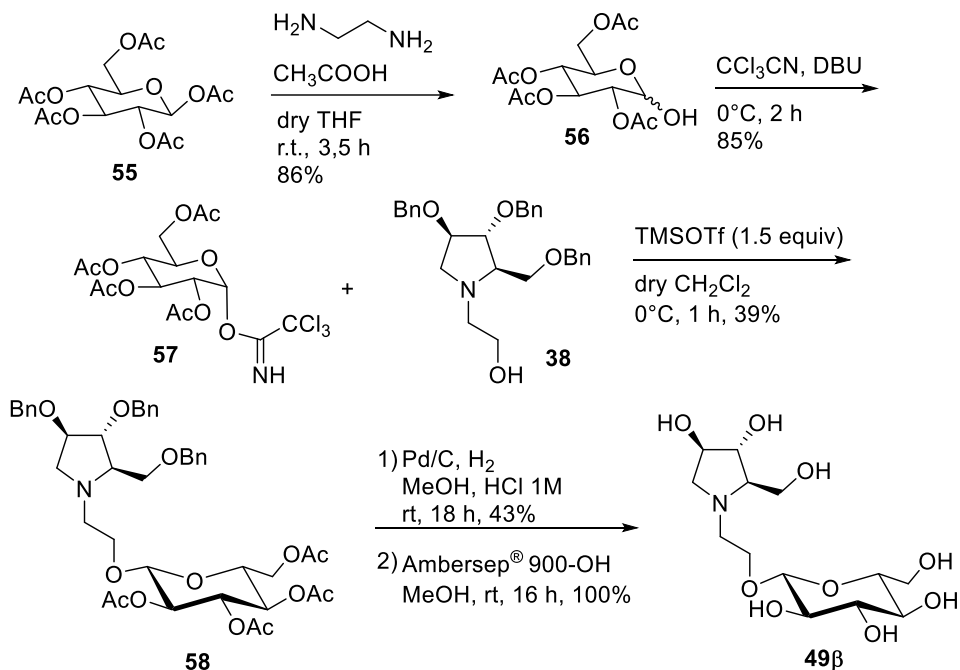
Scheme 2.8: Synthesis of the pseudodisaccharide **49β**.

Compound **49β** was therefore tested against *C. Riparius* and porcine kidney trehalase, giving, to our delight and accordingly to our expectation, a 12-fold more potent inhibition towards *C. riparius* trehalase than its α-anomer, and it was the most potent insect trehalase inhibitor of the pseudodisaccharide pyrrolidine series, with an IC_{50} in the low micromolar range (IC_{50} = 0.784 μM, Table 2.2). Moreover, **49β** showed also a good 7-fold selectivity towards the insect trehalase vs. the porcine enzyme.

2.3 Conclusions

In this part of my PhD thesis the synthesis of new rather good and selectivetrehalase inhibitors was achieved. The hypothesis of the role of both pseudodisaccharide configuration and the importance of pyrrolidine-shape iminosugar bearing the same configuration of natural DAB-1, was confirmed. Moreover, the best tether length between glucose and iminosugar portions was found, suggesting that two carbon atom chain is the ideal distance to allow to all the pseudodisaccharide to place the glucose unit inside the active enzymatic site.

Other investigations are in this moment object of study in our laboratories in collaboration with Prof. Cipolla research group (university of Milano-Bicocca) in particular as a future perspective we would like to synthesize new possible trehalase inhibitors by inserting a

sulphate or a phosphate group on a position of our pyrrolizidine **29** (figure 2.2), in order to mimic the the sulphate ion that is found during the crystallization of the glycoside of 7-homocasuarine within the enzyme (figure 2.3).

2.4 Experimental Section

Here are reported data dealing with the synthesis of the pure **49β** anomer. The other experimental procedures can be found in this paper:

D'Adamio G., Forcella M., Fusi P., Matassini C., Ferhati X., Vanni C., Cardona F.
Probing the Influence of Linker Length and Flexibility in the Design and Synthesis of New Trehalase Inhibitors, *Molecules*, **2018**, *23*, 436.
10.3390/molecules23020436

General Experimental Procedures

All the starting reactants, solvents, and catalysts were commercially available unless otherwise stated. All reactions were carried out under magnetic stirring and monitored by TLC on 0.25 mm silica gel plates (Merck F254). Column chromatographies were carried out on Silica Gel 60 (32–63 µm) or on silica gel (230–400 mesh, Merck). Yields refer to spectroscopically and analytically pure compounds unless otherwise stated. ^{1}H NMR spectra were recorded on a Varian Mercury-400 or on a Varian INOVA 400 instruments at 25 °C. ^{13}C NMR spectra were recorded on a Varian Gemini-200 spectrometer. Chemical shifts are reported relative to TMS (^{1}H: δ = 0.00 ppm) and CDCl3 (^{13}C: δ = 77.0 ppm). Integrals are in accordance with assignments, coupling constants are given in Hz. For detailed peak assignments 2D spectra were measured (COSY, HSQC, NOESY, and NOE as necessary). Small scale microwave assisted syntheses were carried out in a microwave apparatus for synthesis (CEM Discover) with an open reaction vessel and external surface sensor. IR spectra were recorded with a BX FTIR Perkin-Elmer system spectrophotometer. ESIMS spectra were recorded with a Thermo Scientific™ LCQ fleet ion trap mass spectrometer. Elemental analyses were performed with a Perkin-Elmer 2400 analyzer. Optical rotation measurements were performed on a JASCO DIP-370 polarimeter.

Synthesis of 2,3,4,6-Tetra-*O*-acetyl-α/β -D-glucopyranose 56:[77] To a solution of ethylenediamine (93 mg, 1.54 mmol) in 10 mL of dry THF, acetic acid (102 µL, 1.79 mmol)

---

[77] Fernandez-Lorente G., Palomo J.M., Cocca J., Mateo C., Moro P., Terreni M., Fernandez-Lafuenteb R., Guisanb J.M., *Tetrahedron,* **2003**, *59*, 5705–5711.

was slowly added dropwise over 10 min and the reaction mixture was stirred under nitrogen atmosphere at room temperature for 1 h. Then **55** (500 mg, 1.28 mmol) was added and the mixture was stirred for 1 h, until TLC analysis (PE/EtOAc 3:2) showed the disappearance of the starting material (R_f = 0.48) and the formation of a new compound (R_f = 0.24). After washing with HCl 0.1 M (2 × 2 mL) and NaHCO$_3$ (2 × 2 mL), the combined organic layers were dried on Na$_2$SO$_4$, concentrated at reduced pressure and the crude mixture was purified by FCC (PE/AcOEt 1:1) affording pure **56** (α/β 1:9 R_f = 0.30, PE/EtOAc 1:1, 383 mg, 1.100 mmol, 86% yield). ^{1}H-NMR (200 MHz, CDCl$_3$): δ = 5.62 (d, *J*= 9.8 Hz 1H, H-1α), 5.55 (t, *J*= 3.8 Hz, 1H, H-3α), 5.36–5.27 (m, 1H, H-3β), 5.14 (t, *J* = 9.6 Hz, 1Hα + 1Hβ, H-4), 4.96 (dd, *J*= 9.8, 3.4 Hz, 1Hα + 1 Hβ, H-2), 4.80 (t, *J*= 8.1 Hz, 1H, H-1β), 4.37–4.12 (m, 5H, H-6α, H-6 β, H-5α), 3.85–3.77 (m, 1H, H-5β), 2.16 (s, 3Hα + 3 Hβ, OAc), 2.15 (s, 3Hα + 3 Hβ, OAc), 2.09 (s, 3Hα + 3 Hβ, OAc), 2.08 (s, 3Hα + 3 Hβ, OAc) ppm.

Synthesis of 2,3,4,6-Tetra-O-acetyl-α-D-glucopyranosyltrichloroacetimidate 57:[78] A solution of **56** (383 mg, 1.10 mmol) in 8 mL of dry CH$_2$Cl$_2$ was cooled to 0 °C and DBU (32 µL, 0.22 mmol) and trichloroacetonitrile (612 µL, 7.70 mmol) were added. The reaction mixture was stirred under nitrogen atmosphere at room temperature for 2.5 h, when a TLC analysis (Hex/EtOAc 1:1) showed the disappearance of the starting material (R_f = 0.26) and the formation of a new compound (R_f = 0.62). A saturated NH$_4$Cl solution was added and the mixture was transferred to a separating funnel, washing with CH$_2$Cl$_2$. The organic layer was washed with water (3 × 5 mL) and dried over Na$_2$SO$_4$. After concentration under reduced pressure, the crude was purified by flash column chromatography on silica gel (Hex/EtOAc from 3:1 to 2:1) to afford pure **57** (R_f = 0.25 Hex/EtOAc 2:1, 461 mg, 0.939 mmol, 85% yield). ^{1}H-NMR (200 MHz, CDCl$_3$): δ = 8.69 (s, 1H, NH), 6.56 (d, *J* = 3.7 Hz, 1H, H-1), 5.57 (t, *J* = 9.8 Hz, 1H, H-4), 5.23–5.10 (m, 2H, H-2, H-3), 4.32–4.06 (m, 3H, H-5, H-6), 2.08 (s, 3H, OAc), 2.05 (s, 3H, OAc), 2.04 (s, 3H, OAc), 2.02 (s, 3H, OAc) ppm.

Synthesis of Compound 58: A solution of glucopyranosyl tricholoroacetimidate **57** (2 equiv.) and alcohol **38** (1 equiv.) in dry CH$_2$Cl$_2$, was stirred for 10 min at room temperature under nitrogen atmosphere in the presence of 3 Å molecular sieves. After cooling to 0 °C trimethylsilyl trifluoromethanesulfonate (1.5 equiv.) was added and the mixture was stirred for 1.5 h, letting the temperature to rise. To the reaction mixture 1.8 mL of triethylamine was added and the mixture was transferred to a separating funnel, washing with CH$_2$Cl$_2$. The organic layer was washed with HCl 1M (3 × 3 mL), NaOH 1M (1 × 3 mL) and brine (2 × 3 mL). The combined organic layers were dried over Na$_2$SO$_4$ and the solvent was removed under reduced pressure. The resulting crude oil was dissolved in pyridine (3 mL), and acetic anhydride (2 mL) and DMAP (30 µL) were added. The solution was stirred at room temperature overnight, and after concentration under reduced pressure, the crude was purified by flash column chromatography on silica gel (Hex/EtOAc from 1:1 to 1:2) to

_____

[78] Koketsu M., Kuwahara M., *Synth. Commun.* **2004**, *34*, 239–245.

afford the β compound **58** (R$_f$ = 0.516 Hex/EtOAc 1:1, 34 mg, 0.044 mmol, 39% yield) as colorless oil, contaminated with small amounts of partially deacetylated glucoside. **[α]$_{21}^D$**= −15.2 (c = 0.80 in CHCl$_3$); **^{1}H-NMR** (400 MHz, CDCl$_3$): δ=7.32–7.24 (m, 15H, HAr), 5.16 (t, *J* = 9.5 Hz, 1H, H-4'), 5.05 (dd, *J* = 9.8, 9.6 Hz, 1H, H-2'), 4.97 (t, *J* = 9.6 Hz, 1H, H-3'), 4.54–4.43 (m, 7H, H-Bn, H-1'), 4.23 (dd, *J* = 12.2, 4.7 Hz, 1H, Ha-6'), 4.09 (dd, *J* = 12.2, 2.2 Hz, 1H, Hb-6'), 4.00–3.95 (m, 1H, Ha-8), 3.88 (d, *J* = 5.0 Hz, 1H, H-4), 3.81 (d, *J* = 3.8 Hz, 1H, H-3), 3.68–3.58 (m, 2H, Hb-8, H-5'), 3.56–3.43 (m, 2H, H-6), 3.16 (d, *J* = 10.7 Hz, 1H, Ha-5), 3.10–3.04 (m, 1H, Ha-7), 2.77 (q, *J* = 5.7 Hz, 1H, H-2), 2.69–2.61 (m, 2H, Hb-5, Hb-7), 2.06 (s, 3H, OAc), 2.01 (s, 3H, OAc), 1.99 (s, 3H, OAc), 1.93 (s, 3H, OAc) ppm; **^{13}C-NMR** (100 MHz, CDCl$_3$): δ = 170.6, 170.2, 169.4, 169.3 (s, 4C, C=O), 138.3, 138.2, 138.1 (t, 3C, C-Ar), 128.3, 127.8, 127.7, 127.6, 127.5 (d, 15C, C-Ar), 100.6 (d, C-1'), 84.7 (d, C-4), 81.6 (d, C-3), 77.4 (C-2'), 77.1 (d, C-3'), 73.2 (d, C-4'), 72.8 (d, C-2), 71.2, 71.1, 71.0 (s, 3C, C-Ar), 69.4 (d, C-5'), 68.9 (t, C-8), 68.4 (t, C-6), 61.9 (t, C-6'), 58.4 (t, C-5), 54.0 (t, C-7), 20.7, 20.6, 20.6, 20.6 (q, 4C, CH$_3$) ppm; **IR** (CDCl$_3$): ν = 3031, 2945, 2866, 2360, 2331, 1755, 1497, 1454, 1375, 1231, 1171,1039 cm−1. **MS (ESI)**: m/z calcd (%) for C$_{42}$H$_{51}$NO$_{13}$ 777.33; found 800.63 (100%, [M+ Na]$^+$).

Synthesis of Compound 49β: To a solution of **58** (43 mg, 0.055 mmol) in 10 mL of methanol, Pd/C (50%, w/w) and 0.5 mL of HCl 1 M were added under nitrogen atmosphere, then the mixture was stirred under hydrogen atmosphere at room temperature overnight, until an ^{1}H-NMR control showed the disappearance of the starting material. The mixture was then filtered through Celite® and the solvent was removed under reduced pressure. The crude was purified by flash column chromatography on silica gel (CH$_2$Cl$_2$/MeOH 10:1, R$_f$ = 0.585) to afford 12 mg, which were dissolved in 10 mL of methanol, ion exchange resin Ambersep 900-OH was added and the suspension was slowly stirred at room temperature for 16 h. The mixture was filtered through cotton and the solvent was removed under reduced pressure, affording pure **49β** (8 mg, 0.024 mmol, 43% yield) as colourless oil. **[α]$_{19}^D$** = −28.5 (*c* = 0.67 in H$_2$O); **^{1}H-NMR** (400 MHz, D$_2$O): *δ* = 4.34 (d, *J* = 8.0 Hz, 1H, H-1'), 4.02–3.98 (m, 1H, H-4), 3.92 (ddd, *J* = 11.0, 6.4, 4.4 Hz, 1H, Ha-8), 3.82–3.81 (m, 1H, H-3), 3.77 (d, *J* = 2 Hz, 1H, Ha-6'), 3.68–3.56 (m, 4H, Hb-8, H-6, Hb-6'), 3.38–3.21 (m, 3H, H-3', H-4', H-5'), 3.15 (t, *J* = 8.4 Hz, 1H, H-2'), 3.05–2.97 (m, 2H, Ha-7, Ha-5), 2.74 (dd, *J* = 11.4, 5.7 Hz, 1H, Hb-5), 2.61–2.53 (m, 2H, Hb-7, H-2) ppm; **^{13}C-NMR** (100 MHz, D$_2$O): δ = 102.32 (d, C-1'), 79.11 (d, C-3), 76.06 (d, C-3'), 75.79 (d, C-5'), 75.62 (d, C-4), 73.20 (d, C-2'), 72.01 (d, C-2), 69.78 (d, C-4'), 67.88 (t, C-8), 61.19 (t, C-6), 60.88 (t, C-6'), 58.94 (t, C-5), 54.04 (t, C-7) ppm; **MS (ESI)**: *m/z* calcd (%) for C$_{13}$H$_{25}$NO$_9$ 339.15; found: 362.47 (100%, [M+ Na]$^+$); **elemental analysis** calcd (%) for C$_{13}$H$_{25}$NO$_9$ (339.34): C 46.01, H 7.43, N 4.13; found: C 46.37, H 7.45, N 4.17.

Biological experiments

To evaluate the inhibitory pattern, we performed kinetics measurements by varying the trehalose concentration, at two different concentrations of compounds **49α** and **49β**. Results showed a pure competitive inhibitory pattern. To determine the inhibition type, data were plotted according to the Lineweaver-Burk plot, replots were built and an inhibition constant (K_i) was calculated equal to 2.56 ± 0.42 µM for **49α** and 0.40 ± 0.022 µM for **49β**.

Chapter 3

Multivalency in glycosidases inhibition: different approaches to design multivalent iminosugars
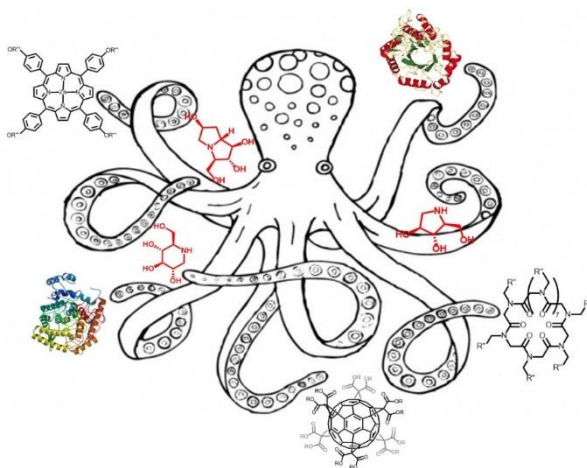
3.1 The Multivalent Effect

3.1.1 Introduction

From a long period, the therapeutic potentiality of iminosugars was known and during the last decades a large part of carbohydrate chemistry has been devoted to the study of new more efficient synthetic strategies to achieve those glycomimetics. In particular, large efforts were done in the search of monovalent iminosugars to target glycosidases. Until a certain point indeed, the basic concept to develop a specific enzyme inhibitor was to consider the lock-key mechanism as effective mode of recognition. Only recently it has been thought to extend to the field of glycosidase inhibition a concept known for a long time in the context of carbohydrate-lectin interactions. The reason is quite clear, indeed lectins are particularly prone for multivalent interactions, as they generally possess several carbohydrate recognition domains to counterbalance their intrinsic weak affinity for their ligands,[79] while glycosidases are generally monomeric, and the oligosaccharides/catalytic sites interactions are often associated with a monovalent process.[60] Nevertheless, at the gates of the 2000s the first example of multivalent glycosidase inhibitors appeared in the literature (dimer **59**, figure 3.1),[80] paving the way for a new line of research: the study of multivalent glycosidases inhibitors.
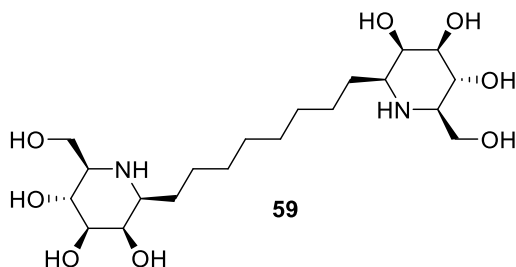

Figure 3.1: First example of multivalent structure, a dimer of DMJ.

The Multivalent Effect (MVE) is defined as the increase in the biological response of compounds that show multiple bioactive units linked together onto a common scaffold, compared to the sum of contributions of the same units alone (see section **1.2.7**, figure 3.2). However, just by incrementing the concentration of the single binding units, an enhancement of activity (relative potency, *rp*) is observed due to the increasing of the local concentration, but not with the same effect observed for a multivalent cluster. Indeed, it's only by the synergy obtained by grafting together several bioactive units, that we observed a real advantage (Figure 3.2).

---

[79] Lis H., Sharon N., *Chem. Rev*., **1998**, *98*, 637–674.

[80] Johns B. A., Johnson C. R., *Tetrahedron Lett*., **1998**, *39*, 749 –752.
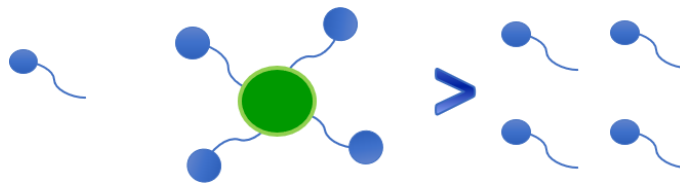
_____

Figure 3.2: Representation of the multivalent effect: increased activity towards the target enzyme when the epitops are covalently linked.

Winum and his collaborators affirmed that there is a positive multivalent effect when the ratio between the relative power (*rp*) and the number of bioactive units in the multivalent system (n) is greater than 1, or *rp* / n> 1 (the relative power *rp* is generally expressed in terms of K_i or IC_{50}). Only in this case there is an effective advantage for the purposes of biological application to use multivalent systems rather than using a higher concentration of the monovalent ligand. Although the effects involved in the interaction between the glycosidases and the multivalent compounds responsible for MVE have not yet been clearly elucidated, affinity enhancements can be expected for enzymes with a single active site presentation, since the high local concentration of the active moiety on the multivalent scaffold, close to the recognition site, may favor a mechanism of recapture, called "statistical rebinding" (see section 3.1.2).

Many iminosugars display high affinity towards the active site of glycosidases, thus making them ideal candidates for the construction of multivalent architectures. Recently, the use of copper (I) azide-alkyne cycloaddition reaction (CuAAC)[63] led to great progresses in the area of research on multivalent iminosugars, allowing the realization of different kind of clusters. For example, in 2009 Gouin and his group reported the systematic evaluation of some clusters of iminosugars as glucosidase inhibitors, providing for the first time also monovalent models to be able to quantify a possible multivalent effect.[81] Indeed, two di- and trivalent derivatives of DNJ (**1**, Figure 3.3) were synthesized using CuAAC, with bi- and tridentate oligoetilene scaffolds (**59**, **60**, Figure 3.3). In addition, the monovalent reference compound **59** was also synthesized. The trivalent derivative **60** in particular showed an *rp*/n = 2.2 with respect to the monovalent **61** towards α-mannosidase from Jack Bean (αManJB).

---

[81] Diot J., García-Moreno M. I., Gouin S. G., Ortiz Mellet C., Haupt K., Kovensky J., *Org. Biomol. Chem.*, **2009**, *7*, 357 363.

n= 2 or 4

59

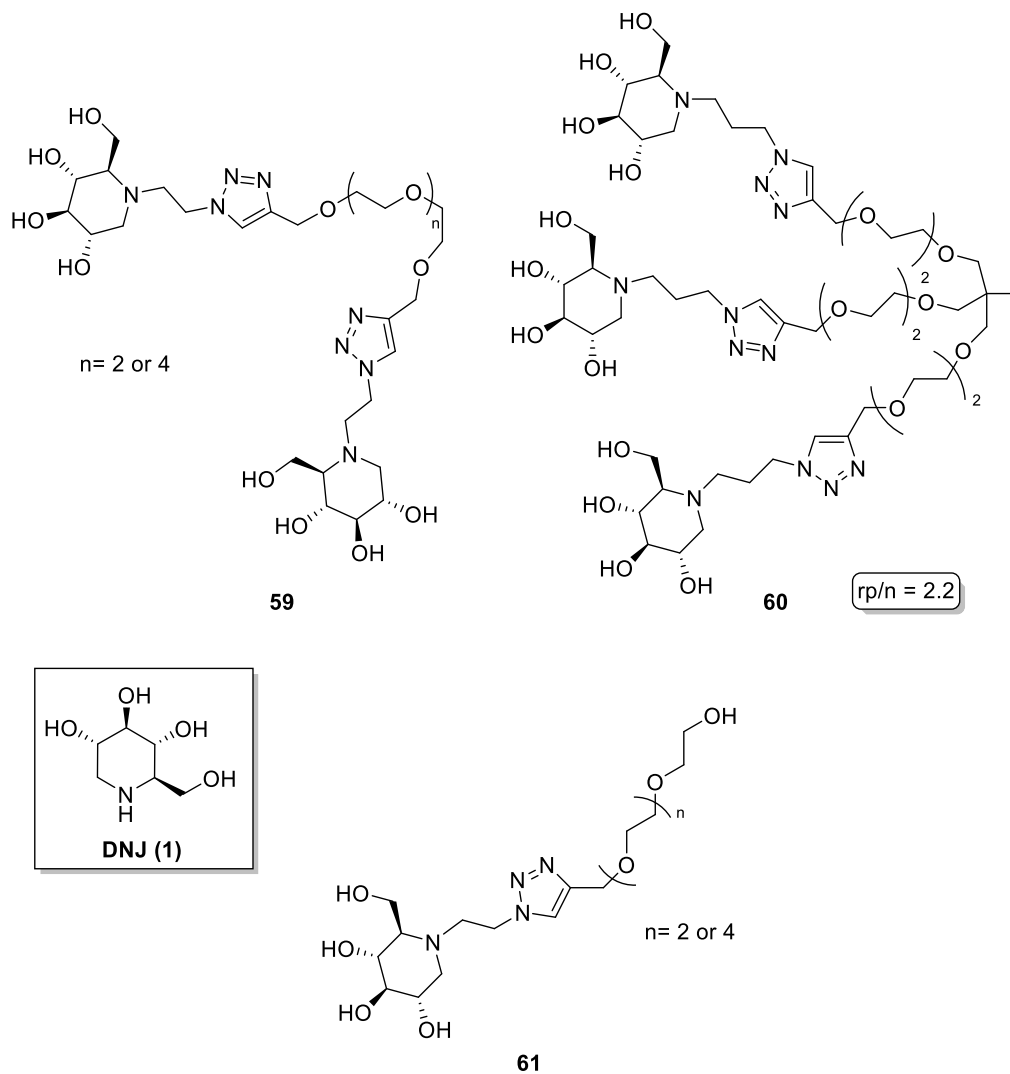**60**

rp/n = 2.2

DNJ (1)

n= 2 or 4

61

Figure 3.3: Di- and trivalent derivatives of DNJ and monovalent reference compound.

However, the first example of a truly remarkable MVE was obtained by Compain and Nierengarten in 2010, when they reported the synthesis of the fullerenic adduct **63** (Figure 3.4),[82] exploiting the synthetic strategy developed in the previous years.[83]

[82] Compain P., Decroocq C., Iehl J., Holler M., Hazelard D., Mena Barragn T., Ortiz Mellet C., Nierengarten J.-F., *Angew. Chem. Int. Ed.*, **2010**, *49*, 5753 –5756.

[83] Iehl J., Nierengarten J.-F., *Chem. Eur. J.*, **2009**, *15*, 7306 –7309.
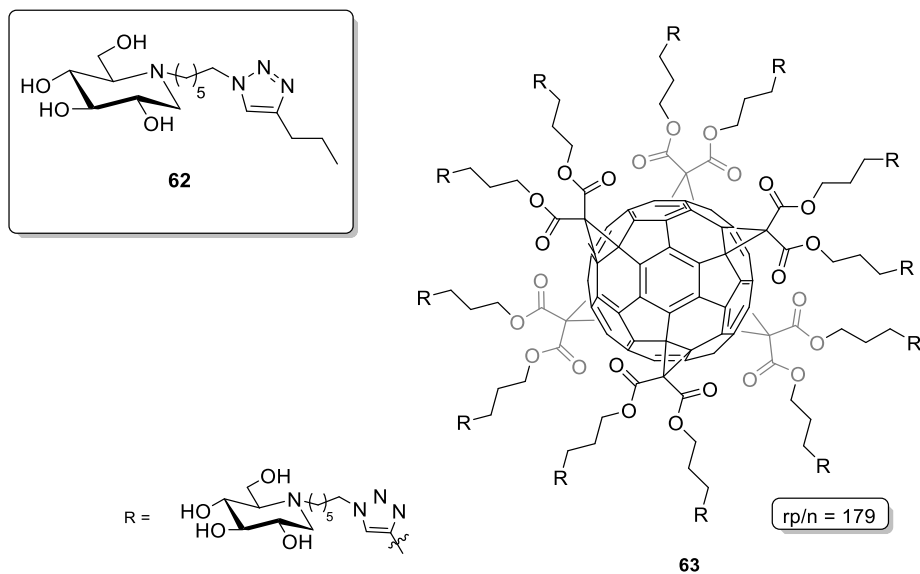
Figure 3.4: Multivalent Cluster C_{60} with *N*-alkylate DNJ.

The multivalent structure consisting of a globular cluster (C_{60} fullerene), decorated with 12 units of a *N*-alkylated derivative of the DNJ (**63**, in Figure 3.4), showed a significant multivalent effect (*rp*/n = 179) against the αManJB compared to the monovalent fee **62**. Following the excellent results, other multivalent structures based on β-cyclodextrins (β-CD)[84] have been synthesized by Compain group. Compound 14-valent **65** (Figure 3.5) consists of 7 iminosugar units on the upper edge and 7 on the lower bound by a chain with 9 carbon atoms to the triazole ring and showed a very high inhibitory activity (*rp*/n = 662, compared to the monovalent compound **64**, taken as a reference). 21-valent cluster **67**, obtained by reacting a trimer of DNJ with each of the seven alkyne functionalities of the β-CD scaffold (and thus called second-generation), inhibits αManJB at nanomolar concentrations (the K_i is 19 ± 3 nM), while the other previously prepared multivalent compounds had K_i values in the order of micromoles. The interesting data for the purpose of rationalizing the multivalent effect is that the 2nd generation cluster 17 has a lower *rp*/n than its corresponding 14-valent **65** (*rp*/n = 470 vs 662), suggesting that the increase in multivalent effect does not grow linearly with valence, but stops at a plateau.

---

[84] (a) Decroocq C., Rodríguez-Lucena D., Russo V., Mena Barragán T., Ortiz Mellet C., Compain P., *Chem. Eur. J.*, **2011**, *17*, 13825 –13831; (b) Decroocq C., Joosten A., Sergent R., Mena Barragán T., Ortiz Mellet C., Compain P., *ChemBioChem,* **2013**, *14*, 2038 –2049.
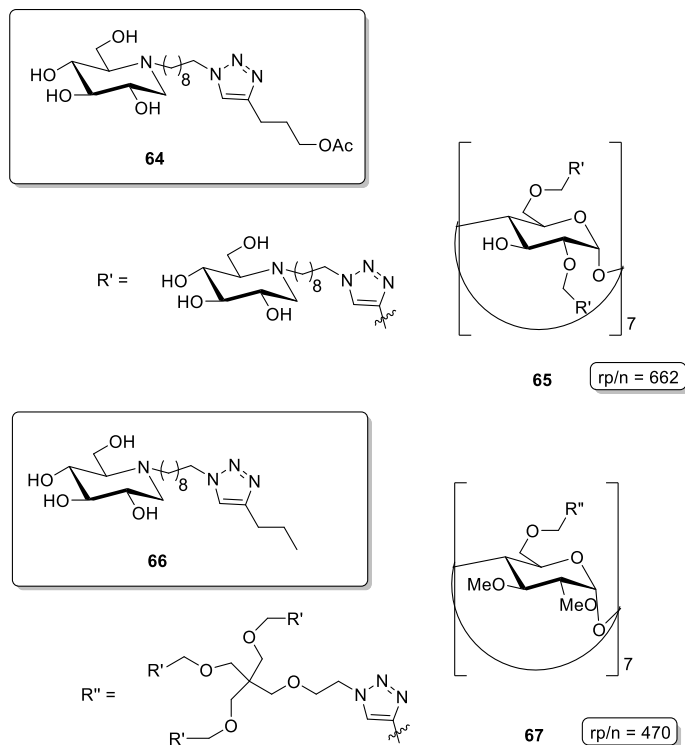
Figure 3.5: Multivalent cluster with scaffold β-CD decorated with N-alkylated DNJ.

This aspect is also highlighted by a following work by Compain, which summarizes a series of cyclopeptoids of different valence (from 18 to 48 units of DNJ).[85] Indeed also in this case the highest inhibition potential does not correspond to the highest valence number, which is instead obtained with the adduct 36-valent **68** (*rp*/n = 4747) (Figure 3.6).
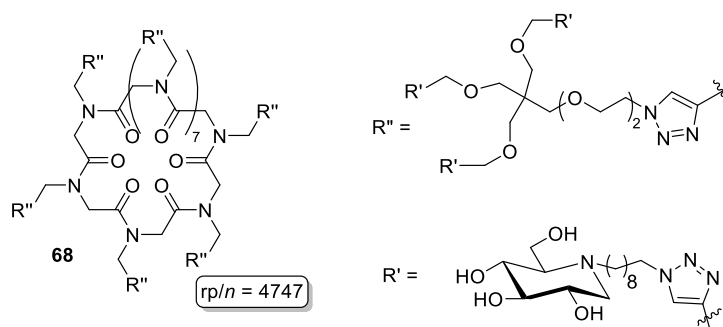

Figure 3.6: Multivalent cyclopeptoid.

[85] Lepage M. L., Schneider J. P., Bodlenner A., Meli A., De Riccardis F., Schmitt M., Tarnus C., Nguyen-Huynh N.-T., Francois Y.-N., Leize-Wagner E., Birck C., Cousido-Siah A., Podjarny A., Izzo I., Compain P., *Chem. Eur. J.,* **2016**, *22*, 5151-5155.

Many other types of scaffolds have been synthesized and tested, such as linear or branched dextrans (DEX) based on polymeric iminosugars,[86] porphyrins,[87] or calixarenic structures.[88] Unlike the many types of scaffolds tested, the iminosugars used as biologically active units are almost exclusively DNJ and its analogue with D-mannose configuration (1-deoxymannojirimicin, DMJ).

Since our research group has many years of experience in the synthesis of iminosugars, we thought to synthesize dendrimeric multivalent adducts with iminosugars which had never been used before, exploiting the CuAAC click chemistry. With this strategy we have synthesized both multivalent pyrrolizidines and piperidines. The first multimerized iminosugars were pyrrolizidines (Figure 3.7), since they already showed a remarkable inhibitory activity against amyloglucosidases, in particular of human maltase glucoamylase, in monovalent form.[58] From the nitrone **30** (Figure 3.7) the derivative **69** (6-azido-6-epi-6,7-dideoxycasuarine) of casuarine **6** was synthesized, which contains an azide moiety in position 6; this made it possible to carry out a CuAAC reaction to build the tetra- and nonavalent systems **70** and **71**.[89]

[86] Brissonnet Y., Ladeveze S., Teze D., Fabre E., Deniaud D., Daligault F., Tellier C., Sestak S., Remaud-Simeon M., Potocki-Veronese G., Gouin S. G., *Bioconjug. Chem.*, **2015**, *26*, 766-772.

[87] Fan J.-Q., *Biol. Chem.*, **2008**, *389*, 1–11.

[88] (a) R. Zelli, J.-F. Longevial, P. Dumy and A. Marra, *New J. Chem.,* **2015**, *39*, 5050-5074; (b) M. Marradi, S. Cicchi, F. Sansone, A. Casnati and A. Goti, *Beilstein J. Org. Chem.*, **2012**, *8*, 951-957; (c) F. Cardona, G. Isoldi, F. Sansone, A. Casnati and A. Goti, *J. Org. Chem.,* **2012**, *77*, 6980-6988.

[89] D'Adamio G., Parmeggiani C., Goti A., Moreno-Vargas A. J., Moreno-Calvijo E., Robina I., Cardona F., *Org. Biomol. Chem.,* **2014**, *12*, 6250-6266.
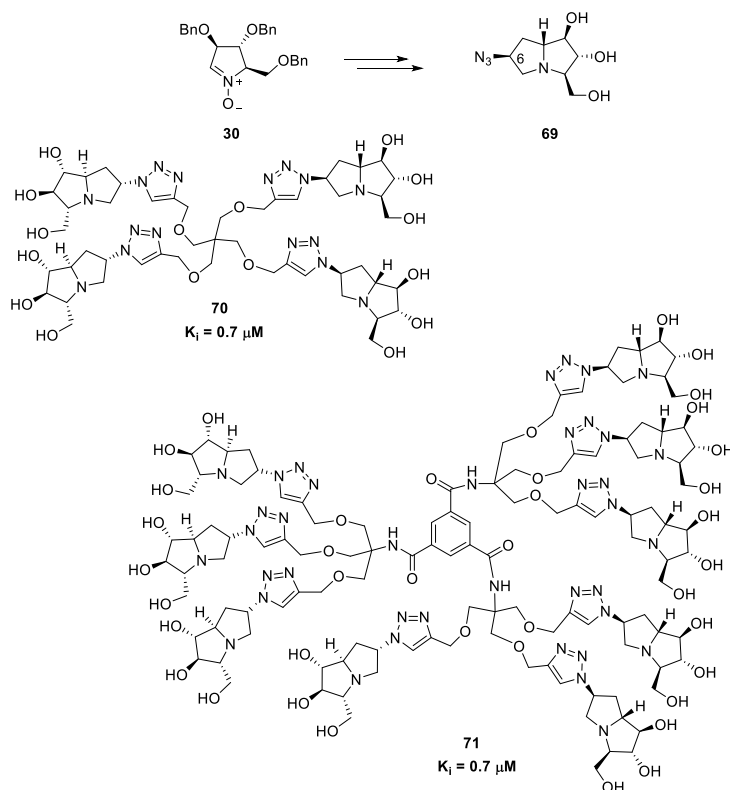
Figure 3.7: Tetra- e nonavalent pyrrolizidines with their K_i.

Compound **71** was the first example of multivalent pyrrolizidine iminosugar with nine bioactive units. However unfortunately, biological enzymatic inhibition tests did not give satisfactory results: both multivalent adducts maintained their activity, but do not show an enhancement compared to their monomeric equivalents against the enzyme amyloglucosidase. Again, using the same scaffolds seen for pyrrolizidines, we prepared multivalent adducts based on piperidine iminosugars (Figure 3.8),[90] exploiting the reductive double amination strategy on the aldehyde derivative **73** developed in our group and obtaining compound **74**,[91] enantiomer of the natural **72**. A simple modification of the synthetic strategy allows to insert on the endocyclic nitrogen a terminal azido alkyl chain, obtaining the derivative **75** that we have exploited to build the structures **76** and **77** through CuAAC.

---

[90] Matassini C., Mirabella S., Goti A., Robina I., Moreno-Vargas A. J., Cardona F., *Beilstein J. Org. Chem.,* **2015**, *11*, 2631-2640.
[91] Matassini C., Mirabella S., Goti A., Cardona F., *Eur. J. Org. Chem.,* **2012**, 3920-3924.
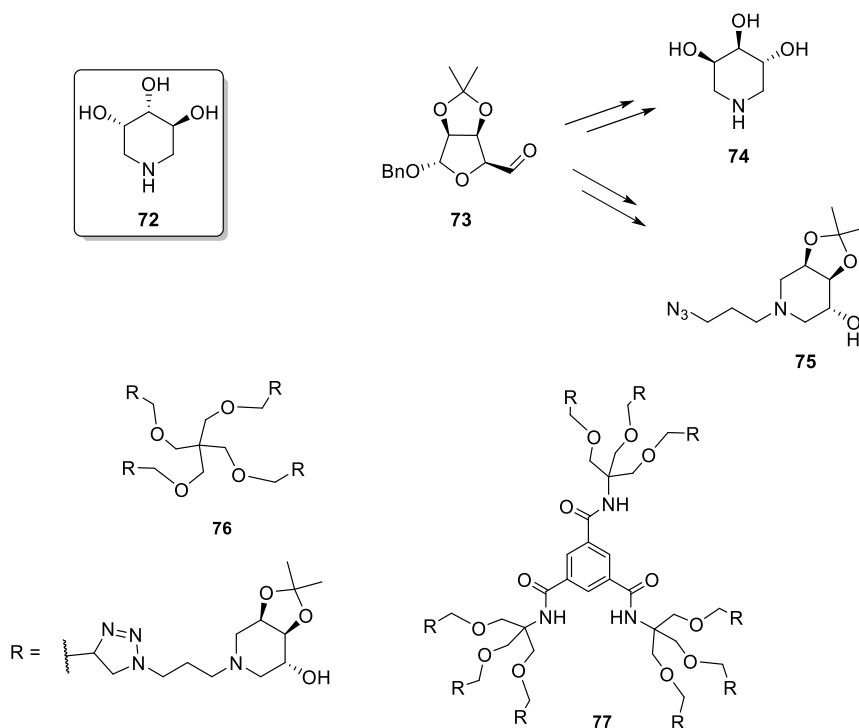
Figure 3.8: Tetra- e nonavalent piperidines.

3.1.2 Mechanistic hypothesis of the multivalent binding

Even if the effects involved in the interaction between the glycosidases and the multivalent compounds responsible for MVE have not yet been unambiguously clarified, the following four mechanisms shown in figure 3.9 are considered possible: 1) *Statistical effect* (Figure 3.9 A), explainable through the increasing of the local concentration and therefore the consequent increase in the possibility to form the bond. 2) *Chelating effect* (Figure 3.9 B), which can attend only if the enzyme possesses more than one catalytic site. 3) *Secondary binding effect*, which can derive from interactions with a non-catalytic site (Figure 3.9 C), or from a steric hindrance effect of the pocket to which the substrate is no longer able to access (Figure 3.9 D). 4) *Cluster effect*, in which the multivalent structure favors the aggregation of several enzymatic units (Figure 3.9 E) or is able to form a sort of cross-linked bonds with multimeric enzymes (Figure 3.9 F).
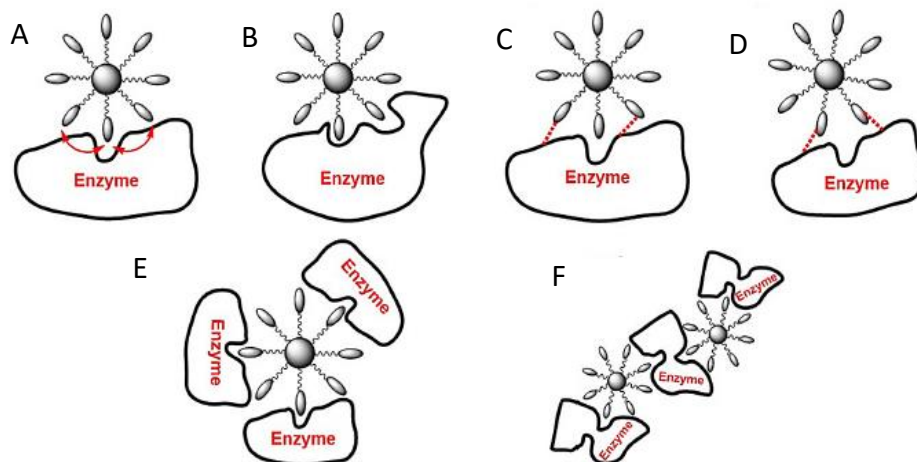
Figure 3.9: Proposed binding models accounting for the multivalent effect.

Several studies have been carried out with the aim of identifying the mechanism of interactions in place. Computational studies demonstrated that mechanism (d) can occur for fullerene-based nanoscale inhibitors of carbonic anhydrase possessing dimensions of the same order of magnitude of the opening of the enzyme cavity.[92] To date the best results have always been obtained towards JBαMan,[45] which is the enzyme most sensitive to the multivalent effect. This propensity can be explained by the dimeric nature hypothesized for this enzyme, which makes possible the involvement of various mechanisms such as the chelating effect (Figure 3.9 B) or the cluster effect (Figure 3.9 F). Furthermore, the results obtained suggest that the spatial distribution of iminosugars proves to be more relevant than the continuous increase in valence. This fact is particularly emphasized in the case of the JBαMan, where a plateau is reached after the repetition of a certain number of biologically active units. For this reason, one hypothesis is that a key role is also played by the multimeric nature of the enzyme itself, which seems to determine a MVE. Once the dimeric nature of the enzyme acetylgalactosamine-6-sulphatase (GALNS) has been demonstrated (see Chapter 1), we decided to test multivalent compounds based on pyrrolidine-based iminosugars inhibitors of this enzyme, whose deficiency causes the onset of a rare metabolic disease: Morquio A. syndrome. We decided to use a *N*-alkylated derivative of the iminosugar DAB-1, since it had already shown a high inhibitory activity (IC_{50} = 0.94 μM) against GCase, to achieve nonavalent compound **77**.[32]

---

[92] Innocenti A., Durdagi S., Doostdar N., Strom T. A., Barron A. R., Supuran C. T., *Bioorg. Med. Chem*. **2010**, *18*, 2822–2828.
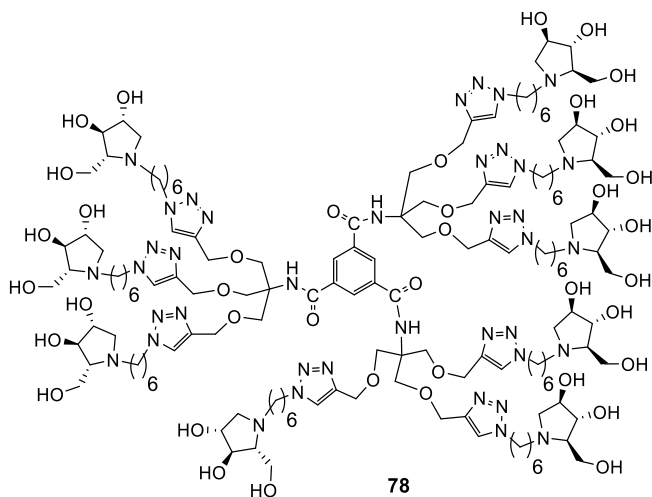
_____

Figure 3.10: Nonavalent pyrrolidine **78**.

The ratio *rp*/n = 9.2 of **78** confirms that also the nature of the enzymatic active site is of significant importance in MVE.

Other studies were carried on in our research group, in order to clarify this phenomenon, by investigating the binding mode of our multivalent pyrrolidine iminosugars with JBMan by a combined NMR/molecular modeling protocol.[93] For the first time it was demonstrated that there is a specific interaction occurring between a multivalent inhibitor and the active site. Moreover, TEM (Transmittance Electron Microscopy) showed that aggregates of enzyme and ligand were formed during their interaction, involving a clustering effect (mode F, figure 3.9).

3.1.3 Our approach to design multivalent architectures

This PhD thesis deals with the purpose to evaluate the MVE by exploiting different kind of scaffolds onto which two type of iminosugars were grafted. Combining our interest in the synthesis of bioactive iminosugars and in the rationalizing of multivalent effect indeed, we chose two kind of iminosugar (a piperidine and a pyrrolidine derivatives, **79** and **80**, figure 3.11) on the basis of the final enzymatic targets. The two azido derivatives were synthetized starting from intermediates **73** and **30**, obtained from natural carbohydrates D-mannose and D-arabinose respectively.

_____

[93] Mirabella S., D'Adamio G., Matassini C., Goti A., Delgado S., Gimeno A., Robina I., Moreno-Vargas A. J., Sestak S., Jimenez-Barbero J., Cardona F., *Chem. Eur. J.*, **2017**, *23*, 14585 – 14596.
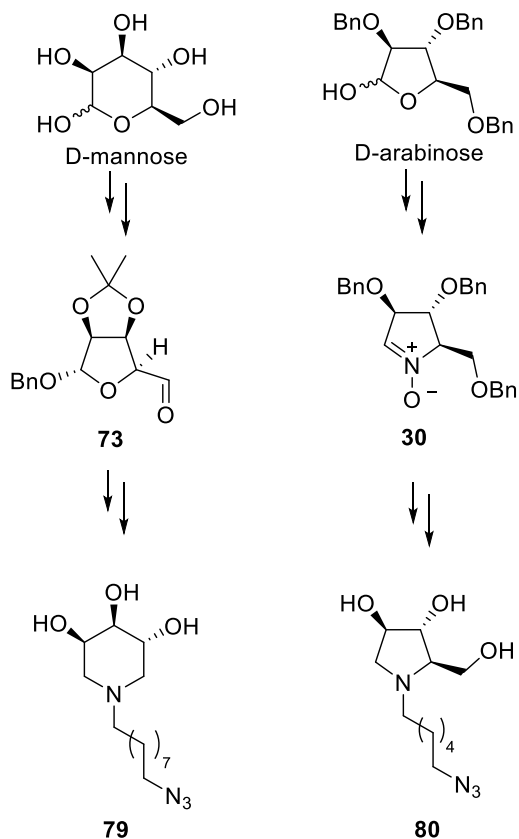
Figure 3.11: Piperidine and pyrrolidine azido derivatives multimerized.

The chapter on Multivalency can be divided in two main parts: the first describes our approach to design multivalent architectures based on the use of click chemistry reaction CuAAC. This synthetic strategy is an ultra-fast and very versatile procedure that allows to achieve a convergent and rapid valency increasing of a bioactive unit. On the other hand, it presents a disadvantage, given by the possible copper complexation by triazole rings and other N atoms that can contaminate the final product with the consequent cytotoxicity. For this reason, we considered alternative methods to avoid the use of copper during the multimerization step. They will be the object of the second part of chapter 3.

3.2 Dendrimeric architectures trough CuAAC

3.2.1 Dendrimers

The copper(I)-catalyzed azide-alkyne cycloaddition (CuAAC), described for the first time by Sharpless and Meldal,[63] has been largely employed for the synthesis of multivalent compounds, due to its efficiency and versatility. Indeed, it allows the conjugation of a great numbers of azide-functionalized moieties on a single alkyl-armed multivalent scaffold with high yields and reduced reaction time. In this PhD thesis the preparation of a library of new multivalent piperidine compounds, by using different monovalent and dendrimeric alkyne scaffolds, is reported. The choice of the 'bioactive warhead' to be multimerized arise from the search of new potent inhibitors of the enzyme GCase. Moreover, following our goal to develop novel pharmacological chaperones to be used in the treatment of LSDs (Gaucher disease in this case), the first step to assess the affinity of our new molecules towards human GCase, is to evaluate their inhibitory activity against the target enzyme in cell lysate. Compounds showing IC_{50} in the micromolar range will be further investigated in '*in vivo*' experiments.
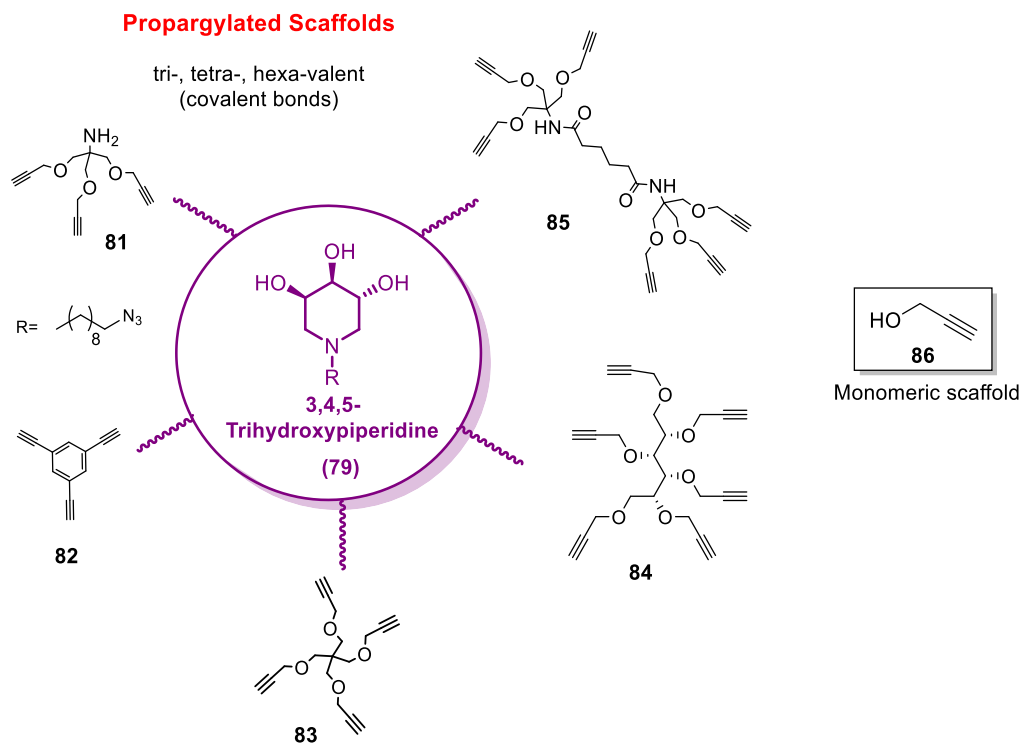
Figure 3.12: Proparglylated multimeric and monomeric dendritic scaffolds.

We chose the azido derivative **79**, a trihydroxypiperidine *N*-alkylated with a 9-carbon chain, encouraged by very promising results in terms of inhibition and rescue of residual GCase activity, obtained with compound **17**, that contains the same piperidine skeleton and a 8-carbon chain on endocyclic nitrogen.[32] In the search of the best valency to achieve our final goal, we explored dendrimeric alkynyl scaffold, differently branched, onto which multimerize piperidine derivative **79**.

To our support in the evaluation of the MVE of our dendrimers bearing the piperidine iminosugar moiety, the promising results in term of multivalency in previous works.[47,93] Indeed, the same piperidine bioactive core was exploited in the synthesis of multivalent architectures (**76** and **77**, figure 3.8). In that case a short alkyl chain (3 carbon atoms) was used as spacer between the scaffold and the iminosugar moiety. The resulting multivalent compounds were tested against a panel of eleven commercially available glycosidases, showing promising results in terms of inhibition towards amyloglucosidase. With the intention to expand our target to the human lysosomal enzyme GCase, we decide to elongate the length of alkyl linker, because of the excellent inhibitory activity obtained in the case of compound **17** that bears an 8-carbon chain on endocyclic nitrogen atom.

Moreover, it also showed a 1.25-fold rescue of GCase activity, thus indicating a very interesting chaperoning potential.

3.2.1.1 Results and discussion

The intermediate *N*-alkylated trihydroxypiperidine was synthesized exploiting a well-known strategy reported in our research group, that allows to achieve the 'masked' aldehyde intermediate **73**, easily synthesized in four steps and 80% overall yield from D-mannose without the need of any chromatographic purification, by following a slight modification of the published procedure[94] (scheme 3.1).
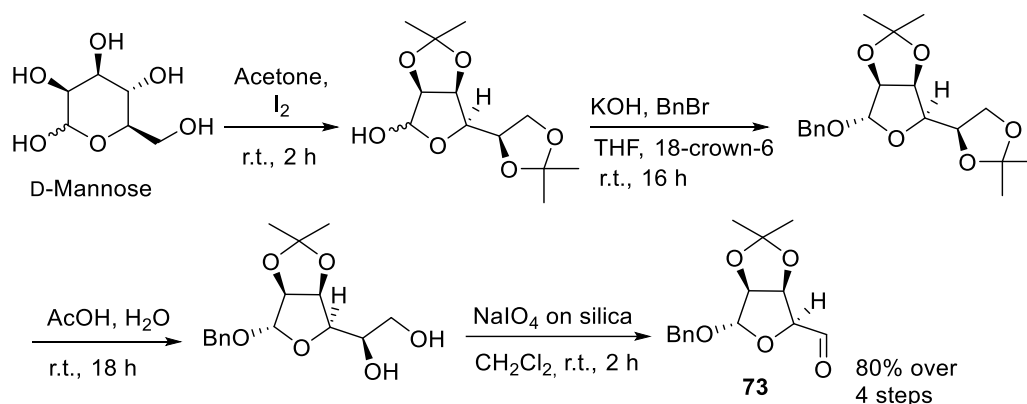
Scheme 3.1: Synthesis of 'masked' dialdehyde **73** from D-mannose.

To get the piperidine skeleton we exploited the DRA (*Double Reductive Amination*)[91] on the intermediate **73**, with benzylamine and H_2 as a reducing agent in the presence of $Pd(OH)_2$ as catalyst (Scheme 3.2).
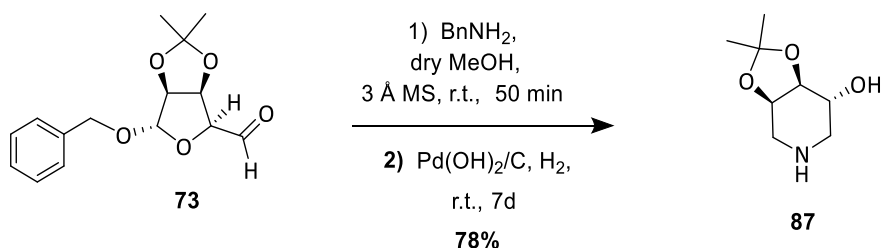

Scheme 3.2: DRA on intermediate **73**.

Compound **73** was solubilized in dry MeOH in the presence of activated 3Å MS molecular sieves, then reacted with an equivalent of benzylamine for 50 minutes at room temperature under N_2 atmosphere. The corresponding formed imine was reduced with H_2

_____

[94] Chen F.-E., Zhao J.-F., Xiong F.-J., Xie B., Zhang P., *Carbohydr. Res.* **2007**, *342*, 2461–2464.

in presence of Pd(OH)$_2$/C as catalyst. After 7 days, piperidine **87** is formed and purified trough flesh column chromatography (FCC).
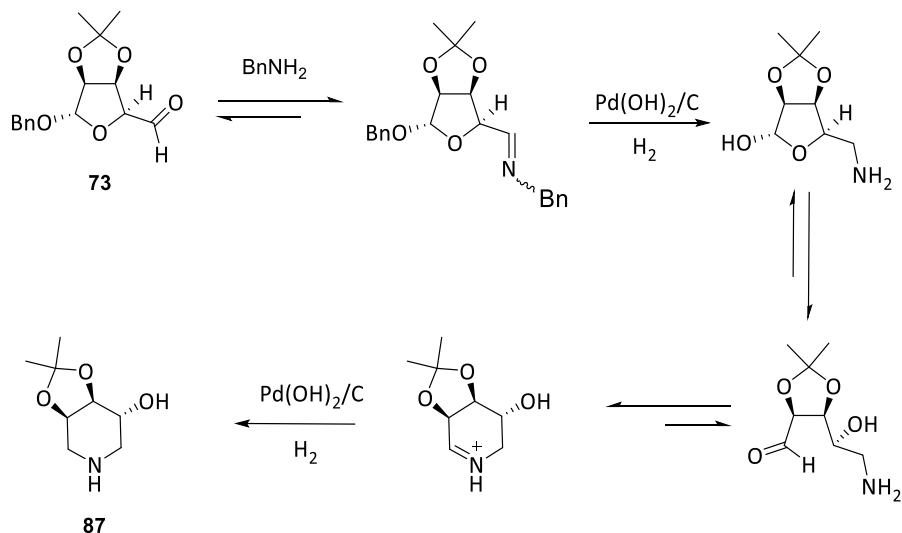
Scheme 3.3: Hypothesized mechanism of piperidine formation.

We hypothesize the reaction mechanism reported in scheme 3.3, in which, after the first nucleophilic attack performed by benzylamine and the consequent Schiff base formation with water elimination (from here the necessity to use molecular sieves in the reaction mixture), the reduction with H$_2$ in presence of palladium hydroxide as catalyst produces an intermediate that is in equilibrium with his opened form. This specie undergoes in this way nucleophilic attack from the nitrogen atom of the primary amine formed (scheme 3.3).

With piperidine skeleton in hands, to introduce the azido moiety on the piperidine scaffold, we resumed our recently developed straightforward synthetic strategy to access *N*-functionalized pyrrolidine,[45b] trying to apply the same method to our piperidine (scheme 3.4).
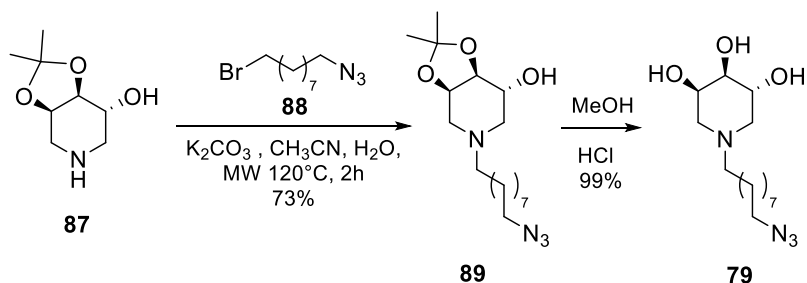
Scheme 3.4: Alkylation of piperidine **87**.

_____

Compound **87** indeed, was reacted with bromo-azido alkyl chain **88** in CH_3CN/H_2O in the presence of K_2CO_3 under MW irradiation at 120°C to yield azide **89** (73%), that was then deprotected in acidic conditions in MeOH, affording the free-hydroxyl group piperidine **79** (99%), necessary to build up the multimeric structures.

We chose a series of propargylated scaffolds with various geometry and number of alkyne moieties, from tri-, tetra- and hexavalents (Figure 3.12), in turn obtained by propargylation of the corresponding alcohols. The trivalent aliphatic scaffold **81** was synthesized from commercial TRIS (hydroxymethylaminomethane), following a reported procedure,[95] while the aromatic trivalent **82** is a commercially available product.

The tetravalent scaffold **83** was prepared by propargylation of the commercial pentaerytritol, as previously reported, as well as hexavalent **85,** obtained by coupling adipic acid with tris[(propargyloxy)methyl]aminomethane **81**.[89] Hexavalent **84** was achieved by propargylation reaction (figure 3.13).[96]

_____

[95] Chabre Y. M., Contino-Pépin C., Placide V., Shiao T. C., Roy R., *J. Org. Chem.* **2008**, *73*, 5602-5605.

[96] Perez-Balderas F., Morales-Sanfrutos J., Hernandez-Mateo F., Isac-García J., Santoyo-Gonzalez F., *Eur. J. Org. Chem.* **2009**, 2441–2453.
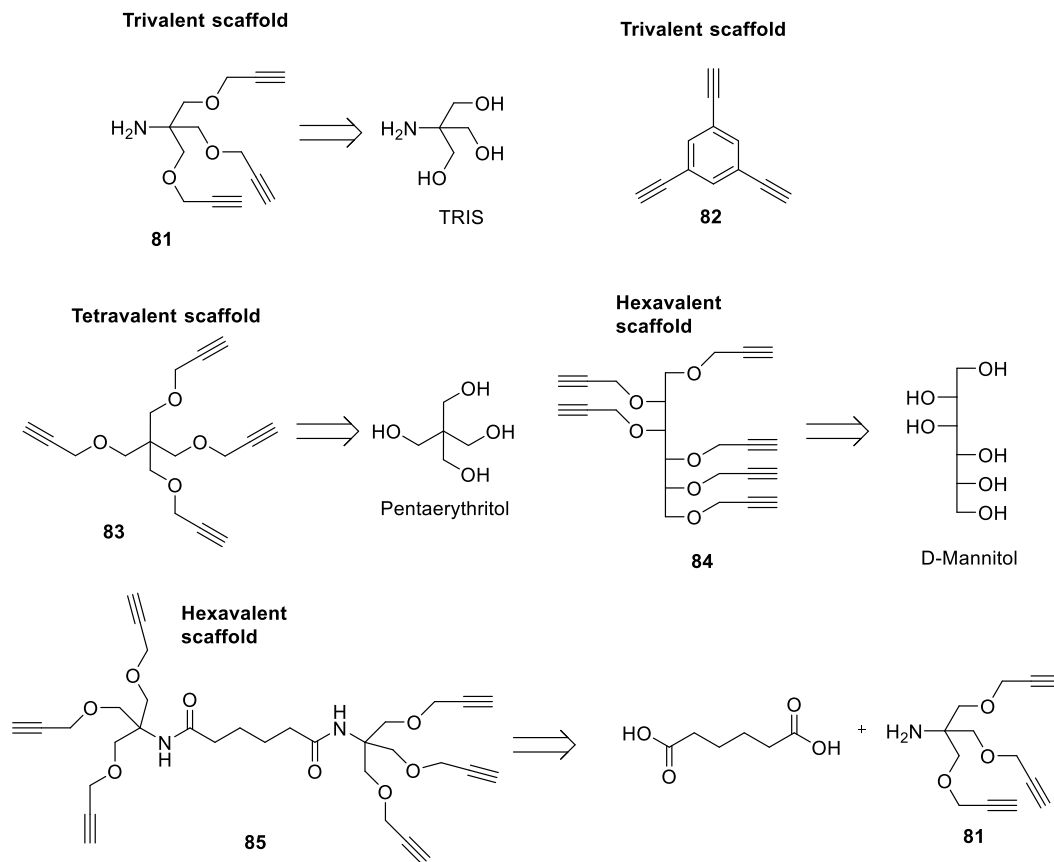
Figure 3.13: Retrosynthesis of the trivalent, tetravalent and hexavalent scaffolds.

To 'click' derivative **79** to the different scaffolds, we asked if it could be better use compound **89**, perform the CuAAC and deprotect the final multivalent once grafted the bioactive unit, or directly react **79** with propargylated scaffolds avoiding the deprotection step on a very big structure such as a multivalent dendrimer. On the basis of previous works,[90] in which the purification procedure resulted much less efficient with such a hydrophilic multivalent adducts with respect to several deprotected monovalent compounds synthesized, we directly applied the strategy a) reported in Scheme 3.5, avoiding in this way all the problems related to the isolation of free amines that we would recover from the DOWEX resin. Indeed, after the requested acidic condition in the deprotection for multivalents bearing protected piperidines, they would have been obtained as hydrochloride salts, therefore needing a treatment with an ion-exchange resin.

_____
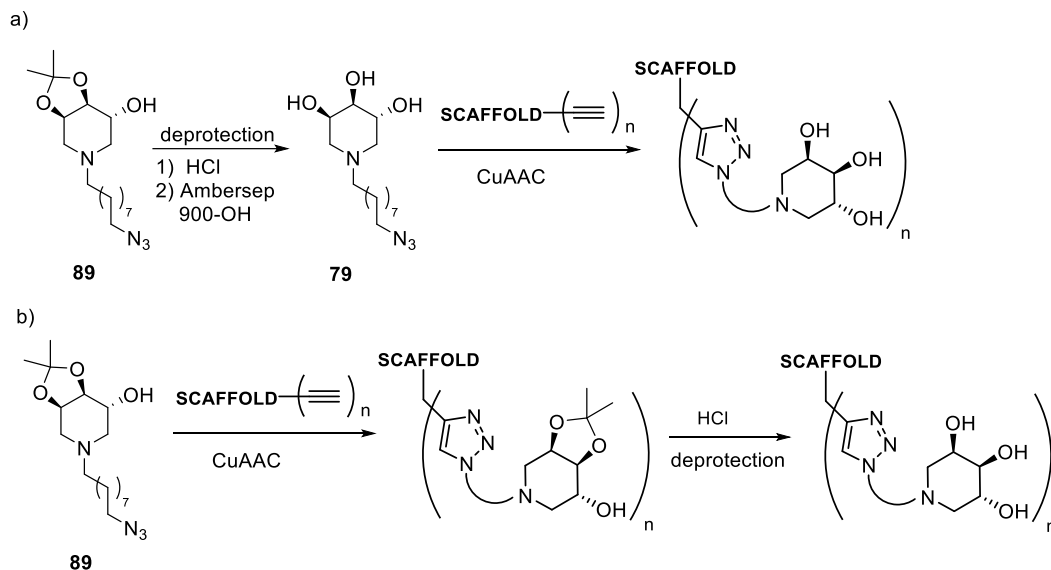
Scheme 3.5: Two investigated routes for the synthesis of multivalent compounds.

Following the first route (a, scheme 3.5), CuAAC reactions of the azido derivative **79** (always n.1 equivalent with respect to each alkynyl moieties number) with the scaffolds previously described were performed: trivalent compounds **81** (Scheme 3.6) and **82** (Scheme 3.7), tetravalent **83** (Scheme 3.8) and hexavalent **84** (Scheme 3.9) and **85** (scheme 3.10), following the same reaction conditions. A catalytic amount of CuSO$_4$, sodium ascorbate, in THF/H$_2$O =2: 1, under MW irradiation at 80 °C for 45 minutes afforded the multivalent compounds **90**-**94** that were first treated with a copper-scavenger resin (QuadraSil® MP resin, 1.0/1.5 mmol/g metal/resin loading) in order to remove every possible residual copper trace, and finally purified through exclusion size chromatography (SEC), using Sephadex LH-20.
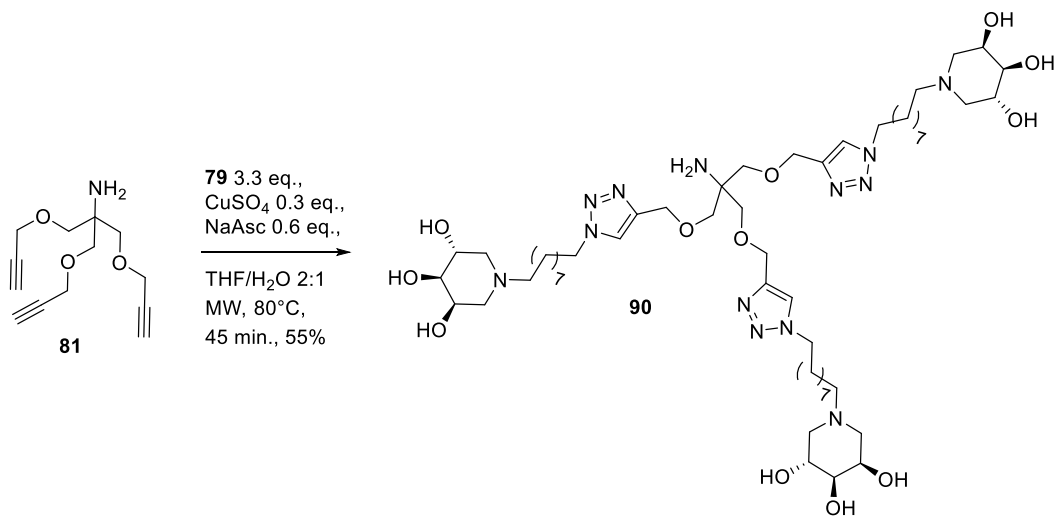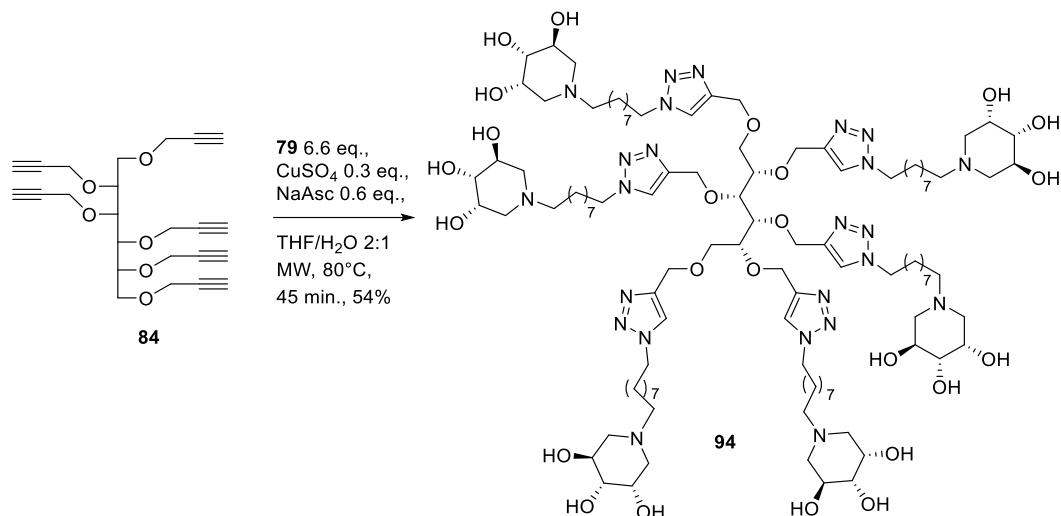
Scheme 3.6: Synthesis of trivalent piperidine **90**.
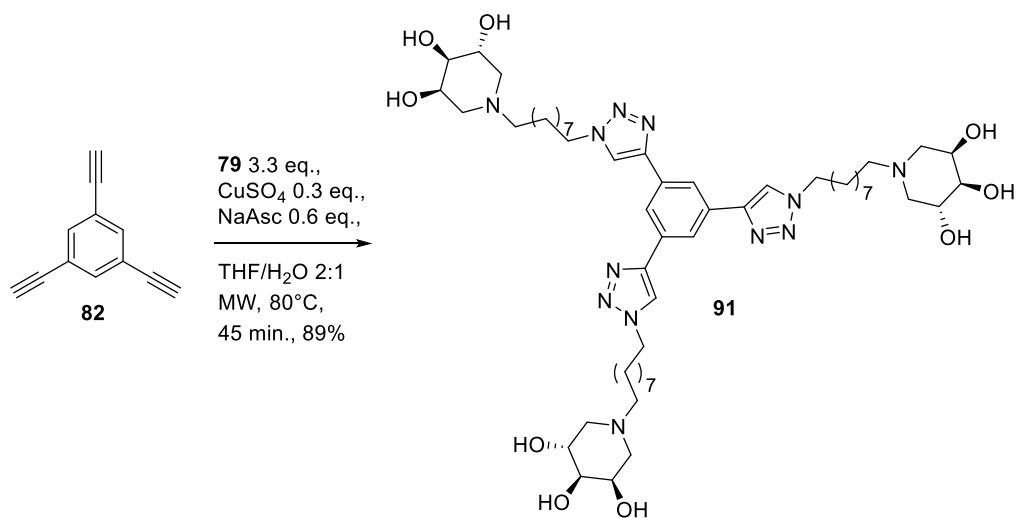
Scheme 3.7: Synthesis of trivalent piperidine **91**.

73
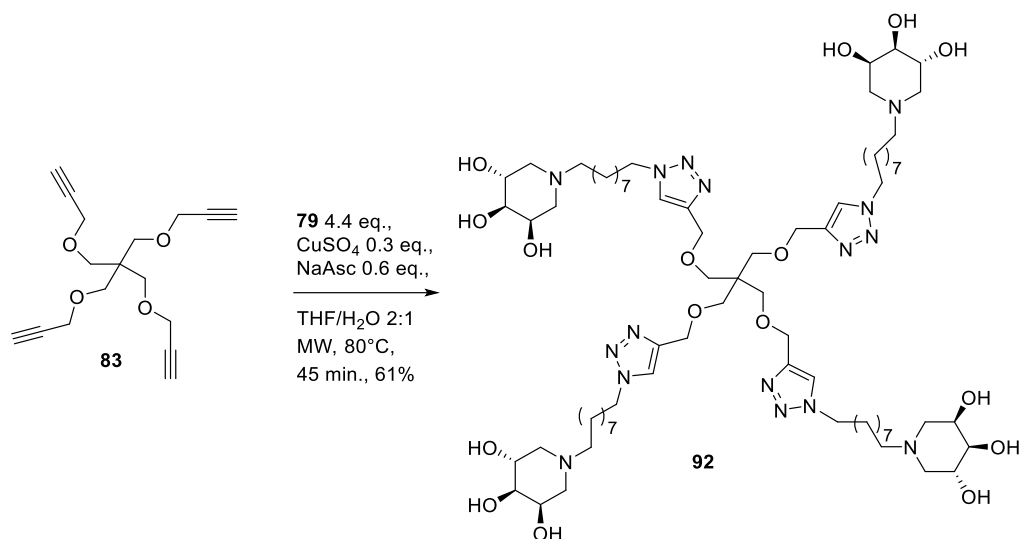
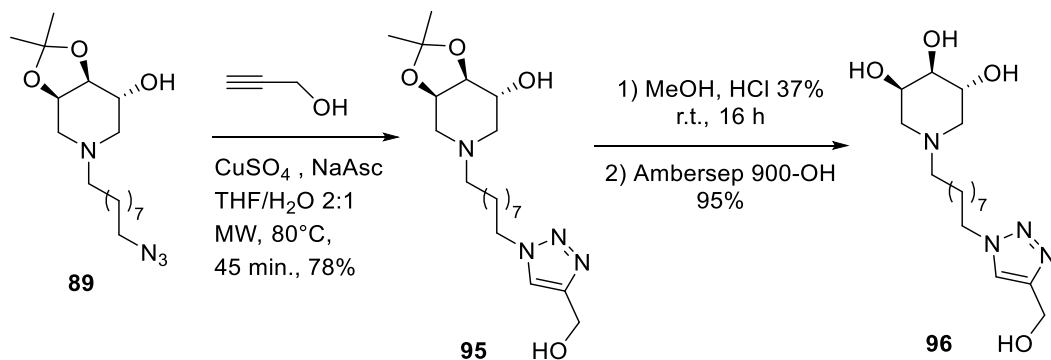**Scheme 3.8**: Synthesis of tetravalent piperidine **92**.
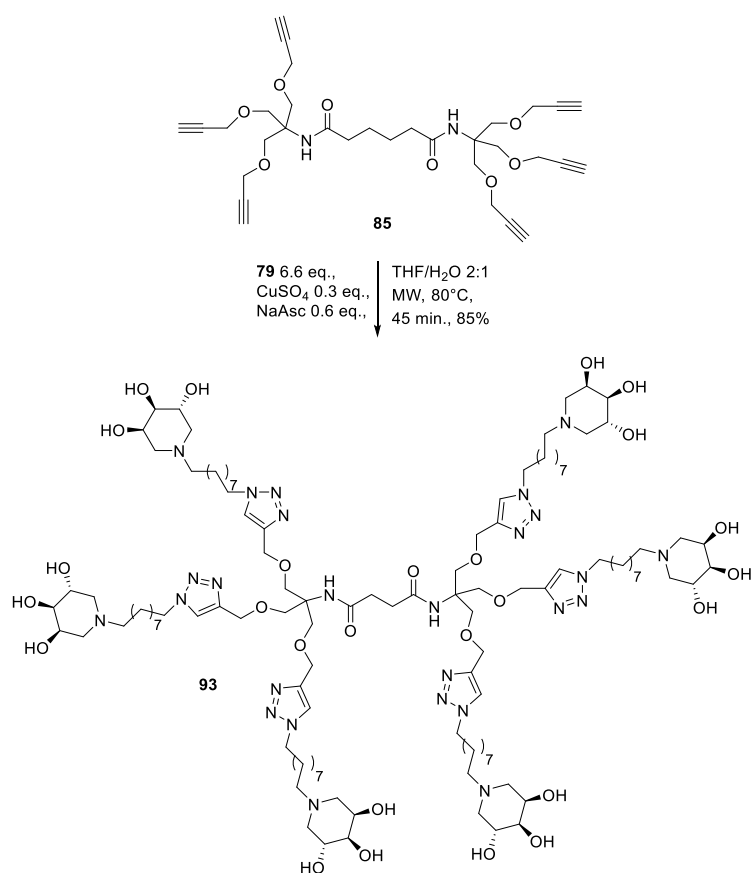
Scheme 3.9: Synthesis of hexavalent piperidine **93**.

Scheme 3.10: Synthesis of trivalent piperidine **94**.

To evaluate the relative inhibitory activity enhancement of these new multimeric systems, giving in this way a quantification of the MVE (by calculating the *rp*/n), a proper monovalent counterpart was also synthesized. In particular, starting from azido-hydroxypiperidine **89**, the CuAAC reaction was performed with propargylalchol in the presence of CuSO₄/sodium ascorbate in THF/H2O = 2:1 at 80°C for 45 minutes, affording adduct **95** in 78% yield (Scheme 3.11). Final deprotection with MeOH/HCl and treatment with strongly basic resin Ambersep 900-OH, afforded the monovalent compound **96** in 95% yield.

Scheme 3.11: Synthesis of reference monovalent compound **94**.

3.2.1.2 Biological evaluation

Preliminary biological evaluation of all the new multivalent piperidines was carried out by measuring their inhibitory activity. All the multivalent compounds **90**-**94** as well as the corresponding monovalent iminosugar **96**, were evaluated towards human GCase enzyme, thanks to a collaboration with Prof. Morrone (Meyer's Children Hospital, Firenze). The compounds were screened in extracts from a pool of human leukocytes isolated from healthy donors (1 mM concentration of inhibitor, 37 °C and optimal pH conditions, see experimental section 3.2.1.4).
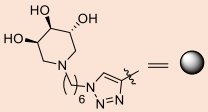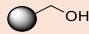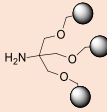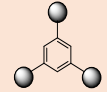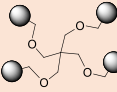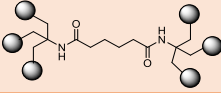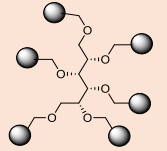
	n.	Valency	% Inhibition (1 mM)	IC_{50} (µM)	rp	rp/n
	96	1	69	500 ± 50	-	-
	90	3	100	27 ± 3	19	6
	91	3	100	7 ± 1	71	24
	92	4	100	9 ± 4	56	14
	93	6	100	11 ± 3	45	8
	94	6	80	6 ± 1	83	14

Table 3.1: Inhibitory activities of multivalent piperidine iminosugars **90**, **91**, **92**, **93** and **94**, with monovalent reference compound **96**, towards GCase β-glucocerebrosidase. Percentages of inhibition at 1mM of inhibitor and IC_{50} [µM] were reported. Relative potency (*rp*) and relative potency per active moiety (*rp*/n) of the tri-, tetra- and hexavalent piperidine **90**, **91**, **92**, **93** and **94** toward GCase.

The results are summarized in Table 3.1, where the inhibition of the monovalent piperidine **96** is also reported for sake of completeness. This one showed around 70% inhibition of GCase, while all the new multivalent piperidines inhibited the enzyme with percentages higher than 80%, suggesting that the simultaneous presentation of the active 2,3,4-trihydroxypiperidine in a multimeric fashion leads to an enhancement of biological activity. As a matter of fact, IC_{50} value for monovalent **96** is higher than those of **90**-**94** which are in the low micromolar range, demonstrating that multivalent inhibitors are more potent than monovalent ones. The best inhibitor of the series is **94**, showing an IC_{50} of 6 μM.

To have a proof of concept about the potentiality of multivalent effect, we calculated the relative potency for all derivatives (*rp*, calculated as the IC_{50} ratio of the reference compound versus that of the corresponding multivalent compounds) that ranges from 19 to 83, suggesting that the inhibitory activity enhancement is not simply due to a concentration effect. Moreover, a positive multivalent effect occurs in all cases (rp/n> 1, where n is the compound valency), in particular the best result is observed with compound **91**, for which a rp/n of 24 was calculated. Following our final goal to apply our iminosugars in the chaperoning activities, we performed chaperoning activity tests for the compounds showing the best values in term of inhibition and IC_{50}. The ability of the multivalent trihydroxypiperidines **91**, **92** and **93** to enhance the activity of GCase was so assayed in human fibroblasts derived from Gaucher patients bearing the N370/RecNcil mutation (table 3.2).

Compound	Inhibition (at 1mM)	IC_{50}	Rescue of GCase activity
91	100	7 ± 1	1.21 at 10 μM
92	100	9 ± 4	1.26 at 10 μM
93	100	11 ± 3	1.21 at 50 μM

Table 3.2: Chaperoning activity assays.

Interestingly, all new compounds showed a moderate increase in GCase activity (around 1.2-fold), after incubation (4 days) with mutated fibroblasts, encouraging us in using multivalent architectures to design new inhibitors to be applied also as pharmacological chaperones. With reference to previous work,[32] where compound **17** (figure 1.15), that bears an 8 atom carbon chain, showed an 1.25-fold GCase enhancement activity at 100 μM concentration, we have improved the chaperoning activity, demonstrating that there is actually an advantage in the multimerization of the bioactive trihydroxypiperidine. Indeed, the GCase activity rescue in this case is obtained at a concentration 10 fold lower.

3.2.1.3 Conclusions

As introduced in the first part of section 3.2, our goal was to evaluate the biological activity of the new multivalent systems against human GCase enzyme, to find new selective inhibitors and, possibly, new pharmacological chaperones to use in the treatment of Gaucher disease. Moreover, we wanted also to define their multivalent potency in terms of *rp*/n in order to verify if an advantage in synthetizing multivalent compounds effectively exists. The synthesis of this small library of multivalent derivatives, including also the monovalent reference compound, was efficiently carried out by multimerizing our iminosugar onto different branched scaffolds through the CuAAC strategy, that allowded us to obtain multivalent 3,4,5-trihydroxypiperidines with a different degree of functionalized 'bioactive arms'. Biological assays finally gave us promising results both in terms of inhibition and of chaperoning activity, with the best inhibitor/chaperone in the trivalent aromatic compound **91**, that additionally shows the best value of *rp*/n revealing itself as the best multivalent iminosugar of the series.

3.2.1.4 Experimental section

For the general details see paragraph 2.4.

Synthesis of piperidine 89: A solution of **87** (63 mg, 0.36 mmol), 1-azido-6-bromohexane (**88**, 135 mg, 0.55 mmol) and K_2CO_3 (75 mg, 0.55 mmol) in 2.4 ml of a mixture CH_3CN/H_2O 5:1 was stirred in microwave at 120°C for 2 h, until a TLC analysis (CH_2Cl_2:MeOH:NH_3 6:1:0.1) showed the disappearance of the starting material (*R*f = 0.00) and the formation of a new product (*R*f = 0.45). After filtration through Celite®, the solvent was removed under reduced pressure and the crude was purified by FCC (EtOAc: PE from 1:1 to 2:1) affording pure **89** (*R*f = 0.18, 89 mg, 0.26 mmol, 73% yield) as a yellow oil. **[α]$_{21}^{D}$**= −30.7 (c = 0.79 in MeOH); **^{1}H-NMR** (400 MHz, CD_3OD): δ= 4.30 (dd, *J* = 8.3, 3.8 Hz, 1H, H-5), 3.89-3.77 (m, 2H, H-3, H-4), 3.29 (t, *J* = 6.8 Hz, 2H, H-1'), 3.04 (d, *J* = 13.1 Hz, 1H, Ha-6), 2.76 (*p*dd, *J* = 12.0, 4.0 Hz, 1H, Ha-2), 2.44 (dd, *J* = 13.3, 3.9 Hz, 1H, Hb-6), 2.39 (dd, *J* = 7.8, 2.7 Hz, 2H, H-9'), 2.02 (dd, *J* = 11.4, 9.0 Hz, 1H, Hb-2), 1.62-1.51 (m, 6H, CH_3), 1.36 (bs, 14H, from H-2' to H-8') ppm; **^{13}C-NMR** (50 MHz, CD_3OD): δ= 110.1 (s, O$\underline{C}$(CH_3)$_2$), 80.2 (d, C-4), 74.5 (d, C-3), 70.4 (d, C-5), 59.2 (t, C-9'), 57.7 (t, C-6), 55.1 (t, C-2), 52.4 (t, C-1'), 30.5-27.8 (t, 7C from C-2' to C-8'), 27.5-26.6 (q, 2C, OC($\underline{C}H_3$)$_2$) ppm; **IR** (CD_3OD): ν = 3022, 2989, 2934, 2856, 2098, 1470, 1383, 1225, 1059 cm^{-1}. **MS (ESI)**: *m/z* calcd (%) for $C_{17}H_{32}N_4O_3$ 340.25; found: 341.25 (100%, [M+ H]$^{+}$), 363.25 (71%, [M+ Na]$^{+}$).

Synthesis of piperidine 79: To a solution of **89** (152 mg, 0.45 mmol) in 18 mL of methanol, 20 drops of 37% HCl were added and the mixture was stirred at room temperature for 18 hours. After that a TLC analysis (CH$_2$Cl$_2$:MeOH 20:1) showed disappearance of the starting material (Rf = 0.44), the solvent was removed under reduced pressure. The crude was purified by FCC (CH$_2$Cl$_2$:MeOH:NH$_3$ from 10:1:0.1 to 6:1:0.1) affording pure **79** (Rf = 0.19, 132 mg, 0.44 mmol, 99% yield) as a colourless oil. **[α]$_{26}$^{D}**= −21.6 (c = 1.02 in MeOH); **^{1}H-NMR** (400 MHz, CD$_3$OD): δ= 3.91 (q, J = 5.8 Hz, 1H, H-3), 3.80 (td, J = 7.9, 4.0 Hz, 1H, H-5), 3.42-3.39 (m, 1H, H-4), 3.29 (t, J = 6.8 Hz, 2H, H-1'), 2.84-2.76 (m, 2H, Ha-6, Ha-2), 2.44-2.32 (m, 2H, Hb-6, Hb-2), 2.29 (d, J = 12.1 Hz, 1H, Ha-9'), 2.15-2.06 (m, 1H, Hb-9'), 1.64-1.57 (m, 2H, H-2'), 1.54-1.51 (m, 2H, H-8'), 1.35 (bs, 10H, from H-3' to H-7') ppm; **^{13}C-NMR** (50 MHz, CD$_3$OD): δ= 75.3 (d, C-4), 69.6 (d, C-5), 69.1 (d, C-3), 59.3 (t, C-9'), 58.2 (t, C-2), 57.6 (t, C-6), 52.4 (t, C-1'), 30.5-27.5 (t, 7C, from C-2' to C-8') ppm; **IR** (CD$_3$OD): ν = 3690, 3585, 3429, 2932, 2856, 2817, 2098, 1469, 1068 cm^{-1}. **MS (ESI)**: m/z calcd (%) for C$_{14}$H$_{28}$N$_4$O$_3$ 300.22; found: 301.33 (100%, [M+ H]$^+$). **Elemental analysis:** C$_{14}$H$_{28}$N$_4$O$_3$ (300.40) calcd. C, 55.98; H, 9.40; N, 18.65; found C, 56.02; H, 9.32, N, 18.55.

Synthesis of protected monovalent piperidine 95: To a solution of **89** (85 mg, 0.250 mmol) in 3 ml of a 2:1 THF:H$_2$O mixture were added CuSO$_4$ (30 mol%), sodium ascorbate (60 mol%) and propargyl alcohol (1 equiv.). The reaction mixture was stirred in a MW reactor at 80 °C for 45 min until TLC analysis (DCM: MeOH 10:1) showed the disappearance of the starting material (Rf = 0.59) and formation of a new product (Rf = 0.00). After filtration through Celite®, the solvent was removed under reduced pressure and the crude was first treated with Quadrasil® MP resin then purified by FCC (CH$_2$Cl$_2$:MeOH:NH$_3$ from 30:1:0.1 to 6:1:0.1) affording pure **95** (Rf = 0.26, 77 mg, 0.19 mmol, 78% yield) as a colourless oil. **[α]$_{25}$^{D}**= + 11.5 (c = 0.90 in CHCl$_3$); **^{1}H-NMR** (400 MHz, CDCl$_3$): δ= 7.51 (s, 1H, H triazole), 4.76 (s, 2H, CH$_2$OH Ar), 4.31 (td, J = 7.1, 2.5 Hz, 2H, H-9'), 4.28-4.26 (m, 1H, H-5), 4.04-4.01 (m, 1H, H-3), 3.95-3.92 (m, 1H, H-3), 3.27 (bs, 1H, OH), 2.72-2.68 (m, 1H, Ha-6), 2.56 (d, J = 11.7 Hz, 1H, Ha-2), 2.44 (d, J = 11.1 Hz, 1H, Hb-2), 2.39 (dd, J = 12.0, 3.2 Hz, 1H, Hb-6), 2.35-2.31 (m, 2H, H-1'), 1.92-1.81 (m, 2H, H-8'), 1.48 (s, 3H, CH$_3$), 1.45-1.37 (m, 2H, H-2'), 1.34 (s, 3H, CH$_3$), 1.28-1.24 (m, 10H, from H-3' to H-7') ppm; **^{13}C-NMR** (50 MHz, CDCl$_3$): δ= 147.9 (s, $\underline{C}$-CH$_2$OH Ar), 121.6 (d, $\underline{C}$H triazole), 109.5 (s, O$\underline{C}$(CH$_3$)$_2$), 76.6 (d, C-4), 72.3 (d, C-5), 67.8 (d, C-3), 57.9 (t, C-1'), 56.7 (t, Ar-$\underline{C}$H$_2$OH), 56.0 (t, C-2), 55.7 (t, C-6), 50.5 (t, C-9'), 30.4 (t, C-8') 29.9-27.4 (t, 6C, from C-2' to C-7') 26.9-26.5 (q, 2C, OC($\underline{C}$H$_3$)$_2$) ppm; **IR** (CDCl$_3$): ν = 3669, 3406, 3005, 2934, 2859, 2361, 1464, 1379, 1142, 1057, 926 cm^{-1}. **MS (ESI)**: m/z calcd (%) for C$_{20}$H$_{36}$N$_4$O$_4$ 396.27; found: 397.53 (100%, [M+ H]$^+$).

Synthesis of deprotected monovalent piperidine 96: To a solution of **95** (73 mg, 0.18 mmol) in 8 mL of methanol, 15 drops of 37% HCl were added and the mixture was stirred at room temperature for 18 hours. After that a TLC analysis (CH$_2$Cl$_2$:MeOH 10:1) showed disappearance of the starting material (Rf = 0.59), the solvent was removed under reduced pressure. The product, obtained as hydrochloric salt, was then treated with the

strongly basic resin Ambersep 900-OH to afford the final product **96** (62 mg, 0.18 mmol, 95% yield) as a colourless oil. $[α]_{27}^D$= - 18.0 (c = 0.94 in CH_3OH); **^{1}H-NMR** (400 MHz, CD_3OD): δ= 7.90 (s, 1H, H triazole), 4.68 (s, 2H, CH_2OH Ar), 4.39 (t, *J* = 6.4 Hz, 2H, H-9'), 3.90-3.89 (m, 1H, H-3), 3.81-3.77 (m, 1H, H-5), 3.40-3.39 (m, 1H, H-4), 2.80-2.69 (m, 2H, Ha-6, Ha-2), 2.37-2.32 (m, 2H, H-1'), 2.26 (d, *J* = 11.0 Hz, 1H, Hb-2), 2.14-1.99 (m, 1H, Hb-6), 1.91-1.88 (m, 2H, H-8'), 1.51-1.48 (m, 2H, H-2'), 1.31 (bs, 10H, from H-3' to H-7') ppm; **^{13}C-NMR** (50 MHz, CD_3OD): δ= 148.8 (s, <u>C</u>-CH_2OH Ar), 123.8 (d, <u>C</u>H triazole), 75.1 (d, C-4), 69.3 (d, C-5), 68.9 (d, C-3), 59.1 (t, C-1'), 58.0 (t, C-2), 57.4 (t, C-6), 56.3 (t, Ar-<u>C</u>H_2OH), 51.1 (t, C-9'), 31.1 (t, C-8') 30.3-27.3 (t, 5C, from C-3' to C-7') 27.7 (t, C-2') ppm; **MS (ESI)**: *m/z* calcd (%) for $C_{17}H_{32}N_4O_4$ 356.24; found: 379.52 (43%, [M+ Na]$^+$), 357.52 (100%, [M+ H]$^+$). **Elemental analysis:** $C_{17}H_{32}N_4O_4$ (356.47) calcd. C, 57.28; H, 9.05; N, 15.72; found C, 57.35; H, 8.99, N, 15.59.

General procedure for CuAAC reaction to synthesize multivalent compounds: To a solution of **79** in a 2:1 THF:H_2O mixture were added $CuSO_4$ (30 mol%), sodium ascorbate (60 mol%) and alkyne **81-85** (1 equiv.). The reaction mixture was stirred in a MW reactor at 80 °C for 45 min until TLC analysis (DCM: MeOH 10:1) showed the disappearance of the starting material (*R*f = 0.21) and formation of the desired product. After filtration through Celite®, the solvent was removed under reduced pressure and the crude was first treated with Quadrasil® MP resin then purified through SEC (with Sephadex LH-20) to obtain the multivalent adducts **90-94**. In the table below (table 3.3) are reported the piperidine **79** equivalents required for each multivalent compound, with the yields of the final products.

Multivalent compound	Alkynyl scaffold (1eq.)	Piperidine 77 (eq.)	Yield %
90	81	3.3	55
91	82	3.3	89
92	83	4.4	61
93	84	6.6	85
94	85	6.6	54

Table 3.3: Multivalent final compounds with relative reaction conditions and yields.

Aliphatic trivalent 90: Obtained as white waxy solid (47 mg, 0.04 mmol). $[α]_{26}^D$= - 12.3 (c = 1.03 in CH_3OH); **^{1}H-NMR** (400 MHz, CD_3OD): δ= 7.98 (s, 3H, H triazole), 4.59 (bs, 6H, H-β), 4.40 (t, *J* = 7.0 Hz, 6H, H-9'), 3.99-3.95 (m, 3H, H-3), 3.87-3.83 (m, 3H, H-5), 3.55-3.45 (m, 9H, H-4, H-α), 3.35 (s, 2H, NH_2), 2.93-2.86 (m, 6H, Ha-6, Ha-2), 2.55-2.47 (m, 9H, H-1', Hb-2), 2.38-2.28 (m, 3H, Hb-6), 1.94-1.89 (m, 6H, H-8'), 1.56-1.55 (m, 6H, H-2'), 1.33 (bs, 30H, from H-3' to H-7') ppm; **^{13}C-NMR** (50 MHz, CD_3OD): δ= 145.5 (s, 3C, <u>C</u>-Ar triazole), 125.0 (d, 3C, <u>C</u>H triazole), 74.3 (t, 3C, C-α), 71.5 (d, 3C, C-4), 69.1 (d, 3C, C-5), 68.3 (d, 3C, C-3), 65.4 (t, 3C, C-β), 59.0 (t, 3C, C-1'), 57.3 (t, 3C, C-2), 56.8 (t, 3C, C-6), 51.4 (t, 3C, C-9'),

29.9 (t, 3C, C-8') 31.2-27.4 (t, 15C, from C-3' to C-7') 26.9 (t, 3C, C-2') ppm; **MS (ESI)**: *m/z* calcd (%) for $C_{55}H_{101}N_{13}O_{12}$ 1136.47; found: 1159.00 (100, [M+ Na]$^+$), 379.83 (77, [(M/3)+ H]$^+$). **Elemental analysis:** $C_{55}H_{101}N_{13}O_{12}$ (1136.47) calcd. C, 58.13; H, 8.96; N, 16.02; found C, 58.19; H, 9.01, N, 15.89.

Aromatic trivalent 91: Obtained as white waxy solid (48 mg, 0.04 mmol). **[α]$_{26}$^{D}**= - 17.5 (c = 1.02 in CH$_3$OH); **^{1}H-NMR** (400 MHz, CD$_3$OD): δ= 8.46 (s, 3H, H-Ar), 8.29 (s, 3H, H triazole), 4.49 (t, *J* = 7.0 Hz, 6H, H-9'), 3.89 (dd, *J* = 5.5, 2.8 Hz, 3H, H-3), 3.80 (td, *J* = 7.7, 3.9 Hz, 3H, H-5), 3.45-3.38 (m, 3H, H-4), 2.83-2.76 (m, 6H, Ha-6, Ha-2), 2.41-2.33 (m, 6H, H-1'), 2.31-2.28 (m, 3H, Hb-2), 2.18-2.05 (m, 3H, Hb-6), 2.02-1.96 (m, 6H, H-8'), 1.54-1.44 (m, 6H, H-2'), 1.36-1.30 (m, 30H, from H-3' to H-7') ppm; **^{13}C-NMR** (50 MHz, CD$_3$OD): δ= 148.0 (s, 3C, C̲-Ar triazole), 133.4 (s, 3C, C̲-Ar), 123.3 (d, 3C, C̲H-Ar), 122.8 (d, 3C, C̲H triazole), 75.0 (d, 3C, C-4), 69.4 (d, 3C, C-5), 68.8 (d, 3C, C-3), 59.2 (t, 3C, C-1'), 57.9 (t, 3C, C-2), 57.3 (t, 3C, C-6), 51.6 (t, 3C, C-9'), 31.2 (t, 3C, C-8') 30.4-27.5 (t, 15C, from C-3' to C-7') 27.3 (t, 3C, C-2') ppm; **MS (ESI)**: *m/z* calcd (%) for $C_{54}H_{90}N_{12}O_9$ 1050.70; found: 1073.92 (73, [M+ Na]$^+$), 526.58 (100, [(M/2)+ H]$^+$), 351.42 (59, [(M/3)+ H]$^+$). **Elemental analysis:** $C_{54}H_{90}N_{12}O_9$ (1051.37) calcd. C, 61.69; H, 8.63; N, 15.99; found C, 61.45; H, 8.35, N, 16.08.

Tetravalent 92: Obtained as white waxy solid (45 mg, 0.03 mmol). **[α]$_{23}$^{D}**= - 14.9 (c = 0.98 in CH$_3$OH); **^{1}H-NMR** (400 MHz, CD$_3$OD): δ= 7.98 (s, 4H, H triazole), 4.51 (s, 8H, H-β), 4.39 (t, *J* = 7.1 Hz, 8H, H-9'), 3.95 (dd, *J* = 3.9, 1.3 Hz, 4H, H-3), 3.84 (td, *J* = 7.1, 3.7 Hz, 4H, H-5), 3.47-3.44 (m, 12H, H-4, H-α), 2.90-2.83 (m, 8H, Ha-6, Ha-2), 2.51-2.42 (m, 12H, H-1', Hb-2), 2.32-2.23 (m, 4H, Hb-6), 1.94-1.87 (m, 8H, H-8'), 1.60-1.47 (m, 8H, H-2'), 1.32 (bs, 40H, from H-3' to H-7') ppm; **^{13}C-NMR** (50 MHz, CD$_3$OD): δ= 146.2 (s, 4C, C̲-Ar triazole), 124.8 (d, 4C, C̲H triazole), 74.6 (t, 4C, C-α), 70.0 (d, 4C, C-4), 69.3 (d, 4C, C-5), 68.5 (d, 4C, C-3), 65.4 (t, 4C, C-β), 59.1 (t, 4C, C-1'), 57.6 (t, 4C, C-2), 57.0 (t, 4C, C-6), 51.3 (t, 4C, C-9'), 46.5 (t, 4C, C-8') 31.3-27.4 (t, 20C, from C-3' to C-7') 27.1 (t, 4C, C-2') ppm; **MS (ESI)**: *m/z* calcd (%) for $C_{73}H_{132}N_{16}O_{16}$ 1489.00; found: 756.92 (100, [(M+ Na)/2]$^+$). **Elemental analysis:** $C_{73}H_{132}N_{16}O_{16}$ (1489.93) calcd. C, 58.85; H, 8.93; N, 15.04; found C, 58.98; H, 8.78, N, 14.49.

Hexavalent 93: Obtained as white waxy solid (58 mg, 0.02 mmol). **[α]$_{23}$^{D}**= - 16.9 (c = 0.74 in CH$_3$OH); **^{1}H-NMR** (400 MHz, CD$_3$OD): δ= 7.92 (s, 6H, H triazole), 4.51 (s, 12H, H-β), 4.35 (t, *J* = 7.0 Hz, 12H, H-9'), 3.94-3.85 (m, 6H, H-3), 3.82-3.77 (m, 6H, H-5), 3.71 (s, 12H, H-α), 3.46-3.37 (m, 6H, H-4,), 2.83-2.72 (m, 12H, Ha-6, Ha-2), 2.41-2.33 (m, 18H, H-1', Hb-2), 2.25-2.11 (m, 10H, Hb-6, H-10', H-13'), 1.88-1.84 (m, 12H, H-8'), 1.57-1.41 (m, 16H, H-2', H-11', H-12'), 1.28 (bs, 60H, from H-3' to H-7') ppm; **^{13}C-NMR** (100 MHz, CD$_3$OD): δ= 176.1 (s, 2C, C=O), 145.8 (s, 6C, C̲-Ar triazole), 124.9 (d, 6C, C̲H triazole), 74.7 (t, 6C, C-α), 69.3 (d, 6C, C-4), 68.6 (d, 6C, C-5), 65.3 (d, 6C, C-3), 61.3 (d, 2C, C-11', C-12'), 59.2 (t, 6C, C-β), 57.7 (t, 6C, C-2, C-6), 57.2 (t, 6C, C-1'), 51.3 (t, 6C, C-9'), 31.3 (t, 6C, C-8'), 30.5-27.3 (t, 30C, from C-3' to C-7') 26.4 (t, 6C, C-2') ppm; **MS (ESI)**: *m/z* calcd (%) for $C_{116}H_{208}N_{26}O_{26}$

_____

2382.58; found: 1203.60 (100, [(M+ Na)/2]$^+$), (84, [(M/2)+Na]$^+$). **Elemental analysis:** C$_{116}$H$_{208}$N$_{26}$O$_{26}$ (2383.10) calcd. C, 58.46; H, 8.80; N, 15.20; found C, 58.29; H, 8.92, N, 15.46.

Hexavalent 94: Obtained as white waxy solid (64 mg, 0.03 mmol). **[α]$_{23}$^{D}**= - 7.3 (c = 0.95 in CH$_3$OH); **^{1}H-NMR** (400 MHz, CD$_3$OD): δ= 8.07, 8.01, 7.97 (s, 6H, H triazole), 4.76-4.57 (s, 12H, H-β), 4.39 (dd, *J* = 13.0, 6.6 Hz, 12H, H-9'), 4.17-4.05 (m, 6H, H-3), 4.02-3.87 (m, 10H, H-5, H-α), 3.85-3.65 (m, 10H, H-4, H-γ), 3.24-3.06 (m, 12H, Ha-6, Ha-2), 3.05-2.74 (m, 24H, H-1', Hb-2, Hb-6), 1.97-1.77 (m, 12H, H-8'), 1.77-1.75 (m, 12H, H-2'), 1.34-1.31 (m, 60H, from H-3' to H-7') ppm; **^{13}C-NMR** (100 MHz, CD$_3$OD): δ= 146.1 (s, 6C, C-Ar triazole), 125.4 (d, 6C, CH triazole), 72.3 (t, 2C, C-α), 69.9 (d, 6C, C-4), 68.1 (d, 4C, C-γ), 66.4 (d, 6C, C-5), 65.2 (d, 6C, C-3), 63.7 (t, 6C, C-1'), 55.4 (t, 6C, C-2), 55.1 (t, 6C, C-6), 51.3 (t, 6C, C-9'), 31.2 (t, 6C, C-8'), 30.1-27.4 (t, 30C, from C-3' to C-7') 25.6 (t, 6C, C-2') ppm; **MS (ESI)**: *m/z* calcd (%) for C$_{108}$H$_{194}$N$_{24}$O$_{24}$ 2212.47; found: 1107.01 (57, [(M/2)+H]$^+$), 738.54 (100, [(M/3)+H]$^+$), 554 (69, [(M/4)+H]$^+$). **Elemental analysis:** C$_{108}$H$_{194}$N$_{24}$O$_{24}$ (2212.84) calcd. C, 58.62; H, 8.84; N, 15.19; found C, 58.88; H, 8.61, N, 15.25.

Biochemical characterization with human GCase: The compounds were screened towards GCase from leukocytes isolated from healthy donors (controls). Isolated leukocytes were disrupted by sonication, and a micro BCA protein assay kit (Sigma–Aldrich) was used to determine the total protein amount for the enzymatic assay, according to the manufacturer instructions. Enzyme activity was measured in a flat-bottomed 96-well plate. Iminosugar solution (3 μL), 4.29 μg/μL leukocytes homogenate (7 μL), and substrate 4-methylumbelliferyl-β-D-glucoside (3.33 mM, 20 μL, Sigma–Aldrich) in citrate/phosphate buffer (0.1:0.2, M/M, pH 5.8) containing sodium taurocholate (0.3%) and Triton X-100 (0.15%) at 37 °C were incubated for 1 h. The reaction was stopped by addition of sodium carbonate (200 μL; 0.5M, pH 10.7) containing Triton X-100 (0.0025 %), and the fluorescence of 4-methylumbelliferone released by β-glucosidase activity was measured in SpectraMax M2 microplate reader (λex=365 nm, λem=435 nm; Molecular Devices). Percentage GCase inhibition is given with respect to the control (without iminosugar).

IC$_{50}$ determination: The IC$_{50}$ values of inhibitors against GCase were determined by measuring the initial hydrolysis rate with 4-methylumbelliferyl-β-D-glucoside (3.33 mM). Data obtained were fitted to the following equation using the Origin Microcal program.

$$\frac{Vi}{Vo} = \frac{Max - Min}{1 + \left(\dfrac{x}{IC_{50}}\right)^{slope}} + Min$$

where V$_i$/V$_o$, represent the ratio between the activity measured in the presence of the inhibitor (V$_i$) and the activity of the control without the inhibitor (V$_0$), "x" the inhibitor

concentration, Max and Min, the maximal and minimal enzymatic activity observed, respectively.

Chaperoning activity assays

Evaluation of the effect of multimeric iminosugars (90-94) on GCase activity in Gaucher patients' cells: Fibroblasts with the N370S/RecNcil mutation from Gaucher disease patients were obtained from the "Cell line and DNA Biobank from patients affected by Genetic Diseases" (Gaslini Hospital, Genova, Italy). Fibroblasts cells (20 x10^4) were seeded in T25 flasks with DMEM supplemented with fetal bovine serum (10 %), penicillin/streptomycin (1%), and glutamine (1%) and incubated at 37 °C with 5% CO_2 for 24 h. The medium was removed, and fresh medium containing the multimeric iminosugars was added to the cells and left for 4 days. The medium was removed, and the cells were washed with PBS and detached with tripsin to obtain cell pellets, which were washed four times with PBS, frozen and lysed by sonication in water. Enzyme activity was measured as reported above.

3.2.2 Study on the aggregation of trihydroxypiperidines

Due to the biological properties of our trihydroxypiperidines, we wanted to investigate the aggregation behaviour, in aqueous solution, of those inhibitors. Indeed, it was expected that such amphiphilic compounds would form aggregates in solution, at given concentration. Understanding the aggregation state in water could be useful to clarify the mechanisms involved in the formation of enzyme-inhibitor complexes. Our aim was to determine if, at the concentration at which these compounds are biologically active (as inhibitors and/or as pharmacological chaperones) they do form aggregates (therefore presenting themselves as a multivalent dynamic micellar system) or they do not.

To study this aspect, we synthesized piperidine **97** exploiting the DRA reaction already used to achieve the *N*-alkylated piperidine **17** (section 1.2.2) with a shorter carbon chain (figure 3.14). Indeed, by elongating the alkyl chain, we enhanced the differentiation between the polar and lipophilic portion of the molecule.
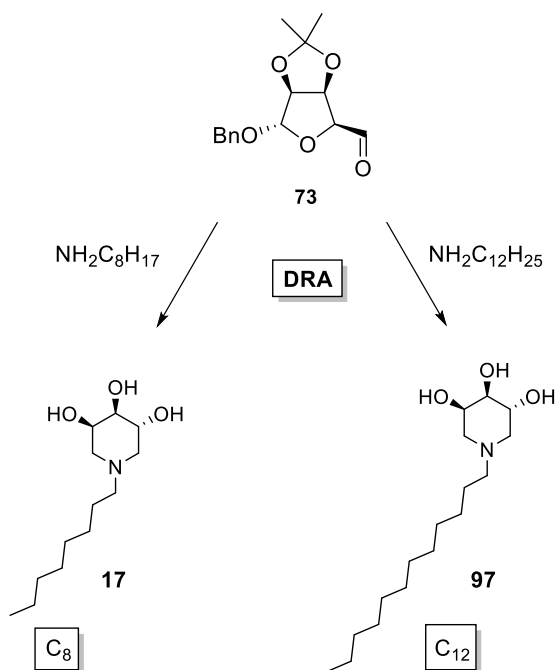

Figure 3.14: Synthetic strategy to obtain piperidine **97**.

Our hypothesis was initially based on the idea that, being the molecule formed by a hydrophilic portion and an apolar chain, and resembling in this way a 'surfactant', once in water there was a sort of a micellar rearrangement of the structures (figure 3.15).
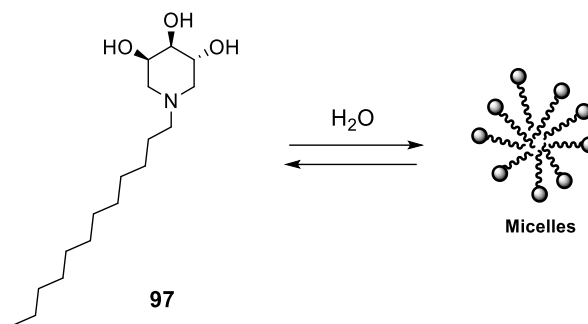
Figure 3.15: Our initial hypothesis: micellar aggregation of piperidine **97**.

To understand the self-assembly of the piperidine amphiphile, we collaborated with Prof. Lo Nostro of the Department of Chemistry of University of Florence, who performed the physico-chemical characterization.

Compound **97** could be treated as a surfactant, due to its amphiphilic nature. Generally, the nature of the polar head of surfactants can be various: neutral, ionic and zwitterionic (figure 3.16).
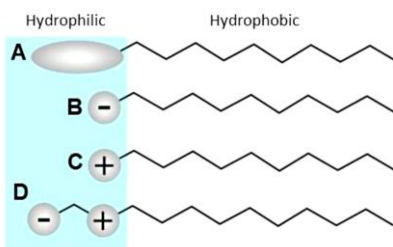

Figure 3.16: Possible forms of polar heads in surfactants: a) neutral; b) anionic; c) cationic; d) zwitterionic

The double nature of the surfactants leads to peculiar behave in aqueous solution, causing a lowering of the surface tension. Indeed, some molecules of the surfactant are placed on the solution surface because of the energetically unfavourable interactions that occur between the alkyl chain of the amphiphile and the water. Increasing the concentration of the amphiphilic compound in solution also increases its amount at the interface, up to the point where the interface is saturated and adsorption is no longer possible; from this point onwards the added surfactant molecules will go into solution leading to an increase in the free energy of the system due to the unfavourable interactions between the surfactant tail and the water, until the so-called "critical micellar concentration" (CMC) is reached. From here, in order to "oppose" the increase in free energy of the system, the surfactant molecules start a process of self-assembly, leading to the formation of micelles (figure 3.17).[97]

---

[97] Moroi Y., Plenum, *J. Dispers. Sci. Technol.*, **1993**, *14 (5)*, 603–604.
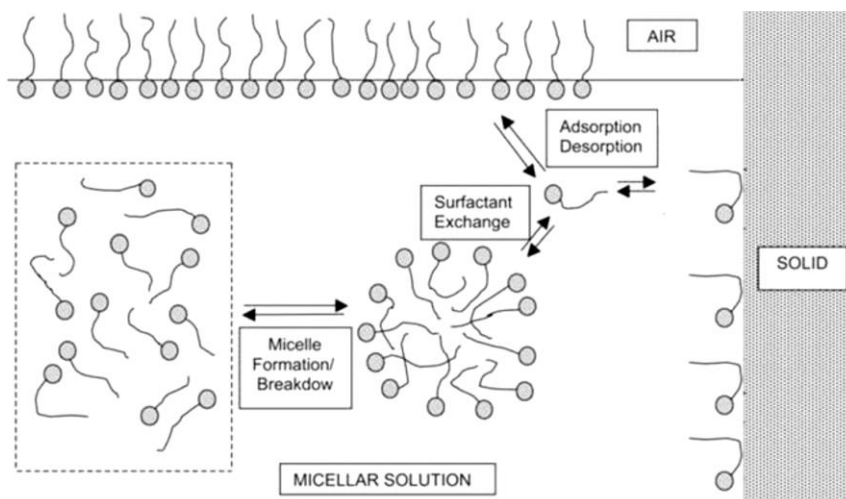
_____

Figure 3.17: Behaviour of a surfactant in aqueous solution.

The process in which single molecules dispersed in a suitable solvent associate themselves to produce complex structures, is called self-assembly and it is caused by the great increase in entropy that occurs after self-association. Moreover, we defined a micellar critical concentration (CMC) the concentration above which the surfactant aggregates, while below the surfactant remains monodisperse in the solvent. Several types of micellar aggregation are known, depending on parameters such as the temperature of the system and the lipophilic chain's length. Once reached the CMC, enhancing surfactant concentration, the micelles can remain spherical or, due to the growth of the volume, aggregate in other types of structures with considerable difference in symmetry with respect to the micellar one, for example assuming a lamellar form.[98] It is possible to predict the type of aggregate that will occur in solution by evaluating the "packing parameter" P, obtained from the following relation: $P = v / a_0 l$, where v and l are respectively the volume and the length of the hydrophobic chain, while a_0 represents the surface occupied by a surfactant in the micelle-water interphase. We have the formation of spherical micelles if $P < 1/3$, while, if the value of $P = 1$ the lamellar aggregation occurs. Once estimated the packaging parameter empirically, SAXS measurements can effectuated for experimentally confirm the hypothesis, then to evaluate the crystalline structures, WAXS and FT-IR data can be recorded. Indeed, by correlating the experimental peaks with some parameters reported in literature,[99] it is possible to understand the type of geometric organization assumed by the crystalline cell. Moreover, performing DSC (Differential Scanning Calorimetry) in the solution (at different concentrations) of the surfactant, we can

_____

[98] Nagarajan R., *Langmuir*., **2002**, *18*, 31-38.

[99] Lo Nostro P., Tempestini E., Bucci M., Mastromartino V., Gori M., Tanini D., Ambrosi M., Fratini M., Capperucci A., *ChemPhysChem.,* **2017**, *18*, 1400–1406.

investigate the interactions between water and amphiphilic substance molecules, understanding the self-assembly in water.

The point was however that: if the micelle formation really occurs, at which piperidine concentration we have it? This is an important issue, because we wanted to understand the aggregation state in the same conditions of the biological tests, and therefore at inhibitory and sub-inhibitory (for the chaperoning activity) concentrations. If our piperidine aggregates in water in a micellar conformation, as we initially theorised, it could be considered as a kind of multivalent system, in which the micelle acts as a piperidine reserve. The main difference with respect to previous dendrimers, is that while they possess a well-defined number of active 'warheads' linked on a common scaffold with covalent bods, in this case the bioactive piperidines are held together by supramolecular forces, in a sort of dynamic equilibrium. For this reason, searching to clarify this concept, we thought to synthesize also a kind of covalently linked micelle, in which the dynamism of the micelle was hampered by the formation of covalent bonds (compound **98**, figure 3.18), and to compare the activity of the polymer with that of monomer.
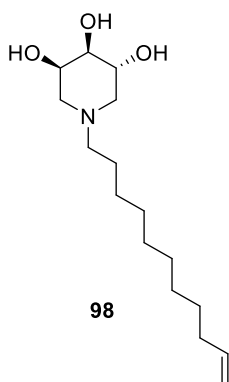

Figure 3.18: Piperidine with unsaturated 11-carbon chain **98**.

But what about the role of the lipophilicity? Investigating this point could be useful to understand something about the nature of the enzymatic site of GCase: in our experience until now, the best results in terms of inhibition and chaperoning activity were obtained indeed with piperidines bearing a quite-long carbon chain (both on the N endocyclic atom, and on C-2).[32,36] For this reason, to prove or confute the importance of a lipophilic portion, we carried on the synthesis of a molecule that contains the same trihydroxypiperidine skeleton and a water soluble more polar chain with a comparable length (compound **99**, figure 3.19), but bearing a PEG chain instead of an alkyl chain.
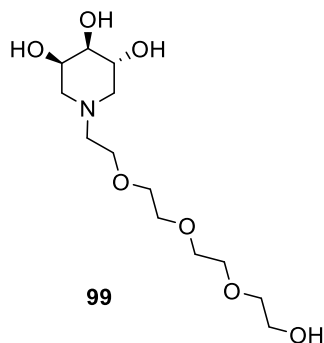
Figure 3.19: Trihydroxypiperidine **99** *N*-alkylated with a polar PEG-ylated chain.

The final step in those preliminary studies was the evaluation of all those compounds as GCase inhibitors and, if they would show promising results, as chaperones.

3.2.2.1 Results and discussion

For the synthesis of piperidine **97** we started from the same D-mannose derived dialdehyde intermediate **73**, applying again the DRA strategy (scheme 3.12). We first remove the benzyl group of dialdehyde **73** affording **100**,[91] then, using dodecylamine in the double reductive amination, we got piperidine intermediate **101** that was finally deprotected in acidic conditions affording the final compound **97** (32% over 2 steps).
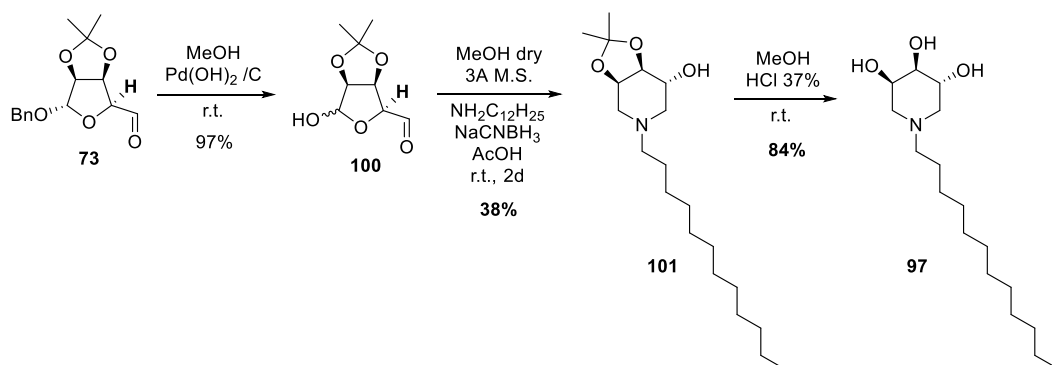
Scheme 3.12: Synthetic strategy for compound **97**.

Physico-chemical characterization:

The physico-chemical characterization of **97** was carried out by Prof. Lo Nostro group (Department of Chemistry, University of Florence). At first the packing parameter of compound **97** was estimated using Tanford formulas, through which it was possible to derive the volume and the length of the apolar tail of the compound **97**. The area per polar head was found by approximating the piperidine polar heads with cylinders.
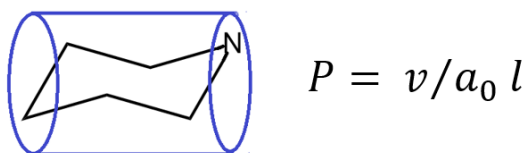
$$P = v/a_0 \, l$$

Figure 3.20: Cylindric approximation of polar heads.

The P value found is of about 0.9, for which the formation of a planar lamellar structure with the solvent distributed between the bilayers formed by the amphiphilic molecules is expected. This happens when we have a high amphiphile concentrations (see table 3.4). Moreover, through Tanford formulas the length of the polar head (l_p) was calculated: it is of 6 Å; the length of the tails (l_c) is about 15.4 Å. The structural unit (d) is composed of two tails and two heads that are placed at limited distance, in order to maximize the hydrogen bonds. Comparing the hydrocarbon thickness (d-2l_h) with the length of the two tails, the degree of interdigitation G.I.% is obtained. The hypothesized structure, together with the G.I% formula, is reported in figure 3.21.

$$G.I.(\%) = 100 \cdot \frac{d-2lp}{2lc} \approx 56.49\%$$

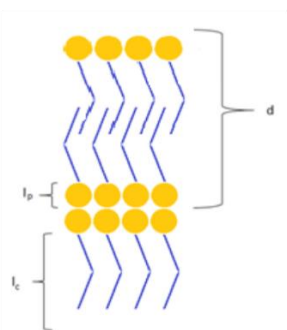**Figure 3.21:** Hhypothetical scheme of the structure envisaged by G.I%.

Performing DSC measurements, a melting temperature of 64.37 °C with a ΔH_{fus} of 75.03 J/g (248.89 kJ/mol) was found; moving towards higher temperatures another peak much smaller than the first is present, probably given by a polymorph or an improbable impurity remained following the synthesis (figure 3.22).
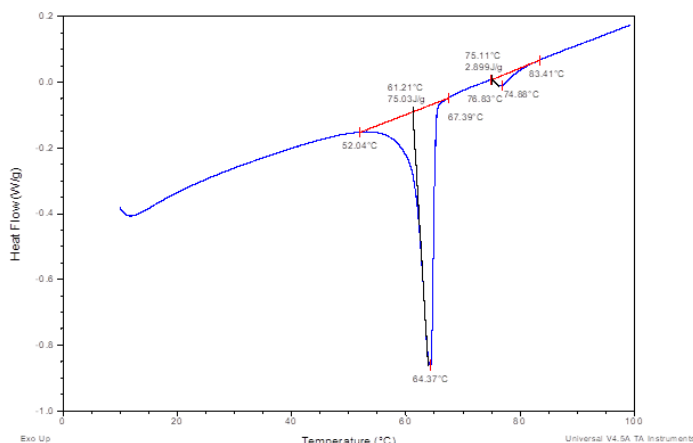
Figure 3.22: DSC thermogram.

The lamellar structure was then confirmed by SAXS experiments, in which two peaks at the scattering vector "q" value equal to 0.21 Å^{-1} and 0.43 Å^{-1} were obtain, relative respectively to the first and second reflection of the 'lamella'. The thickness of a 'lamella' can be derived from the ratio q = 2π / d, which is therefore equal to 29.4 Å. Analyzing WAXS profile of the solid, a tricline type geometric organization of the crystalline cell was found, also confirmed by IR spectroscopy. Moreover, the sample was characterized by SAXS, WAXS and DSC techniques at various concentrations in aqueous solution, respectively at 8, 12, 20 and 40% w/w concentrations: it was possible to quantify the temperature at which there is a passage from a lamellar phase to a disordered gel-like phase (around 21°C), and to obtain the number of water molecules strongly linked to the polar heads of the surfactant (W_b), which do not freeze or melt during the heating/cooling cycles and the number of strongly bound molecules by the polar head of the surfactant (N_b) (table 3.4). Finding these values for several solutions at different concentrations (table 3.4) we note how the number of strongly bound molecules increases as the concentration of the dispersed **97** surfactant increases, while the number of molecules per polar surfactant head shows an opposite trend.

W/W%	ΔH$_{fus}$ (J/g)	W_b %	N_b%
7.9	331.1	0.81	6.82
11.85	300.1	10.09	5.21
19.53	271.6	18.63	2.57
41.5	77	76.93	0.45

**Table 3.4:** Values obtained by calorimetric experiments.

Moreover, aiming also to understand if the piperidine self-assemblies in micellar aggregates, we performed surface tension measurements. A 12 μM value of CMC was found. This value can be compared to the IC_{50} graph in order to understand if our compound is active in monomeric form or the micellar aggregates, at least in part, are responsible of biological activity (see biological evaluation 3.2.2.2).

For the synthesis of piperidine containing the terminal double bond **98**, we investigated two different pathways: the first one in which 1,11-undecyl,bromo-nonane was directly reacted with piperidine **102**, obtained through acidic deprotection and consequent treatment with strongly acid resin DOWEX, of compound **87** (scheme 3.13).[91]
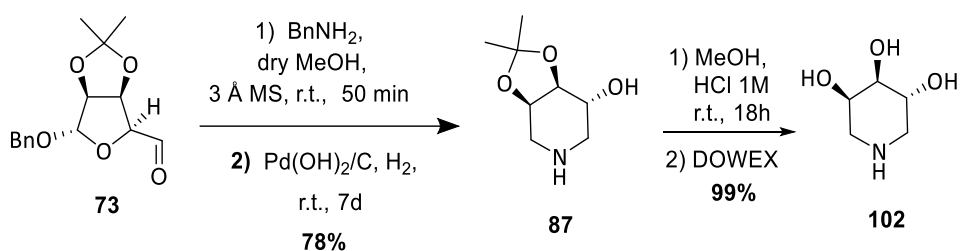
Scheme 3.13: Synthesis of compound **102**.

Compound **102** was reacted with 1,11-undecyl,bromo-nonane using the alkylation procedure already exploited in the synthesis of azido-piperidine **89** (see section 3.2.1.1), as described in scheme 3.14.
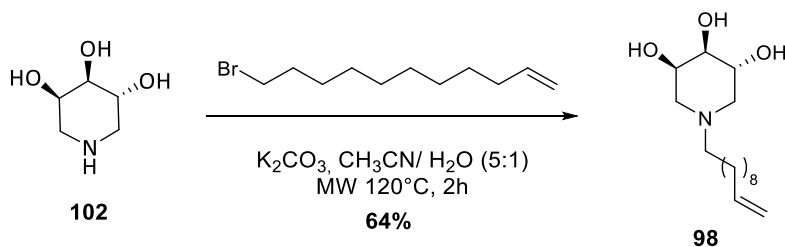
Scheme 3.14: Synthesis of compound **98**.

We observed in this case, the formation of a byproduct in a consistent amount (66 mg, 0.23 mmol, 28% yield), that we identified, through ESI-MS and NMR, in the bis-alkylated piperidine **103** (scheme 3.15).

_____
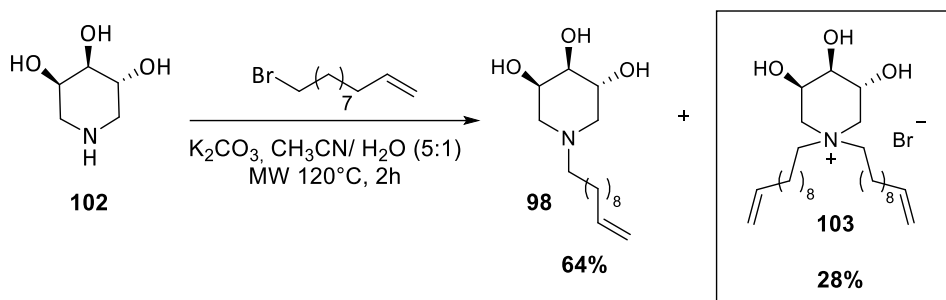
Scheme 3.15: Formation of byproduct **103**.

Trying to avoid to recover the bis-alkylated compound, we thought to perform the alkylation starting from the protected piperidi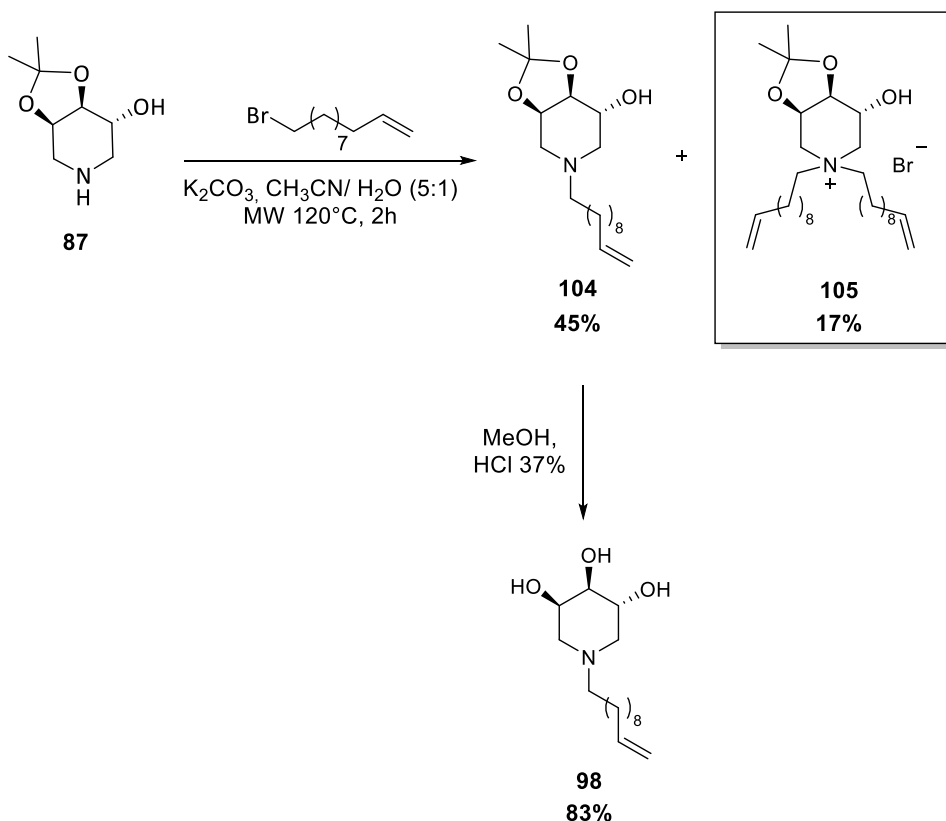ne **87**, and deprotect the product in the final step with an acidic cleavage of the hydroxyl groups on C-3 and C-4 (scheme 3.16), but also in this case, we obtained the corresponding protected bis-alkylated compound **105** (140 mg, 0.32 mmol, 17%).

Scheme 3.16: Alternative synthetic strategy.

We reasoned that this problem was probably due to the terminal double bond that could provoke a sort of packaging, because in the case of the azido derivatives **79** and **89**, we did not observe the same analogous by-product. Anyway, once obtained derivative **98**, we

tried to perform a polymerization reaction exploiting the olefin moiety with several attempts.

We decided to perform the polymerization using AIBN (2,2'-azobisisobutyronitrile) as radical initiator and we planned the experiment in order to induce the micellar formation, dissolving amphiphile **98** in deuterium dioxide (to follow the reaction profile through NMR spectroscopy; concentration: 10 mg/0.1 ml) and adding drop by drop a solution of AIBN in methanol. According to our hypothesis compound **98** would dispose itself displaying the polar portion of the molecule outwards (showing a lipophobic nature) and the lipophile tails inwards; the initiator, dissolved in organic medium, would have reach the internal part of the micelle, performing its role and starting in that way the polymerization reaction, catalysed by the temperature (50°C) and helped by the use of UV radiation. To attest the formation of the polymer, we performed a ^{1}H-NMR after one hour, but the situation seemed to be the same: the ratio between the integrals of H-3 (or H-4 or H-5) and H-7' (the olefin proton) was still equal to 1, while, if the polymerization occurred, we expected at list a reduction of H-7' integral. The same spectrum was observed after 4 hours and addition of AIBN (4% in mol with respect to initial 2%). We decided to add more AIBN (to reach a total percentage of 8%) and left the reaction for other 6 hours, but a further NMR control, showed again no decrease of olefin proton integrals. In the second attempt we changed some parameters, setting the temperature to 100°C for 15 minutes,[100] but nothing happened also in this case. In the third and final procedure, we first tried to re-crystallize AIBN from methanol and then we enhanced the amount (10% in mol) of initiator and also the concentration of starting material in the solvent, passing from 100 mg/1 ml to 100 mg/2 ml (see table 3.5). Unfortunately, even in these conditions the desired polymerization did not occurr, letting us think that for some reason it was no possible to achieve the covalently linked micelle.

	T	t	C	conditions
2	50 °C	24 h	100 mg/ 1mL	UV lamp
3	100 °C	15 min	100 mg/ 1mL	-
4	100 °C	18 h	from100 mg/ 1mL to 100 mg/ 2mL	recrystallized AIBN from MeOH Purification with Sephadex®

Table 3.5: Polymerization conditions.

---

[100] Krstina J., Moad G., Willing I., Danek S.K., Kelly D.P., Jones S.L., Solomon D.H., *Eur. Polym. J.*, **1993**, *29*, 379-388.

For the synthesis of 'PEG-ylated' piperidine **99**, we followed the alkylation procedure already used in the synthesis of azido-piperidine **89** (see section 3.2.1.1), reported in scheme 3.17: the trihydroxypiperidine **87** was reacted with tetraethylene glycol *p*-toluenesulfonate respectively, in CH_3CN/H_2O in the presence of K_2CO_3 under MW irradiation at 120°C to yield piperidine **106** (64%), that was then deprotected in acidic conditions in MeOH, to afford the **99** in quantitative yield.
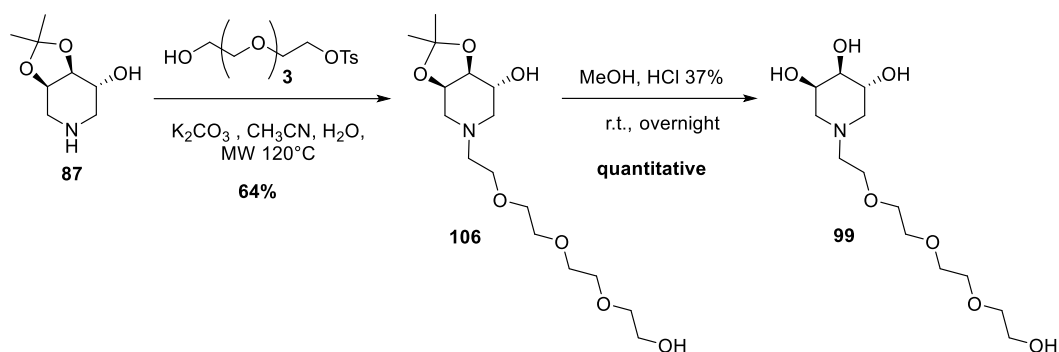

Scheme 3.17: Synthesis of piperidine **99**.

3.2.2.2 Biological evaluation

The inhibitory activity of all the synthesized piperidines was evaluated towards GCase enzyme, moreover chaperone activity of piperidine **97** was assayed on human fibroblasts derived from Gaucher patients bearing the N370/RecNcil mutation, thanks to a collaboration with Prof. Morrone (Meyer's Children Hospital). First of all, compounds **97**, **98**, and **103** were screened in extracts from a pool of human leukocytes isolated from healthy donors (1 mM concentration of inhibitor, 37 °C and optimal pH conditions, see experimental section 3.2.1.4), using 4-methylumbelliferyl β-D-glucopyranoside as substrate.

Piperidine **97** showed great inhibition value (99% at 1mM) and excellent results in terms of IC_{50} (Table 3.6), for this reason it was also tested as pharmacological chaperone revealing itself as the best chaperone of the series of *N*-alkylated trihydroxypiperidines synthesized in our group.[32] Indeed, compound **97** was able to rescue the GCase activity of 1.3 fold at 100 nM when incubated with fibroblasts bearing the N370/RecNcil mutation, for four days.

97
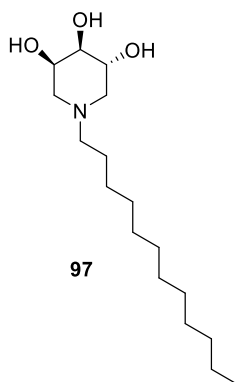
	Inhibition	IC$_{50}$	Rescue of GCase activity on N370/RecNcil mutated fibroblasts
	(conc. 1mM) 99%	3.4 μM	1.3 fold at 100 nM

Table 3.6: Biological data for piperidine **97**.

From the superficial tension measurements, we found a critical micellar concentration (CMC) of 12 μM, 1 magnitude order higher than the IC$_{50}$ concentration, thus suggesting that our compound is probably active in the monomeric form. However, further investigations are ongoing addressing this issue.

We assayed also the two piperidines with unsatured 11 carbons chain **98** and **103**, that revealed a good inhibitory profile and good IC$_{50}$ values, especially for monoalkylated compound **98** (table 3.7).

98

103
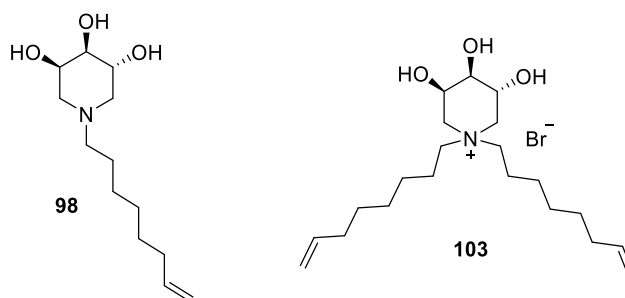
Piperidine	Inhibition	IC$_{50}$
98	97 %	4.0 ± 0.7 μM
103	98 %	20.0 ± 7.0 μM

Table 3.7: Biological inhibition and IC$_{50}$ data for piperidines **98** and **103**.

The good inhibition results achieved for bis-alkylated piperidine **103** lead us reasoned on the role played by the protonation of endocyclic nitrogen atom. Indeed, this compound results permanently charged, due to the formation of four bonds. Consequently, we asked

ourselves what could happen if we were able to give to piperidine the possibility to accept a proton donation from the enzymatic site and to be consequently positively charged in a reversible way, but still continuing to maintain the double chain on the piperidine *N*, a necessary condition to well mimic the natural substrate glucosyl ceramide (**9**, figure 3.23). Thus, as a future plan we aim to synthesize a 3,4,5-trihydroxypiperidine substituted on the endocyclic N with a bifurcate alkyl chain, that however has the possibility to be protonate in a reversible way during the interaction with the enzyme, such as the derivative showed in figure 3.23.
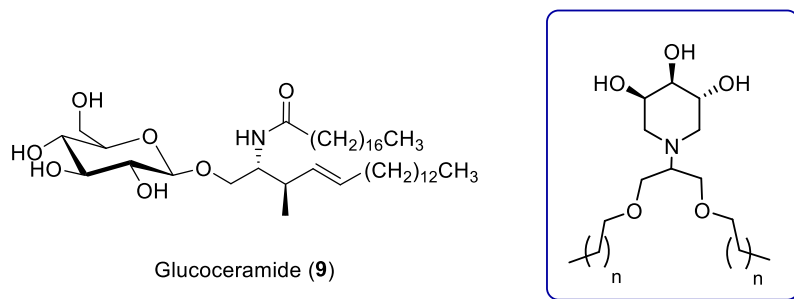
Glucoceramide (**9**)

Figure 3.23: Natural GCase substrate glucosyl ceramide **9**.

In order to understand the importance of a lipophilic portion in such inhibitors, we tested piperidine **99** that contains a polar chain (due to the presence of oxygen atoms instead of carbons), and effectively it showed no inhibition power (table 3.8), thus demonstrating that the cavity of the enzymatic site of GCase seems to be prone to accept preferentially lipophilic molecules. This result can be useful in the future design of new more potent inhibitors and chaperones.

Inhibition
0 %

Table 3.8: Biological inhibition and IC_{50} data for piperidine **99**.

3.2.2.3 Conclusions

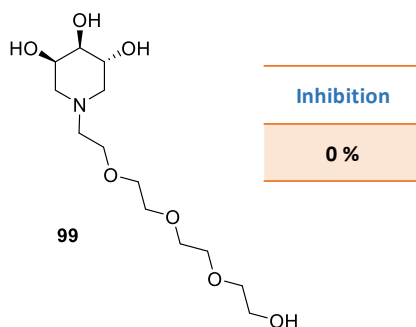In conclusion, in this part of the project trihydroxypiperidines differently functionalized at the nitrogen atom were synthesized and assayed as inhibitors/chaperones against GCase enzyme. Moreover, in order to understand the aggregation mode in water of the most active piperidine of the series (compound **97**), we characterized it through physical-chemical techniques. Through different kind of measurement, we found that our piperidine self-assemblies in water in a lamellar conformation.

New synthesized compounds (**97**, **98**, **103**) have revealed to be excellent GCase inhibitors, especially piperidine *N*-alkylated with C-12 carbon chain (compound 95) that is also able to restore the catalytic activity of the enzyme bearing the N370/RecNcil mutation. Moreover, it shows the best chaperoning activity between all the *N*-alkylated piperidines ever synthesized in our research group.

Thanks to the synthesis and the biological evaluation of piperidine **99**, that is substituted on the N endocyclic atom with a polar chain, we also were able to confirm that the enzymatic cavity of the GCase enzyme prefers to interact with a lipophilic moiety.

To better understand the structure-activity relationship between trihydroxypiperidines and GCase, docking studies will be object of future investigation in our laboratories, together with the synthesis of a derivative bearing a bifurcate alkyl chain that allowed the piperidine to undergo a reversible protonation (figure 3.23), maybe using a double reductive amination reaction (scheme 3.18).
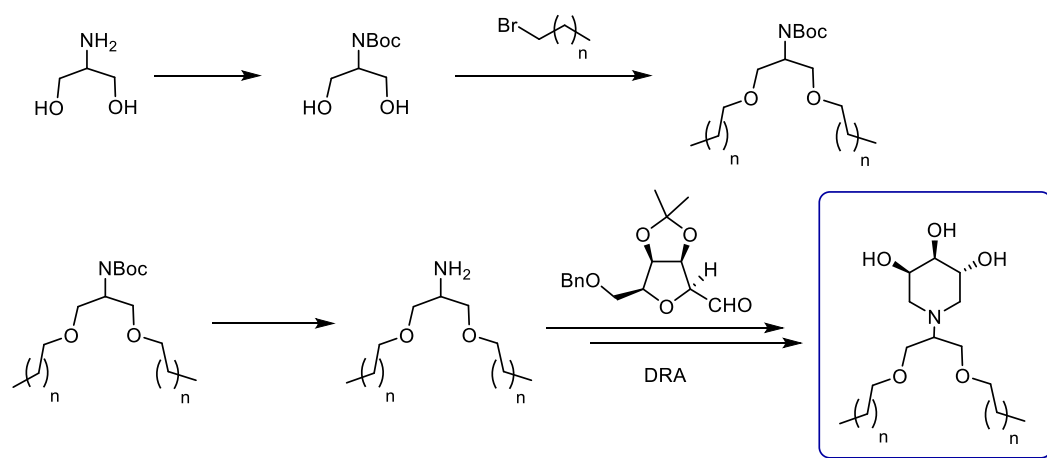
Scheme 3.18: Synthesis of a reversible protonatable GCase inhibitor.

3.2.2.4 Experimental section

For the general details see paragraph 2.4.

Synthesis of piperidine 101: A 0.1 M solution of dialdehyde **100** (819 mg, 4.35 mmol) in dry MeOH was stirred in the presence of 3Å molecular sieves powder for 15 min, under nitrogen atmosphere, then dodecylamine (806 mg, 4.35 mmol) was added. After 3 hours the reaction mixture was cooled at 0°C, NaBH$_3$CN (820 mg, 13.05 mmol) and AcOH (500 μl, 8.70 mmol) were added and the mixture was allowed to warm to room temperature and stirred for two days under nitrogen atmosphere. The molecular sieves were removed by filtration through Celite and the filtrate was concentrated under vacuum. The residue was purified by flash chromatography (CH$_2$Cl$_2$:MeOH from 50:1 to 10:1) affording **101** in 38% yields (*R*f = 0.32, 563 mg, 1.65 mmol) as a colourless waxy solid. **[α]$_{22}$^{D}**= + 11.5 (c = 0.31 in CHCl$_3$); **^{1}H-NMR** (400 MHz, CDCl$_3$): δ= 4.31 (pq, *J* = 6.2 Hz, 1H, H-3), 4.07 (t, *J* = 4.4 Hz, 1H, H-4), 3.97-3.93 (m, 1H, H-5), 2.81 (dd, *J* = 12.0, 6.0 Hz, 1H, Ha-2), 2.57 (d, *J* = 2.9 Hz, 2H, H-6), 2.42-2.34 (m, 3H, Hb-2, H-1'), 1.50-1.45 (m, 5H, CH$_3$, H-2'), 1.35 (s, 3H, CH$_3$), 1.31-1.25 (m, 18H, from H-3' to H-11'), 0.87 (t, *J* = 6.8 Hz, 3H, CH$_3$) ppm; **^{13}C-NMR** (50 MHz, CDCl$_3$): δ= 109.2 (s, C(CH$_3$)$_2$), 76.9 (d, C-4), 72.1 (d, C-3), 67.5 (d, C-5), 57.8 (t, C-1'), 55.8 (t, C-2), 55.5 (t, C-6), 31.8-26.3 (12C, t from C-2' to C-11', q CH$_3$), 14.0 (q, CH$_3$) ppm; **IR** (CHCl$_3$): ν = 3458, 2928, 2854, 1468, 1456, 1404, 1383, 1246, 1144 cm^{-1}. **MS (ESI)**: *m/z* calcd (%) for C$_{20}$H$_{39}$NO$_3$ 341.29; found: 342.33 (100%, [M+ H]$^+$). **Elemental analysis:** C$_{20}$H$_{39}$NO$_3$ (341.53) calcd. C, 70.33; H, 11.51; N, 4.10; found C, 70.51; H, 11.72, N, 4.22.

Synthesis of piperidine 97: To a solution of **101** (563 mg, 1.65 mmol) in 55 mL of methanol, 1.38 ml of 37% HCl were added and the mixture was stirred at room temperature for 18 hours. After that an ^{1}H-NMR showed disappearance of the methyl groups, the solvent was removed under reduced pressure. The crude was purified by FCC (CH$_2$Cl$_2$:MeOH:NH$_3$ 10:1:0.1) affording pure **97** (*R*f = 0.25, 419 mg, 1.39 mmol, 84% yield) as a white powder. **[α]$_{22}$^{D}**= −19.6 (c = 0.91 in MeOH); **^{1}H-NMR** (400 MHz, CD$_3$OD): δ= 3.90 (dt, *J* = 5.7, 2.9 Hz, 1H, H-3), 3.80 (td, *J* = 7.9, 4.0 Hz, 1H, H-5), 3.42-3.39 (m, 1H, H-4), 2.85-2.73 (m, 2H, Ha-6, Ha-2), 2.44-2.17 (m, 3H, H-1', Hb-2), 2.06-2.02 (m, 1H, Hb-6), 1.54-1.45 (m, 2H, H-2'), 1.31-1.27 (m, 18H, from H-3' to H-11'), 0.89 (t, *J*= 6.8 Hz, 3H, CH$_3$) ppm; **^{13}C-NMR** (50 MHz, CD$_3$OD): δ= 73.7 (d, C-4), 68.1 (d, C-5), 67.5 (d, C-3), 57.8 (t, C-1'), 56.5 (t, C-2), 56.0 (t, C-6), 31.6-22.2 (12C, t from C-2' to C-11', q CH$_3$), 12.9 (q, CH$_3$) ppm; **MS (ESI)**: *m/z* calcd (%) for C$_{17}$H$_{35}$N$_4$O$_3$ 301.26; found: 302.42 (100%, [M+ H]$^+$). **Elemental analysis:** C$_{17}$H$_{35}$NO$_3$ (301.53) calcd. C, 67.73; H, 11.70; N, 4.65; found C, 67.91; H, 11.53, N, 4.40.

Synthesis of piperidine 98 and 103: A solution of **98** (71 mg, 0.53 mmol), 1-11,bromoundecene (187 mg, 0.80 mmol) and K$_2$CO$_3$ (111 mg, 0.80 mmol) in 2.3 ml of a mixture CH$_3$CN/H$_2$O 5:1 was stirred in microwave at 120°C for 2 h, until a TLC analysis

(CH$_2$Cl$_2$:MeOH:NH$_3$ 6:1:0.1) showed the disappearance of the starting material (*R*f = 0.00). After filtration through Celite®, the solvent was removed under reduced pressure and the crude was purified by FCC (CH$_2$Cl$_2$:MeOH:NH$_3$ from 10:1:0.1 to 8:1:0.1) affording pure **98** (*R*f = 0.24, 87 mg, 0.34 mmol, 64% yield as white waxy solid) and, as byproduct, compound **103** (*R*f = 0.18, 66 mg, 0.23 mmol, 28% yield).

Piperidine 98: $[\alpha]_{21}^{D}$= −30.7 (c = 0.79 in MeOH); **^{1}H-NMR** (400 MHz, CD$_3$OD): δ= 5.82 (ddt, *J* = 17.0, 10.2, 6.7 Hz, 1H, H-10'), 5.02-4.91 (m, 2H, H-11'), 3.91 (dt, *J* = 5.7, 3.0 Hz, 1H, H-3), 3.80 (td, *J* =7.9, 4.0 Hz, 1H, H-5), 3.41-3.40 (m, 1H, H-4), 2.83-2.77 (m, 2H, Ha-6, Ha-2), 2.42-2.34 (m, 2H, H-1'), 2.29 (d, *J* = 11.3 Hz, 1H, Hb-2), 2.13-2.03 (m, 3H, Hb-6, H-9'), 1.56-1.46 (m, 2H, H-2'), 1.41-1.32 (m, 12H, from H-3' to H-8') ppm; **^{13}C-NMR** (50 MHz, CD$_3$OD): δ= 140.0 (d, C-10'), 114.7 (t, C-11'), 75.2 (d, C-4), 69.5 (d, C-5), 69.1 (d, C-3), 59.3 (t, C-1'), 58.1 (t, C-2), 57.5 (t, C-6), 34.8 (t, C-9'), 30.6-28.6 (t, 6C, from C-3' to C-8'), 27.5 (t, C-2') ppm; **MS (ESI)**: *m/z* calcd (%) for C$_{16}$H$_{31}$NO$_3$ 285.23; found: 286.42 (100%, [M+ H]$^+$);. **Elemental analysis:** C$_{16}$H$_{31}$NO$_3$ (285.43) calcd. C, 67.33; H, 10.95; N, 4.91; found C, 67.46; H, 11.03, N, 4.78.

Piperidine 103: $[\alpha]_{26}^{D}$= − 5.5 (c = 1.0 in MeOH); **^{1}H-NMR** (400 MHz, CD$_3$OD): δ= 5.83 (ddt, *J* = 17.0, 10.2, 6.7 Hz, 2H, H-10'), 5.03-4.93 (m, 4H, H-11'), 3.32-4.26 (m, 1H, H-3), 4.17-4.07 (m, 1H, H-5), 3.83 (dd, *J* = 5.7, 3.0 Hz, 1H, H-4), 3.69-3.39 (m, 8H, H-6, H-2, H-1'), 2.08 (q, *J* = 6.9 Hz, 4H, H-9'), 1.85-1.68 (m, 4H, H-2'), 1.42-1.37 (m, 24H, from H-3' to H-8') ppm; **^{13}C-NMR** (100 MHz, CD$_3$OD): δ= 140.1 (d, 2C, C-10'), 114.7 (t, 2C, C-11'), 71.3 (d, C-4), 68.1 (d, C-5), 64.3 (d, C-3), 64.2 (t, 2C, C-1'), 62.0 (t, C-2), 59.4 (t, C-6), 34.9 (t, 2C, C-9'), 30.4-27.3 (t, 12C, from C-3' to C-8'), 22.7 (t, 2C, C-2') ppm; **MS (ESI)**: *m/z* calcd (%) for C$_{27}$H$_{52}$NO$_3$$^+$ 438.39; found: 438.51 (100%, [M]$^+$).

Synthesis of piperidine 104 and 105: A solution of **87** (143 mg, 0.83 mmol), 1-11,bromoundecene (252 mg, 1.08 mmol) and K$_2$CO$_3$ (172 mg, 1.25 mmol) in 3.6 ml of a mixture CH$_3$CN/H$_2$O 5:1 was stirred in microwave at 120°C for 2 h, until a TLC analysis (CH$_2$Cl$_2$:MeOH:NH$_3$ 6:1:0.1) showed the disappearance of the starting material (*R*f = 0.00). After filtration through Celite®, the solvent was removed under reduced pressure and the crude was purified by FCC (AcOEt:Hexane from 1:5 to 1:1) affording pure **104** (*R*f = 0.31, 121 mg, 0.37 mmol, 45% yield as white waxy solid) and, as byproduct, compound **105** (*R*f = 0.10, 67 mg, 0.14 mmol, 17% yield).

Piperidine 104: $[\alpha]_{21}^{D}$= + 9.97 (c = 1.0 in CHCl$_3$); **^{1}H-NMR** (400 MHz, CDCl$_3$): δ= 5.80 (dqd, *J* = 19.8, 6.7, 5.9 Hz, 1H, H-10'), 5.00-4.91 (m, 2H, H-11'), 4.29 (dd, *J* = 12.6, 5.9 Hz, 1H, H-5), 4.05 (t, *J* = 4.5 Hz, 1H, H-4), 3.94 (dd, *J* = 7.1, 4.2 Hz, 1H, H-3), 2.76 (dd, *J* = 11.8, 6.1 Hz, 1H, Ha-6), 2.56 (dd, *J* = 11.7, 2.7 Hz, 1H, Ha-2), 2.51 (dd, *J* = 11.8, 4.8 Hz, 1H, Hb-2), 2.39-2.34 (m, 3H, Hb-6, H-1'), 2.03 (q, *J* = 6.9 Hz, 2H, H-9'), 1.50 (s, 3H, CH$_3$), 1.46-1.43 (m, 2H, H-2'), 1.35 (s, 3H, CH$_3$), 1.26 (s, 12H, from H-3' to H-8') ppm; **^{13}C-NMR** (50 MHz, CDCl$_3$): δ= 138.7 (d, C-10'), 113.6 (t, C-11'), 108.8 (s, C̲-(CH$_3$)$_2$), 75.9 (d, C-4), 71.5 (d, C-5), 66.9 (d, C-3), 57.3 (t, C-1'), 55.4 (t, C-6), 54.9 (t, C-2), 33.3 (t, C-9'), 29.0-25.9 (q, 2C, C-(C̲H$_3$)$_2$, t, 7C,

_____

from C-2' to C-8') ppm; **IR** (CHCl$_3$): ν = 3338, 2936, 2859, 2492, 2456, 2197, 2100, 2061, 1458, 1384, 1246, 1221, 1153 cm^{-1}. **MS (ESI)**: *m/z* calcd (%) for C$_{19}$H$_{35}$NO$_3$ 325.26; found: 326.20 (100%, [M+H]$^+$).

Piperidine 105: $[α]_{21}{}^D$= −10.22 (c = 1.0 in CHCl$_3$); **^{1}H-NMR** (400 MHz, CDCl$_3$): δ= 5.81-5.71 (m, 2H, H-10'), 4.97-4.88 (m, 4H, H-11'), 4.63 (bs, 1H, H-3), 4.49 (bs, 1H, H-4), 4.22 (bs, 1H, H-5), 4.03 (d, *J* = 14.0 Hz, 1H, Ha-2), 3.92 (bs, 1H, Ha-6), 3.69-3.30 (m, 6H, Hb-2, Hb-6, H-1'), 2.02-1.97 (m, 4H, H-9'), 1.68 (bs, 4H, H-2'), 1.46 (s, 3H, CH$_3$), 1.30-1.24 (m, 27H, CH$_3$, from H-3' to H-8') ppm; **^{13}C-NMR** (100 MHz, CDCl$_3$): δ= 139.1 (d, 2C, C-10'), 114.3 (t, 2C, C-11'), 109.8 (s, C-(CH$_3$)$_2$), 72.8 (d, C-4), 70.4 (d, C-3), 65.0 (d, C-5), 63.6 (t, 2C, C-1'), 58.8 (t, C-6), 56.7 (t, C-2), 33.8 (t, 2C, C-9'), 29.4-22.3 (q, 2C, C-(CH$_3$)$_2$ t, 14C, from C-2' to C-8') ppm; **IR** (CHCl$_3$): ν = 3340, 3006, 2874, 2437, 2402, 2221, 1998, 1976, 1497, 1396, 1266, 1146 cm^{-1}.**MS (ESI)**: *m/z* calcd (%) for C$_{30}$H$_{56}$NO$_3{}^+$ 478.43; found: 478.40 (100%, [M]$^+$).

Synthesis of piperidine 106: A solution of **87** (60 mg, 0.35 mmol), tetraethylene glycol *p*-toluenesulfonate (181 mg, 0.52 mmol) and K$_2$CO$_3$ (72 mg, 0.52 mmol) in 3.6 ml of a mixture CH$_3$CN/H$_2$O 5:1 was stirred in microwave at 120°C for 2 h, until a TLC analysis (CH$_2$Cl$_2$:MeOH:NH$_3$ 5:1:0.2) showed the disappearance of the starting material (*R*f = 0.37) and the formation of a new product (*R*f = 0.73). After filtration through Celite®, the solvent was removed under reduced pressure and the crude was purified by FCC (Et$_2$O:AcOEt from 15:1 to AcOEt) affording pure **106** (*R*f = 0.52, 78 mg, 0.22 mmol, 64% yield) as a yellow oil. $[α]_{25}{}^D$= + 12.6 (c = 0.76 in CHCl$_3$); **^{1}H-NMR** (400 MHz, CDCl$_3$): δ= 4.32 (dd, *J* = 12.7, 6.2 Hz, 1H, H-5), 4.07 (s, 1H, H-4), 3.94 (s, 1H, H-3), 3.70-3.69 (m, 2H, H-2'), 3.65 (s, 8H, from H-3' to H-6'), 3.60-3.50 (m, 4H, H-7', H-8'), 2.87 (dd, *J* = 11.6, 6.1 Hz, 1H, Ha-6), 2.68 (dd, *J* = 11.7, 9.3 Hz, 1H, Ha-2), 2.63-2.58 (m, 3H, H-1', Hb-2), 2.33 (dd, *J* = 11.5, 8.0 Hz, 1H, Hb-6), 1.49 (s, 3H, CH$_3$), 1.35 (s, 3H, CH$_3$) ppm; **^{13}C-NMR** (50 MHz, CDCl$_3$): δ= 109.2 (s, C(CH$_3$)$_2$), 76.5 (d, C-4), 72.8 (t, C-7'), 72.0 (d, C-5), 70.7-70.2 (d, 4C, from C-3' to C-6'), 68.9 (t, C-8'), 67.3 (d, C-3), 61.8 (t, C-2'), 57.0 (t, C-2), 56.3 (t, C-1'), 55.8 (t, C-6), 28.4 (q, CH$_3$), 26.5 (q, CH$_3$) ppm; **IR** (CDCl$_3$): ν = 3447, 3005, 2876, 1655, 1458, 1354, 1246, 1101, 1059 cm^{-1}. **MS (ESI)**: *m/z* calcd (%) for C$_{16}$H$_{31}$NO$_7$ 349.21; found: 372.49 (100%, [M+ Na]$^+$), 350.43 (49%, [M+ H]$^+$).

Synthesis of piperidine 99: To a solution of **106** (71 mg, 0.20 mmol) in 8 mL of methanol, 15 drops of 37% HCl were added and the mixture was stirred at room temperature for 18 hours. After that a TLC analysis (CH$_2$Cl$_2$:MeOH:NH$_3$ 5:1:0.2) showed disappearance of the starting material (*R*f = 0.73), the solvent was removed under reduced pressure. Piperidine **99** was obtained without further purification (*R*f = 0.10, 62 mg, 0.20 mmol, quantitative yield) as a colourless oil. $[α]_{26}{}^D$= −17.1 (c = 0.84 in MeOH); **^{1}H-NMR** (400 MHz, CD$_3$OD): δ= 3.98 (s, 1H, H-3), 3.58 (td, *J* = 8.7, 4.3 Hz, 1H, H-5), 3.72-3.71 (m, 10H, from H-2' to H-6'), 3.65-3.63 (m, 4H, H-7', H-8'), 3.49 (d, *J* = 10.4 Hz, 1H, H-4), 2.91 (dd, *J* =22.2, 2.1 Hz, 2H, Ha-6, Ha-2), 2.66 (t, *J* = 5.5 Hz, 2H, H-1'), 2.40 (d, *J* = 12.3 Hz, 1H, Hb-2), 2.20-2.11 (m, 1H, Hb-6) ppm; **^{13}C-NMR** (100 MHz, CD$_3$OD): δ= 73.6 (d, C-4), 71.6 (d, C-5),69.6-69.3 (t, 5C, from C-3' to C-7'), 67.6 (C-8'), 67.4 (d, C-3), 60.3 (t, C-2'), 56.6 (t, C-2), 56.0 (t, C-

6), 55.8 (t, C-1') ppm; **MS (ESI)**: *m/z* calcd (%) for $C_{13}H_{27}NO_7$ 309.18; found: 332.45 (100%, [M+ Na]$^+$). **Elemental analysis:** $C_{13}H_{27}NO_7$ (309.36) calcd. C, 50.47; H, 8.80; N, 4.53; found C, 50.55; H, 8.69, N, 4.61.

For the procedures of biochemical characterization with human GCase, IC$_{50}$ determination and chaperoning activity assays, see section 3.2.1.4.

3.2.3 Resorcinarenes

To extend the study of multimerization of our iminosugar onto different scaffolds, we started a project in collaboration with the groups of Prof. Neri from the University of Salerno and of Dr. Sestak from the Centre for Glycomics Slovak Academy of Sciences of Bratislava. Our aim was to design a new class of mannosidases inhibitors starting from pyrrolidine DAB-1 derivatives conjugated to resorcinarene scaffolds. Combining our expertise in the total synthesis of iminosugar glycomimetics and Prof. Neri experience in the synthesis of resorcinarenes, we wanted to obtain a new class of selective inhibitors of different families of mannosidase enzymes, towards whom the new glycocalyx systems would be tested by Dr. Sestak. We decided to multimerize onto resorcinarenic scaffolds a bioactive unit that contains as iminosugar skeleton, the pyrrolidine DAB-1, a well-known inhibitor of a wide range of mammalian glycosidases.[101] Indeed, in its multivalent fashion, it showed very impressive results in our previous works towards different enzymes, such as *N*-acetylgalactosamine-6-sulfatase (GALNS), which is the deficient enzyme in mucopolysaccharidosis Morquio A syndrome (see section 1.2.4)[47] and JBMan, that can be taken as model for other two mannosidases of therapeutic interest (Golgi α-mannosidase GManII and lysosomal α-mannosidase LManII), due to its dimeric nature and its commercially availability (see section 1.2.5).[93] In particular this project was focused in the synthesis of new multivalent compounds that could selectively target GManII, in order to find new potential anticancer drugs, being it involved in *N*-glycan processing. Indeed, an altered cell surface carbohydrate decoration compared to normal cells has been found in many types of cancer. Swainsonine is a potent inhibitor of GManII, blocking tumour growth and metastasis, but it is not selective towards this enzyme, because it inhibits also the close lysosomal α-mannosidase LManII, leading to swainsonine-induced mannosidosis symptoms.[53] However, previous work showed that the multimerization of DAB-1 pyrrolidine iminosugar[93] and DNJ,[102] produced multivalent inhibitors more potent towards GManII than towards LManII. In other words, GManII is much more prone to accept multivalent inhibitors than LManII (**78**, **107**, figure 3.24).

---

[101] Asano N., Oseki K., Kizu H., Matsui K., *J. Med. Chem*., **1994**, *37*, 3701 –3706.

[102] Brissonet Y., Ortiz Mellet C., Morandat S., Garcia-Moreno M. I., Deniaud D., Matthews S. E., Vidal S., Sestak S., Kirat K. El, Gouin S. G., *J. Am. Chem. Soc*., **2013**, *135*, 18427–18435.
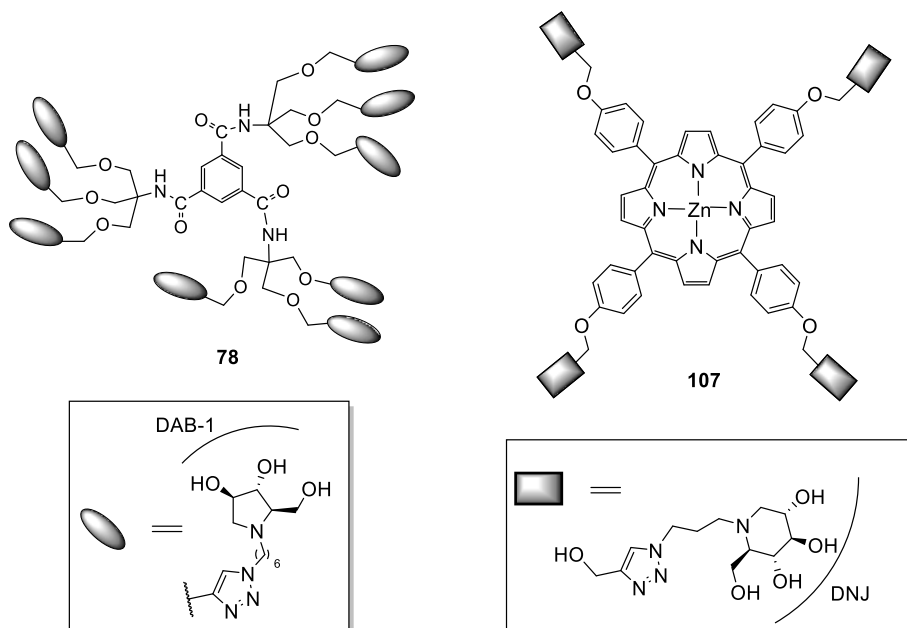
Figure 3.24: Multivalent GManII inhibitors **78** and **107**.

For this reason, the synthesis of multivalent compounds can help us in finding increasingly selective inhibitors for Golgi mannosidase without affecting the lysosomal enzyme, avoiding in this way undesired drawbacks such as the onset of mannosidosis.

Among the multitude of scaffolds reported in the literature for the multimerization of glycosidases inhibitors, we can find bowl-shaped macrocycles called resorcinarenes, resorcinol-formaldehyde cyclic oligomers that furnish the opportunity to attach several bioactive functions on different positions thereby accessing different topologies of the multivalent constructs. Because of their structural resemblance to calixarenes, chalice-like shape compounds which are phenol-derived cyclo-oligomers, they are also called calix[4]resorcinarenes.[103] Resorcinarenes are non-planar systems and they exist in different isoforms, classified by a combination of stereochemical criteria: the conformation of the macrocyclic ring; the relative configuration of the substituents at the methylene bridges; and the individual configuration of methylene bridge substituents (figure 3.25).[104]

[103] Gutsche C. D, *Calixarenes; Monographs in Supramolecular Chemistry*, **1989**, *1*, Ed. J F Stoddart.

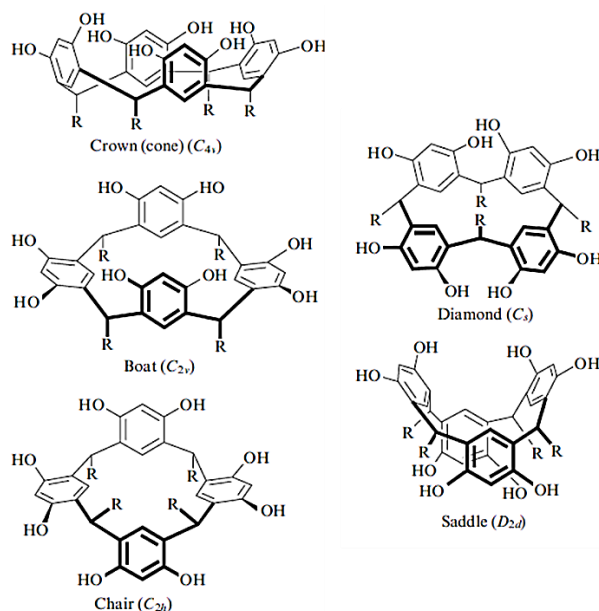[104] Högberg A. G. S., *J. Am. Chem. Soc.*, **1980**, *102*, 6046-6050.

Figure 3.25: The five highly symmetrical conformations: crown (C_{4v}), boat (C_{2v}), chair (C_{2h}), diamond (C_s) and saddle (D_{2d}).

Calix[4]resorcinarenes are very versatile scaffolds because they can be functionalized at two, four, six, eight, twelve, sixteen or more sites depending on the reagent, aldehyde, resorcinol and conditions used to carry out the reaction.

In this project, we wanted to access new selective GManII inhibitors by multimerizing our bioactive DAB-1 based iminosugar derivative with calix[4]resorcinarenes and calix[6]resorcinarenes synthesized by Prof. Neri group.

3.2.3.1 Results and discussion

As already mentioned before, this project has been developed in collaboration with Prof. Neri from the University of Salerno, and our contribution involved the synthesis of the iminosugar azido derivatives that were then conjugated to resorcinarenes by Prof. Neri group. In our initial plans, we thought to multimerize onto Prof. Neri's resorcinarenes pyrrolidine iminosugar **108**, that we obtained starting from the same intermediate **38** used in the synthesis of trehalase inhibitors (see chapter 2). Compound **108** was achieved from D-arabinose, that once transformed to pyrrolidine **38** through a reduction with NaBH₄ followed by a N-O cleavage performed with Zn in acetic acid of nitrone **30**, was first alkylated with 1-bromo-2-ethanol to afford alcohol **38**, then exposed to a Mitsunobu

reaction with diphenil phosphoryl azide (DPPA) as the nucleophile to obtain the azido intermediate **108** (scheme 3.19).[105]
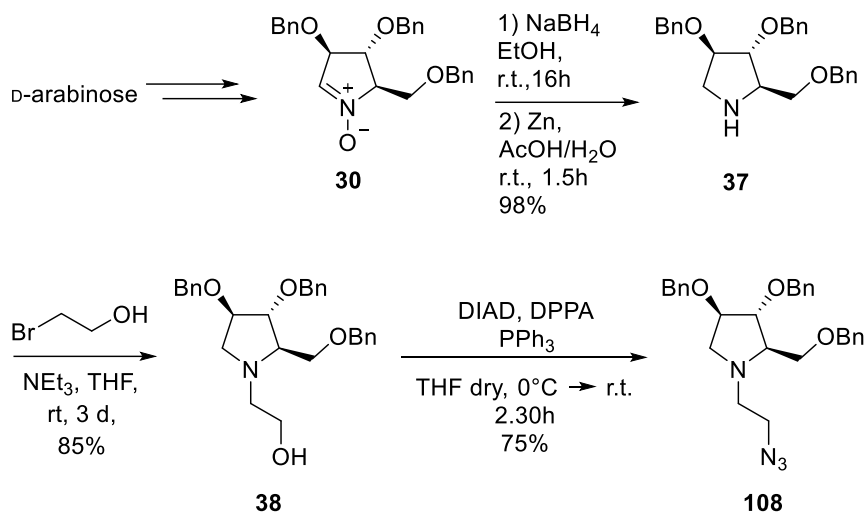
Scheme 3.19: Synthetic strategy to obtain pyrrolidine derivative **108**.

The deprotection of the hydroxyl groups of the pyrrolidine was not a trivial task, indeed we could not perform a reductive cleavage of the benzyl groups through a catalytic hydrogenation due to the presence of the azido moiety that is not resistant to those strong conditions and would undergo the reduction to amine. Furthermore, we could not exploit the same route used in previous cases of piperidine iminosugars (see section 3.2.1 and section 3.2.2), consisting in the alkylation of pyrrolidine skeleton with 1-bromo-2-azidoethanol, because of the explosivity of such low molecular weight azides. For this reason we thought to use a reduction milder than hydrogenation, using BCl_3 that in a previous work allowed to perform a benzyl cleavage in similar conditions.[105] In that way, we were able to obtain a sufficient amount of the final deprotected azido derivative to be characterized, but not enough to be 'clicked' to resorcinarenes (scheme 3.20).
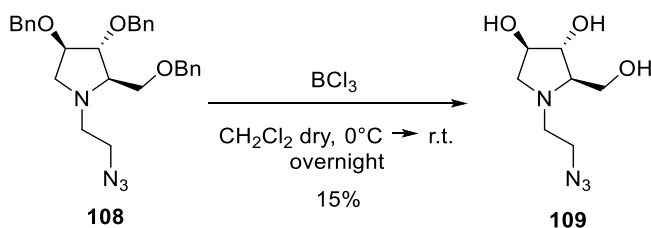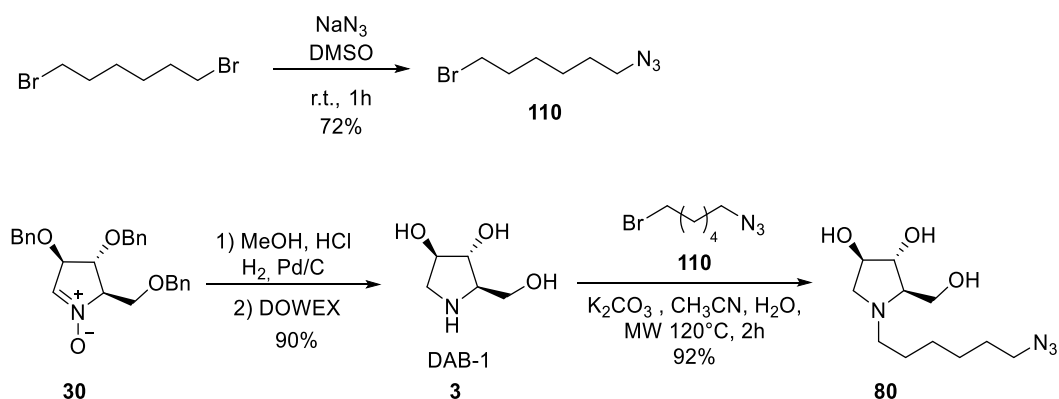

Scheme 3.20: Synthesis of pyrrolidine **109**.

---

[105] Ferhati X., Matassini C., Fabbrini M.G., Goti A., Morrone A., Cardona F., Moreno-Vargas A. J., Paoli P., *Bioorg. Chem.*, **2019**, *87*, 534-549.

For this reason, we though to elongate the alkyl chain from 2 to 6 carbon atoms, whose synthesis had been already accomplished in our laboratories for other projects (see section 3.3.1), and easily allows to obtain a bromo-azide chain without the risk of explosivity. Additionally, this longer derivative could furnish more flexible inhibitors with respect to those obtained using azido-pyrrolidine **109**. The starting point was again nitrone **30**, that was however hydrogenated to DAB-1, that already possesses the free hydroxyl groups, and successively alkylated with 1-bromo,6-hexanol **110** previously obtained from a mono-substitution with NaN$_3$ of 1,6-dibromohexane (scheme 3.21).

Scheme 3.21: Synthesis of pyrrolidine **80**.

We sent bioactive iminosugar **80** to Prof. Neri's laboratories, where the conjugation through a click CuAAC reaction to three different resorcinarenes was accomplished, since they possess a wide experience in the synthesis of this kind of multivalent systems.[106]

The synthesis of monovalent pyrrolidine compound **111** (figure 3.26), necessary to estimate the multivalent effect of our resorcinarenes, was already reported in our previous work.

---

[106] (a) Talotta C., De Rosa M., Soriente A., Spinella A., Gaeta C., Neri P., *Supramol. Chem*., **2019**, *31*, 62-68. (b) Iuliano V., Ciao R., Vignola E., Talotta C., Iannece P., De Rosa M., Soriente A., Gaeta C., Neri P., *Beilstein J. Org. Chem.*, **2019**, *15*, 2092–2104. (c) Concilio G., Talotta C., Gaeta C., Neri P., Monaco G., Zanasi R., Tedesco D., Bertucci C., *J.Org.Chem*., **2017**, *82*, 202–210.
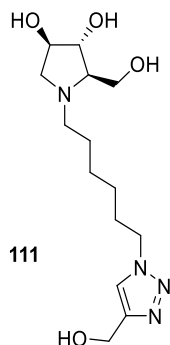
Figure 3.26: Monovalent reference compound **111**.

The multimeric scaffold structures are octavalent (**112** and **113**, scheme 3.22) and dodecacavalent (**114**) resorcinarenes, or calix[4]resorcinarenes, with different degree of rigidity (scheme 3.22). Indeed, while the scaffold **112** is conformationally more rigid thanks to the presence of methyl groups between the resorcinol units, compounds **113** and **114** are more flexible, and this could reflect, in our hypotheses, in a different biological activity. Moreover, calix[6]resorcinarenes such as compound **114**, much less common than calix[4]resorcinarenes, are interesting in terms of valency enhancement in the final conjugate.
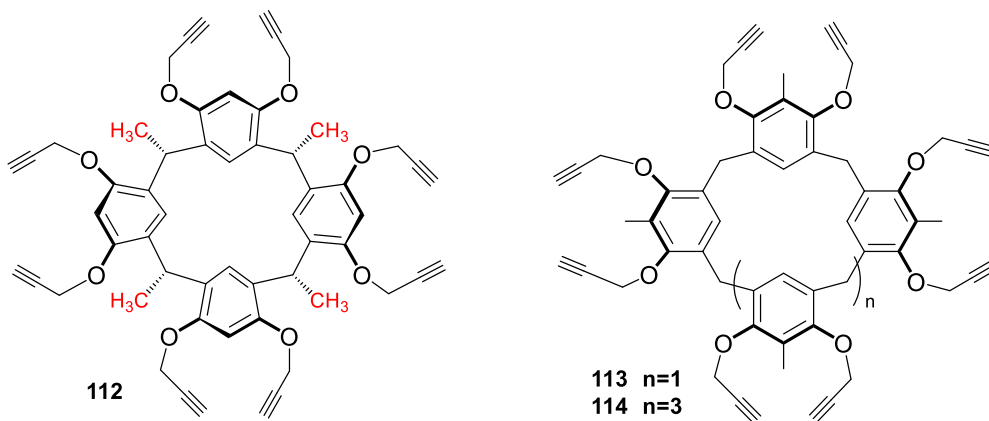

Scheme 3.22: Resorcinarene scaffolds **112**, **113** and **114**.

Once conjugated to our pyrrolidine iminosugars, we obtained the final resorcinarenes derivatives **115**, **116** and **117** (scheme 3.23). While compound **115** results to be stable in a cone conformation displaying bioactive pyrrolidine units in a syn orientation, the conformational mobility of the resorcinol rings in derivatives **116** and **117**, leads the pyrrolidine epitope to adopt different orientations.

_____
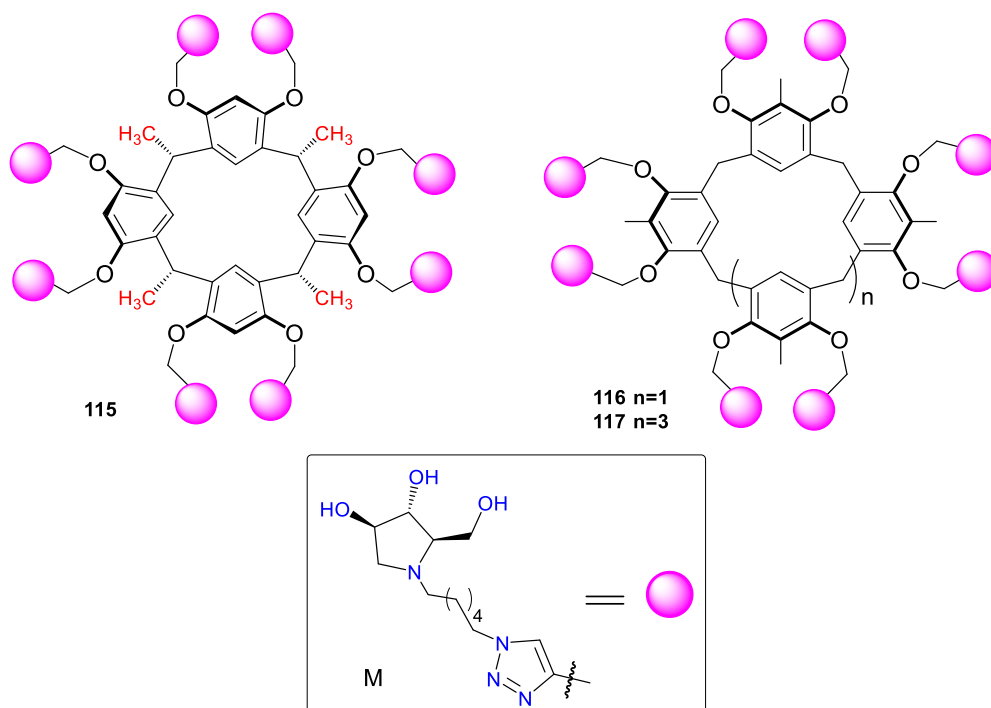
Scheme 3.23: Resorcinarene derivatives **115**, **116** and **117**.

All the glycocalix- were tested in the laboratories of Dr. Sestak, with whom we collaborated in several projects,[93] towards different mannosidases (see section 3.2.3.2). Since they noticed some problems in dissolving the glycoresorcinarenes in water, we wanted to find a method to increase the water solubility of the final compounds. Thus, we thought to functionalize the DAB-1 skeleton with a more polar linker to properly space the bioactive component from the resorcinarene scaffolds, for example exploiting a PEG-ylated chain similar to the one used in the synthesis of piperidine **99** (see section 3.2.2.1), but with a length comparable to pyrrolidine **111** (scheme 3.24). At first, we had to synthesize an appropriate PEG-ylated chain that could allow us to perform an alkylation using the same condition exploited for the piperidine (see section 3.2.1 and 3.2.2) and to obtain final compound **120**.
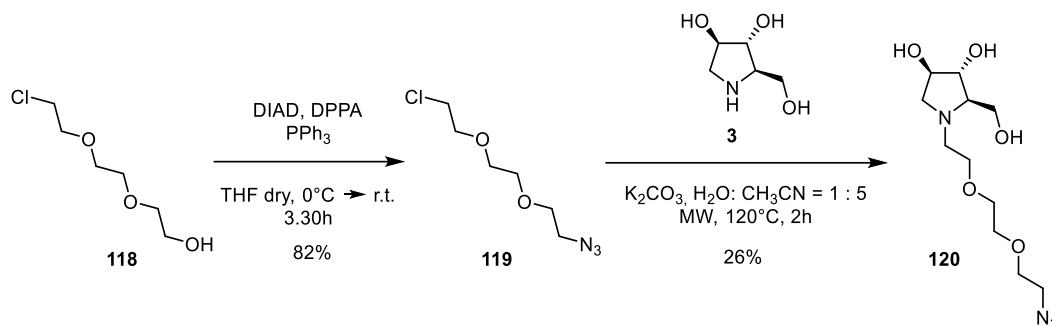
Scheme 3.24: Synthetic pathway to obtain PEG-ylated pyrrolidine **120**.

Starting from the commercial 2-[2-(2-chloroethoxy)ethoxy]ethanol **118**, we transformed the alcohol in an azido moiety with a Mitsunobu reaction to afford the azido derivative **119**, used in the following alkylation performed in a mixture of acetonitrile and water (1:5) in the presence of a base by heating with microwaves for two hours. In the case of pyrrolidine, we had some problems in the efficiency of alkylation reaction in fact, the first time that we tried, only a low amount of product was recovered (26% yield). We tried thus to avoid the microwave heating and to perform the reaction at reflux overnight. In this case we obtained an improvement in the results (38% yield, scheme 3.25), but without reaching the good yields obtained for the piperidines.
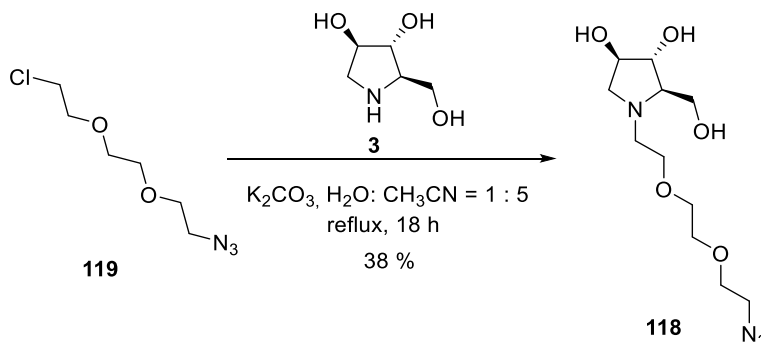
Scheme 3.25: Attempt of synthesis of pyrrolidine **120** using reflux heating.

We thought therefore that, by substituting chlorine atom with a more effective leaving group such as iodine, maybe we could enhance the percentage of recovered product, and so we decided to try this method, but unfortunately, the yield was comparable to the previous attempt (scheme 3.26). Anyway, we were able to obtain enough pyrrolidine azido derivative to send to Prof. Neri.
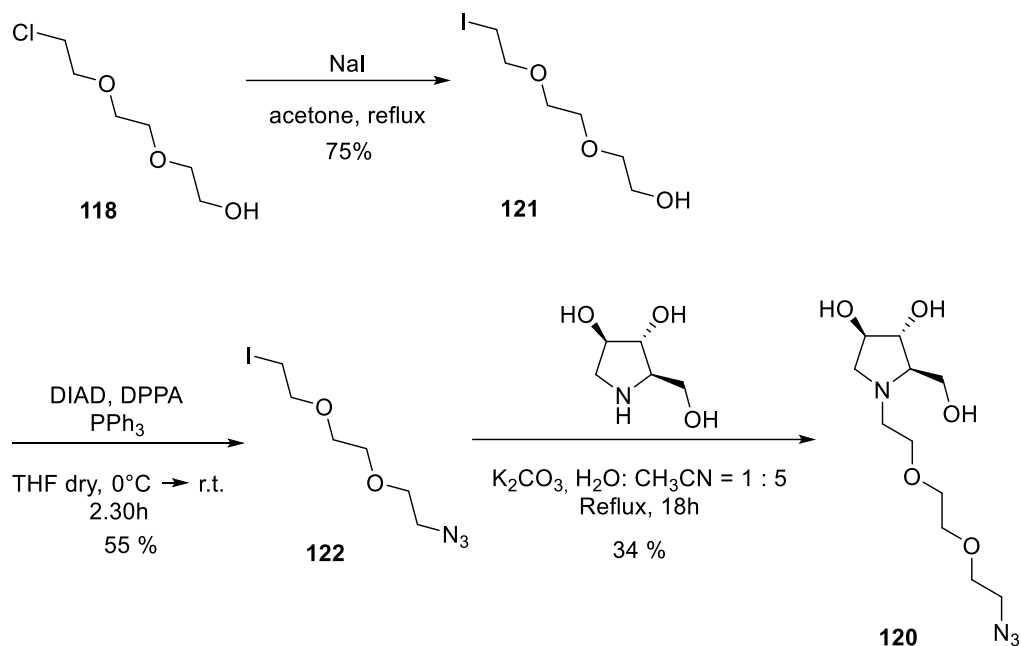
Scheme 3.26: Attempt with ioduration of compound **118**.

3.2.3.2 Biological evaluation

The three resorcinarene derivatives **115**, **116** and **117** bearing our pyrrolidine **80** were tested against a panel of commercial mannosidases by Prof. Sestak and co-workers. Moreover, rp and rp/n with respect to the reference monovalent compound **111**, were also evaluated. The data shown in table 3.9 show a good inhibitory profile, expressed in terms of IC_{50}, for all three compounds. Indeed, they all have the IC_{50} values in the micromolar range, thus demonstrating to be good mannosidases inhibitors. In particular, towards the commercial JB mannosidase the best result was achieved with the dodecavalent compound **117**, that showed an IC_{50} value of 3.8 μM. Also compounds **115** and **116**, both displaying a valency of 8 bioactive units, are potent JBMan inhibitors, with IC_{50} of 5.3 μM and 14.8 μM respectively. In the case of the Golgi mannosidase GManII, that is our target enzyme due to its involvement in some cancer growth processes, excellent inhibition values were obtained, with the best IC_{50} of the series showed by dodecavalent compound **117** (IC_{50} =1.7 μM). Comparing these inhibition data with the IC_{50} obtained towards lysosomal mannosidase LManII, that ranged between 173 μM and 865 μM, we can affirm that our resorcinarene pyrrolidines are selective for Golgi mannosidase with respect to the lysosomal mannosidase LManII, paving the way for a potential application of these compounds as anticancer agent.

Compound	Valency	JBMan		GManII		LManII	
		IC$_{50}$ (μM)	rp (rp/n)	IC$_{50}$ (μM)	rp (rp/n)	IC$_{50}$ (μM)	rp (rp/n)
111	1	1300	-	175	-	2450	-
115	8	5.3	248 (31)	3.7	47 (6)	173	14 (1.8)
117	12	3.8	342 (29)	1.7	103 (8.6)	523	4.7 (0.4)
116	8	14.8	88 (11)	5.3	33 (4.1)	865	2.8 (0.35)

Table 3.9: Relative potency (rp) and relative potency per active unit (rp/n) of compounds **115**, **116** and **117** as related to monovalent iminosugar **111**. Inhibitory activity towards the three α-mannosidases presented in IC$_{50}$ [μM].

Moreover, also in terms of multivalent effect quantification we had encouraging feedback, considering first that the monovalent reference compound showed an IC$_{50}$ value in the micromolar range only in one case (IC$_{50}$ = 175 μM towards GManII) while towards other mannosidases the inhibition is in the millimolar range. Moreover, all compounds had rp higher than 30; in particular, the best results of the series were obtained with dodecavalent compound **117** towards both JBman (rp = 342) and GManII (rp= 103), once again confirming the huge potentiality of a multivalent structure in the inhibition of some glycosidases of therapeutic interest. Comparing the two octavalent resorcinarenes instead, which differs for the conformational mobility of the pyrrolidine units, we can say that, given the same valency, a higher rigidity of the resorcinol rings (in derivative **115**) leads to an enhancement of the biological activity towards all the mannosidases, with IC$_{50}$ values of 5.3 μM, 5.7 μM and 173 μM (towards JBMan, GManII and LManII respectively), versus 14.8 μM, 5.3 μM and 865 μM (see table 3.9).

3.2.3.3 Conclusions

Three new multivalent compounds based on pyrrolidine DAB-1 derivatives anchored to resorcinarene scaffolds, were synthesized and tested against some mannosidases of therapeutic interest, thanks to the collaborations that we have with the two groups of Prof. Neri and Dr. Sestak. Once obtained the pyrrolidine ligands, they were multimerized onto resorcarenes with different valency and conformational orientations. The results obtained with biological tests showed a good inhibitory profile and precious information about the importance to find multivalent glycosidases inhibitors. Indeed, we obtained excellent results in term of both inhibition potency and selectivity towards the

enzyme we were interested in inhibiting, due to its involvement in anticancer applications, as reported in table 3.9. It will be of our interest to rationalize the differences in biological activity between the two derivatives with the same valency **115** and **116**, and in our future plans there will be some modelling studies, such as docking on the commercial JB mannosidase, considering that it was recently solved in its apo form by Prof. Compain and co-workers,[51] to better understand the mechanism of interaction between our inhibitors and the target enzyme. Moreover, the grafting of the pyrrolidine ligand **120** onto the same resorcinarenes **112**-**114** is now ongoing in the laboratories of Prof. Neri, and they will be tested by Prof. Sestak in the near future, in order to understand if the use of a more soluble bioactive unit could be enhanced in someway the inhibitory potential of whole multivalent structure.

3.2.3.4 Experimental section

For the general details see paragraph 2.4.

Synthesis of pyrrolidine 109: To a solution of **108** (256 mg, 0.54 mmol) in dry CH_2Cl_2 (48 mL) cooled to 0 °C by means of an ice bath, 4.88 mL of BCl_3 solution 1.0 M in hexane were added and the reaction mixture was stirred at room temperature under nitrogen atmosphere for 16 h. A TLC analysis (AcOEt: EP 2:1) showed the disappearance of starting material (Rf = 0.89) and formation of a new product (Rf = 0.50). To the reaction mixture 20 mL of a EtOH were added, and the reaction mixture was stirred until the solution was transparent, subsequently 20 mL of H_2O and 10 mg of basic resin Ambersep® 900-OH were added and left stirred for 1 hour. The mixture was filtered on cotton to remove the resin, washed thoroughly with MeOH. The solvent was evaporated at reduced pressure and the crude **109** was purified by FCC (CH_2Cl_2:MeOH: 12 %NH_3 1:5:0.3). The hydrochloride salt obtained from the first fraction of the column was then passed through DOWEX 50WX8 ion-exchange resin, by eluting sequentially with MeOH, H_2O and 12 % NH_4OH, affording free amine **109** as pale yellow oil (17 mg, 0.08 mmol, 15% yield). **[α]$_{28}^{D}$**= −25.1 (c = 0.84 in MeOH); **^{1}H-NMR** (400 MHz, D_2O): δ= 4.09-4.07 (m, 1H, H-3), 3.90-3.88 (m, 1H, H-4), 3.68 (dd, J = 5.1, 1.2 Hz, 2H, H-6), 3.45 (t, J = 6.0 Hz, 2H, H-2'), 3.07-3.01 (m, 2H, Ha-2, Ha-1'), 2.77 (dd, J = 11.1, 5.8 Hz, 1H, Hb-2), 2.62-2.55 (m, 2H, H-5, Hb-1') ppm; **^{13}C-NMR** (50 MHz, D_2O): δ= 79.0 (d, C-4), 75.6 (d, C-3), 71.9 (d, C-5), 61.2 (t, C-6), 58.6 (t, C-2), 53.4 (t, C-1'), 49.2 (t, C-2') ppm; **MS (ESI)**: *m/z* calcd (%) for $C_7H_{14}N_4O_3$ 202.11; found: 225.26 (100%, [M+ Na]$^+$). **Elemental analysis:** $C_7H_{14}N_4O_3$ (202.21) calcd. C, 41.58; H, 6.98; N, 27.71; found C, 41.46; H, 6.89, N, 27.60.

Synthesis of piperidine 120: A solution of **3** (60 mg, 0.45 mmol), 2-[2-(2-azidoethoxy)ethoxy]ethanol **119** (175 mg, 0.90 mmol) and K_2CO_3 (93 mg, 0.68 mmol) in 2.4 ml of a mixture CH_3CN/H_2O 5:1 was stirred at reflux for 24 h, until a TLC analysis (CH_2Cl_2:MeOH:NH$_3$ 2:1:0.2) showed the disappearance of the starting material (*R*f = 0.10) and the formation of a new product (*R*f = 0.79). After filtration through Celite®, the solvent was removed under reduced pressure and the crude was purified by FCC (CH_2Cl_2:MeOH:NH$_3$ from 6:1:0.1 to 2:1:0.1) affording pure **120** (*R*f = 0.21, 50 mg, 0.17 mmol, 38% yield) as a yellow oil. **[α]$_{21}^D$**= -41.5 (c = 0.68 in H_2O); **^{1}H-NMR** (400 MHz, D_2O): δ= 4.00 (ps, 1H, H-3), 3.81 (ps, 1H, H-4), 3.61-3.54 (m, 10H, H-6, from H-2' to H-5'), 3.39 (t, *J* = 4.7 Hz, 2H, H-6'), 3.02-2.94 (m, 2H, Ha-2, Ha-1'), 2.71 (dd, *J* = 11.2, 5.7 Hz, 1H, Hb-2), 2.55-2.46 (m, 2H, H-5, Hb-1') ppm; **^{13}C-NMR** (50 MHz, D_2O): δ= 78.9 (d, C-4), 75.5 (d, C-3), 72.0 (d, C-5), 69.6-68.7 (t, 4C, from C-2' to C-5'), 61.0 (t, C-6), 58.9 (t, C-2), 53.9 (t, C-1'), 50.2 (t, C-6') ppm; **MS (ESI)**: *m/z* calcd (%) for $C_{11}H_{22}N_4O_5$ 290.16; found: 313.04 (55%, [M+ Na]$^+$), 291.06 (100%, [M+ H]$^+$). **Elemental analysis:** $C_{11}H_{22}N_4O_5$ (290.32) calcd. C, 45.51; H, 7.64; N, 19.30; found C, 45.49; H, 7.48, N, 19.34.

3.3 Multivalent iminosugars through Copper free-methodologies

As mentioned before, most of the strategies used to design multivalent architectures require the use of the click chemistry reaction CuAAC (copper catalysed alkyne azide cycloaddition), that represents the most proficient way to rapidly access compounds with a high valency degree. Using that methodology, however, a wide range of scaffolds of different nature, such as dendrimers, calixarenes and recently also glycopolymers formed by iminosugars can be exploited. [107] Even if to date it is the predominant protocol to achieve the large variety of multivalent glycosidases inhibitors, CuAAC is associated with a general drawback consisting in the possibility of complexation of copper that could occur by the several triazole moieties and enhanced by the nitrogen atoms presents in iminosugar units, traducing in the possibility of a cytotoxicity of the final products if traces of copper remain as impurities.

Trying to overcome all the possible drawbacks related to the use of copper in the synthetic methodologies illustrated until now, we also thought to exploit alternative strategies to multimerize our bioactive iminosugar warheads, in particular we focused our efforts in the synthesis of Au glyconanoparticles (Au GNPs), adducts formed by a gold nanometric core decorated with sugars. Those systems were initially projected as a survey tool for the study of carbohydrate-lectin interaction[108] indeed, given their chemical and physical properties, they have all the characteristics necessary for this purpose: they are a colloidal system which is soluble and stable in water and able to cross the cell membrane thanks to the surface shell formed by carbohydrates. One of the main features that makes GNPs particularly attractive for our purposes is their multi-functionality, reflecting in the possibility of simultaneously insert more ligand units on the gold nano-core and modulating their arrangement, thus making them an advantageous alternative to other dendrimeric scaffolds previously seen (see section 3.1). The synthesis of glyconanoparticles is provided by a one-step procedure described for the first time by Brust and collaborators.[109] It is called "*in situ* direct synthesis", and it consists in the reduction *in situ* of a gold (III) salt (HAuCl$_4$) in the presence of glycoconjugates functionalized with a terminal thiol group and of NaBH$_4$ as a reducing agent (Figure 3.27).

_____

[107] Martínez-Bailén M., Galbis E., Carmona A. T., de-Paz M.V., Robina I., *Eur. Polymer J.*, **2019**, *119*, 213–221.

[108] (a) de La Fuente J. M., Barrientos A. G., Rojas T. C., Rojo J., Cañada J., Fernández A., Penadés S., *Angew. Chem. Int. Ed.* **2001**, *40*, 2257-2261. (b) Barrientos A. G., de La Fuente J. M., Rojas T. C., Fernández A., Penadés S., *Chem. Eur. J.*, **2003**, *9*, 1909-1921. (c) de La Fuente J. M., Penadés S., *BBA-Gen. Subjects,* **2006**, *1760*, 636.

[109] Brust M., Walker M., Bethell D., Schiffrin D. J., Whyman R., *J. Chem. Soc., Chem. Commun.*, **1994**, 801-802.
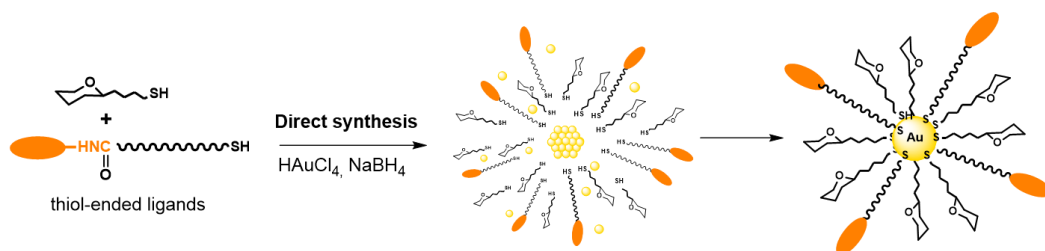
Figure 3.27: The direct method for the synthesis of A GNPs.

The Au GNPs formed are made up of self-assembled mono-layers (SAMs) of glycoconjugates, bound to the metal surface by S-Au bonds (Figure 3.28).
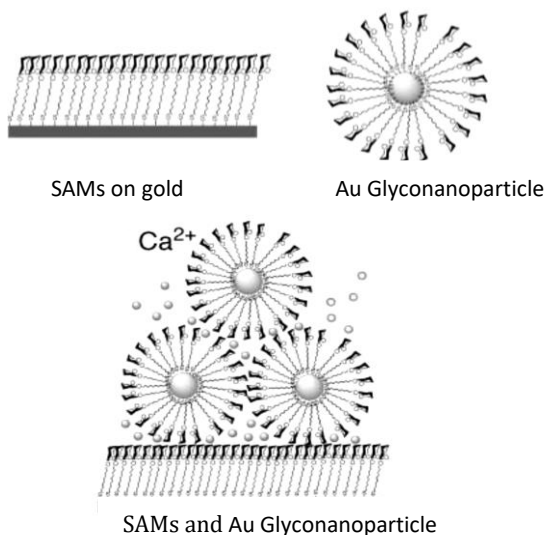

SAMs on gold   Au Glyconanoparticle

SAMs and Au Glyconanoparticle

Figure 3.28: SAMs glyconanoparticles.

The approach based on the use of carbohydrate self-assembled monolayers (SAMs) on two- and three-dimensional gold surfaces is termed glyconanotechnology, and it allows to obtain multivalent structures without employing the click CuAAC approach, thus avoiding the risk of finding copper residues in the final products. Since the direct synthesis allows to insert different ligands on the same core, it becomes possible to prepare a wide range of glyco-adducts with different "load" of ligands. In fact, together with the biologically active part of the GNPs (the *active component*), it is necessary to introduce components that modulate the rigidity and flexibility without interfering in their biological activity.[110] These

---

[110] Marradi M., Chiodo F., García I., Penadés S., *Chem. Soc. Rev.*, **2013**, *42*, 4728-4245.

_____

are called *inner components*, and allow to obtain a better spatial arrangement of the active component on the gold surface and an adequate solubility of the final system in water, and on the basis of previous studies, a fairly long and amphiphilic linker was the ideal to impart flexibility and to assist the dispersion of the glyconano-adducts in water.[111]

Our group recently contributed to the field by synthesizing the first example of multivalent glyconanoadducts containing biologically active iminosugars as active component, and monosaccharides as inner component to target different glycosidases. A synthetic strategy that allowed the inclusion of iminosugars (pyrrolizidines and piperidines) on a very small gold core (the diameter is less than 2 nm) has been developed, to verify the presence of a positive multivalent effect. Moreover, this approach has made possible the achievement of multivalent iminosugars with a density modulable by simply varying the mutual percentage between the inner and the active component (figure 3.29).[112]
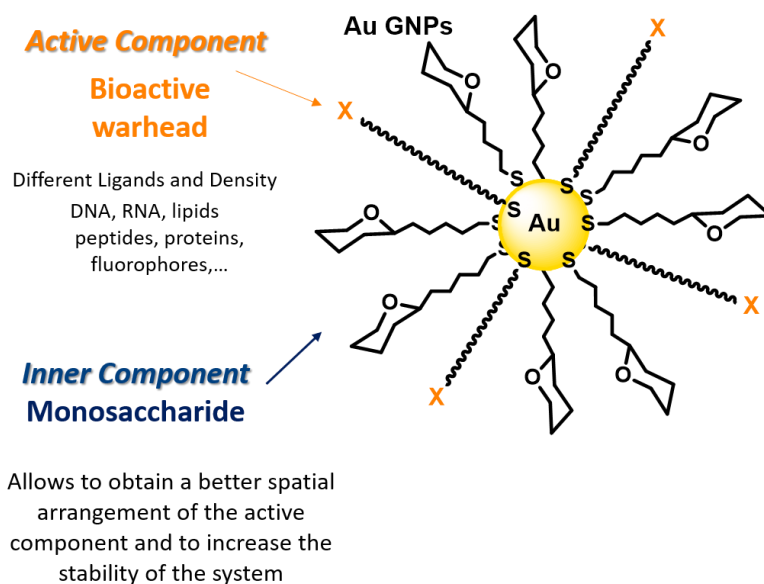

Active Component
Bioactive warhead

Different Ligands and Density
DNA, RNA, lipids peptides, proteins, fluorophores,…

Au GNPs

Inner Component
Monosaccharide

Allows to obtain a better spatial arrangement of the active component and to increase the stability of the system

Figure 3.29: General scheme of gold glyconanoparticles (GNPs).

The obtained Au GNPs contained as inner component two kind of iminosugars previously synthesized in our laboratories and then properly functionalized, of piperidine and pyrrolizidine nature (figure 3.30).

_____

[111] (a) Martínez-Ávila O., Hijazi K., Marradi M., Clevel C., Campion C., Kelly C., Penadés S., *Chem. Eur. J.*, **2009**, *15*, 9874-9888. (b) Safari D., Marradi M., Chiodo F., Th Dekker H. A., Shan Y., Adamo R., Oscarson S., Rijkers G. T., Lahmann M., Kamerling J. P., Penadés S., Snippe H., *Nanomedicine*, **2012**, *7*, 651-662.

[112] Matassini C., Marradi M., Cardona F., Parmeggiani C., Robina I., Moreno-Vargas A.J., Penadés S., Goti A., *RSC Adv.*, **2015**, *5*, 95817-95822.
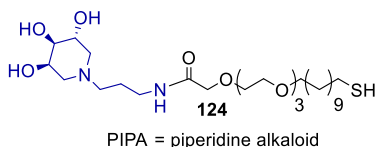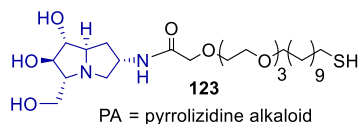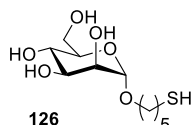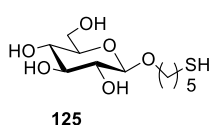
Active component

Au-GNPs

123

PA = pyrrolizidine alkaloid

124

PIPA = piperidine alkaloid

127a: 20% PA-Au-βGlc
127b: 40% PA-Au-βGlc
127c: 20% PA-Au-αMan
127d: 40% PA-Au-αMan

127

Inner component

125 **126**

128a: 20% PIPA-Au-βGlc
128b: 40% PIPA-Au-βGlc

128
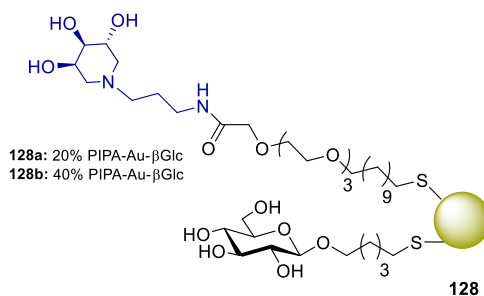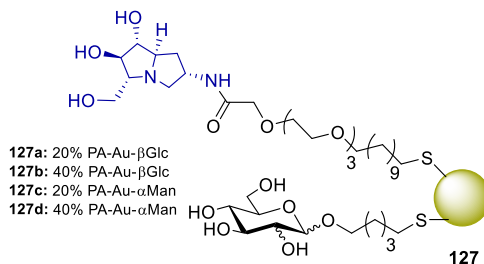
Figure 3.30: Glyconanoparticles with pyrrolizidine and piperidine iminosugars.

The glyconano-adducts **127** and **128** were prepared with different active and inner component percentages and then tested towards commercial glycosidases, showing only retention of the inhibitory activity, but any positive multivalent effect. Moreover, it was also observed that using **125** or **126** as inner component made no difference in the biological activity.

Following this procedure, in part of the PhD thesis we decided to apply the same strategy seen now to multimerize other two kind of iminosugars, already proved to be good inhibitors towards two glycosidase enzymes: the first one is a pyrrolidine derivative of natural DAB-1 (section 3.3.1), to be tested against the two sulfatases IDS and GALNS (see chapter 1). The other bioactive warhead is the widely envisaged DNJ piperidine iminosugar, available in our laboratories thanks to the collaboration with Prof. Compain from the University of Strasbourg, that we would like to test against JBMan (scheme 3.27).
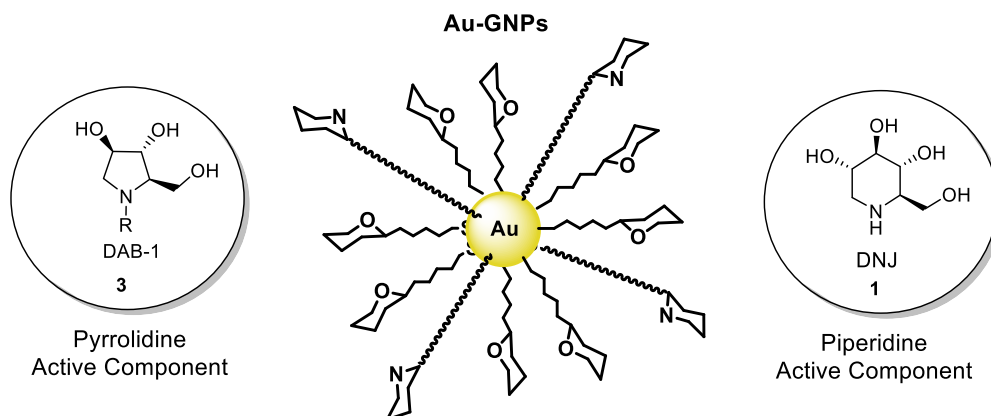
Scheme 3.27: Aim of this work: synthesis of gold glyconanoparticles decorated with DAB-1 and DNJ derivatives as active component.

Additionally, in searching novel methodologies to avoid the use of click CuAAC reaction, we envisaged a strategy based on a sequence of 1,3-dipolar cycloaddition with a high stereo and regioselectivity (section 3.3.3).

3.3.1 Hybrid Gold Glyconanoparticles (DAB-1 based)

When multimerized on a dendrimeric scaffold, the natural DAB-1 pyrrolidine iminosugar was demonstrated to be an excellent inhibitor of two lysosomal sulfatases, namely *N*-acetylgalactosamine-6-sulfatase (GALNS) and iduronate-2-sulfatase (IDS), whose deficiency leads to lysosomal storage diseases (Morquio A and Hunter diseases, respectively. See section 1.2.4).[47] These pathologies are currently treated by infusion of recombinant enzymes, which suffer from low stability in vivo. Hence, the identification of inhibitors of these recombinant enzymes represents the starting point for the development of enzyme stabilizers.[113] Based on our previous findings, where we developed a straightforward strategy to build gold glyconanoparticles containing a bioactive iminosugar component, we aimed to achieve the multimerization of DAB-1 onto Au GNPs, in order to find new GALNS and/or IDS inhibitors. Our results are the object of this part of the PhD thesis and can be also found in this paper:

Matassini C., Vanni C., Goti A., Morrone A., Marradi M., Cardona F.
Multimerization of DAB-1 onto Au GNPs affords new potent and selective *N*-acetylgalactosamine-6-sulfatase (GALNS) inhibitors, *Org. & Biomol. Chem.*, **2018**, *16*, 8604– 8612.

_____

[113] Boyd R. E., Lee G., Rybczynski P., Benjamin E. R., Khanna R., Wustman B. A., Valenzano K. J., *J. Med. Chem.*, **2013**, *56*, 2705-2725.

3.3.1.1 Results and discussion

With the aim to synthesize the gold glyconanoparticles (Au GNPs) decorated with pyrrolidine iminosugars, we started with the design of the active and inner components. It was necessary indeed to insert in our pyrrolidine ligand a properly functionalized linker (**129**, scheme 3.28), in order to allow the formation of a Au-S bond,[114] and to space the bioactive warhead from the gold core in order to avoid the whole system collapse.
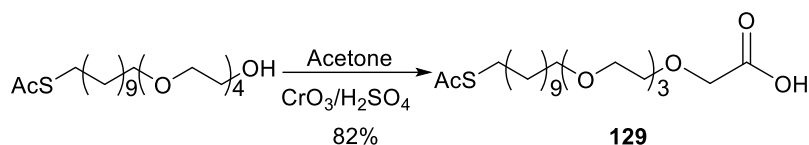

Scheme 3.28: Synthesis of PEG-ylated linker **129**.[114]

To achieve this derivative, we started from the D-arabinose derived nitrone **30**, that was first alkylated with 1,6-bromo,azidohexane **110**, then catalytically hydrogenated to afford the corresponding amino derivative **131** with 65% yield after basic elution over an ion exchange acid resin DOWEX-50WX8 (scheme 3.29).[47]
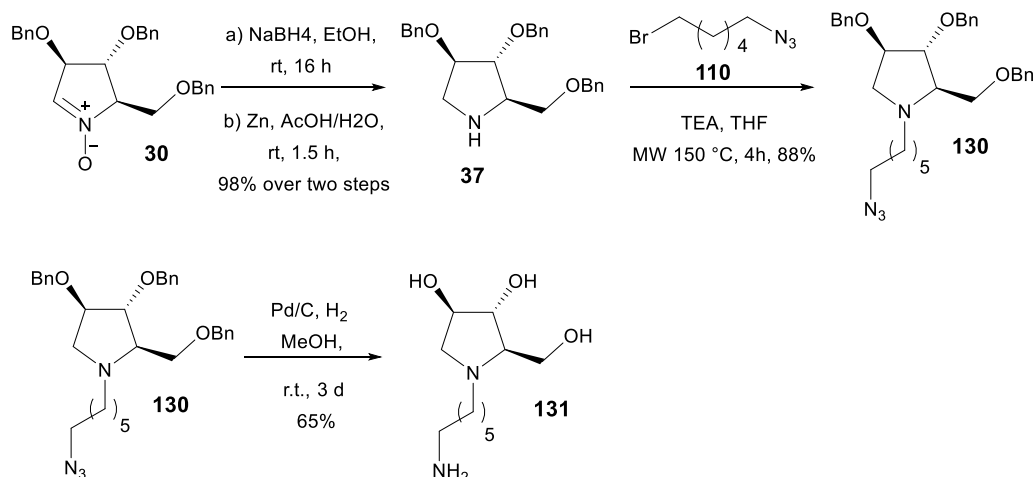
Scheme 3.29: Synthesis of pyrrolidine amino derivative **131**.[47]

However, coupling of **131** with the linker **129** was not selective, and afforded an inseparable mixture of the two regioisomers: the desired amide **132** and its ester derivative **133** (scheme 3.30).

[114] He S., Garcia I., Gallo J., Penadés S., *CrystEngComm*, **2009**, *11*, 2605.

_____
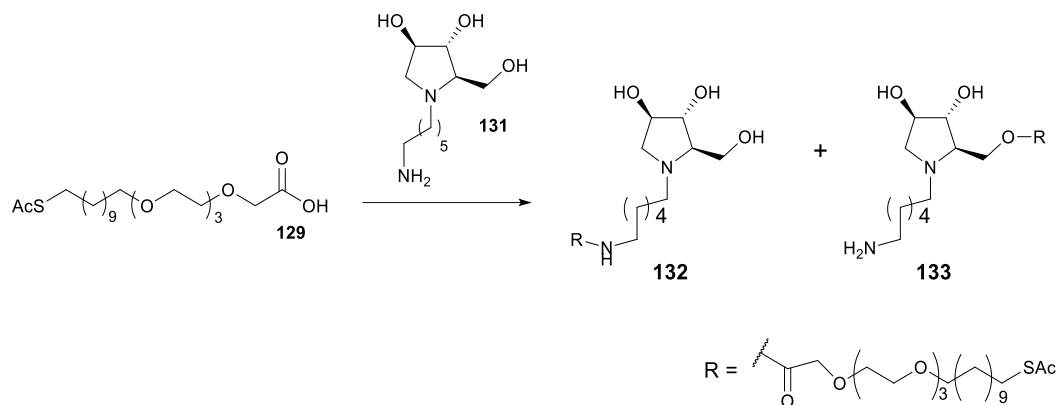
Scheme 3.30: First attempt for the synthesis of **132**.

Therefore, we thought to use an alternative strategy, which eliminated the problem of poor regioselectivity in the formation of the amide bond: to introduce the terminal amino moiety on the pyrrolidine, we first alkylated the endocyclic nitrogen of DAB-1 **3** with an azido-terminal aliphatic chain, thus obtaining derivative **80**; then, we protected the hydroxyl moieties with acetyl groups to give compound **134**, considering that the O-acetyl protecting groups would be removed when liberating the thiol-ending moiety. At this point we reduced the azide group to amine **135** using the Staudinger reaction. However, the reaction was troublesome, due to problematic product isolation from the formed triphenylphosphine oxide. We managed to overcome this problem by using polymer-bound Ph$_3$P [115] and the amine **135** was isolated in quantitative yield after refluxing for 4 h in THF/H$_2$O. In this way we were able to drive the reaction towards the formation of a single regioisomer, thus making the coupling with **129** to give the compound **132** (Scheme 3.31).

_____

[115] Ayesa S., Samuelsson B., Classon B., *Synlett.*, **2008**, *1*, 97-99.
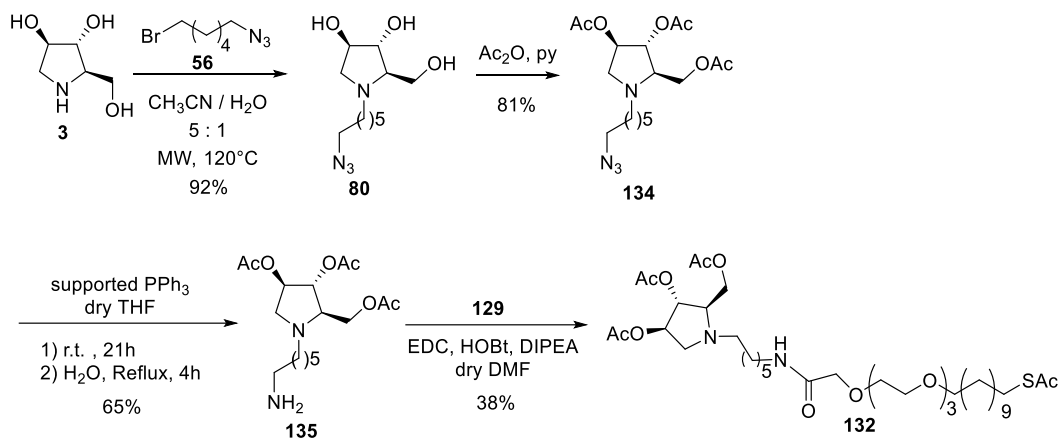
Scheme 3.31: Synthethic patway fo the synthesis of **132**.

As inner component we used βGlcC$_5$S **125**, obtained starting from β-glucose pentaacetylate **54**, which was first glycosylated at the anomeric oxygen by Fisher esterification with 4-penten-1-ol alcohol (yield = 30%) and then thioacetylate with thioacetic acid (yield = 85%). Final deprotection with sodium metanoate in MeOH led to the obtainment of product **125** in 63% yield (Scheme 3.32).[116]
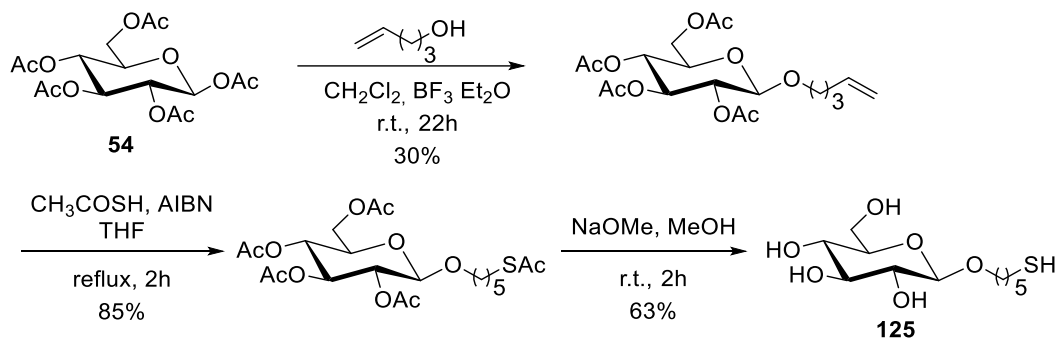
**Scheme 3.32:** Synthesis of inner component **125**.

It is worth noting that while ligand **132** has a long and amphiphilic linker to impart flexibility and assist the water dispersibility of the final GNPs, the sugar ligand **125** has a shorter and hydrophobic linker to ensure the rigidity of the nanoparticle core.

With active and inner components in hands, we could provide the glyconanoadduct formation, by preliminary establishing the mutual percentage between the two components. In that way we built a small library of Au GNPs at different percentages of

---

[116] Love J. C., Estroff L. A., Kriebel J. K., Nuzzo R. G., Whitesides G. M., *Chem. Rev.* **2005**, *105*, 1103-1169.

_____

iminosugar. As mentioned before, the *in situ* synthesis allows to control the growth of the gold cluster by simply varying the ligands mixture/Au(III) molar ratio and the simultaneous insertion of different ligands. Water-soluble and stable gold GNPs of 2-nm average diameter were obtained by adding an aqueous solution of tetrachloroauric acid (HAuCl$_4$, 1 equiv.) to a methanolic solution of a mixture of thiol-derivatized conjugates (active iminosugar conjugate and inner sugar component, 3 equiv.) in the desired proportion. The resulting mixture was reduced with an excess of NaBH$_4$ (27 equiv.) as reducing agent and the suspension was vigorously shaken for 2 h at 25 °C. The supernatant was removed, the nanoparticles were washed with methanol and the residue was dissolved in milliQ water, purified by dialysis and characterized by ^{1}H NMR spectroscopy, transmission electron microscopy (TEM), infrared spectroscopy (IR), and ultraviolet spectroscopy (UV). Glyconanoparticles with different density of active component were obtained by changing the ratio of iminosugar conjugate with respect to sugar derivative as inner component in the initial mixture before GNP formation. The ratio of the components was controlled by ^{1}H NMR. The proportion of the ligands on the gold surface was also examined by ^{1}H NMR after cluster formation (analysis of the supernatant and washings) as well as performing qNMR of GNPs in deuterium oxide with an internal reference. This well established protocol employed for the quantification of different ligands onto Au GNPs,[117] allowed the quantitative ^{1}H NMR determination of the iminosugar on the nanoparticle by integration of a diagnostic signal (see the section 3.3.1.3) with respect to the internal standard signal.[112] The ^{1}H NMR spectra of the GNPs featured broader peaks with respect to those of the corresponding free ligands, testifying for nanoparticle formation. Regarding the sugar/iminosugar ligand ratio, its uniformity was ascertained by ^{1}H NMR performed on the reaction mixture (before) and, after nanoparticle formation, on both the supernatant and the washings (after). The Au GNPs were also characterized by UV-vis spectroscopy and transmission electron microscopy (TEM). Following the above procedure, Au GNPs decorated with 30% (**138a**), 40% (**138b**) and 50% (**138c**) densities of iminosugar were prepared (Scheme 3.33). Au GNPs **138a** and **138b** were dispersible in water and TEM images showed metallic cores with average diameters ranging from 1.7 nm to 1.9 nm. These nanoparticles could be freeze-dried and re-dispersed in water without flocculation. Conversely, 50% iminosugar-coated Au GNPs (**138c**) showed difficulties in isolation after washing with MeOH and could not be properly redispersed in water after freeze-drying.

_____

[117] (a) Manea F., Bindoli C., Fallarini S., Lombardi G., Polito L., Lay L., Bonomi R., Mancin F., Scrimin P., *Adv. Mater.*, **2008**, *20*, 4348; (b) Chiodo F., Enríquez-Navas P. M., Angulo J., Marradi M., Penadés S., *Carbohydr. Res*., **2015**, *405*, 102.
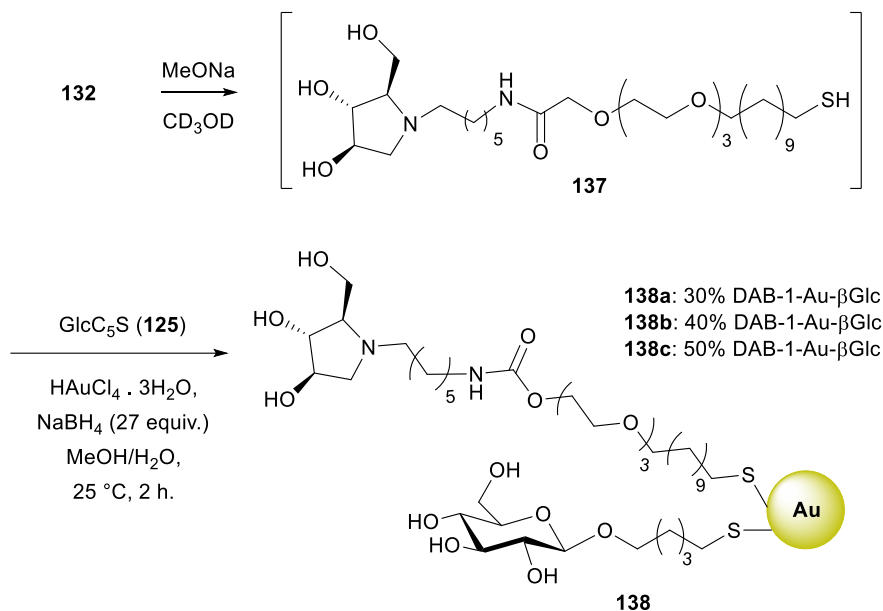
Scheme 3.33: Synthesis of the DAB-1-decorated Au GNPs **138**.

If on one hand the exceptionally small dimensions of the gold core have the advantage to give to the glyconanocomposites better biological properties (such as, for example, an efficient internalization in the cell), on the other side they limit the possibility to increase the percentage of the iminosugar beyond a certain limit. As a matter of fact, we could not increase the loading of the iminosugar ligand more than 40% without losing water dispersibility. For this reason, we also set out a strategy that would allow us to expand the valency of the system prior to the formation of the gold nanoparticles, by combining the dendrimeric technique (see section 3.1), using suitable bioactive dendrons equipped with a thiol-ending functionality, in order to increase the valency without affecting water stability properties, thanks to a more favorable balance between hydrophilic heads and hydrophobic chains. In that case we decided to use the same trimeric alkyne scaffold used in the synthesis of multimeric trihydroxypiperidines (**81**, see section 3.2.1.1) to multimerize our pyrrolidine azido derivative **134**: indeed, it possesses the alkyne moieties necessary to click the azido active warhead, and an amine that could be coupled with the thiol-ended linker **129** (scheme 3.34). Moreover, the CuAAC reaction that contemplates the 'critical' use of copper as catalyst, is done several steps before the grafting of the active component to the gold core, reducind in this way the risk of contamination. Furthermore, compounds bearing the trimeric linker, have been subjected to ICP analysis to assess the absence of copper traces.
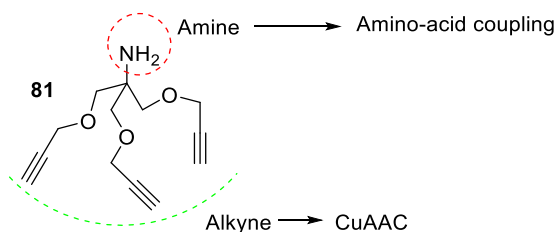
Scheme 3.34: Trivalent scaffold to build dendrimeric ligand.

Reaction of the azido-armed acetyl protected **134** with the trivalent amine **81**[118] gave the trivalent compound **139** in excellent 91% yield after purification by FCC (scheme 3.35).
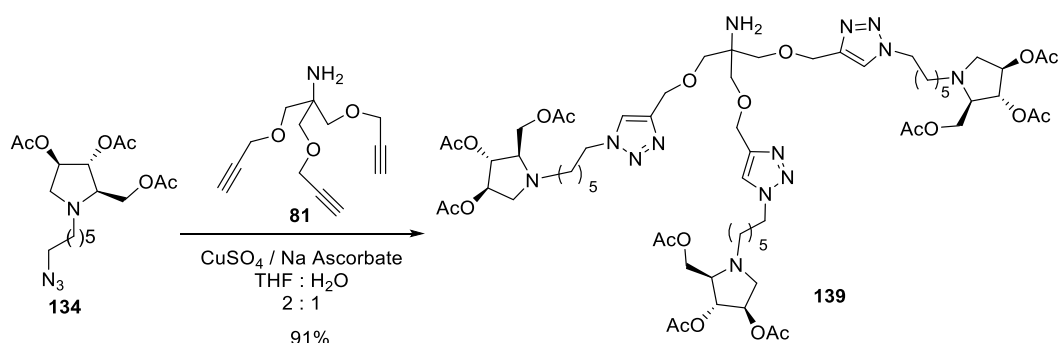

Scheme 3.35: Synthesis of trivalent active component **139**.

Unfortunately, reaction of the amine **139** with the acid **129** under the same conditions used for amine **135** (1-ethyl-3-(3-dimethylaminopropyl)carbodiimide (EDC), 1–hydroxybenzotriazole (HOBt) and diisopropylethylamine (DIPEA) in dry DMF at room temperature) failed to yield the desired product **140**. However, coupling of **139** with the acid **129** in the presence of 3-(diethoxyphosphoryloxy)-1,2,3-benzotriazine-4(3H)-one (DEPBT)[119] and DIPEA in dry THF for 6 days at room temperature afforded the compound **140** with a remarkable 85% yield (scheme 3.36). Based on this result, the amine **135** was reacted with the acid **129** using DEPBT as coupling agent (reaction conditions: DEPBT, DIPEA, dry THF, 6 d, r.t.), in order to verify if we could obtain a yield enhance, but no improvement (around 40% with respect to 38%) was observed.

---

[118] Chabre Y. M., Contino-Pépin C., Placide V., Shiao T. C., Roy R., *J. Org. Chem.*, **2008**, *73*, 5602.
[119] Li H., Jiang X., Ye Y.-h., Fan C., Romoff T., Goodman M., *Org. Lett.*, **1999**, *1*, 91.
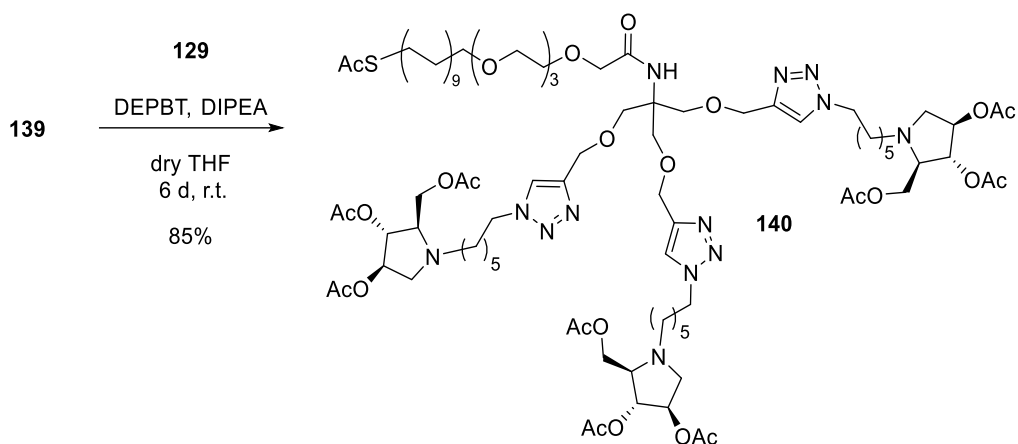
Scheme 3.36: Coupling between amine **139** and acid **129** with DEPBT.

With trivalent ligand **140** in hand, the preparation of Au GNPs **142** decorated with 30% of the trivalent DAB-1 was achieved following the same protocol employed for the synthesis of Au GNPs **138** (scheme 3.37).

142: 30% tri-DAB-1-Au-βGlc
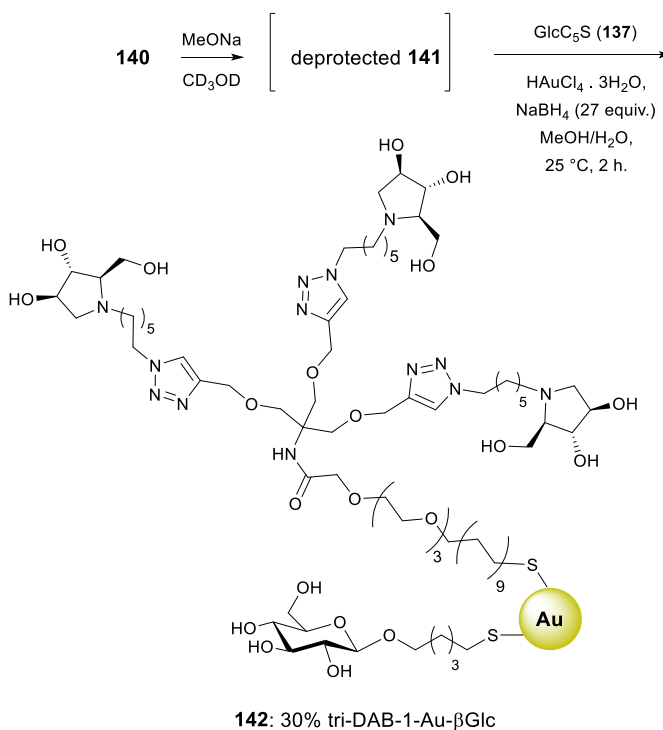
Scheme 3.37: Synthesis of tri-DAB-1-decorated Au GNPs **141**.

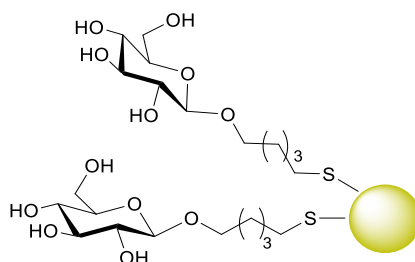After work-up (MeOH washings) and purification (dialysis), the Au GNPs **142** resulted dispersible and very stable in water and they were characterized analogously to the Au GNPs **138**.
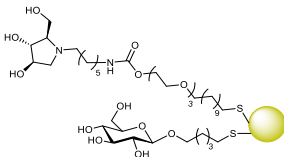
Au GNPs functionalized with 100% of GlcC$_5$S (100% Au βGlc, **143**, scheme 3.38) were also prepared following a reported procedure[111a] to be employed as control systems.

143: 100% Au-βGlc

Scheme 3.38: Au GNPs **143** functionalized with 100% of GlcC$_5$S.

The small library of Au GNPs synthesized in this project, is summarized in the table below, with all data related to them, experimentally extrapolated. In the table the estimated molecular weight of the Au GNP is also reported, calculated by following an empirical formula reported in literature that correlates the gold core diameter with the molecular weights of the nanoparticles.[120] Moreover, in the last column of the table it is reported the amount of the active component DAB-1 as measured by qNMR. It is worth noting that the concentrations found with these two different methods (by TEM and qNMR) are quite in agreement (the same order of magnitude) for the GNPs 138a and 138b while, for GNPs 142, bearing the dendrimer as *active component*, the two values are not in accordance.

Au-GNPs	Characterization			
	TEM	**Estimate M.W.** (from TEM)	**DAB-1 amount** (from TEM)	**DAB-1 amount** (from qNMR)
30% DAB-1 **70% Au-βGlc** **138a**	1.7±0.4 nm	(C$_{30}$H$_{59}$N$_2$O$_8$S)$_3$(C$_{11}$H$_{21}$O$_6$S)$_{12}$ Au$_{140}$ M.W. = 32775	0.54mg Correspond to **49 nmol**	0.54mg Correspond to **50 nmol**

[120] Martinez-Avila O., Hijazi K., Marradi M., Clavel C., Campion C., Kelly C., Penadés S., *Chem. Eur. J.*, **2009**, *15*, 9874-9888.
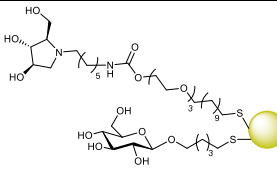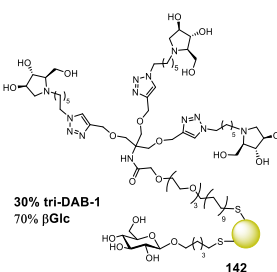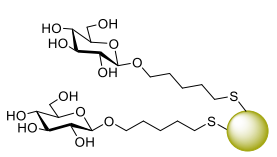
40% DAB-1 **60% Au-βGlc** **138b**	1.9±0.3 nm	$(C_{30}H_{59}N_2O_8S)_6(C_{11}H_{21}O_6S)_{11}$ Au_{140} M.W. = 34317	0.2mg Correspond to **35 nmol**	0.2mg Correspond to **32 nmol**
30% tri-DAB-1 **70% βGlc** **142**	2.0±0.5 nm	$(C_{65}H_{118}N_{13}O_{17}S)_2(C_{11}H_{21}O_6S)_5$ Au_{140} M.W. = 31754	0.27mg Correspond to **51 nmol**	0.27mg Correspond to **35 nmol**
143: 100% Au-βGlc	1.7±0.4 nm	$(C_{11}H_{21}O_6S)_{35}Au_{140}$ M.W. = 37422	/	

Table 3.10: Resume table of DAB-1-based Au GNPs.

3.3.1.2 Biological evaluation

As mentioned before, the purpose of this project was to evaluate the inhibitory activity of the new synthesized Au GNPs towards the two sulfatases GALNS and IDS, involved respectively in the metabolic diseases Morquio A Syndrome and Hunter's Disease. The glyconanoparticles **138a-b**, **142** and **143** obtained were subjected to preliminary inhibition tests, carried out thanks to the collaboration with the group of Prof. A. Morrone at the laboratory of Metabolic Diseases of the Meyer Hospital of Florence. They were initially evaluated at 0.2 mg/mL concentration in extracts from a pool of human leukocytes isolated from healthy donors by fluorimetric test. Compound **80** was used as the monovalent reference compound, and the percentage of inhibition towards GALNS and IDS was evaluated at 1 mM of inhibitor, as previously reported.[121] The collected data are summarized in table 3.11. For percentages of inhibition higher than 70%, the corresponding IC_{50} values were evaluated by measuring human enzyme activity at different Au GNPs

---

[121] (a) Van Diggelen O. P., Zhao H., Kleijer W. J., Janse H. C., Poorthuis B. J. H. M., Van Pelt J., Kamerling J. P., Galjaard H., *Clin. Chim. Acta*, **1990**, *187*, 131. (b) Voznyi Y. V., Keulemans J. L., van Diggelen O. P., *J. Inher. Metabol. Dis.*, **2001**, *24*, 675.

concentrations (see section 3.3.1.4).

| GNP	Iminosugar conc. (µM) in 0.2 mg/mL^{-1} of Au GNPs	% of Inhibition	
		IDS IC$_{50}$, µM	GALNS IC$_{50}$, µM
138a	18.5	15%	83%[a] **0.025 mg/mL^{-1}** (2.31)[b]
138b	32.0	39%	88% **0.016 mg/mL^{-1}** (2.56)[b]
142	26.0	16%	97% **0.004 mg/mL^{-1}** (0.52)[b]
143	0	18%	75% 0.028 mg/mL^{-1}
Compound	**Iminosugar conc. (µM)**	**IDS**	**GALNS**
80	1000	0%	52%[c]
144	3000	n.d.	29%[c]
78	9000	96%[c,d] (**140**)[d]	94%[c,d] (**47**)[d]

Table 3.11: Percentage of inhibition towards human GALNS and IDS at 0.2 mg mL^{-1} in terms of Au GNPs. IC$_{50}$ values were measured for inhibition percentage higher than 70% and are reported as mg L^{-1} of Au GNPs in bold and as µM concentration of iminosugar in parentheses.

[a] Percentage of inhibition obtained at 0.15 mg mL−1 concentration of Au GNPs.
[b] IC50 (µM) in terms of the iminosugar concentration. [c] Percentage of inhibition obtained at 1 mM concentration. [d] Data taken from ref. 47. The reported IC$_{50}$ value was obtained using the same experimental protocol of this manuscript (e.g. same substrate concentration).

The effective iminosugar component concentration of Au GNPs **138a**, **138b** and **142** was determined by qNMR. This allowed us to measure the IC$_{50}$ values not only as mg L^{-1} of Au GNPs, but also as the µM concentration of the iminosugar in the nanoparticles (for **138a**, **138b** and **142**, values are in parentheses). Monovalent reference compound **80** showed around 50% inhibition of GALNS, while multivalent Au GNPs decorated with DAB-1

inhibited GALNS with percentages ranging from 83% to 97%. In terms of DAB-1 concentration, these results indicate that GALNS was strongly inhibited in the low micromolar/high nanomolar range. In other words, the presentation of the multiple DAB-1 units at the gold glyconanoparticle surface generates more potent GALNS inhibitors, confirming our previous observation reported with DAB-1 based dendrons (scheme 3.39).[47]
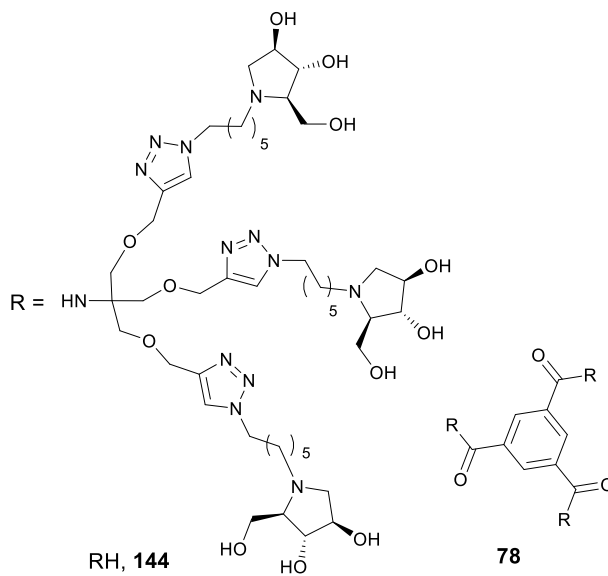
Scheme 3.39: Trivalent DAB-1 based dendron **144** and nonavalent DAB-1 based dendrimer **78**.

A moderate enhancement of inhibitory activity was observed when the number of grafted active units was increased from 30% DAB-1 βGlc (**138a**) to 40% DAB-1 βGlc (**138b**), being the IC_{50} = 0.016 mg mL^{-1} for vs. IC_{50} = 0.025 (table 3.29). In terms of the iminosugar concentration, no enhancement of inhibitory activity was observed at all, being IC_{50} = 2.56 µM vs. IC_{50} = 2.31 µM). This trend parallels that previously observed on Au GNPs coated with a pyrrolizidine iminosugar in the inhibition of a different enzymatic target, namely amyloglucosidase from *Aspergillus niger*.[112] Also in this case, the inhibitory activity was insensitive to the increase of the percentage of the iminosugar ligand with respect to the sugar inner component. However, while towards amyloglucosidase from *Aspergillus niger* 100% Au βGlc **143** did not show any inhibitory activity when tested at 0.2 mg mL^{-1}, with GALNS an unexpected remarkable inhibition was observed (75% inhibition, IC_{50} = 0.028 mg mL−1, table 3.29). This prompted us to reflect on the role of the sugar (the inner component). Indeed, the sugar part, which constitutes an essential component of our nanoparticle/scaffold, exerts a considerable inhibitory activity itself. As a matter of fact, it has been recently reported that sugars, when multivalently presented on nanodiamond

particles[122] and on magnetic nanoparticles,[123] may afford a significant inhibitory activity, even if the monovalent sugar ligand is not an inhibitor. Also in our case, neither the thiol ending GlcC$_5$SH nor its disulfide dimer showed any inhibitory activity towards GALNS when screened up to 2 mM inhibitor concentration (see section 3.3.1.4). The significant inhibition observed for **143** suggests that the GALNS enzyme is particularly prone to accept multivalent ligands. Moreover, these results confirm that GALNS, unlike lysosomal glycosidases that show exquisite specificity for the saccharide to hydrolyze, has substantial promiscuity in substrate recognition, as previously reported.[89] Our data suggest that the simultaneous presentation of the sugar and the iminosugar units results in the enhancement of the affinity towards the GALNS enzyme, thus acting in a synergistic way. The greatest improvement was achieved by protruding the trivalent DAB-1 moiety (deprotected **141**) from the glyconanoparticle core. This was achieved with the synthesis of Au GNPs **142** by combining the dendrimeric technique with the nanoparticle formation. The Au GNPs **142** decorated with 30% of trivalent DAB-1 resulted in 97% inhibition of GALNS with an observed IC$_{50}$ value of 0.004 mg mL^{-1} in terms of Au GNP concentration, corresponding to 0.52 µM of iminosugar (table 3.29). The advantage of employing the glyconanoparticle strategy to afford new more potent inhibitors of GALNS based on DAB-1 (AuGNPs **142**) is clearly demonstrated. Indeed, the previously reported trivalent DAB-1 compound **144**[47] (scheme 3.39) inhibited GALNS by only 29% at 1 mM concentration (table 3.29). The inhibitory activity found for Au GNPs **142** far exceeds that previously obtained with nonavalent DAB-1 dendrimer **78**, for which an IC$_{50}$ = 47 µM was observed when tested under the same experimental conditions (the same substrate concentration). Indeed, Au GNPs **142** are two orders of magnitude more active than the nonavalent dendrimer **76**. Regarding IDS, Au GNPs **138a**, **138b** and **142** did not significantly inhibit this enzyme (15–39% inhibition at 0.2 mg mL^{-1}), and **80** did not inhibit IDS at all. Interestingly, Au GNPs coated with DAB-1 (12a, 12b) or tri-DAB-1 **142** showed high selectivity towards GALNS with respect to IDS, while the previously reported dendrimer **78** showed no substantial selectivity.

3.3.1.3 Conclusions

In this project, Au GNPs decorated with the iminosugar active component DAB-1 were synthesized, in search of new potent multivalent inhibitors of lysosomal sulfatases GALNS and IDS, therapeutically relevant enzymes involved in lysosomal storage diseases

_____

[122] Siriwardena A., Khanal M., Barras A., Bande O., Mena-Barragán T., Ortiz Mellet C., Garcia-Fernández J. M., Boukherroub R., Szunerits S., *RSC Adv.*, **2015**, *5*, 100568.

[123] Alvarez-Dorta D., Brissonnet Y., Saumonneau A., Deniaud D., Bernard J., Yan X., Telluer C., Daligault F., Gouin S., *ChemistrySelect*, **2017**, *2*, 9552.

(Morquio A and Hunter disease, respectively). Exploiting the nanoparticle direct synthesis protocol, Au GNPs decorated with different loadings of the iminosugar component were achieved. This methodology allows indeed to vary the mutual percentage between active and inner component. A remarkable inhibitory activity was found for the whole set of Au GNPs **138a**, **138b**, **142** and **143** towards GALNS, while IDS was not significantly inhibited. Surprisingly, a good inhibition was observed also for 100% Au-βGlu **143**, prepared as a control system, thus suggesting a synergistic effect of the sugar component (which is a part of the scaffold) and the iminosugar moiety in imparting the inhibitory activity, at least towards this particular enzyme target. Loading higher than 40% could not be attained due to the small dimensions of the gold cores. To enhance the multivalent presentation of the iminosugar component, combination with the dendrimeric technique was used by synthesizing the trivalent DAB-1 ligand **139**, subsequently employed in the preparation of Au GNPs **142**. Multimerization of DAB-1 onto Au GNPs resulted in new multivalent inhibitors selective for GALNS in the low micromolar range in all cases, with the best result obtained with the Au GNPs **142** decorated with 30% of trivalent DAB-1, for which an IC_{50} value of 0.52 μM was measured. This result far exceeds that obtained with a previously reported nonavalent dendrimer **78**, for which an IC_{50} value of 47 μM had been obtained. Therefore, Au GNPs coated with DAB-1 are between 18-fold (**138b**, IC_{50} = 2.56 μM) and 90-fold more active than **78** (**142**, IC_{50} = 0.52 μM), thus representing the most potent GALNS inhibitor reported so far to the best of our knowledge. Work is underway in our lab to deeply investigate the role of the sugar component, in order to find the best synergistic effect in inhibiting GALNS.

3.3.1.4 Experimental section

For the general details see paragraph 2.4. Additionally, UV/Vis spectra were recorded with a Varian CaryWin 4000 UV/Vis spectrophotometer. TEM analysis was performed with a Philip CM12 instrument with CRYO-GATAN UHRST 3500 Technology, digital camera and EDAX microanalysis and with a JEOL JEM-2100F microscope, both operating at 200 kV. ICP analysis was performed with a Thermo Scientific™ iCAP 7400 ICP-OES analyzer.

Synthesis of pyrrolidine 131: To a solution of 2 (89 mg, 0.17 mmol) in MeOH (5 mL) and 12 M HCl (6 drops), Pd/C (45 mg) was added and the reaction mixture was left stirring at room temperature under a H_2 atmosphere for three days. The catalyst was filtered through a Celite® pad and the filtrate was concentrated under vacuum to quantitatively yield the hydrochloride of 3, which was eluted through an ion-exchange resin (DOWEX® 50XW8-100) with MeOH, H_2O and 6% NH_4OH to give the free amine **131** (25 mg, 0.11 mmol, 65%). **[α]$_{20}^{D}$** = −49.4 (c = 0.69 in H_2O); **^{1}H-NMR** (400 MHz, D_2O): δ = 3.98 (dt, *J* = 5.4, 2.4 Hz,

_____

1H, H-3), 3.80 (dd, *J* = 4.9, 2.9 Hz, 1H, H-4), 3.63–3.54 (m, 2H, H-6), 2.87 (dd, *J* = 11.2, 2.4 Hz, 1H, Ha-2), 2.72–2.65 (m, 3H, Ha-1', H-6'), 2.60 (dd, *J* = 11.2, 5.8 Hz, 1H, Hb-2), 2.39 (dd, *J* = 10.5, 5.1 Hz, 1H, H-5), 2.24 (td, *J* = 10.7, 5.4 Hz, 1H, Hb-1'), 1.48–1.19 (m, 8H, from H-2' to H-5') ppm; **13C-NMR** (50 MHz, D_2O) δ = 79.3 (d, C-4), 75.5 (d, C-3), 71.9 (d, C-5), 61.4 (t, C-6), 58.3 (t, C-2), 55.3 (t, C-1'), 39.8 (t, C-6'), 28.2–25.5 (t, 4C, from C2' to C5')ppm; **MS (ESI)**: m/z calcd (%) for $C_{11}H_{24}N_2O_3$ 232.18; found: 233.23 (100%, [M + H]+). **Elemental analysis**: (%) for $C_{11}H_{24}N_2O_3$ (232.32) calcd: C, 56.87; H, 10.41; N, 12.06; found C, 56.36; H, 10.31; N 11.84.

Synthesis of pyrrolidine 134: To a solution of **80** (336 mg, 1.3 mmol) in pyridine (9.6 mL), acetic anhydride (6.2 mL, 65.0 mmol) was added. The solution was stirred at room temperature overnight. Then, after concentration under reduced pressure, the crude product was purified by FCC (pentane/AcOEt from 5 : 1 to 2 : 1) to afford pure **134** (216 mg, 0.56 mmol, *R*f = 0.5, 81% yield) as a colorless oil. **[α]21D** = −50.8 (c = 0.91 in $CHCl_3$). **1H-NMR** (400 MHz, $CDCl_3$): δ ppm = 5.07 (pt, *J* = 5.3 Hz, 2H, H-3, H-4), 4.17 (dd, *J* = 5.6, 11.6 Hz, 2H, H-6), 3.26 (t, *J* = 6.9 Hz, 2H, H-6'), 3.14 (d, *J* = 11.2 Hz, 1H, Ha-5), 2.79–2.71 (m, 3H, Hb-5, H-2, Ha-1'), 2.36–2.32 (m, 1H, Hb-1'), 2.08 (s, 9H, OAc), 1.63–1.25 (m, 8H, from H-2' to H-5'). **13C-NMR** (100 MHz, $CDCl_3$): δ = 170.8–169.6 (s, 3C, –O$\underline{C}$OCH_3), 78.9–76.4 (d, 2C, C-3, C-4), 67.8 (t, C-1'), 63.3 (t, C-6), 57.5 (t, C-5), 54.7 (d, C-2), 51.4 (t, C-6'), 29.7–26.6 (t, 4C, from C2' to C5'), 21.0–20.6 (q, 3C, O$\underline{C}H_3$) ppm; **IR** ($CDCl_3$): ṽ = 2939, 2862, 2811, 2258, 2099, 1740, 1455, 1372, 1236, 1049 cm⁻¹; **MS (ESI)**: calcd (%) for $C_{17}H_{28}N_4O_6$ 384.20; found: 407.09 (100 %, [M + Na]+). **Elemental analysis**: (%) for $C_{17}H_{28}N_4O_6$ (384.43): calcd C, 53.11; H, 7.34; N, 14.57; found: C, 53.61; H, 7.52; N, 14.95.

Synthesis of pyrrolidine 135: To a solution of supported-PPh_3 (Fluka, ~3.2 mmol g⁻¹ crosslinked with 2% DVB, 50 mg, 0.2 mmol) in dry THF (1 mL), a solution of **134** (30 mg, 0.08 mmol) in dry THF (1 mL) was added. The reaction mixture was stirred under a nitrogen atmosphere at room temperature overnight. After a TLC control ($CHCl_3$/MeOH = 20: 1) showing the presence of both the starting material (*R*f = 0.8) and the product (*R*f = 0.9), 4 µL of H_2O were added and the mixture was refluxed for 3 hours, until a TLC analysis showed the complete disappearance of the starting material **134**. The obtained crude product was filtered over cotton and purified by FCC (from CH_2Cl_2/MeOH 10: 1 to CH_2Cl_2/MeOH/NH_3 5: 1: 0.1) to give pure **135** (17 mg, 0.05 mmol, 59% yield) as a pale-yellow oil. **1H-NMR** (400 MHz, $CDCl_3$): δ ppm = 5.08–5.05 (m, 2H, H-3, H-4), 4.21–4.13 (m, 2H, H-6), 3.15 (d, *J* = 11.6 Hz, 1H, Ha-5), 2.81–2.66 (m, 5H, Hb-5, H-2, Ha-1', H-6'), 2.37–2.23 (m, 1H, Hb-1'), 2.08 (s, 9H, OAc), 1.49–1.26 (m, 8H, from H-2' to H-5'). **13C-NMR** (50 MHz, $CDCl_3$): δ ppm = 170.7–169.9 (s, 3C, –O$\underline{C}$OCH_3), 79.2–76.5 (d, 2C, C-3, C-4), 67.8 (t, C-1'), 63.4 (t, C-6), 57.5 (t, C-5), 54.7 (d, C-2), 42.2 (t, C-6'), 33.8 (t, C-5'), 28.0–26.8 (t, 3C, from C-2' to C4'), 21.0–20.9 (q, 3C, O$\underline{C}H_3$). **MS (ESI)**: calcd (%) for $C_{17}H_{30}N_2O_6$ 358.21; found: 359.44 (100%, [M + H]+).

Synthesis of DAB-1 based ligand 132: A solution of compound **129** (102 mg, 234

µmol), 1-hydroxybenzotriazole (HOBt, 46.4 mg, 343 µmol) and N-(3-dimethylaminopropyl)-N'-ethylcarbodiimide (EDC, 66.0 µL, 374.4 µmol) in dry DMF (2.0 mL) was stirred at room temperature under a nitrogen atmosphere. After 10 min, a solution of **135** (56.0 mg, 156 µmol) and N,Ndiisopropylethylamine (DIPEA 73.0 µL, 421.0 µmol) in dry DMF (1.5 mL) was added. The reaction mixture was stirred at room temperature for 18 h, until a TLC analysis (CH_2Cl_2/MeOH 2: 1) confirmed the formation of a new product (Rf = 0.5) and the complete disappearance of compound **135** (Rf = 0.1). The reaction mixture was diluted with AcOEt (10 mL) and washed with H_2O (1 × 8 mL) and the organic layer was then washed with a saturated solution of $NaHCO_3$ (1 × 8 mL), water (1 × 8 mL) and brine (1 × 8 mL), dried over anhydrous Na_2SO_4 and concentrated under vacuum. Purification through gradient column chromatography (CH_2Cl_2/MeOH from 30: 1 to 10: 1) afforded pure **132** (46 mg, 59 µmol) as a pale-yellow oil, in 38% yield. **[α]$_{23}^D$** = −25.2 (c = 0.63 in CHCl3). **^{1}H-NMR** (400 MHz, CDCl3): δ = 5.06 (br s, 2H, H-3, H-4), 4.22–4.06 (m, 2H, H-6), 3.97 (s, 2H, H-L1), 3.74–3.55 (m, 12H, H-L2/L7), 3.43 (t, J = 6.8 Hz, 2H, H-L8), 3.24 (dt, J = 14.3, 6.7 Hz, 2H, H-6'), 3.14 (d, J = 12.0 Hz, 1H, Ha-5), 2.85 (t, J = 7.4 Hz, 2H, H-L18), 2.79–2.65 (m, 3H, Hb-5, H-2, Ha-1'), 2.31 (s, 1H, Hb-1'), 2.31 (s, 3H, SAc), 2.12–2.02 (m, 9H, OAc), 1.59–1.18 (m, 26H, from H-2' to H-5', from H-L9 to H-L17) ppm; **^{13}C-NMR** (100 MHz, CDCl3): δ = 196.1 (s, S$\underline{C}$OCH$_3$), 170.9–169.7 (s, 4C, OAc (3), $\underline{C}$ONH–), 78.8–76.4 (d, 2C, C-3, C-4), 71.6–70.6 (t, 7C, OCH$_2$– from L1 to L7), 67.7 (t, CH$_2$, L-8), 63.2 (t, C-6), 57.5 (t, C-5), 54.8 (d, C-2), 39.5 (t, C-6'), 38.8 (t, C-1, O–$\underline{C}$H$_2$–CH$_2$–R), 30.6 (q, SCO$\underline{C}$H$_3$), 29.7–26.1 (t, 14C, CH$_2$SAc; C from L9 to L18; form C 2' to 5'), 21.1–20.9 (q, 3C, OCH$_3$) ppm; **MS (ESI)**: calcd (%) for $C_{38}H_{68}N_2O_{12}S$ 776.45; found: 799.07 (100 %, [M + Na]$^+$). **IR** (CDCl$_3$): ṽ = 3690, 3422, 2930, 2856, 2256, 2245, 1737, 1669, 1601, 1535, 1465, 1370, 1234, 1112, 1045 cm^{-1}. **Elemental analysis**: (%) for $C_{38}H_{68}N_2O_{12}S$ (777.02): calcd C, 58.74; H, 8.82; N, 3.61; found: C, 58.83; H, 8.68; N, 3.60.

Synthesis of trivalent DAB-1 derivative 139: To a solution of **134** (52.3 mg, 140 µmol) in 1.2 mL of THF/H_2O = 2: 1 $CuSO_4$ (1.9 mg, 12 µmol), sodium ascorbate (5 mg, 25 µmol) and **81** (9.7 mg, 41 µmol) were added. The reaction mixture was stirred under microwave irradiation at 80 °C for 45 min, until a TLC analysis (AcOEt) showed the disappearance of the starting material (Rf = 0.75) and the formation of a new product (Rf = 0.00). After filtration through a Celite® pad, the solvent was removed under reduced pressure and the crude product was purified by FCC (CH_2Cl_2/MeOH/NH$_3$ from 10: 1: 0.1 to 5: 1: 0.1) affording pure **139** (52 mg, 37.4 µmol, Rf = 0.41 in CH_2Cl_2/MeOH/NH$_3$ 10: 1: 0.1) as a colorless oil, in 91% yield. **[α]$_{23}^D$** = −37.3 (c = 0.88 in CHCl$_3$). **^{1}H-NMR** (400 MHz, CDCl$_3$): δ = 7.59 (br s, 3H, triazole), 5.06 (pd, J = 5.6 Hz, 6H, H-3, H-4), 4.63 (br s, 6H, H-β), 4.34 (t, J = 7.2 Hz, 6H, H-6'), 4.15 (ddd, 6H, J = 11.6, 5.6, 4.72 Hz, 6H, H-6), 3.52 (br s, 6H, H-α), 3.13 (d, J = 11.2 Hz, 3H, H-5), 2.77–2.70 (m, 9H, Hb-5, H-2, Ha-1'), 2.34–2.31 (m, 3H, Hb-1'), 2.07 (s, 27H, OAc), 1.95–1.85 (m, 6H, H-5'), 1.51–1.41 (m, 6H, H-2'), 1.34–1.25 (m, 12H, H-3', H-4') ppm; **^{13}C-NMR** (100 MHz, CDCl$_3$): δ = 170.8–169.6 (s, 9C, OAc), 144.9 (s, 3C, triazole),

122.3 (d, 3C, triazole), 78.7 (d, 3C, C-3), 76.3 (d, 3C, C-4), 72.3 (t, 3C, C-α), 67.7 (d, 3C, C-2), 64.9 (t, 3C, C-β), 63.1 (t, 3C, C-6), 57.4 (t, 3C, C-5), 56.0 (s, HN$\underline{C}$(CH$_2$O)$_3$–), 54.5 (t, 3C, C-1'), 50.2 (t, 3C, C-6'), 30.2

(t, 3C, C-5'), 27.7 (t, 3C, C-2'), 26.6 (t, 3C, C-3'), 26.3 (t, 3C, C-4'), 21.0 (q, 9C, $\underline{C}$H$_3$CO) ppm; **MS (ESI)**: calcd (%) for C$_{64}$H$_{101}$N$_{13}$O$_{21}$ 1364.54; found: 1387.76 (100 %, [M + Na]$^+$); **IR** (CDCl$_3$): ṽ = 3675, 3148, 3029, 3005, 2938, 2863, 2813, 1739, 1465, 1438, 1372, 1218, 1210, 1143, 1095, 1051 cm^{-1}. **Elemental analysis**: (%) for C$_{64}$H$_{101}$N$_{13}$O$_{21}$ (1388.56): calcd C, 55.36; H, 7.33; N, 13.11; found: C, 55.13; H, 7.18; N, 13.13.

Synthesis of trivalent DAB-1 based ligand 140: To a solution of compound **129** (8.6 mg, 19.7 μmol) in dry THF (225 μL) at 0 °C, 3-(diethoxyphosphoryloxy)-1,2,3-benzotriazin-4(3H)-one (DEPBT 13 mg, 43.2 μmol) and N,N-diisopropylethylamine (DIPEA 7.4 μL, 43.2 μmol) were added. The mixture was stirred at 25 °C for 15 min under a nitrogen atmosphere, then a solution of **139** (30.0 mg, 21.6 μmol) in dry THF (225 μl) was added and the reaction mixture was stirred at room temperature for 6 days, until a TLC analysis (CH$_2$Cl$_2$/MeOH 20: 1) showed the formation of a new product (*R*f = 0.9). The reaction mixture was diluted with AcOEt (5 mL), washed with NH$_4$Cl (2 × 3 mL), NaHCO$_3$ (2 × 3 mL) and H$_2$O (2 × 3 mL), dried over anhydrous Na$_2$SO$_4$ and concentrated under vacuum. Purification through gradient column chromatography (CH$_2$Cl$_2$/MeOH from 20: 1 to 10: 1) afforded pure **140** (30 mg, 17 μmol) as a yellow oil, in 85% yield. **[α]$_{23}^D$** = −29.1 (c = 0.35 in CHCl$_3$). **^{1}H-NMR** (400 MHz, CDCl$_3$): δ = 7.56 (br s, 3H, triazole), 5.06 (t, *J* = 5.3 Hz, 6H, H-3, H-4), 4.59 (br s, 6H, H-β), 4.33 (t, *J* = 7.3 Hz, 6H, H-6'), 4.16 (qd, 6H, *J* = 16.3, 11.5, 5.5 Hz, 6H, H-6), 3.87 (s, 2H, L-1), 3.80 (s, 6H, H-α), 3.65–3.40 (m, 14H, from L-2 to L-8), 3.13 (d, *J* = 11.2 Hz, 3H, Ha-5), 2.85 (m, 2H, L-18), 2.79–2.68 (m, 9H, Hb-5, H-2, Ha-1'), 2.36–2.29 (m, 6H, Hb-1', SAc), 2.07 (s, 27H, OAc), 1.91 (br s, 6H, H-5'), 1.58–1.25 (m, 36H, from L-9 to L-17, H-2', H-3', H-4') ppm; **^{13}C-NMR** (100 MHz, CDCl$_3$): δ = 196.6 (s, S$\underline{C}$OCH$_3$), 170.7–169.6 (s, 9C, OAc), 169.5 (s, $\underline{C}$ONH–), 144.9 (s, 3C, triazole), 122.4 (d, 3C, triazole), 78.9 (s, 3C, C-3), 76.4 (d, 3C, C-4), 71.5–70.1 (t, 7C, from L-1 to L-7), 69.9 (s, L-8), 68.9 (t, 3C, C- α), 67.8 (d, 3C, C-2), 65.0 (t, 3C, C-β), 63.2 (t, 3C, C-6), 59.7 (s, HN$\underline{C}$(CH$_2$O)$_3$–), 57.4 (t, 3C, C-5), 54.6 (t, 3C, C-1'), 50.2 (t, 3C, C-6'), 30.2 (q, –CH$_2$SCOCH$_3$), 29.7–26.1 (t, 22C, from L-9 to L-18, C-2'– C-5'), 20.9, 20.8 (s, 9C, CO$\underline{C}$H$_3$) ppm; **MS (ESI)**: calcd (%) for C$_{85}$H$_{139}$N$_{13}$O$_{27}$S 1807.60; found: 926.25 (100%, [(M+ Na)/2]$^+$); IR (CDCl$_3$): ṽ = 3690, 3396, 3029, 3007, 2930, 2858, 1739, 1681, 1603, 1530, 1465, 1372, 1234, 1207, 1097, 1052, 1021 cm^{-1}. **Elemental analysis**: (%) for C$_{85}$H$_{139}$N$_{13}$O$_{27}$S (1807.15): calcd C, 56.49; H, 7.75; N, 10.08; found: C, 56.64; H, 7.38; N, 9.85.

General procedure for the "in situ" deprotection of S-acetyl conjugates 132 and 140: To a solution of **132** and **140** in CD$_3$OD (20 mg ml^{-1} and 10 mg ml^{-1}, respectively), 30 equivalents of NaOMe were added and the reaction mixture was left stirring for 2 hours at 25 °C under a nitrogen atmosphere. The complete disappearance of the starting material

was confirmed via ^{1}H-NMR and the crude product was directly used for the preparation of Au GNPs.

Preparation and characterization of Au GNPs: The Au GNPs coated with DAB-1 derivatives (mono- and trivalent) and simple monosaccharide βGlcC$_5$S (DAB-1-βGlc-Au NPs **143** and tri-DAB1-βGlc-Au NPs **142**) were prepared by the reduction of an Au(III) salt using sodium borohydride in the presence of a mixture of thiol-ending iminosugar conjugate and βGlcC$_5$S **137** as ligands, in different ratios following a reported procedure.[112] For the analysis of the ratio between the iminosugar ligands and βGlcC$_5$S, ^{1}H-NMR spectra of the initial mixture and the supernatant after Au-GNP formation were recorded. The ligand loading on the Au-GNPs was also evaluated by quantitative NMR (qNMR) using 3-(trimethylsilyl)propionic-2,2,3,3-d$_4$ acid (TSP-d$_4$) as an internal standard in the D$_2$O solution of the Au GNPs. The prepared Au GNPs were freeze-dried and stored at 4 °C. Under these conditions, the Au GNPs can be stored for months maintaining their biophysical properties. The Au GNPs **143**, coated only with the simple monosaccharide βGlcC$_5$S, were also prepared as previously described.

General procedure for the preparation of Au GNPs coated with iminosugars: An aqueous solution of HAuCl$_4$ (25 mM, 1 equiv.) was added to a 12 mM methanolic solution of a suitable mixture of thiol-ending sugar and iminosugar conjugates (3 equiv. overall). An aqueous solution of NaBH$_4$ (1 M, 27 equiv.) was then added in four portions, with vigorous shaking. The black suspension formed was shaken for 2 hours at 25 °C. After that, the supernatant was removed and analysed by ^{1}H-NMR to study the nanoparticle ligand composition. The residue was washed several times with MeOH. In order to separate well the nanoparticles from the supernatant centrifugation (12 000 rpm, 2 min) was performed. The residue was dissolved in a minimal volume of HPLC gradient grade water and purified by dialysis (SnakeSkin® Pleated Dialysis Tubing, 10 000 MWCO and Slide-A-Lyzer® 10K Dialysis Cassettes, 10 000 MWCO). Iminosugar coated Au GNPs were obtained as a dark-brown powder after freeze-drying and characterized via ^{1}H-NMR, UV-Vis spectroscopy and TEM analysis.

The spectra relatives to the Au GNPs **138a-c 142** can be found in the ESI of the paper cited before.

Preparation of 30% DAB-1-βGlc NPs (138a): A 1: 2.3 mixture of thiol-ending **132** (7.83 mg, 12.9 µmol) and βGlcC$_5$S **137** (8.3 mg, 29.6 µmol) in CD$_3$OD (1.4 mL) was used to obtain 4.7 mg of AuGNPs **138a**. **TEM** (average diameter): 1.7 ±0.4 nm. **Quantitative ^{1}H-NMR** (400 MHz, D$_2$O containing 0.05 wt. % of 3-(trimethylsilyl)propionic-*2,2,3,3-d*$_4$ acid, sodium salt as an internal standard): 0.54 mg of **138a** were dissolved in 120 µL of D$_2$O and

_____

40 µL of D_2O containing 0.05 wt.% TSP were added and 50 nmoles of DAB-1 conjugate were found. Significant peaks: δ = 4.24 (br s, from βGlcC5S), 3.95-2.95 (m), 2.82-2.70 (m, 1H, from DAB-1 conjugate) 2.62-2.53 (m, 1H, from DAB-1 conjugate), 1.90-1.00 ppm (m).

Preparation of 40% DAB-1-βGlc NPs (138b): A 1: 1.5 mixture of thiol-ending **132** (7.80 mg, 12.9 µmol) and βGlcC₅S **137** (5.4 mg, 19.3 µmol) in CD_3OD (2.7 mL) was used to obtain 0.4 mg of Au GNPs **138b**. **TEM** (average diameter): 1.9 ±0.3 nm. **Quantitative ^{1}H-NMR** (400 MHz, D_2O containing 0.05 wt. % of 3-(trimethylsilyl)propionic-*2,2,3,3-d₄* acid, sodium salt as an internal standard): 0.20 mg of 12b were dissolved in 150 µL of D_2O and 15 µL of D_2O containing 0.05 wt.% TSP were added and 32 nmoles of DAB-1 conjugate were found. Significant peaks: δ = 3.98 (br s, NHCOCH₂- from DAB-1 conjugate), 3.81-2.98 (m), 2.87-2.75 (m, 1H, from DAB-1 conjugate), 2.67-2.57 (m, 1H, from DAB-1 conjugate), 1.90-1.00 ppm (m).

Preparation of 50% DAB-1-βGlc NPs (138c): A 1: 1 mixture of thiol-ending **132** (7.80 mg, 12.9 µmol) and βGlcC₅S **137** (3.6 mg, 12.9 µmol) in CD_3OD (2.1 mL) was used to obtain 0.45 mg of Au GNPs **138c.** These nanoparticles were difficult to isolate after washing with MeOH and they were not stable when dispersed in water; indeed flocculation was observed after a few hours. For this reason a qNMR was impossible to be recorded (15-18 h of acquisition time are usually necessary for these experiments).**TEM** (average diameter): 2.5 ±0.5 nm.

Preparation of 30% tri-DAB-1-βGlc NPs (142): A 1: 4 mixture of thiol-ending **141** (10.0 mg, 5.5 µmol) and βGlcC₅S **137** (6.3 mg, 22.1 µmol) in CD_3OD (2.3 mL) was used to obtain 2.2 mg of AuGNPs **142**. TEM (average diameter): 1.7 ±0.5 nm. The ^{1}H-NMR spectrum of the "before mixture" showed a 1: 2.3 ratio between **141** and **137**, corresponding to 30% tri-DAB-1-βGlc NPs, also confirmed by the ^{1}H NMR spectrum of the "after mixture". **Quantitative ^{1}H-NMR** (400 MHz, D_2O containing 0.05 wt. % of 3-(trimethylsilyl)propionic-*2,2,3,3-d₄* acid, sodium salt as an internal standard): 0.27 mg of **142** were dissolved in 150 µL of D_2O and 15 µL of D_2O containing 0.05 wt.% TSP were added and 35 nmoles of DAB-1 conjugate were found. Significant peaks: δ = 7.85 (br s, 3H, triazole from DAB-1 conjugate), 4.29 (br s, from βGlcC₅S), 4.03 (br s, NHCOCH₂-, 6H, from DAB-1 conjugate), 3.93-3.00 (m), 2.90-2.65 (m, 9H, from DAB-1 conjugate), 2.48-2.30 (m, 6H, from DAB-1 conjugate), 1.92-0.93 ppm (m).

Determination of GALNS and IDS activity in leukocytes homogenate from healthy donors. For compounds **80**, **138a-b**, **142**, **143** and **144** the percentage of inhibition (at 1 mM concentration for **80** and **144** and at 0.2 mg/mL for AuGNPs **138a-b**, **142** and **143**) towards GALNS and IDS, using leukocyte extracts from healthy donors, was evaluated. Leukocyte pellets were disrupted by sonication in water and the micro BCA protein assay kit (Sigma-

Aldrich) was used to set up the protein amount for the enzymatic assay, according to the manufacturer's instructions.

GALNS enzymatic test: Enzyme activity was measured by setting the reaction in 0.2 ml tubes and performing the experiments in triplicates as follows.

Step 1: Iminosugars solution (3 µl), leukocytes homogenate (7 µl) and 20 µl of 4-methylumbelliferyl-ßgalactoside-6-sulphate.Na (Moscerdam Substrates) substrate solution in Na-Acetate/acetic acid buffer (0.1 M/0.1 M, pH 4.3) containing 0.1 M NaCl , 0.02% (w/v) NaN$_3$ and 5 mM Pb-acetate were incubated for 17 h at 37 °C.

Step 2: After step 1 the tubes were placed on an ice cooler and the reaction was stopped by addition of 5 µl of Na-phosphate buffer (0.9 M, pH 4.3) containing 0.02 % of NaN$_3$ and by efficient mixing with vortex. Then, 10 µl of β-Gal-A-10U were added to each sample and the suspension mixed again in vortex apparatus, then samples were incubated for 2 h at 37°C. At the end of this period the tubes were placed on an ice cooler and the samples were transferred in a cooled flat–bottomed 96 well plate and the reaction was immediately stopped with 200 µl of NaHCO$_3$/Na$_2$CO$_3$ buffer (0.5M/0.5M pH 10.7) containing 0.025% (w/v) of Triton X-100. Fluorescence was measured in a SpectraMax M2 microplate reader (Molecular-Devices) using a 365 nm excitation wavelength and a 435 nm emission wavelength. Percentage of GALNS inhibition was given with respect to the control (without iminosugar). Experiments were performed in triplicate, and the mean ± S. D. was calculated.

IDS enzymatic test: Enzyme activity was measured by setting the reaction in 0.2 ml tubes and performing the experiments in triplicates as follows.

Step 1: Iminosugars solution (3 µl), leukocytes homogenate (7 µl) and 20 µl of 4-methylumbelliferyl-α-LIduronide-2-sulphate.2Na (Moscerdam Substrates) substrate solution were incubated for 4 h at 37 °C.

Step 2: After step 1 the tubes were placed on an ice cooler and the reaction stopped by addition of 20 µl of Na-Phosphate/Citrate buffer (0.2M/ 0.1M pH 4.5) and by efficient mixing with vortex. Then, 10 µl of LEBT (Lysosomal Enzymes purified from Bovine Testis) were added to each sample and the incubation was continued for 24 hours at 37°C. At the end of this period tubes were placed on an ice cooler and the samples were transferred in a cooled flat–bottomed 96 well plate and the reaction was immediately stopped by addition of 200 µl of NaHCO$_3$/Na$_2$CO$_3$ buffer (0.5M/0.5M pH 10.7) containing 0.025% (w/v) of Triton X-100. Fluorescence was then measured in a SpectraMax M2 microplate reader (Molecular-Devices) using a 365 nm excitation wavelength and a 435 nm emission wavelength. Percentage of IDS inhibition was given with respect to the control (without iminosugar). Experiments were performed in triplicate, and the mean ± S. D. was calculated.

For the IC$_{50}$ determination, see section 3.2.1.4

3.3.2 Hybrid Gold Glyconanoparticles (DNJ based)

The first synthesis of **deoxynojirimycin** DNJ (1966, Paulsen) and the discovery of its important biological properties,[1] has prompted the interest in imino analogues of carbohydrates. The first rational of the MVE observed for a trimeric DNJ derivative, ten years ago,[81] extended the multivalency concept to carbohydrate-processing enzymes. Until then indeed, this phenomenon was considered an exclusive prerogative of the lectins-carbohydrates interaction due to the multimeric nature of such enzymes. But in 2009, by clicking a DNJ azido derivative to some bi- and tridentate oligoetilene scaffolds, for the first time a systematic evaluation of multivalent iminosugar-based glycosidase inhibitors were furnished, paving the way for a wide research in this field (see section 3.2). The concept was validated in 2010, when Compain and Nierengarten, reported the synthesis of a fullerene-based 12-valent DNJ compound (**63,** section 3.2) that showed a binding enhancements towards JBα-man up to three orders of magnitude over the monovalent counterpart (K_i = 0.15 μM *vs* K_i = 188 μM).[82] Starting from these multivalency 'milestones', a large variety of multimeric DNJ compounds were synthesized by exploiting the CuAAC reaction, for example in 2011 Ortiz Mellet and Compain reported the synthesis of multivalent structures based on β-cyclodextrins (β-CD).[84] Many other different scaffolds were exploited, ranging from porphyrins[87] or calixarenes,[88] to more complex micellar self-assembled glycopeptides and polymeric dextrans.[51] In 2016 again Compain built a series of cyclopeptoids of different valency (from 18 to 48 units of DNJ), including the one decorated with 36 DNJ units which showed the best inhibition value ever reported until now (K_i = 0.0011 μM).[85] Moreover, the recent obtainment of the first high resolution crystal structure of its complex with JBα-man, allowed the rationalization of multivalent effect observed with this 36-valent cluster,[51] revealing that the binding modes involved in the inhibition of JBα-man and the multivalent effect observed, strongly depend on the size and shape of the prepared multivalent architecture. Indeed, the crystal structure clearly confirmed the previously hypothesized formation of a 2:1 JBα-man:inhibitor complex, revealing a sandwich-type complex in which four DNJ units bind the catalytic pockets of two JBα-man molecules.

Despite the large variety of studied scaffolds, until now nobody has ever grafted a DNJ derivative onto gold nanoparticles. Only magnetic nanoparticles coated with DNJ (DNJ@Fe$_3$O$_4$) to apply in biocatalysis[123] and a nanostructured porous silicon (PS) particles covalently attached with DNJ to study brain tumor inhibitors,[124] are reported.
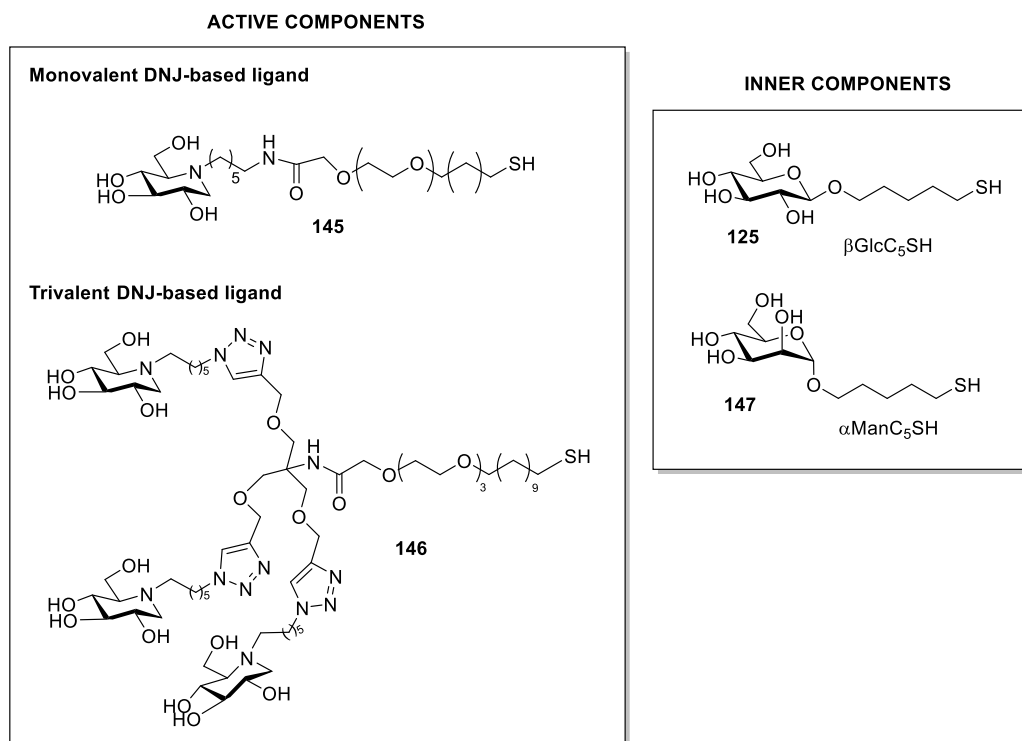
For this reason and thanks to our group's expertise in the synthesis of Au glyconanoparticles,[112,45b] we thought to synthesized Au GNPs decorated with a DNJ

_____

[124] Kleps I., Ignat T., Miu M., Craciunoiu F., Trif M., Simion M., Bragaru A., Dinescu A., *J. Nanosci. Nanotechnol*., **2010**, *10*, 2694-2700.

derivative to target JBαMan enzyme, to be applied in anticancer research. Indeed, Jack Bean mannosidase can be taken as model for Golgi α-mannosidase II, that was demonstrated to be involved in some cancer growth processes (see section 1.2.5). Moreover, being JBα-Man commercially available, it is possible to use it as a model enzyme for structural and mechanistic studies, mostly considering that its structure was recently solved Prof. Compain.[51] To deal with this goal, we collaborated with Prof. Compain (University of Strasbourg, France), who furnished us the DNJ unit that we properly functionalized and grafted on the gold nanometric core, following the protocol developed in our recent work (see section 3.3.1).[45b]

3.3.2.1 Results and discussion

Aiming to target JBα-Man using DNJ based Au GNPs, we followed the guidelines achieved in our previous work where we multimerized two kinds of DAB-1 linkers on gold nanosized core.[45b] For this reason, the strategy was to synthesized Au GNPs containing the monovalent ligand **145** in a percentage of 40%, since in previous case, this was the optimal amount of active component to insert onto the gold core. On the other hand, trying to expand the effective amount of iminosugar units, we wanted to vary the percentage of the trivalent iminosugar linker **146** to find if any implementation of the bioactive compound on the nanoparticle was possible (scheme 3.40). Moreover, we also investigated the consequence of changing the inner component, by using α-mannose **147** as well as β-glucose ligand **125** (scheme 3.40). Again, it was necessary to connect our bioactive iminosugar derivative to a properly functionalized linker (**129** scheme 3.28), in order to allow the formation of a Au-S bond, and to space the bioactive warhead from the gold core in order to avoid the whole system collapse.
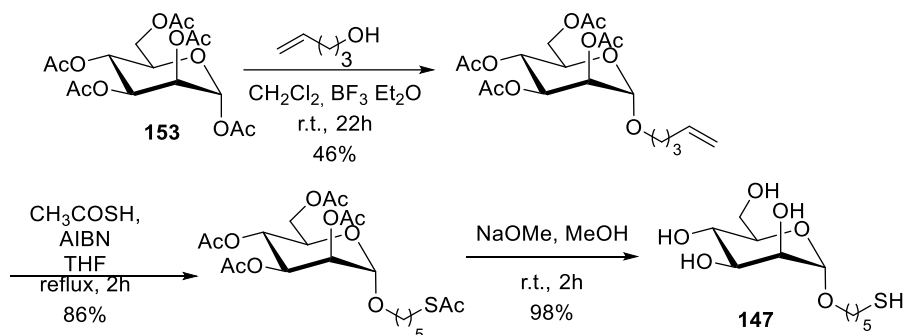
ACTIVE COMPONENTS

Monovalent DNJ-based ligand

145

Trivalent DNJ-based ligand

146

INNER COMPONENTS

125 βGlcC$_5$SH

147 αManC$_5$SH

Scheme 3.40: Scheme of the ligands, active and inner components.

In this case the azido DNJ derivative **148** (scheme 3.41) was directly furnished by prof. Compain and we did not need to synthesize it. Starting from the same azido key intermediate, we were able to get the two ligands: the monovalent **145**, by reducing the azido to amine through the Staudinger reaction seen before, and the trivalent **146** by performing a simple CuAAC click reaction. For the synthesis of amine **149**, we exploited the Staudinger reaction conditions optimized before (section 3.3.1), consisting in the use polymer-bound Ph$_3$P and refluxing for 4 h in THF/H$_2$O. With intermediate **149** in hands, a coupling reaction using EDC and HOBt in dry DMF, was performed, and allowed to achieve compound **150** in good yield (67%). Starting from the same azido intermediate **148** we also synthesized the trivalent dendron **151**, by 'clicking' it onto the trivalent scaffold **81** with a CuAAC reaction (CuSO$_4$ and sodium ascorbate). Subsequently we coupled it with linker **129** to get the peracetylated ligand **152** (scheme 3.41). In this case, to reproduce the same coupling conditions exploited in the case of trivalent pyrrolidine-based ligand (section 3.3.1), we used DEPBT as coupling agent (reaction conditions: DEPBT, DIPEA, dry THF, 6 d, r.t.) that afforded the final ligand **152** in excellent yield (94%).
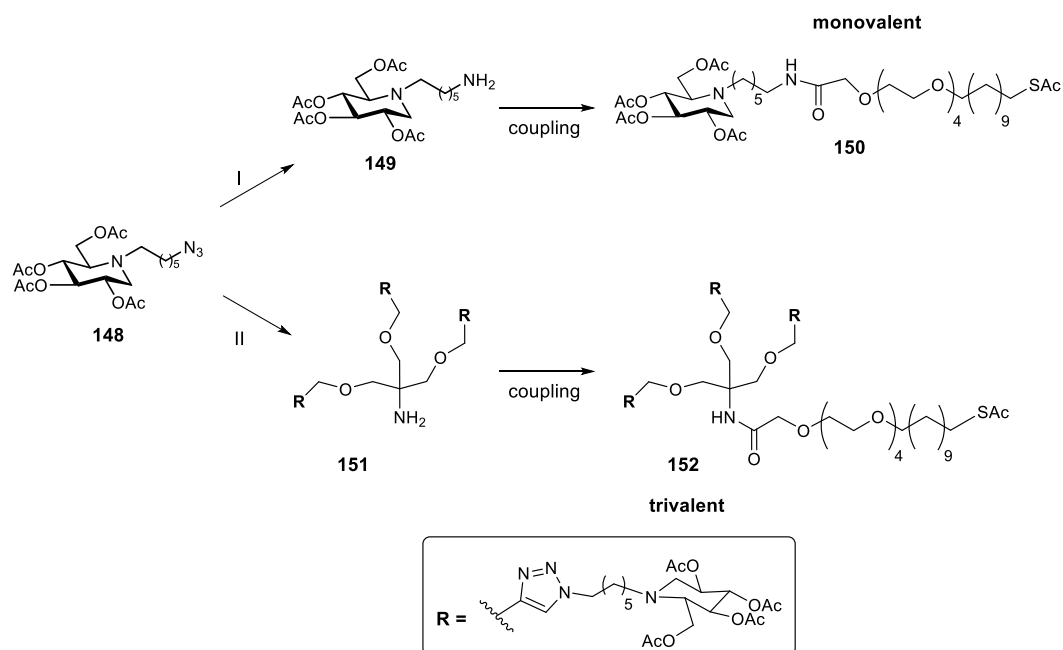
Scheme 3.41: Synthesis of two ligands **150** and **152**. I) Staudinger reduction; II) CuAAC.

As mentioned before, we also wanted to use two different inner components (**125** and **147**, scheme 3.40). GlcC$_5$S and ManC$_5$S conjugates **125**[116] (section 3.3.1, scheme 3.32) and **147**[125] (Scheme 3.42) were easily prepared starting from the peracetylated sugars which are commercially available, according to published procedures (Scheme 3.42). Briefly, the pentacetylated glycoside was glycosylated with 4-penten-1-ol in Fisher conditions, followed by free radical mediated thioacetilation with thioacetic acid; the subsequent deprotection with sodium methoxide in MeOH afforded desired derivative in good overall yields.
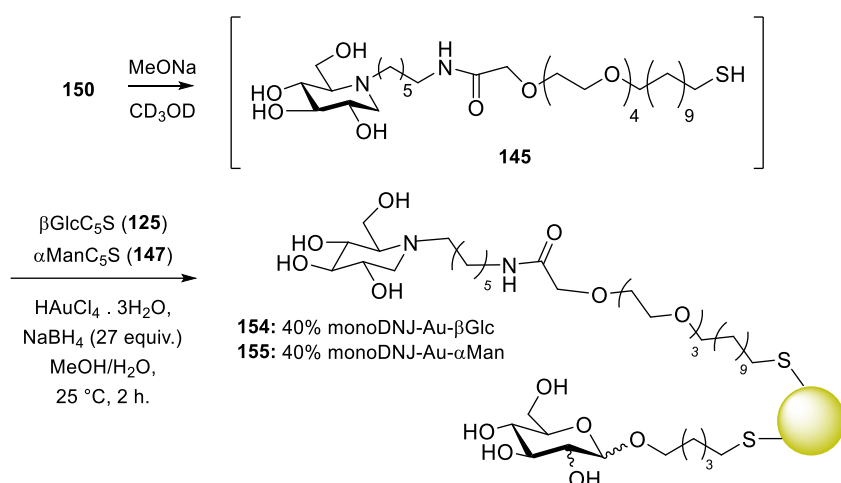

Scheme 3.42: Synthesis of inner component **147**.

[125] Buskas T., Sçderberg E., Konradsson P., Fraser-Reid B., *J. Org. Chem*., **2000**, *65*, 958 – 963.

With active and inner components in hands, we could provide the glyconanoadduct formation, by preliminary establishing the mutual percentage between the two components, following the same protocol employed for the synthesis of Au GNPs with DAB-1 ligands (section 3.3.1). In that way we built a small library of Au GNPs at different percentages of iminosugar, in its monovalent (scheme 3.43) and trimeric form (scheme 3.44). Briefly, water-soluble and stable gold GNPs of 2-nm average diameter were obtained by adding an aqueous solution of tetrachloroauric acid (HAuCl$_4$, 1 equiv.) to a methanolic solution of a mixture of thiol-derivatized conjugates (active iminosugar conjugate and inner sugar component, 3 equiv.) in the desired proportion. The resulting mixture was reduced with an excess of NaBH$_4$ (27 equiv.) as reducing agent and the suspension was vigorously shaken for 2 h at 25 °C.

Scheme 3.43: Au GNPs containing monovalent DNJ ligand as active component βGlcC$_5$S (**154**) and αManC$_5$S (**155**) as inner component.

With the same procedure, we synthesized also Au GNPs grafting on the gold core the trivalent ligand **146** (scheme 3.44).
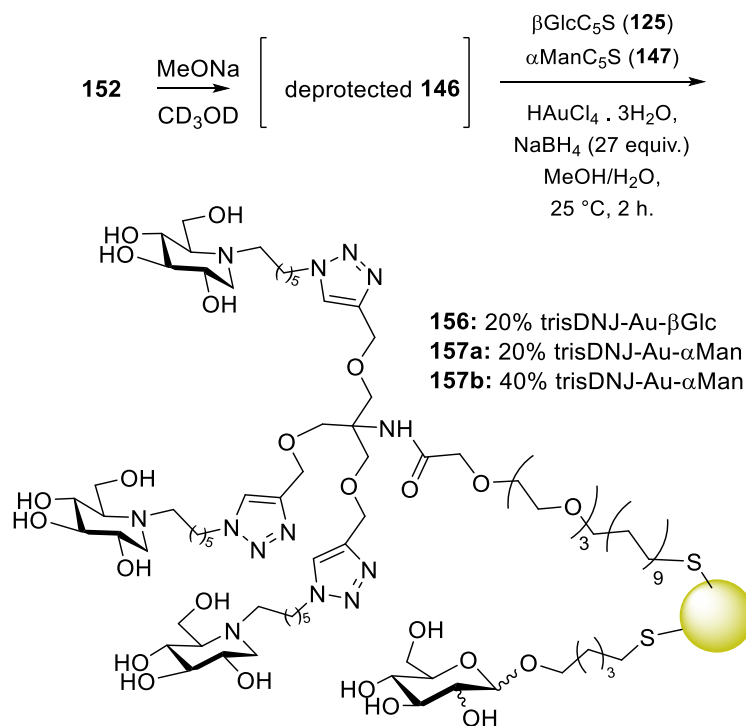
Scheme 3.44: Au GNPs containing trivalent DNJ ligand as active component and βGlcC₅S (**156**) and different percentages of αManC₅S (**157a**, **157b**) as inner component.

After 2 hours, the supernatant was removed, the nanoparticles were washed with methanol and the residue was dissolved in milliQ water, purified by dialysis and characterized by ¹H NMR spectroscopy, transmission electron microscopy (TEM), infrared spectroscopy (IR), and ultraviolet spectroscopy (UV). Glyconanoparticles with different density of active component were obtained by changing the ratio of iminosugar conjugate with respect to sugar derivative as inner component in the initial mixture before GNP formation. The ratio of the components was controlled by ¹H NMR. The proportion of the ligands on the gold surface was also examined by ¹H NMR after cluster formation (analysis of the supernatant and washings) as well as performing qNMR of GNPs in deuterium oxide with an internal reference. This well stablished protocol employed for the quantification of different ligands onto Au GNPs, allowed the quantitative ¹H NMR determination of the iminosugar on the nanoparticle by integration of a diagnostic signal with respect to the internal standard signal.[112] The ¹H NMR spectra of the GNPs featured broader peaks with respect to those of the corresponding free ligands, testifying for nanoparticle formation. Regarding the sugar/iminosugar ligand ratio, its uniformity was ascertained by ¹H NMR performed on the reaction mixture (before) and, after nanoparticle formation, on both the supernatant and the washings (after). The Au GNPs were also characterized by UV-vis

spectroscopy and transmission electron microscopy (TEM).

Au GNPs functionalized with 100% of GlcC$_5$S (100% Au βGlc, **143**, scheme 3.45) and with 100% of ManC$_5$S (100% Au αMan, **158**, scheme 3.45) were also prepared following a reported procedure[111a] to be employed as control systems.

143: 100% Au-βGlc   **158:** 100% Au-αMan
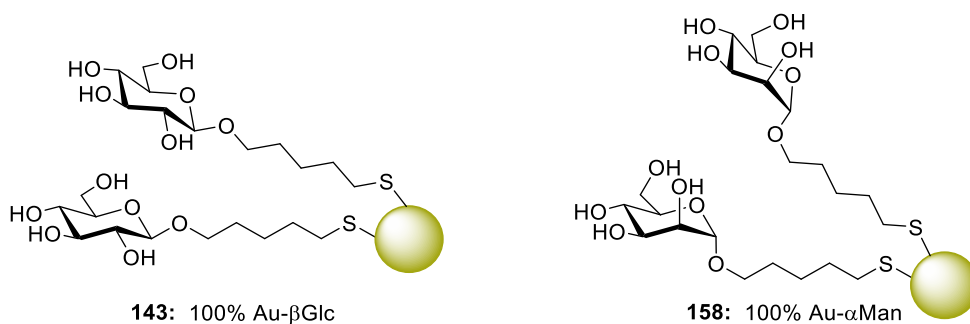
Scheme 3.45: Au GNPs **143** functionalized with 100% of GlcC5S and **158**.

The small library of Au GNPs synthesized in this project, is summarized in the table below, with all data related to them. In the table are also reported the estimated molecular weight of the Au GNP, calculated by following an empirical formula reported in literature that correlates the gold core diameter (measured with TEM) with the molecular weights of the nanoparticles.[120] Moreover, in the last column of the table it is reported the amount of the active component DNJ as measured by qNMR. It is worth noting that the concentrations found with these two different methods (by TEM and qNMR) are quite in agreement (the same order of magnitude).

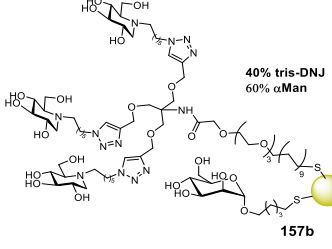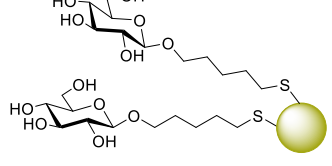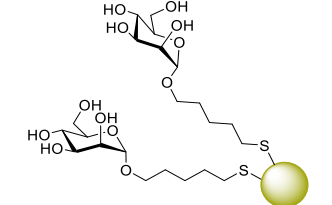| Au-GNPs	Characterization			
	TEM	Estimate M.W. (from TEM)	DNJ amount (from TEM)	DNJ amount (from qNMR)
40% monoDNJ 60% αMan **155**	2.1±0.6 nm	$(C_{31}H_{61}N_2O_9S)_9(C_{11}H_{21}O_6S)_{14}$ Au_{140} M.W. = 37255	2mg/mL Correspond to **483 μM**	2mg/mL Correspond to **467 μM**
40% monoDNJ 60% βGlc **154**	1.8±0.4 nm	$(C_{31}H_{61}N_2O_9S)_8(C_{11}H_{21}O_6S)_{12}$ Au_{140} M.W. = 36055	2mg/mL Correspond to **444 μM**	2mg/mL Correspond to **413 μM**
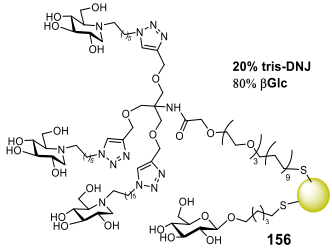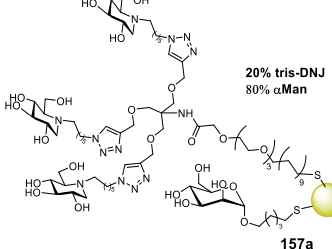
|	2.1±0.5 nm	$(C_{68}H_{125}N_{13}O_{20}S)_4(C_{11}H_{21}O_6S)_{18}Au_{140}$ M.W. = 38543	2mg/mL Correspond to **623 µM**	2mg/mL Correspond to **567 µM**
	2.0±0.4 nm	$(C_{68}H_{125}N_{13}O_{20}S)_3(C_{11}H_{21}O_6S)_{14}Au_{140}$ M.W. = 35942	2mg/mL Correspond to **501 µM**	2mg/mL Correspond to **450 µM**
	2.1±0.5 nm	$(C_{68}H_{125}N_{13}O_{20}S)_3(C_{11}H_{21}O_6S)_5Au_{140}$ M.W. = 33410	2mg/mL Correspond to **539 µM**	2mg/mL Correspond to **503 µM**
	1.7±0.4 nm	$(C_{11}H_{21}O_6S)_{35}Au_{140}$ M.W. = 37422	/	/
	1.6±0.4 nm	$(C_{11}H_{21}O_6S)_{73}Au_{140}$ M.W: = 48000	/	/

Table 3.12: Resume table of DNJ-based Au GNPs.

3.3.2.2 Biological evaluation

As mentioned before, the purpose of this project was to evaluate the inhibitory activity of newly synthesized Au GNPs towards JBαMan glycosidase, taken as a model enzyme for Golgi mannosidase, important enzyme for anticancer applications.

The obtained glyconanoparticles **154**, **155**, **156**, **157a** and **157b** were subjected to preliminary inhibitory tests, carried out thanks to the collaboration with the group of Prof. P. Compain at the University of Strasbourg, France.

They were evaluated at 2 mg/mL concentration towards commercially available (Sigma Aldrich) JBαMan. Compound **62** (scheme 3.46) was used as the monovalent reference compound. The collected data are summarized in table 3.32.
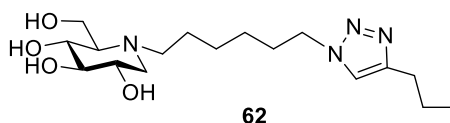
Scheme 3.46: Monovalent reference compound **62**.

GNP	Iminosugar conc. (µM) in 2 mg/mL^{-1} of Au GNPs	Jack-bean α mannosidase K_i
154	413	8 ± 2 µM *Competitive*
155	467	16 ± 2 µM *Competitive*
156	567	0.198 ± 0.060 µM *Competitive*
157a	450	0.175 ± 0.171 µM *Competitive*
157b	503	0.084 ± 0.066 µM *Competitive*
143	0	n.i. at 0.5 mg/mL
158	0	n.i. at 0.5 mg/mL
Compound	**Iminosugar conc. (µM)**	**Jack-bean α mannosidase K_i**
62	1000	322 µM

Table 3.13: IC$_{50}$ values measured for Au GNPs towards JBαMan.

The effective iminosugar component concentration of Au GNPs **154**, **155**, **156**, **157a** and **157b** was determined by qNMR. This allowed us to measure the IC_{50} values as the µM concentration of the iminosugar in the nanoparticles. Monovalent reference compound **62** showed an IC_{50} value of 322 µM, while all the multivalent Au GNPs bearing DNJ iminosugar derivatives display IC_{50} in the low micromolar range, thus validating that a multivalent presentation of the iminosugar generates a real advantage in the biological activity. The best activity of the series was that obtained for Au GNPs **157b**, decorated with 40% of tris-DNJ and 60% of α-mannose as inner component (0.084 µM). This is also the best result obtained with a glyconanoadduct towards JBMan, considering that it is twice better than the best result obtained with some glycopeptides self-assembled in micelles synthesized by Compain in 2014, also glyconanoclusters but with another NP size and loading (among 30 nm).[126] Moreover, it is the first DNJ-based NP evaluated on JBMan.

The effective advantage of an additional synthetic step, consisting in the trimerization of the bioactive ligand before the formation of AuGNPs, could be justified by comparing the biological activities of GNPs **155** and **157a** which display the same number of *active component* (i.e. approximately 9 DNJ units). Indeed, from qNMR (measured at 2mg/mL in terms of nanoparticles) the concentration of DNJ was confirmed to be 467 µM and 450 µM for GNPs **155** and **157a** respectively. Despite the comparable DNJ concentrations, GNPs **157a** showed a much lower Ki with respect to **155** (0.175 µM vs 16 µM). While the multivalent effect in **155** arises exclusively from the multimerization of monovalent DNJ on the gold nanoparticle platform, in **157a** we can ascribe the much higher biological activity to the multivalent synergy of the platform (AuGNPs) and the previous trimerization of DNJ units, suggesting that the preorganization of the ligand in trimeric heads plays a fundamental role.

Activities of Au GNPs displaying mono DNJ ligands **154** and **155** and β-glucose and α-mannose respectively, were active in a similar range, as we previously observed for pyrrolizidine-based Au GNPs **127a**-**127c** and **127b**-**127d**.[112] Moreover, their activity is comparable to the glycopeptides reported by Compain in 2014.[126] The same comparison in terms of inner component can be done also for compounds bearing the tripod tris-DNJ **156** and **157a-b**, confirming that the biological activity depends only from the iminosugar part of the glyconanoadducts. It is worth noting that this aspect is not always glaring, given the results obtained with 100% β-Glc Au GNPs 143 in the case of GALNS inhibition (see section 3.3.1).

_____

[126] Bonduelle C., Huang J., Mena-Barragan T., Ortiz Mellet C., Decrocq C., Etame E., Heise A., Compain P., Lecommandoux S., *Chem. Commun.*, **2014**, 5*0*, 3350-3352.

3.3.2.3 Studies by TEM

To better rationalize the binding interactions largely enhanced by a multimeric presentation of our DNJ ligand, we aim to analyse the complexes JBMan-ligands through Transmission Electron Spectroscopy (TEM) with negative staining. This kind of studies are now ongoing in our laboratories, in collaboration with the laboratory of GLycoNanoTechnology of CIC biomaGUNE in San Sebastian, Spain.

JBMan is a high molecular weight metalloenzyme of about 220 KDa, which comprises two pairs of subunits that have molecular weights of 66 and 44 KDa, respectively,[127] and is visible by TEM. By exploiting the technique of TEM with negative staining, we will be able to see how our glyconanoparticles interact with the enzyme and how the enzyme will display its conformation in the presence of such inhibitors. Those experiments will enrich this study about the multimerization of DNJ onto gold nanoparticles as scaffolds, that until now, were not still reported in literature.

3.3.2.4 Conclusion

In this project, Au GNPs decorated with the iminosugar active component DNJ were synthesized, in searching for new potent inhibitors of JBMan enzyme. Following the *in situ* direct synthesis protocol reported in 1994 by Brust and co-workers,[109] that we demonstrated to be successful to graft on a gold nanoparticle surface ligands of iminosugar nature,[112] Au GNPs decorated with different loadings of DNJ component were obtained. Being not possible to overcharge the percentage of iminosugar component onto gold surface, we trimerized the bioactive compound before grafting it on the nanoparticle, following the procedure already performed in the previous work with DAB-1 Au GNPs.[45b] A remarkably inhibitory activity was found for both Au GNPs **154** and **155**. By grafting onto the gold core the DNJ tripod **146**, Au GNPs **156**, **157a** and **157b** was achieved and they showed the best activity of the series. In particular, **157b** with a Ki of 0.084 μM, is the best among multivalent nanosized DNJ inhibitors ever reported in literature to the best of our knowledge.

Given the excellent results achieved with these Au GNPs and being DNJ a potent GCase inhibitor (see section 1.2.2), in the next future we would like to test these derivatives also against the GCase enzyme, in order to find new selective inhibitors/chaperones to be apply in the treatment of Gaucher Disease. Additionally, we are also planning to follow the same synthetic protocol to multimerize our bioactive trihydroxypiperidine already multimerized with dendrimeric scaffolds, onto gold glyconanoparticles, in order to study the effect of another type of scaffold on the GCase inhibition.

_____

[127] Gnanesh Kumar B. S., Pohlentz G., Schulte M., Mormann M., Kumar N. S., *Glycobiology*, **2014**, *24*, 252–261.

3.3.2.4 Experimental section

For the general details see paragraph 3.3.1.4. TEM analysis was performed with a Philip CM12 instrument with CRYO-GATAN UHRST 3500 Technology, digital camera and EDAX microanalysis and with a JEOL JEM-2100F microscope, both operating at 200 kV. ICP analysis was performed with a Thermo Scientific™ iCAP 7400 ICP-OES analyzer.

Synthesis of piperidine 149: To a solution of **148** (36 mg, 79 µmol) in 4.6 mL of THF/H_2O = 2:1, PPh_3 (25 mg, 75 µmol) was added. The reaction mixture was then refluxed for 5.30 h, until a TLC analysis (CH_2Cl_2/MeOH 10: 1) showed the disappereance of the starting material (*R*f= 0.91) and the formation of a new product (*R*f= 0.10). The solvent was removed under reduced pressure and the crude was purified by FCC (CH_2Cl_2/MeOH/NH_3 from 10: 1 to 5: 1: 0.2) affording pure **149** (25 mg, 58.1 µmol, *R*f = 0.10 in CH_2Cl_2/MeOH 10: 1) as colourless oil in 74% yield. **[α]$^D_{22}$** = + 4.75 (c = 0.59 in $CHCl_3$); **^{1}H-NMR** (400 MHz, $CDCl_3$): δ = 5.05 (dt, *J* = 17.1, 9.2 Hz, 2H, H-3, H-4), 4.94 (td, *J* = 10.0, 5.0 Hz, 1H, H-5), 4.19-4.09 (m, 2H, H-7), 3.18 (dd, *J* = 11.5, 5.1 Hz, 1H, Ha-6), 2.75-2.68 (m, 1H, Ha-1'), 2.62 (dt, *J* = 11.6, 2.5 Hz, 1H, H-2), 2.57-2.50 (m, 1H, Hb-1'), 2.43 (bs, 2H, H-6'), 2.30 (t, *J* = 10.5 Hz, 1H, Hb-6), 2.06 (s, 3H, OAc), 2.01 (s, 6H, OAc), 2.00 (s, 3H, OAc), 1.48-1.22 (m, 8H, H-2', H-3', H-4', H-5') ppm; **^{13}C-NMR** (100 MHz, $CDCl_3$): δ = 171.0-169.9 (s, 4C, -O$\underline{C}$OCH_3), 74.8 (d, C-5), 69.7 (C-3), 69.6 (d, C-4), 61.7 (d, C-2), 59.7 (t, C-7), 53.0 (t, C-6), 51.8 (t, C-1'), 27.1-26.8 (t, 4C, from C2' to C5'), 24.9 (t, C-6'), 21.0-20.8 (q, 4C, -CO$\underline{C}H_3$) ppm; **MS (ESI)**: m/z 431.04 (100, H$^+$). **IR** ($CDCl_3$): $\tilde{v}$ = 2935, 2860, 2255, 1744, 1664, 1601, 1508, 1369, 1234, 1061, 1032 cm^{-1}. **Elemental analysis** (%) for $C_{20}H_{34}N_2O_8$ (430.49): calcd C, 55.80; H, 7.96; N, 6.51; found: C, 55.74; H, 7.87; N, 6.60.

Synthesis of DNJ based ligand 150: A solution of EDC·HCl (1-Ethyl-3-(3-dimethylaminopropyl) carbodimide hydrochloride (18.2 mg, 95 µmol), 1–hydroxybenzotriazole (HOBt, 11.7 mg, 87 µmol) and **129** (25.9 mg, 59 µmol) in dry DMF (0.2 mL) was left stirring for 10 min. and then added to a solution of DNJ derivative **149** (17.0 mg, 40 µmol) and *N*,*N*-diisopropylethylamine (19 µL, 107 µmol) in DMF (0.9 mL). The reaction mixture was left stirring at room temperature, under nitrogen atmosphere, for 6 hours, then diluted with AcOEt (10 mL) and washed with H_2O (2 x 3 mL). The organic layer was then washed with a satured solution of $NaHCO_3$ (1 x 3 mL) and brine (1 x 4 mL), dried over anhydrous Na_2SO_4 and concentrated under vacuum. The crude was purified by column chromatography (DCM/MeOH from 30:1 to 10:1) affording 22 mg of **150** (26 µmol, 67% yield). *R*f = 0.32 (CH_2Cl_2/MeOH 10: 1). [α]$^D_{26}$ = 3.33 (c = 0.69 in $CHCl_3$). **^{1}H-NMR** (400 MHz, $CDCl_3$): δ = 5.06 (dt, *J* = 9.2, 2.8 Hz, 2H, H-3, H-4), 4.99-4.92 (m, 1H, H-5), 4.17-4.13 (m, 2H, H-7), 3.98 (s, 2H, L-1), 3.69-3.56 (m, 12H, from L-2 to L-7), 3.44 (t, *J* = 6.8 Hz, 2H, L-8), 3.29-

3.16 (m, 3H, H-6', Ha-6), 2.85 (t, *J* = 3.6 Hz, 2H, L-18), 2.77-2.69 (m, 1H, Ha-1'), 2.64-2.61 (m, 2H, H-2), 2.58-2.52 (m, 1H, Hb-1'), 2.32 (bs, 4H, SAc, Hb-6), 2.08 (s, 3H, OAc), 2.02 (s, 6H, OAc), 2.01 (s, 3H, OAc), 1.59-1.51 (m, 4H, L-9, L-17), 1.36-1.25 (m, 22H, from H-2' to H-5', from L-10 to L-16) ppm; **¹³C-NMR** (50 MHz, CDCl₃): δ = 195.9 (s, S$\underline{C}$OCH₃), 170.8-170.0 (s, 4C, -O$\underline{C}$OCH₃), 169.7 (s, $\underline{C}$ONH-), 74.7 (d, C-5), 71.6-70.0 (t, 8C, from L-1 to L-8), 69.5 (C-3), 69.4 (d, C-4), 61.5 (d, C-2), 59.2 (t, C-7), 52.9 (t, C-6), 51.7 (t, C-1'), 38.7 (t, C-6'), 30.6 (q, -SCO$\underline{C}$H₃), 29.6-28.9 (t, 11C, from L-9 to L-18, C-5'), 26.9-26.1 (t, 3C, C-2', C-3', C-4'), 20.8-20.7 (q, 4C, -CO$\underline{C}$H₃) ppm; **MS (ESI)**: m/z 871.35 (100, M+Na⁺). **IR** (CDCl₃): $\tilde{v}$ = 3005, 2929, 2856, 1744, 1673, 1540, 1466, 1370, 1237, 1107, 1033 cm⁻¹; **Elemental analysis** (%) for C₄₁H₇₂N₂O₁₄S (849.08): calcd C, 58.00; H, 8.55; N, 3.30; found: C, 57.94; H, 8.50; N, 3.39.

Synthesis of trivalent piperidine 151: To a solution of **148** (63 mg, 138 µmol) in 3 mL of THF/H₂O = 2:1 CuSO₄ (2.1 mg, 13 µmol), sodium ascorbate (5 mg, 25 µmol) and **81**[128] (9.9 mg, 42 µmol) were added. The reaction mixture was stirred in microwave at 80 °C for 45 min, until a TLC analysis (CH₂Cl₂/MeOH 10: 1) showed the disappearance of the starting material (*R*f = 0.46) and the formation of a new product (*R*f = 0.00). The solvent was removed under reduced pressure and the crude was purified by FCC (CH₂Cl₂/MeOH/NH₃ from 30: 1 to 5: 1: 0.1) affording pure **151** (57 mg, 35.4 µmol, *R*f = 0.33 in CH₂Cl₂/MeOH/NH₃ 10: 1: 0.1) as a pale yellow oil, in 85% yield. **[α]$^D_{22}$** = + 7.47 (c = 0.91 in CHCl₃). **¹H-NMR** (400 MHz, CDCl₃): δ = 7.58 (br s, 3H, triazole), 5.09-5.01 (m, 6H, H-3, H-4), 4.96-4.91 (m, 3H, H-5), 4.60 (s, 6H, H-β), 4.34 (t, *J* = 7.2 Hz, 6H, H-6'), 4.18-4.10 (m, 6H, H-7), 3.44 (s, 6H, H-α), 3.18 (dd, *J* = 11.4, 5.0 Hz, 3 H, Ha-6), 2.76-2.69 (m, 3H, Ha-1'), 2.63-2.60 (m, 3H, H-2), 2.56-2.49 (m, 3H, Hb-1'), 2.29 (t, *J* = 10.8 Hz, 3H, Hb-6), 2.07-1.84 (m, 36H, OAc), 1.45-1.25 (m, 24H, H-2', H-3', H-4', H-5') ppm; **¹³C-NMR** (100 MHz, CDCl₃): δ = 170.8-169.7 (s, 12C, -O$\underline{C}$OCH₃), 145.1 (s, 3C, triazole), 122.4 (s, 3C, triazole), 74.7 (d, 3C, C-5), 72.3 (t, 3C, C-α), 69.6 (d, 3C, C-3), 69.4 (d, 3C, C-4), 65.1 (t, 3C, C-β), 61.8 (d, 3C, C-2), 59.7 (t, 3C, C-7), 52.9 (t, 3C, C-6), 51.6 (t, 3C, C-1'), 50.2(t, 3C, C-6'), 30.3 (t, 3C, C-5'), 26.7 (t, 3C, C-2'), 26.4 (t, 3C, C-3'), 25.0 (t, 3C, C-4'), 20.9 (q, 12C, $\underline{C}$H₃CO) ppm; **MS (ESI)**: m/z 1626.58 (100, Na⁺); **IR** (CDCl3): $\tilde{v}$ = 3690, 3606, 2937, 2862, 2257, 1745, 1602, 1438, 1370, 1234, 1097, 1052, 1032 cm⁻¹. **Elemental analysis** (%) for C₇₃H₁₁₃N₁₃O₂₇ (1604.75): calcd C, 54.64; H, 7.10; N, 11.35; found: C, 54.60; H, 7.25; N, 11.37.

Synthesis of trivalent DNJ based ligand 152: To a solution of compound **151** (56.8 mg, 35.4 µmol) in dry THF (570 µL) at 0 °C, 3-(diethoxyphosphoryloxy)-1,2,3-benzotriazin-4(3H)-one (DEPBT 21.2 mg, 70.8 µmol) and *N,N*-diisopropylethylamine (DIPEA 12.0 µL, 70.8 µmol) were added. The mixture was stirred at 25 °C for 15 min under a nitrogen atmosphere, then a solution of **129** (30.0 mg, 21.6 µmol) in dry THF (225 µl) was added and the reaction mixture was stirred at room temperature for 6 days, until a TLC analysis

---

[128] Y. M. Chabre, C. Contino-Pépin, V. Placide, T. C. Shiao and R. Roy, *J. Org. Chem.*, 2008, **73**, 5602.

(CH$_2$Cl$_2$/MeOH 6: 1) showed the formation of a new product (*R*f = 0.7). The reaction mixture was diluted with AcOEt (5 mL), washed with NH$_4$Cl (2 × 3 mL), NaHCO$_3$ (2 × 3 mL) and H$_2$O (2 × 3 mL), dried over anhydrous Na$_2$SO$_4$ and concentrated under vacuum. Purification through gradient column chromatography (CH$_2$Cl$_2$/MeOH from 20: 1 to 10: 1) afforded pure **152** (61 mg, 30.1 µmol) as a yellow oil, in 94% yield. **[α]$^D_{18}$** = + 5.29 (c = 0.87 in CHCl$_3$). **^{1}H-NMR** (400 MHz, CDCl$_3$): δ = 7.54 (br s, 3H, triazole), 6.81 (s, 1H, CON-H), 5.06-4.98 (m, 6H, H-3, H-4), 4.94-4.88 (m, 3H, H-5), 4.57 (s, 6H, H-β), 4.31 (t, *J* = 7.2 Hz, 6H, H-6'), 4.15-4.07 (m, 6H, H-7), 3.84 (s, 2H, L-1), 3.77 (s, 6H, H-α), 3.63-3.51 (m, 12 H, from L-2 to L-7), 3.39 (t, *J* = 6.8 Hz, 2H, L-8), 3.15 (dd, *J* = 11.5, 5.1 Hz, 3H, Ha-6), 2.82 (t, *J* = 7.4 Hz, 2H, L-18), 2.74-2.67 (m, 3H, Ha-1'), 2.60-2.58 (m, 3H, H-2), 2.53-2-46 (m, 3H, Hb-1'), 2.28-2.24 (m, 6H, Sac, Hb-6), 2.03 (s, 9H, OAc), 1.99 (s, 18H, OAc), 1.98 (s, 9H, OAc), 1.91-1.84 (m, 6H, H-5'), 1.48 (quint., *J* = 14.1, 6.8 Hz, 4H, L-9, L-17), 1.33-1.22 (m, 32H, H-2', H-3', H-4', from L-10 to L-16) ppm; **^{13}C- NMR** (50 MHz, CDCl$_3$): δ = 196.0 (s, SCOCH$_3$), 170.8–169.7 (s, 12C, -OCOCH$_3$), 169.6 (s, CONH–), 144.9 (s, 3C, triazole), 122.5 (d, 3C, triazole), 74.7 (d, 3C, C-5), 71.6-70.0 (t, 8C, from L-1 to L-8), 69.6 (d, 3C, C-3), 69.4 (d, 3C, C-4), 68.9 (t, 3C, C-α), 65.0 (t, 3C, C-β), 52.9 (t, 3C, C-6), 51.6 (t, 3C, C-1'), 50.2 (t, 3C, C-6'), 30.3 (q, 30.2 (q, –CH$_2$SCOCH$_3$), 29.6–24.9 (t, 22C, from L-9 to L-18, C-2'- C-5'), 20.8, 20.7 (s, 12C, COCH3) ppm; **MS (ESI)**: m/z 1033.92 (100, (m/z) + 2Na$^+$); **IR** (CDCl3): ṽ = 3022, 2932, 2858, 1744, 1675, 1525, 1369, 1220, 1098, 1032 cm^{-1}. **Elemental analysis** (%) for C$_{94}$H$_{151}$N$_{13}$O$_{33}$S (2023.34): calcd C, 55.80; H, 7.52; N, 9.00; found: C, 55.76; H, 7.62; N, 8.92.

General procedure for the "in situ" deprotection of S-acetyl conjugates 150 and 152: To a solution of **150** and **152** in CD$_3$OD (20 mg ml^{-1} and 10 mg ml^{-1}, respectively), 30 equivalents of NaOMe were added and the reaction mixture was left stirring for 2 hours at 25 °C under a nitrogen atmosphere. The complete disappearance of the starting material was confirmed via ^{1}H-NMR and the crude product was directly used for the preparation of Au GNPs.

Preparation and characterization of Au GNPs: The Au GNPs coated with DNJ derivatives (mono- and trivalent) and simple monosaccharides βGlcC$_5$S and aManC$_5$S (DNJ-βGlc-Au NPs **154**, DNJ-αMan-Au NPs **155** and tri-DAB1-βGlc-Au NPs **156**, and tri-DNJ-αMan -Au NPs **157a-b**) were prepared by the reduction of an Au(III) salt using sodium borohydride in the presence of a mixture of thiol-ending iminosugar conjugate and βGlcC$_5$S **125** and αManC$_5$S **147** as ligands, in different ratios following a reported procedure.[112] For the analysis of the ratio between the iminosugar ligands and βGlcC$_5$S or αManC$_5$S, ^{1}H-NMR spectra of the initial mixture and the supernatant after Au-GNP formation were recorded. The ligand loading on the Au-GNPs was also evaluated by quantitative NMR (qNMR) using 3-(trimethylsilyl)propionic-2,2,3,3-d$_4$ acid (TSP-d$_4$) as an internal standard in the D$_2$O solution of the Au GNPs. The prepared Au GNPs were freeze-dried and stored at 4 °C. Under these conditions, the Au GNPs can be stored for months maintaining their biophysical

_____

properties. The Au GNPs **143**, coated only with the simple monosaccharide βGlcC$_5$S, and **158**, coated only with the simple monosaccharide αManC$_5$S were also prepared as previously described.

General procedure for the preparation of Au GNPs coated with iminosugars: An aqueous solution of HAuCl$_4$ (25 mM, 1 equiv.) was added to a 12 mM methanolic solution of a suitable mixture of thiol-ending sugar and iminosugar conjugates (3 equiv. overall). An aqueous solution of NaBH$_4$ (1 M, 27 equiv.) was then added in four portions, with vigorous shaking. The black suspension formed was shaken for 2 hours at 25 °C. After that, the supernatant was removed and analysed by ^{1}H-NMR to study the nanoparticle ligand composition. The residue was washed several times with MeOH. In order to separate well the nanoparticles from the supernatant centrifugation (12 000 rpm, 2 min) was performed. The residue was dissolved in a minimal volume of HPLC gradient grade water and purified by dialysis (SnakeSkin® Pleated Dialysis Tubing, 10 000 MWCO and Slide-A-Lyzer® 10K Dialysis Cassettes, 10 000 MWCO). Iminosugar coated Au GNPs were obtained as a dark-brown powder after freeze-drying and characterized via ^{1}H-NMR, UV-Vis spectroscopy and TEM analysis.

Preparation of 40% DNJ-βGlc NPs (154): A 1: 2.3 mixture of thiol-ending **145** (4.5 mg, 2.65 μmol) and βGlcC$_5$S **125** (1.0 mg, 3.72 μmol) in CD$_3$OD (1.1 mL) was used to obtain 0.35 mg of AuGNPs **154**. **TEM** (average diameter): 1.8 ±0.4 nm. **Quantitative ^{1}H-NMR** (400 MHz, D$_2$O containing 0.05 wt. % of 3-(trimethylsilyl)propionic-*2,2,3,3-d*$_4$ acid, sodium salt as an internal standard): 0.15 mg of **154** were dissolved in 200 μL of D$_2$O and 15 μL of D$_2$O containing 0.05 wt.% TSP were added and 31 nmoles of DNJ conjugate were found.[129] Significant peaks: δ = 2.84 (br s, 1H, from DNJ conjugate), 2.60-2.45 (m, 2H, from DNJ conjugate) ppm.

_____

[129] In the quantitative NMR (qNMR) a mediated value of the multiplet corresponding to Ha-1' proton signal (δ = 2.84 ppm, 1H) of DNJ conjugate and the multiplet corresponding to H-6 (δ = 2.60-2.45 ppm, 2H) was selected for integration as it falls in a spectral region free of other signals.
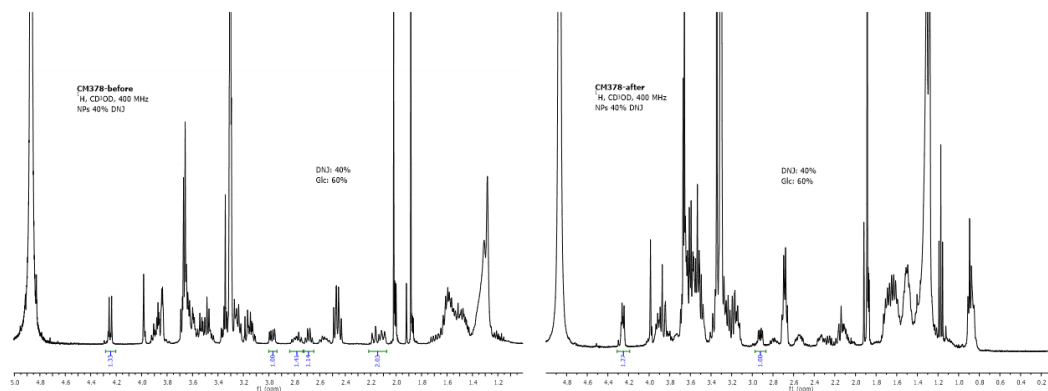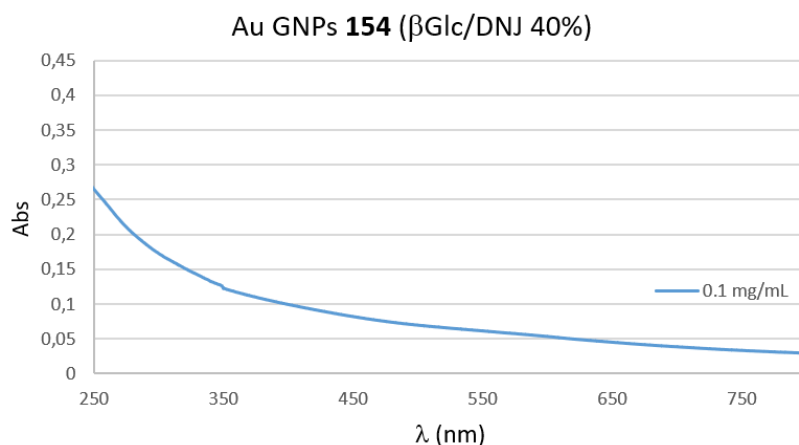
^{1}H NMR of sugar/iminosugar ligands mixture before (left) and after (right) formation of Au GNPs **154** (400 MHz, CD$_3$OD).
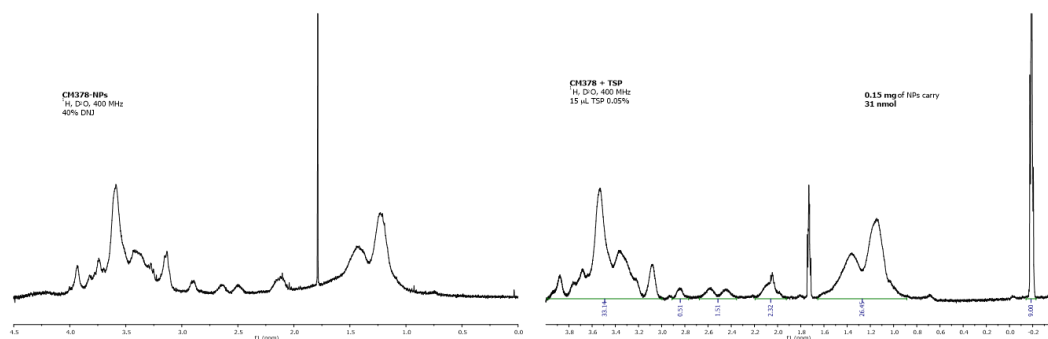
^{1}H NMR and ^{1}H qNMR with TSP-d$_4$ of Au GNPs **154** (400 MHz, D2O).
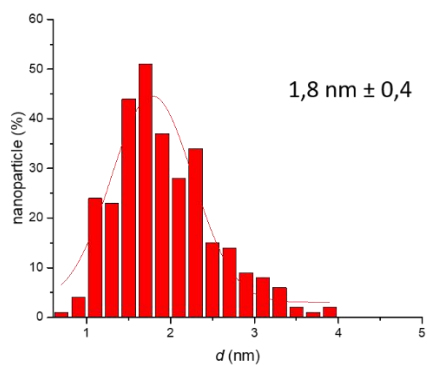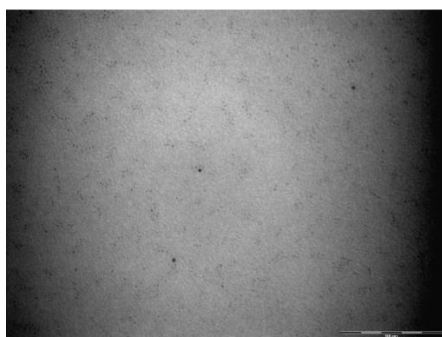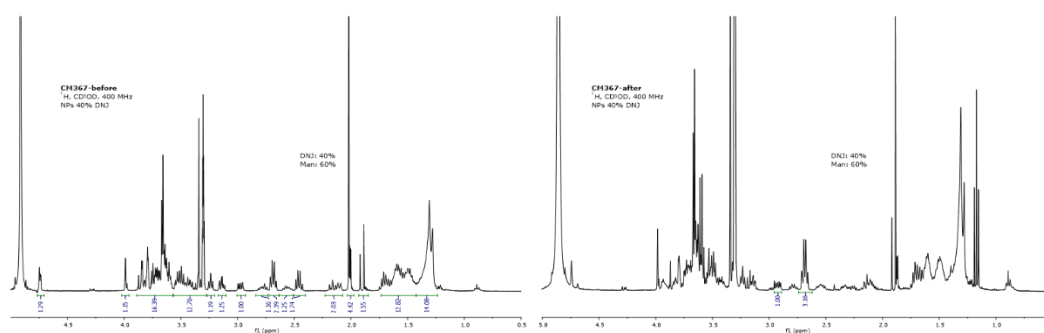

TEM micrograph in H$_2$O and size-distribution histogram obtained by measuring 300 nanoparticles (average diameter double distribution: 1.8 ±0.4 nm).

_____

Au GNPs **154** (βGlc/DNJ 40%)

UV/vis spectrum of H$_2$O solution of Au GNPs **154** recorded at concentration of 0.1 mg/mL.

Preparation of 40% DNJ-αMan NPs (155): A 1: 2.3 mixture of thiol-ending **145** (3.8 mg, 5.89 μmol) and αManC$_5$S **147** (4.2 mg, 14.73 μmol) in CD$_3$OD (1.2 mL) was used to obtain 1.33 mg of AuGNPs **155**. **TEM** (average diameter): 2.1 ±0.6 nm. **Quantitative ^{1}H-NMR** (400 MHz, D$_2$O containing 0.05 wt. % of 3-(trimethylsilyl)propionic-*2,2,3,3-d$_4$* acid, sodium salt as an internal standard): 0.60 mg of **155** were dissolved in 200 μL of D$_2$O and 40 μL of D$_2$O containing 0.05 wt.% TSP were added and 140 nmoles of DNJ conjugate were found.[130] Significant peaks: δ = 2.89 (m, 1H, from DNJ conjugate).
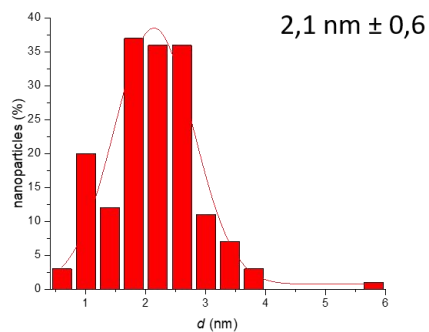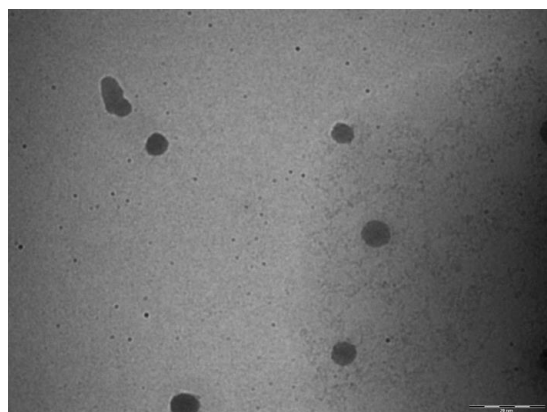

^{1}H NMR of sugar/iminosugar ligands mixture before (left) and after (right) formation of Au GNPs **155** (400 MHz, CD$_3$OD).

---

[130] In the quantitative NMR (qNMR) the multiplet corresponding to Ha-1' proton signal (δ = 2.89 ppm, 1H) of DNJ conjugate, was selected for integration as it falls in a spectral region free of other signals.
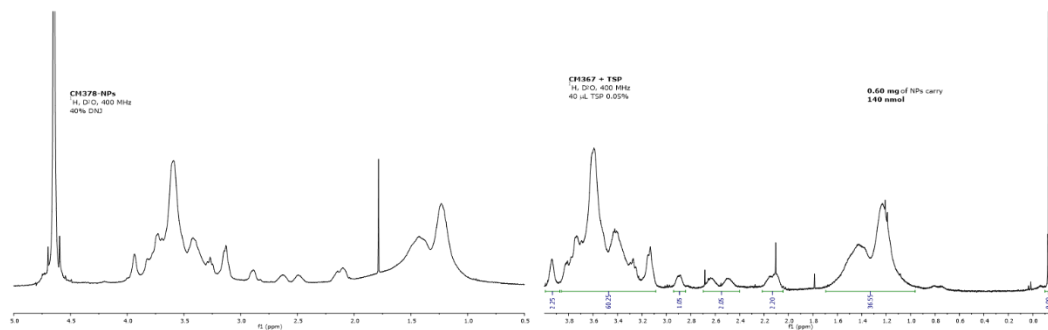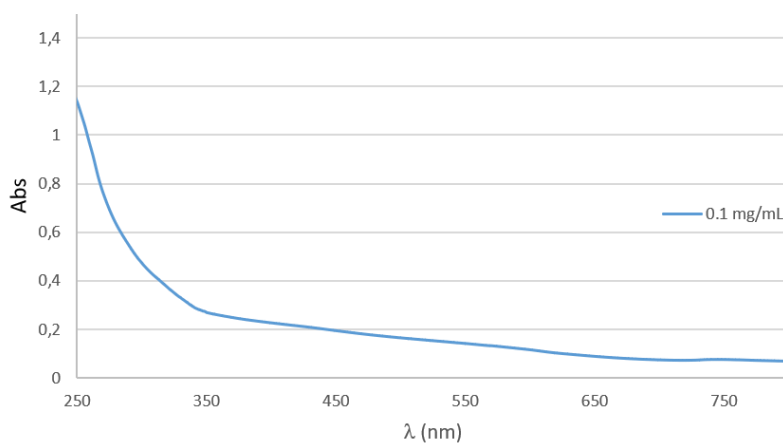
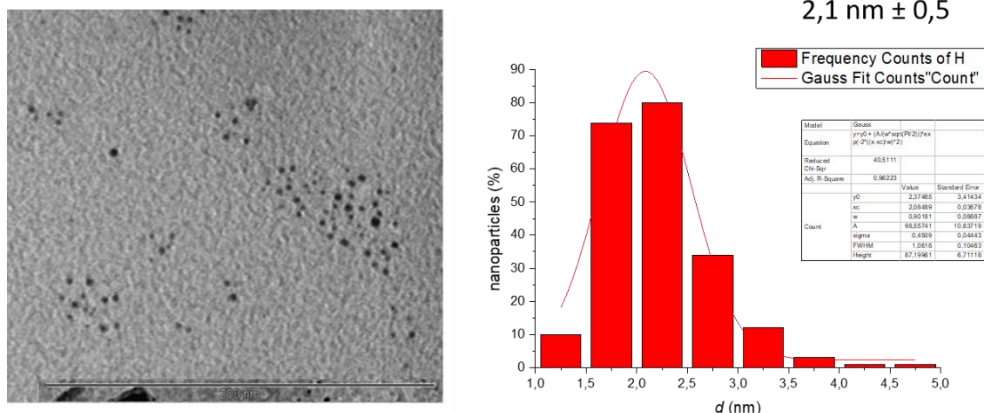^{1}H NMR and ^{1}H qNMR with TSP-d_4 of Au GNPs **155** (400 MHz, D$_2$O).

TEM micrograph in H$_2$O and size-distribution histogram obtained by measuring 300 nanoparticles (average diameter double distribution: 2.1 ±0.6 nm).
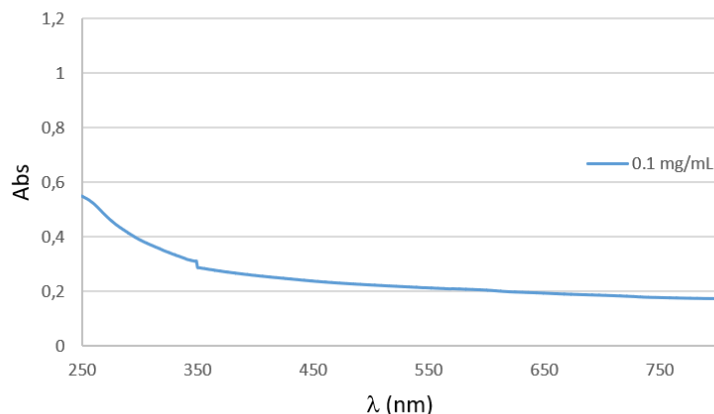
Au GNPs **155** (αMan/DNJ 40%)

UV/vis spectrum of H$_2$O solution of Au GNPs **155** recorded at concentration of 0.1 mg/mL.

Preparation of 20% DNJ-βGlc NPs (156): A 1: 2.3 mixture of thiol-ending **152** (10.9 mg, 7.41 μmol) and βGlcC$_5$S **125** (8.4 mg, 29.64 μmol) in CD$_3$OD (3.1 mL) was used to obtain 4.5 mg of AuGNPs **156**. **TEM** (average diameter): 2.1 ±0.5 nm. **Quantitative ^{1}H-NMR** (400 MHz, D$_2$O containing 0.05 wt. % of 3-(trimethylsilyl)propionic-*2,2,3,3-d$_4$* acid, sodium salt as an internal standard): 0.60 mg of **156** were dissolved in 180 μL of D$_2$O and 40 μL of D$_2$O containing 0.05 wt.% TSP were added and 170 nmoles of DNJ conjugate were found.[131] Significant peaks: δ = 7.83 (br s, 3H, triazole from DNJ derivative) ppm.

^{1}H NMR of sugar/iminosugar ligands mixture before (left) and after (right) formation of Au GNPs
156 (400 MHz, CD3OD).

^{1}H NMR and ^{1}H qNMR with TSP-d$_4$ of Au GNPs **156** (400 MHz, D$_2$O).

---

[131] In the quantitative NMR (qNMR) the multiplet corresponding to the triazole signal (δ = 7.83 ppm, 3H) of DNJ conjugate, was selected for integration as it falls in a spectral region free of other signals.

2,1 nm ± 0,5

TEM micrograph in H$_2$O and size-distribution histogram obtained by measuring 300 nanoparticles (average diameter double distribution: 2.1 ±0.5 nm).
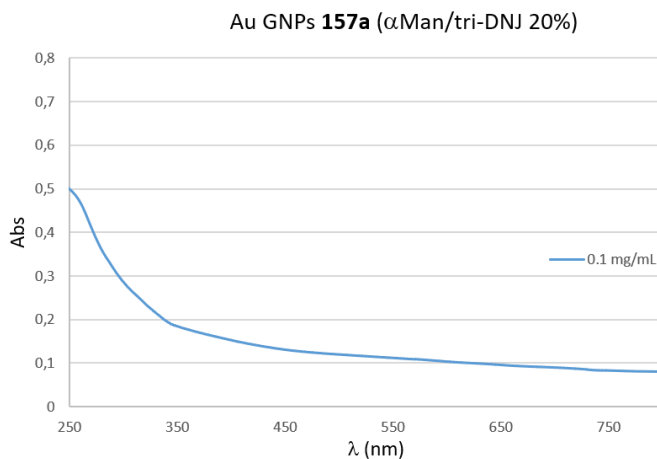

Au GNPs **156** (βGlc/tri-DNJ 20%)

UV/vis spectrum of H$_2$O solution of Au GNPs **156** recorded at concentration of 0.1 mg/mL.

Preparation of 20% DNJ-αMan NPs (157a): A 1: 2.3 mixture of thiol-ending **152** (10.9 mg, 7.41 µmol) and αManC$_5$S **147** (8.3 mg, 29.64 µmol) in CD$_3$OD (3.1 mL) was used to obtain 3.7 mg of AuGNPs **157a**. **TEM** (average diameter): 2.0 ±0.4 nm. **Quantitative ^{1}H-NMR** (400 MHz, D$_2$O containing 0.05 wt. % of 3-(trimethylsilyl)propionic-*2,2,3,3-d$_4$* acid, sodium salt as an internal standard): 0.60 mg of **157a** were dissolved in 180 µL of D$_2$O and 40 µL of D$_2$O containing 0.05 wt.% TSP were added and 135 nmoles of DNJ conjugate were found.[132] Significant peaks: δ = 7.84 (br s, 3H, triazole from DNJ derivative) ppm.

---

[132] In the quantitative NMR (qNMR) the multiplet corresponding to the triazole signal (δ = 7.84 ppm, 3H) of DNJ conjugate, was selected for integration as it falls in a spectral region free of other signals.

^{1}H NMR of sugar/iminosugar ligands mixture before (left) and after (right) formation of Au GNPs **157a** (400 MHz, CD$_3$OD).

^{1}H NMR and ^{1}H qNMR with TSP-d$_4$ of Au GNPs **157a** (400 MHz, D$_2$O).

TEM micrograph in H$_2$O and size-distribution histogram obtained by measuring 300 nanoparticles (average diameter double distribution: 2.0 ±0.4 nm).

Au GNPs **157a** (αMan/tri-DNJ 20%)

UV/vis spectrum of H₂O solution of Au GNPs **157a** recorded at concentration of 0.1 mg/mL.

Preparation of 40% DNJ-αMan NPs (157b): A 1: 2.3 mixture of thiol-ending **152** (6.9 mg, 4.70 μmol) and αManC₅S **147** (1.27 mg, 4.51 μmol) in CD₃OD (0.97 mL) was used to obtain 1.7 mg of AuGNPs **157b**. **TEM** (average diameter): 2.1 ±0.5 nm. **Quantitative ¹H-NMR** (400 MHz, D₂O containing 0.05 wt. % of 3-(trimethylsilyl)propionic-*2,2,3,3-d₄* acid, sodium salt as an internal standard): 0.60 mg of **157b** were dissolved in 180 μL of D₂O and 40 μL of D₂O containing 0.05 wt.% TSP were added and 151 nmoles of DNJ conjugate were found.[133] Significant peaks: δ = 7.81 (br s, 3H, triazole from DNJ derivative), 2.57-2.44 (m, 6H, from DNJ conjugate) ppm.
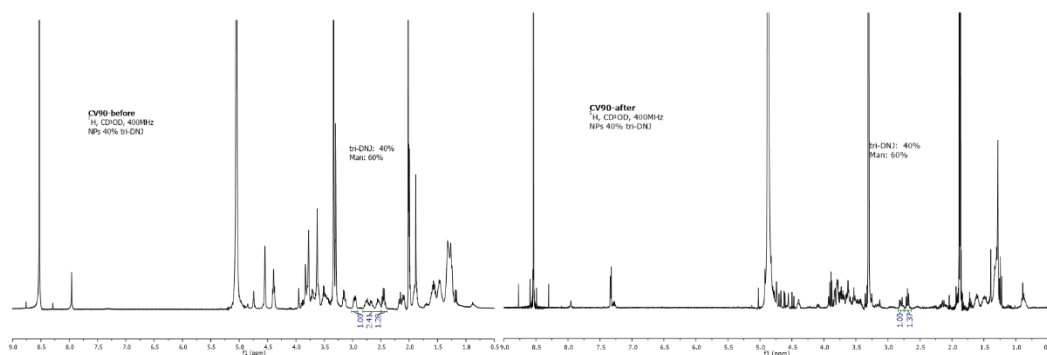

¹H NMR of sugar/iminosugar ligands mixture before (left) and after (right) formation of Au GNPs **157b** (400 MHz, CD₃OD).

---

[133] In the quantitative NMR (qNMR) a mediated value of the multiplet corresponding to the triazole signal (δ = 7.84 ppm, 3H) of DNJ conjugate and the multiplet corresponding to H-6 (δ = 2.57-2.44 ppm, 6H) was selected for integration as it falls in a spectral region free of other signals.
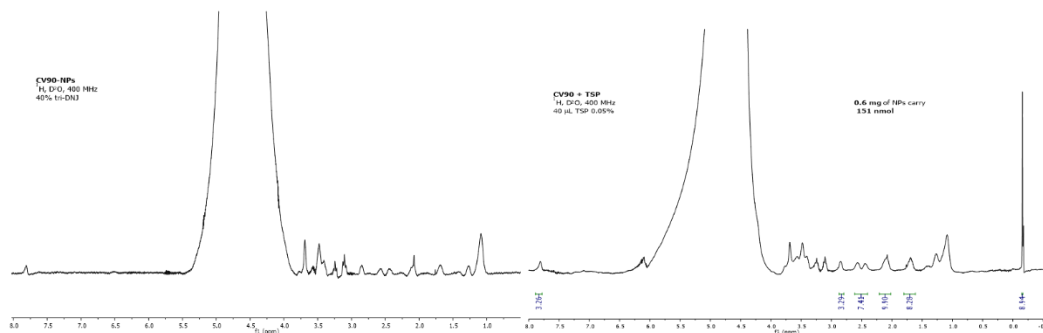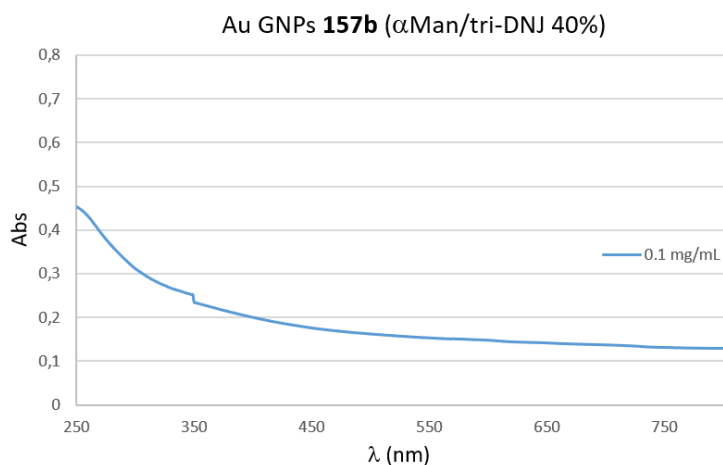
^{1}H NMR and ^{1}H qNMR with TSP-d$_4$ of Au GNPs **157b** (400 MHz, D$_2$O).
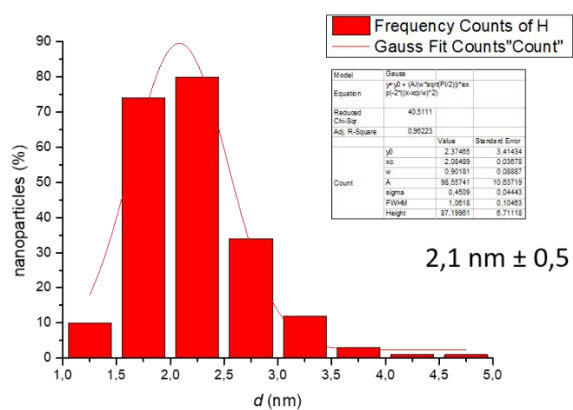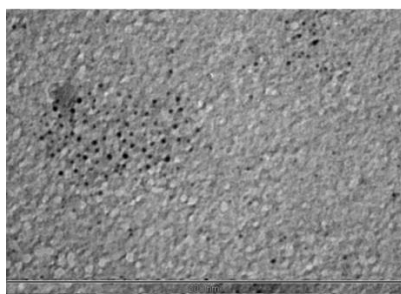
TEM micrograph in H$_2$O and size-distribution histogram obtained by measuring 300 nanoparticles (average diameter double distribution: 2.1 ±0.5 nm).

UV/vis spectrum of H$_2$O solution of Au GNPs **157b** recorded at concentration of 0.1 mg/mL.

3.3.3 1,3-dipolar cycloadditions

Aiming to find new methods that do not comprehend the use of copper in synthetic procedures, we developed a strategy that totally avoids the CuAAC reaction, by using the iteration of three selective and high-yielding steps (1,3-dipolar cycloaddition to nitrone **30**, N-O bond cleavage of the adduct and selective *N*- and/or *O*-allylation), that allows the preparation of different multivalent clusters iminosugars based on the natural DAB-1 moiety as the bioactive epitope. The 1,3-DC of nitrones with alkenes, like the CuAAC reaction, is a 100% atom economy reaction. Moreover, it does not need the presence of any additive or metal catalyst and requires only heating as the energy source. However, a major problem arises, since the 1,3-DC of cyclic nitrones to non-symmetric alkenes affords, in principle, two bicyclic isomeric isoxazolidines, each one possessing up to three new stereocentres formed in one-step (Figure 3.31).
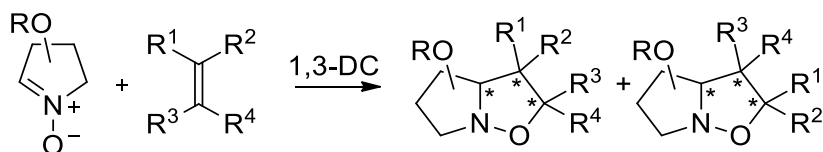

Figure 3.31: Schematic representation of 1,3-DC of pentaatomic cyclic nitrones to alkenes.

In order to represent an advantageous method, one must be sure that the 1,3-DC is highly stereoselective, reducing drastically the number of the possible diasteroisomers that may results from the reaction. In previous work we have proved that the peculiar all-*trans* relative stereochemistry of the D-arabino derived nitrone **30** allows it to undergo highly regio- and stereoselective 1,3-DC with mono- and disubstituted alkenes.[134]

We envisaged that the high selectivity shown by nitrone **30** may be exploited in a stepwise strategy with iteration of the 1,3-DC reaction, expecting formation of a single diastereoisomer (or a largely prevalent one) in each cycloaddition step. The proof of concept of this strategy for the building of new multivalent iminosugars based on DAB-1 is demonstrated in this work with the synthesis of dimeric and trimeric DAB-1 based architectures. This procedure, despite its lengthening compared to usual click techniques, allows placement of the bioactive units with different topologies, thus increasing the chance of achieving optimal interaction with the biological target.

---

[134] Martella D., D'Adamio G., Parmeggiani C., Cardona F., Moreno-Clavijo E., Robina I., Goti A., *Eur. J. Org. Chem.,* **2016**, 1588-1598.

Our results are object of this part of PhD thesis and can be also found in this paper:

3.3.3.1 Results and discussion

Nitrone **30** was synthesized from commercially available tribenzylated D-arabinose[134] and allyl benzyl ether **159** was obtained from benzyl alcohol as previously reported.[135] We envisaged that the iteration of the whole sequence (N-O bond cleavage, *N*- or *O*-allylation and 1,3-DC) would afford a growing linear oligomer chain with controlled size that contains the pyrrolidine bioactive unit either within the chain (structure A) or as a pendant (structure B), or mixed. The first step was the cycloaddition of **30** to **159**, performed by heating a toluene solution in a closed vial at 110 °C either with an oil bath for 2.5 h or using a MW reactor (1.5 h) affording, after purification by flash column chromatography (FCC), similar yield (85-86%, scheme 3.47) of the *exo-anti* isoxazolidine **160**. In both cases, a mixture of two other inseparable stereoisomers was isolated in a very small amount (15% and 8% yield). The structure of **160** was assigned on the basis of analogies of the ^{1}H NMR spectrum with other cycloadducts obtained with different dipolarophiles, and ascertained through 1D NOESY experiments, which showed correlation peaks between H-2, H-4 and H-6 protons that are located on the same side of the pyrrolizidine ring. Indeed, the dipolarophiles approach *anti* with respect to the vicinal benzyloxy group, and the *exo* mode is preferred to avoid repulsive steric interactions with substituent at C-4 placed on the opposite face, due to the nitrone *trans-trans* relative configuration.[69] Reductive cleavage of the N-O bond with 10 equiv of Zn in a 1:1 mixture of AcOH/H_2O at room temperature for 1.5 h gave quantitatively the amino alcohol **161**, which did not require further purification (scheme 3.47), then a selective *N*-allylation of **161** to the new dipolarophile **162** was performed using allyl bromide as the electrophile heating at 150 °C for 2 h under MW irradiation. In these conditions, *N*-allyl pyrrolidine **162** was obtained in 86% yield (Scheme 2). To confirm the selective *N*-allylation, compound **162** was acetylated to **163** in 66% yield.

---

[135] Ilardi E. A., Stivala C. E., Zakarian A., *Org. Lett.* **2008**, *10*, 1727-1730.
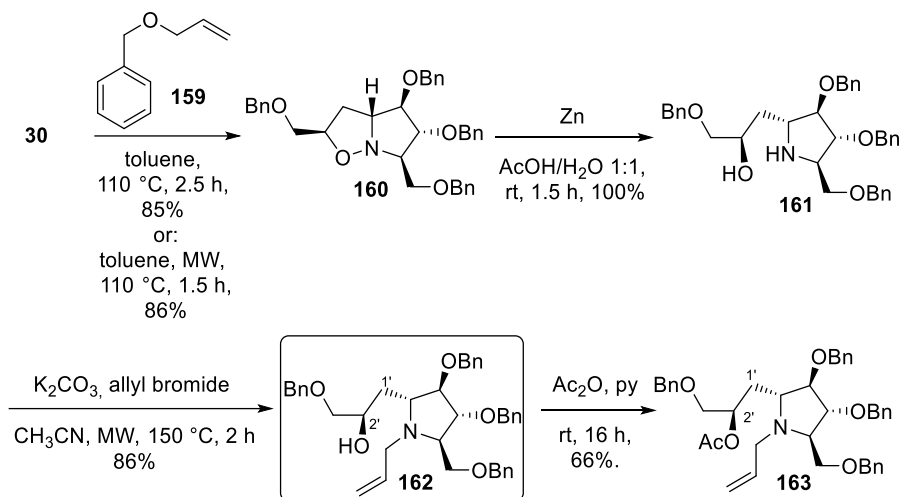
Scheme 3.47: 1,3-DC reaction of nitrone **30** to allyl benzyl ether **159**, N-O bond cleavage reduction and selective *N*-allylation.

Although it is known that selective *O*-allylation in the presence of a free amine is troublesome, we initially employed a hard base such as NaH to verify if satisfactory amounts of the desired compound **165** might be afforded avoiding lengthy protecting groups strategies. Under these conditions, a mixture of *N*-allylated **163**, *O*-allylated **165** and the *N,O*-bis allylated pyrrolidines **166** was obtained (scheme 3.48). The selectivity in favor of the *O*-allylated compound **165** was improved considerably (from 8 to 39%) when the less basic potassium tert-butoxide was employed as the base, but it was still unsatisfactory.
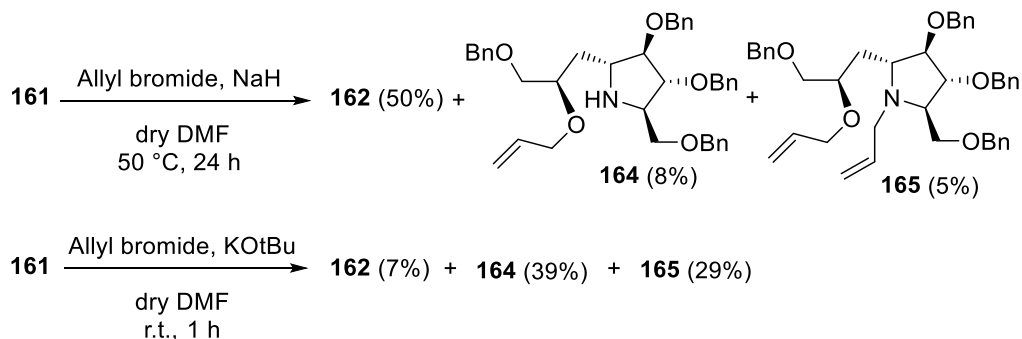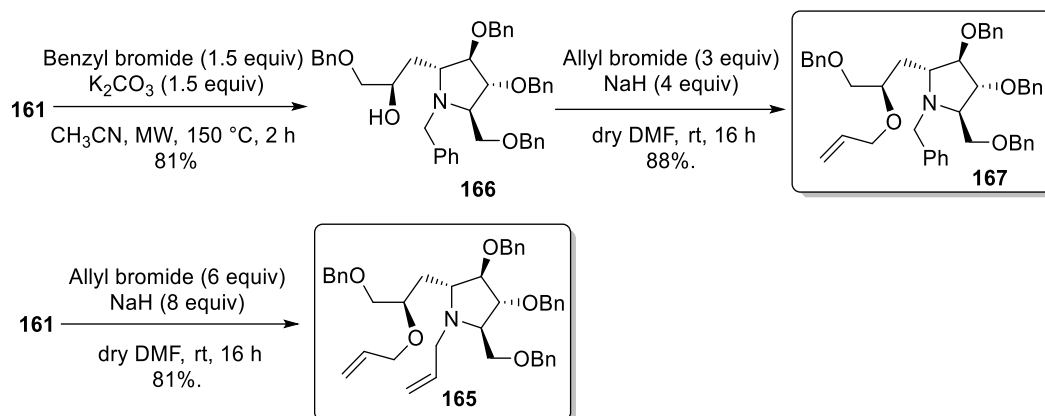

Scheme 3.48: Attempted selective *O*-allylation of amino alcohol **161**.

For this reason, we tried a different methodology, consisting in reacting **161** with benzyl bromide in CH₃CN with K₂CO₃ under MW irradiation at 150 °C for 2 h. The *N*-benzyl protected pyrrolidine **166** was then obtained in 81% yield (scheme 3.49), and it was expected to be less prone to undergo *N*-allylation and would be easily deprotected in the final debenzylation step. Indeed, allylation of **166** with allyl bromide (3 equiv) and NaH (4

_____

equiv) in dry DMF at room temperature afforded the allyl ether **167** in 88% yield (scheme 3.49). Moreover, direct treatment of **161** with a high excess of allyl bromide (6 equiv) and NaH (8 equiv) in dry DMF at room temperature for 16 h afforded exclusively the *N,O*-bis allylated pyrrolidine **165** (81% yield), which was employed as a bivalent dipolarophile in the 1,3-DC strategy.


Scheme 3.49: Selective *O*-allylation of amino alcohol **161** and *N,O*-bis allylation.

With the three new dipolarophiles **162**, **167** and **165** in hand, we investigated their 1,3-dipolar cycloaddition reactions with nitrone **30**. Reaction of *N*-allylated **162** with **30**, performed in toluene under MW irradiation at 110 °C for 2.5 h, afforded the *exo-anti* adduct **168** as a single diastereoisomer in 94% yield (Scheme 3.50). The deprotection of the perbenzylated adduct **168** was not a trivial task, due to the high basicity and hydrophilicity of the final products. When I began this work, a new strategy to obtain the final free amines had to be found, and here my contribution to this works inserts. I started with a catalytic hydrogenation with Pd/C in MeOH with a few drops of 37% aqueous HCl caused also the isoxazolidine ring opening and afforded the bis-pyrrolidinium hydrochloride **169** in quantitative yield. By passing the hydrochloride salt **169** through the ion exchange resin Dowex 50WX8-200 and eluting successively with MeOH, H_2O and 12% aqueous ammonia, the free amine **170** was recovered in the ammonia fraction with low yield (13%). However, further free amine **170** was obtained by treatment of the MeOH fraction with the strongly basic Ambersep 900-OH resin, to reach 40% overall yield of **170**.
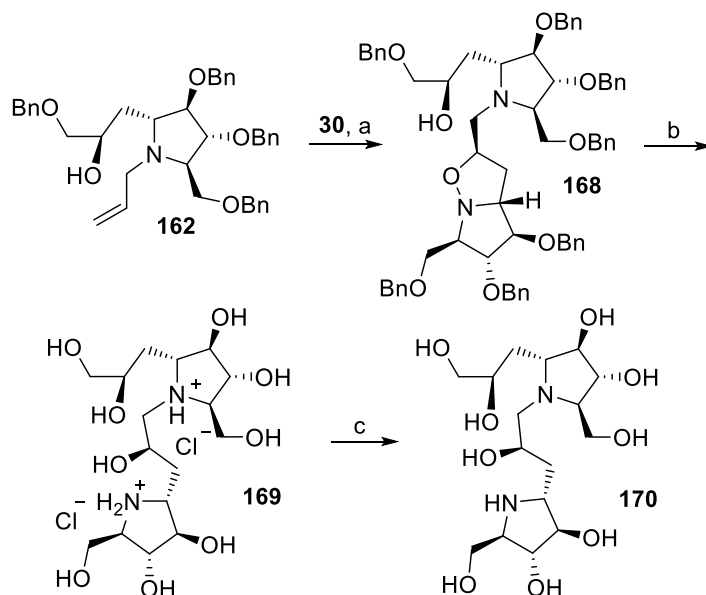
Scheme 3.50: Synthesis of the dimeric pyrrolidine **170**. Reaction conditions: a) Toluene, MW, 110 °C, 2.5 h, 94%; b) H$_2$, Pd/C, MeOH, HCl, rt, 16 h, 100%; c) Dowex 50WX8-200, and Ambersep 900-OH, 40%.

The cycloaddition of **167** with nitrone **30** was performed by heating in toluene under MW irradiation at 110 °C for 2.5 h. The reaction afforded the *exo-anti* adduct **171** as a single diastereoisomer in 87% yield (scheme 3.51). Subsequent catalytic hydrogenation with Pd/C in MeOH with some drops of 37% aqueous HCl gave the hydrochloride salt **172** in quantitative yield. Treatment with Dowex 50WX8-200 and eluting successively with MeOH, H$_2$O, and 12% aqueous ammonia afforded the free amine **173** in the ammonia fraction in 95% yield.
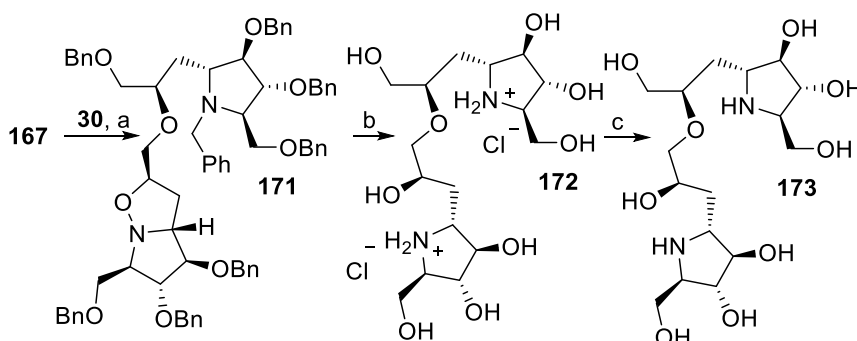
Scheme 3.51: Synthesis of the dimeric pyrrolidine **173**. Reaction conditions: a) Toluene, MW, 110 °C, 2.5 h, 87%; b) H$_2$, Pd/C, MeOH, HCl, rt, 16 h, 100%, c) Dowex 50WX8-200, 95%.

The cycloaddition of **165** to yield the bis-isoxazolidine adduct was finally undertaken. To

our delight, a single stereoisomer **174** was recovered in 53% yield, which derived from the *exo-anti* approach of the nitrone to both dipolarophile moieties. Catalytic hydrogenation with Pd/C in MeOH with some drops of 37% aqueous HCl gave the trimeric pyrrolidinium hydrochloride **175** in quantitative yield. Treatment with Dowex 50WX8-200 and with Ambersep 900-OH yielded the free amine **176** (scheme 3.52) in 60% overall yield.
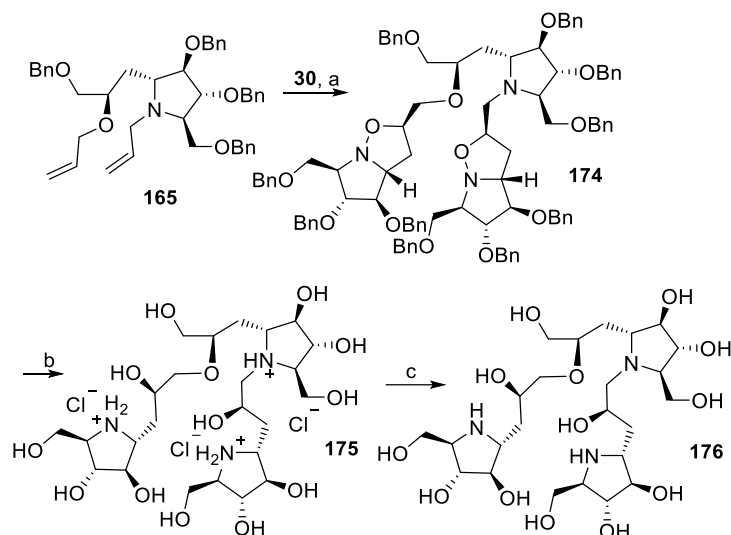
Scheme 3.52: Synthesis of the trimeric pyrrolidine **176**. Reaction conditions: a) Toluene, MW, 110 °C, 1.5 h, 53%; b) H$_2$, Pd/C, MeOH, HCl, rt, 16 h, 100%; c) Dowex 50WX8-200 and Ambersep 900-OH, 60%.

3.3.3.2 Biological evaluation

All the three free amines **170**, **173** and **176** were tested against GALNS enzyme, that we recently demonstrated to be particularly prone to accept multivalent iminosugars[45b] due to its dimeric nature.[44] No inhibition was showed by DAB-1 at 1 mM inhibitor concentration, however both dimer **170** and trimer **176** showed IC$_{50}$ in the low micromolar range (0.3 and 0.2 μM, respectively), thus confirming that multimerization of DAB-1 epitopes generates potent GALNS inhibitors. On the contrary, the dimer **173** possesses only a 55% inhibitory activity against GALNS, thus suggesting that the ligand topology strongly affects the affinity of the oligomeric constructs towards this enzyme, indeed, with type B oligomers, presenting the bioactive DAB-1 units more exposed and accessible, it could better interact with GALNS (scheme 3.53).
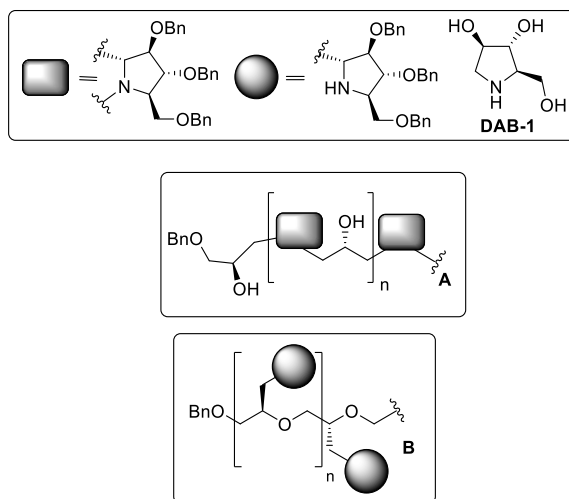
Scheme 3.53: Type A andtype B oligomers obtained by the iterative strategy.

3.3.3.3 Conclusions

In conclusions, in this project we explored an alternative synthetic pathway to achieve multimeric iminosugars without the use of copper mediated azide alkyne cycloaddition. This study could be used as proof of concept for the iteration of 1,3-dipolar cycloaddition, N-O-ring opening and selective *N*-allylation, or *O*-allylation, or both. The synthesis relies on the highly regio- and stereoselective of the 1,3-DC step that allows to obtain the new dipolarophiles **162**, **165** and **167** which were added again to nitrone **30** and finally converted to divalent DAB-1 based pyrrolidines **170** and **173** and trivalent **176**, respectively. This new strategy for the preparation of multimeric iminosugars involves the 100% atom economic 1,3-DC in the key steps, it does not employ homogeneous metals nor additives, and allows to access three different types of ligand topologies of the final DAB-1 clusters.

3.3.3.4 Experimental section

For the general details see paragraph 2.4.

Here are reported data dealing with the synthesis of the free amines **170**, **173**, **175**, **176**. The other experimental procedures can be found in this paper:

Matassini C., D'Adamio G., Vanni C., Goti A., Cardona F.
Studies for the Multimerization of DAB-1-Based Iminosugars through Iteration of the Nitrone Cycloaddition/Ring-Opening/Allylation Sequence, *Eur. J. Org. Chem*., **2019**, *30*, 4897-4905.

Synthesis of bis-pyrrolidine 170: The free amine was obtained by passing the hydrochloride salt **169** (35 mg, 0.075 mmol) through a Dowex 50WX8 ion-exchange resin, by eluting sequentially with MeOH, H_2O and 12% NH_4OH. The fraction eluted with 12% ammonia afforded the free base **170** (4 mg, 0.010 mmol, 13%). However, the fraction eluted with MeOH contained the unaltered hydrochloride salt **169**, which after treatment with the strongly basic Ambersep 900-OH resin afforded further 8 mg (0.020 mmol) of the free amine **170**. Compound **170** (12 mg, 0.030 mmol) was therefore obtained as a waxy white solid with a 40% overall yield. **[α]$^D_{25}$** = +5.7 (c = 0.14 in MeOH); **^{1}H-NMR** (400 MHz, D_2O): δ = 3.99-3.96 (m, 2H, H-3 and H-4'), 3.90-3.80 (m, 3H, H-4, H-8 and H-8'), 3.78-3.71 (m, 4H, H-3', H-9 and Ha-6'), 3.68 (dd, *J* = 11.7, 5.9 Hz, 1H, Hb-6'), 3.60 (dd, *J* = 11.7, 3.9 Hz, 1H, Ha-6), 3.48 (dd, *J* = 11.7, 6.3 Hz, 1H, Hb-6), 3.24-3.18 (m, 1H, H-2'), 3.16-3.11 (m, 1H, H-5), 3.06 (dt, *J* = 7.8, 3.4 Hz, 1H, H-2), 3.00 (q, *J* = 4.4 Hz, 1H, H-5'), 2.83 (dd, *J* = 13.7, 2.5 Hz, 1H, Ha-9'), 2.63 (dd, *J* = 13.7, 8.5 Hz, 1H, Hb-9'), 1.86 (dt, *J* = 14.1, 3.9 Hz, 1H, Ha-7), 1.76 (ddd, *J* = 13.7, 9.3, 4.4 Hz, 1H, Ha-7'), 1.72-1.65 (m, 1H, Hb-7'), 1.55 (dt, *J* = 14.2, 8.3 Hz, 1H, Hb-7) ppm; **^{13}C-NMR** (50 MHz, D_2O): δ = 80.7 (d, C-3), 80.3 (d, C-3'), 78.9 (d, C-4'), 76.5 (d, C-4), 70.0 (d, C-8'), 67.6 (d, C-5), 65.5 (d, C-8), 65.1 (t, C-6), 65.0 (d, C-2), 61.5 (d, C-5'), 60.0 (t, C-6'), 59.1 (t, C-9), 57.2 (d, C-2'), 52.3 (t, C-9'), 37.0 (t, C-7'), 30.7 (t, C-7) ppm; **MS (ESI):** m/z calcd for $C_{16}H_{32}N_2O_9$ $^+$ H^+ 396.99; found: 397.22 (100, [M+H]$^+$); **Elemental analysis** calcd (%) for $C_{16}H_{32}N_2O_9$ (396.43): C 48.48, H 8.14, N 7.07; found: C 48.46, H 8.10, N 7.06.

Synthesis of bis-pyrrolidine 173: The free amine **173** was obtained by passing the hydrochloride salt **172** (15 mg, 0.032) through a Dowex 50WX8 ion-exchange resin eluting sequentially with MeOH, H_2O and 12% NH_4OH. Elution with ammonia 12% afforded the free base **173** (12 mg, 0.030 mmol, 94% yield) as a white waxy solid, that tends to spontaneously form the corresponding mono-carbonate salt. **[α]$^D_{22}$**= + 51.6 (c = 0.45 in MeOH); **^{1}H-NMR** (400 MHz, D_2O): δ = 3.97-3.94 (m, 1H, H-8'), 3.91-3.86 (m, 2H, H-3, H-4'), 3.81-3.66 (m, 9H, H-4, H-3', H-6', H-6, Ha-9', H-9), 3.61-3.56 (m, 1H, H-8), 3.49-3.44 (m. 1H, Hb-9'), 3.23-3.07 (m, 4H, H-2, H-2', H-5', H-5), 2.02-1.90 (m, 1H, Ha-7), 1.84-1.76 (m, 1H, Ha-7'), 1.72-1.61 (m, 2H, Hb-7, Hb-7') ppm; **^{13}C-NMR** (50 MHz, D_2O): δ = 160.3 (q, 1C, HCO3-), 80.8, 77.8, 77.1, 77.0 (d, 4C, C-3, C-3', C-4, C-4'), 73.6 (t, 1C, C-9'), 67.9 (d, 1C, C-8'), 62.6-61.4 (6C, C-5, C-5', C-6, C-6', C-8, C-9), 57.0, 56.8 (2C, C-2', C-2), 36.0 (t, 1C, C-7'), 34.1 (t, 1C, C-7) ppm; **MS (ESI):** m/z calcd for $C_{17}H_{34}N_2O_{12}^+$ 397.22; found: 397.28 (100, [M]$^+$); **Elemental analysis** calcd (%) for $C_{17}H_{34}N_2O_{12}^+$ (458.46): C 44.54, H 7.48, N 6.11; found: C 45.05, H 7.44, N 5.84.

Synthesis of trimeric pyrrolidinium hydrochloride 175: To a solution of **174** (58 mg, 0.039 mmol) in 20 mL of MeOH, 29 mg of 10% Pd on carbon and four drops of HCl 37% were added while stirring under nitrogen atmosphere, then the mixture was stirred under hydrogen atmosphere at room temperature for 16 h. After TLC analysis (PE:AcOEt 2:1) showed the disappearance of the starting material (*R*f = 0.21) and formation of a new product, the mixture was filtered through Celite® and the solvent was removed under reduced pressure affording the trimeric pyrrolidinium hydrochloride **175** (27 mg, 0.039 mmol, 100% yield) as a yellow waxy solid. **[α]$^D_{24}$** = + 2.1 (c = 0.43 in MeOH); **^{1}H-NMR** (400 MHz, D$_2$O): δ = 4.34 (bs, NH), 4.13-4.03 (m, 7H), 3.99-3.88 (m, 7H), 3.73-3.57 (m, 8H), 3.46-3.39 (m, 5H), 2.20-2.08 (m, 6H) ppm; **^{13}C-NMR** (50 MHz, D$_2$O): δ = 77.8, 77.3, 76.3, 74.1 (d, 7C), 69.0 (d, 2C), 65.3, 63.0, 62.7, 58.2, 58.0, 56.5, 53.1 (11C), 49.2 (t, 1C), 34.6 (t, 2C), 28.2 (t, 1C) ppm; **MS (ESI):** m/z calcd for C$_{24}$H$_{49}$N$_3$O$_{13}$ 293.67; found: (100, [M]$^{2+}$).

Synthesis of trimeric pyrrolidine 176: The free amine was obtained by passing the hydrochloride salt **175** (67 mg, 0.096 mmol) through a Dowex 50WX8 ion-exchange resin, by eluting sequentially with MeOH, H$_2$O and 12% NH$_4$OH. The fraction eluted with 12% ammonia afforded free base **176** (11 mg, 0.019 mmol, 20%). However, the fraction eluted with MeOH contained the unaltered hydrochloride salt **175**, which after treatment with the strongly basic Ambersep 900-OH resin afforded further 23 mg (0.039 mmol) of the free amine **176**. Compound **176** (34 mg, 0.058 mmol) was therefore obtained as a waxy white solid with a 60% overall yield. **[α]$^D_{24}$** = + 7.0 (c = 0.70 in MeOH); **^{1}H-NMR** (400 MHz, D$_2$O): δ = 3.98 (bs, 1H), 3.93-3.84 (m, 1H), 3.82-3.54 (m, 16H), 3.46 (dd, J = 10.2, 7.0 Hz, 1H), 3.09-2.96 (m, 5H), 2.86-2.79 (m, 2H), 2.61-2.56 (m, 1H), 1.88-1.81 (m, 1H), 1.76-1.56 (m, 5H) ppm; **^{13}C-NMR** (50 MHz, D$_2$O): δ = 81.8 (1C), 81.7 (1C), 80.6 (1C), 79.8 (1C), 79.4 (1C), 78.1 (1C), 77.9 (1C), 73.5 (1C), 68.3 (1C), 68.1 (1C), 66.2 (1C), 64.6 (1C), 62.5, 62.3, 61.8, 61.7 (4C), 59.5 (1C), 57.8 (1C), 57.2 (1C), 52.1 (1C), 49.0 (1C), 38.6, 36.9 (t, 2C), 27.8 (t, 1C) ppm; **MS (ESI):** m/z calcd for C$_{24}$H$_{47}$N$_3$O$_{13}$ 585.31; found: 586.38 (100, [M+H]$^+$); **Elemental analysis** calcd (%) for C$_{24}$H$_{47}$N$_3$O$_{13}$ (585.64): C 49.22, H 8.09, N 7.18; found: C 48.95, H 8.32, N 9.95.
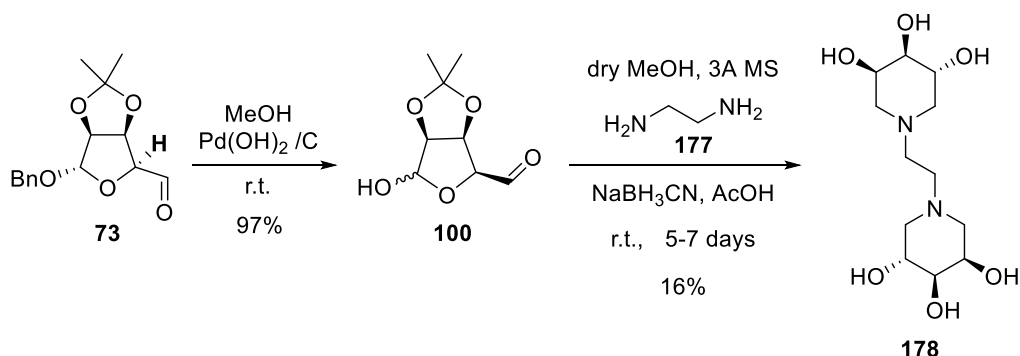
3.3.4 Multimeric trihydroxypiperidines through DRA

In the context of the multimerization techniques without the involvement of click CuAAC strategy, we are dealing with the development of a new strategy based on the double amination reaction (DRA) of the D-mannose derived intermediate **73**, whose condition were previously developed by our research group,[91,136] with different branched amines (scheme 3.54), in order to access new multivalent trihydroxypiperidines.
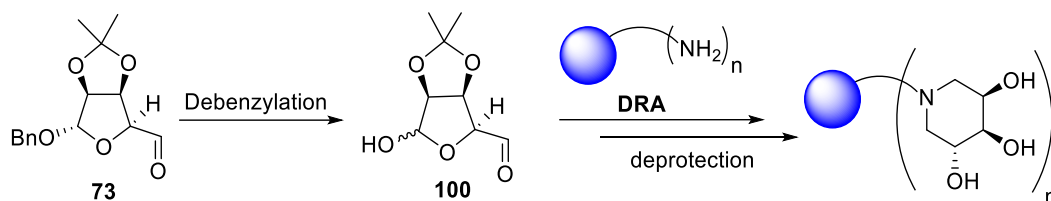
Scheme 3.54: Schematic representation of DRA strategy to obtain multivalent trihydroxypiperidines.

This strategy, once set up the optimal conditions to be used in the DRA, which is not as trivial as CuAAC, can represent another alternative pathway to those analyzed in chapter 3. We started the study of this strategy by using ethylenediamine **177** as amine dimeric scaffold. We envisaged two synthetic strategies: the first one consisting in the previous deprotection of the hydroxyl group in anomeric position of dialdehyde **73** to afford intermediate **100**, followed by reaction with diamine **177** in the presence of NaBH$_3$CN as the reducing agent. Compound **100** indeed was treated with ethylenediamine **177** and NaBH$_3$CN (3.0 equiv.) in dry methanol, in the presence of 3Å molecular sieves and AcOH (2.0 equiv.) for 5-7 days (scheme 3.55), affording dimeric trihydroxypiperidine **178**.

Scheme 3.55: Scheme of DRA to access dimeric trihydroxypiperidine **178**.

---

[136] Matassini C., Mirabella S., Ferhati X., Faggi C., Robina I., Goti A., Moreno-Clavijo E., Moreno-Vargas A. J., Cardona F., *Eur. J. Org. Chem.* **2014**, 5419–5432.

However, compound **178** was recovered in low yields (16%) after purification by FCC, probably due to the difficulties encountered in the extraction from the aqueous phase, in which it remains trapped due to its hydrophilic nature. For this reason, we tried an alternative strategy, in which we directly performed the DRA on the benzylated aldehyde **73**, that, in slight excess (1.2 equiv.), was reacted with ethylenediamine **177** (0.5 equiv.) in dry methanol and in the presence of 3 Å molecular sieves. After about 2 hours, Pd(OH)$_2$ /C was added and the reaction mixture was left stirring under H$_2$ atmosphere for 6 days (scheme 3.56); after purification by FCC, compound **179** was obtained in good yield (69%). The final deprotection in acidic conditions and treatment with strongly basic resin Ambersep 900-OH, afforded compound **178** in 86% overall yield.
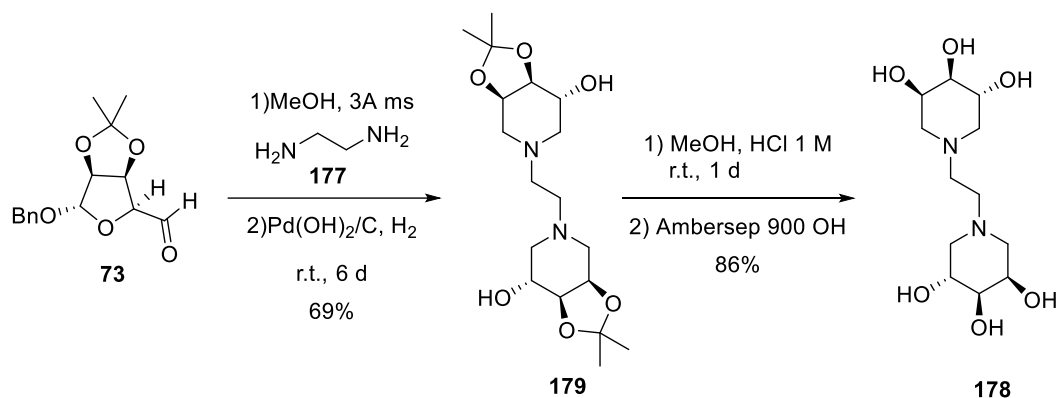
Scheme 3.56: Synthesis of dimeric piperidine **178** starting from protected dialdehyde **73**.

Having found these optimal reaction conditions for DRA with protected dialdehyde **73**, we are now planning to apply them to a list of 'polibranched' amines (for example we have started with 1,6-hexanediamine) that could allow the synthesis of a small library of multimeric trihydroxypiperidines without the use of copper mediated azide alkyne cycloaddition CuAAC with all the drawbacks related to it.

Preliminary inhibition tests were effectuated on a panel of six different human lysosomal glycosidases, in collaboration with Prof. Morrone from the Metabolic Diseases laboratory of the Meyer Pediatric Hospital of Florence. In particular, the activity of compound **178** was tested on the following glycosidases: α-fucosidase (α-Fuc), α- and β-galactosidase (α- and β-Gal), α- and β-mannosidase (α- and β-Man) and β-glucosidase (β-Glu or GCase).

	α -Fuc	α-Gal	β-Gal	α -Man	β-Man	β-Glu
178	12 (%)	3 (%)	34 (%)	-	3 (%)	17 (%)

Table 3.33: Inhibitory activity (%) towards a panel of six glucosidases

The inhibitory activity of compound **178** towards the lysosomal glycosidases was evaluated in leukocytes isolated from healthy donors by measuring enzymatic activity by means of a fluorimetric assay: compound **178** (1 mM), leukocyte homogenate and specific synthetic substrate (buffered at an appropriate pH) were incubated at 37 ° C for 1 hour. The reaction was stopped with pH 10.7 buffer and the fluorescence measured in a SpectraMax M2 microplate reader. Glycosidase inhibition was calculated with respect to the corresponding control.

A weak inhibition was observed for all the glycosidases towards it was tested: the α-fucosidase and β-glucosidase enzymes were inhibited in a range lower than 20% (12% and 17%, respectively), while β-galactosidase was inhibited by 34%. In the case of α-Gal and β-Man the inhibition values are lower than 10%. A particular behaviour was observed for α-mannosidase, whereby compound **178** appears to function as an activator (increase in activity by 28%). Few examples are reported in literature of glycosidases activators, but they represent a great opportunity in therapeutics, allowing the modulation of the biological activity from inhibition to activation.[137] We thought that maybe the reason of low biological activity of dimeric piperidine **178** is related to the shortness of tether length between the two hydroxypiperidine polar heads that could hamper the dimer flexibility. For this reason, attempts to synthesize a dimeric piperidine bearing a longer spacer than two carbon atoms, are now ongoing in our laboratories, in particular we are synthesizing a **178** analogue with a six-atom tether length (**180**, scheme 3.57).
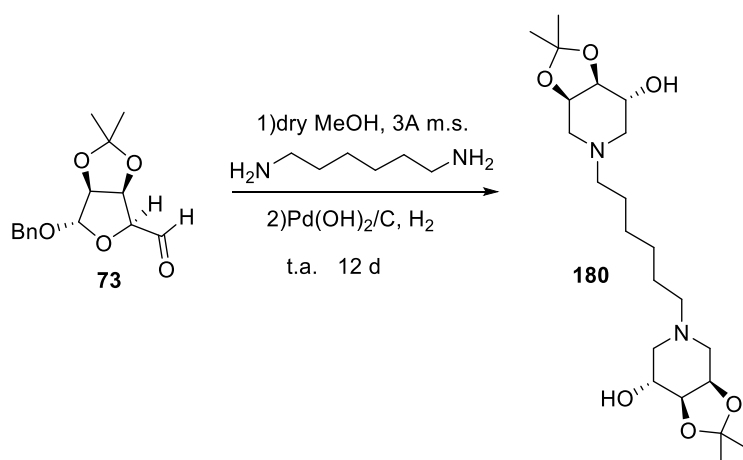
Scheme 3.57: Synthesis of six atom tether length dimeric piperidine **180**.

---

[137] Alvarez-Dorta D., Brissonnet Y., Saumonneau A., Deniaud D., Bernard J., Yan X., Tellier C., Daligault F., G. Gouin S., *Chem. Sel.*, **2017**, *2*, 9552 – 9556.

3.3.4.1 Experimental section

For the general details see paragraph 2.4.

Strategy A for the synthesis of piperidine 178: A solution of dialdehyde **100** (107 mg, 0.57 mmol) in dry MeOH (1 mL) was stirred in the presence of 3Å molecular sieves powder for 15 min, under nitrogen atmosphere, NaBH$_3$CN (107 mg, 1.71 mmol), AcOH (65 μL, 1.14 mmol) and ethylenediamine (19 μL, 0.28 mmol) were added. The mixture was stirred for five days under nitrogen atmosphere. The molecular sieves were removed by filtration through Celite and the filtrate was concentrated under vacuum. The residue was purified by flash chromatography (CH$_2$Cl$_2$: MeOH: NH$_3$ from 20:1:0.1 to 10:1:1) affording **178** (27 mg, 0.09 mmol) in 16% as waxy white solid.

Strategy B for the synthesis of piperidine 179: A solution of dialdehyde **73** (240 mg, 0.86 mmol) in dry MeOH (10 mL) was stirred in the presence of 3Å molecular sieves powder for 15 min, under nitrogen atmosphere and then ethylenediamine (24 μL, 0.36 mmol) was added. Reaction mixture was stirred for 1 hour under nitrogen atmosphere, then Pd(OH)$_2$/C (260 mg, in two portions) was added and left stirring under H$_2$ atmosphere for six days. The molecular sieves were removed by filtration through Celite and the filtrate was concentrated under vacuum. The residue was purified by flash chromatography (CH$_2$Cl$_2$: MeOH: NH$_3$ 5:1:0.1) affording **179** (93 mg, 0.25 mmol) in 69% as waxy white solid. **[α]$^D_{23}$** = -14.9 (c= 0.80 in MeOH); **^{1}H NMR** (400 MHz, CD$_3$OD) δ = 4.30-4.25 (m, 2H, H-3 e H-3'), 4.87-4.82 (m, 2H, H-4 e H-4'), 4.82-4.77 (m, 2H, H-5 e H-5'), 2.97 (dd, *J*= 12.8, 2.6 Hz, 2H, Ha-2 e Ha-2'), 2.75 (dd, *J* = 11.9, 2.8 Hz, 2H, Ha-6 e Ha-6'), 2.59 (br s, 4H, H-7 e H-7'), 2.56 (dd, *J* = 12.9, 3.3 Hz, 2H, Hb-2 e Hb-2'), 2.19-2.11 (m, 2H, Hb-6 e Hb-6'), 1.48 (s, 6H, Me), 1.33 (s, 6H, Me) ppm; **^{13}C NMR** (100 MHz, CD$_3$OD) δ = 108.8 (s, 2C, -$\underline{C}$(CH$_3$)$_2$), 78.5 (d, 2C, C-4 e C-4'), 73.0 (d, 2C, C-3 e C-3'), 68.8 (d, 2C, C-5 e C-5'), 56.3 (t, 4C, C-6 e C-6'), 54.2 (t, 2C, C-7 e C-7'), 54.0 (t, 2C, C-2 e C-2'), 27.1 (q, 2C, Me), 25.2 (q, 2C, Me) ppm; **MS (ESI)** m/z (%) = 373.26 (100, [M+H]+), 395.31 (71, [M+Na]+); **IR** (CD$_3$OD): 3345, 2990, 2938, 2630, 1595, 1564, 1462, 1379, 1244, 1221.

Synthesis of piperidine 178: To a solution of **179** (15 mg, 0.04 mmol) in 2 mL of methanol, 4 drops of 1M HCl were added and the mixture was stirred at room temperature for 20 hours. The solvent was removed under reduced pressure, and the crude was treated with strongly basic resin Ambersep 900-OH and triturated with CH$_2$Cl$_2$: MeOH: NH$_3$ 10:1:0.1 to afford pure piperidine **178** (10 mg, 0.03 mmol) as a waxy white solid in 86% yield. **[α]$^D_{23}$** = -30.1 (c= 0.40 in MeOH). **^{1}H NMR** (400 MHz, D$_2$O) δ =3.81-3.77 (m, 2H, H-3 e H-3'), 3.68-3.61 (m, 2H, H-5 e H-5'), 3.32-3.26(m, 2H, H-4 e H-4'), 2.75-2.60 (m, 4H, Ha-2, Ha-2', Ha-6 e Ha-6'), 2.41-2.34 (m, 4H, H-7 e H-7'), 2.14 (m, 2H, Hb-2 e Hb-2'), 1.98-1.87 (m, 2H, Hb-6 e Hb-6') ppm; **^{13}C NMR** (100 MHz, D$_2$O) δ = 73.7 (d, 2C, C-4 e C-4'), 67.7 (d, 2C, C-3 e C-3'), 67.6 (d, 2C, C-5 e C-5'), 56.8 (t, 2C, C-2 e C-2'), 56.0 (t, 2C, C-6 e C-6'), 53.5 (t, 2C, C-7 e C-7') ppm; **MS (ESI)** m/z (%) = 293.26 (100, [M+H]+), 315.26 (26, [M+Na]+).

Chapter 4

Iminosugars as modulators in Carbonic Anhydrase inhibition
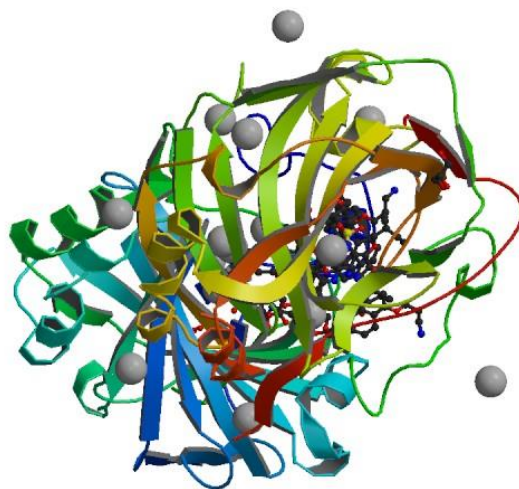
4.1 Introduction

The carbonic anhydrases (CA, EC 4.2.1.1) are ubiquitous zinc(II) metalloenzymes that are found in higher vertebrates, green plants, algae, bacteria, and archaea.[138] CA catalyzes the reversible hydration of carbon dioxide (CO_2) to give bicarbonate (HCO_3^-) and a proton (H^+), a fundamental physiological reaction that underpins a multitude of essential cellular processes associated with respiration and transport of CO_2/HCO_3^- between metabolizing tissues and the lungs, photosynthesis in higher plants, provision of HCO_3^- for biosynthetic pathways (gluconeogenesis, lipogenesis and ureagenesis), pH regulation and CO_2 homeostasis, electrolyte and fluid secretion.[139] In all organisms, this reaction occurs very slowly at physiological pH, and for this reason, CAs have the primary function of accelerating the reaction.
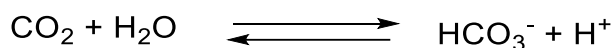
$$CO_2 + H_2O \rightleftharpoons HCO_3^- + H^+$$

Figure 4.1: Interconversion catalyzed by the carbonic anhydrase.

There are 7 families known to date, (from α to θ-CAs), which differ in their preference for metal ions used within the active site for performing the catalysis, but most importantly for the three-dimensional folding of the protein. 15 Different isozymes are present in humans, designated as hCA1, several of which are cytosolic (hCA I-III, hCA VII, hCA XIII), four are membrane bound or transmembrane proteins (hCA IV, IX, XII and XIV), two are mitochondrial (hCA VA and VB), and one is secreted into the saliva and milk (hCA VI).[140] The hCAs I and II isoforms are used in humans for the treatment of edema and glaucoma, the IV isoform is involved in the extracellular regulation of pH in neurons and in glial cells, hCA IX has instead a fundamental role in tumor progression, in acidification and metastasis in numerous types of tumors, such as carcinomas of the lungs, colon, breast, esophagus and cervix.[141] The modulation of CA activity through inhibition (or activation) is therefore a promising avenue for the treatment of a wide range of acquired and inherited diseases. Moreover, due to the presence of different hCAs isoforms, it is necessary to increase the selectivity of the inhibitory activity in order to avoid the side effects connected to the inhibition of isoforms not involved in certain pathologies.[142]

The most important class of compounds used in the design of such inhibitors are

[138] Maren, T. H. *Physiol. Rev.* **2017**, *47*, 595–781.

[139] Supuran, C. T.; Casini, A.; Scozzafava, A. *Med. Res. Rev.* **2003**, 535–558.

[140] Lolak N., Akocak S., Bua S., Koca M., Supuran C. T., *Bioorg. Chem*. **2018**, 77, 542–547.

[141] Sapegin A., Kalinin S., Angeli A., Supuran C. T., Krasavin M., *Bioorg. Chem.,* **2018**, 76, 140–146.

[142] D'Ambrosio K., Smaine F.-Z., Carta F., De Simone G., Winum J.-Y., Supuran C. T., *J. Med. Chem.*, **2012**, 55, 6776-6783.

sufonamides ($R-SO_2NH_2$), the most effective zinc binding moiety.[143] Indeed, in all the investigated enzyme-inhibitor complexes, the binding of the sulfonamide derivatives is mainly driven by the coordination of the deprotonated sulfonamide nitrogen to the catalytic Zn^{2+} ion, with consequent substitution of the zinc-bound water molecule, and by two H-bonds of the sulfonamide moiety with residue Thr199 of the enzyme (figure 4.2).[144]
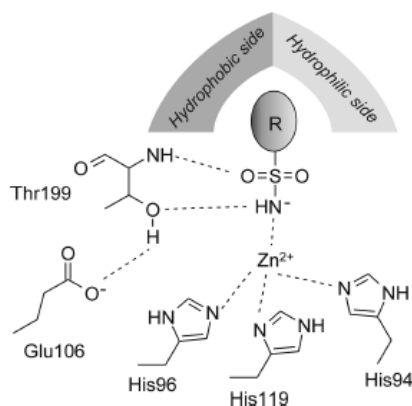

Figure 4.2: Binding mechanism of sulfonamides.

Nevertheless, we have to consider that the substituents linked to $-SO_2NH_2$ also play a key role, in fact they are carefully selected to be able to interact both with one of the pockets of the active site and with the amino acid residues around the prosthetic group,[141] and they are necessary to improve the interaction between sulfonamide scaffold and CA (Figure 4.3).
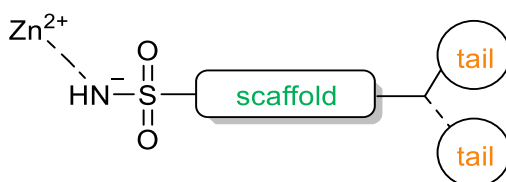

Figure 4.3: Schematic representation of the interaction between the sulfonamide scaffold and the active site of the CA.

The first sulfonamide studied in 1940 by Mann and Keilin was the simple benzenesulfonamide (figure 4.4).[145]

[143] Vullo D., Kumar R. S. S., Scozzafava A., Ferry J. G., Supuran C. T., *J. Enz. Inhib. Med. Chem.*, **2017**, 33, 31–36.

[144] Alterio V., Di Fiore A., D'Ambrosio K., Supuran C. T., De Simone G., *Chem. Rev.* **2012**, *112*, 4421–4468.

[145] Mann T., Keilin D., *Nature*. **1940**, 164–165.

SO$_2$NH$_2$

NH$_2$
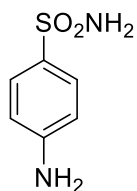
181

Figure 4.4: Benzensulfonamide, the first CAs inhibitor studied.

In later years it was of great interest to note that in almost all the adducts studied, the interaction of the benzene sulfonamide fraction with the active site of the enzyme is rather similar, i.e. the sulfonamide group is involved in the coordination of the Zn^{2+} catalytic ion and the benzene ring establishes different Van der Waals interactions with amino acid residues of the active site (figure 4.5). On the contrary, the substituents on the aromatic ring can establish different types of interaction that involve the hydrophobic / hydrophilic regions of the active site.[144]
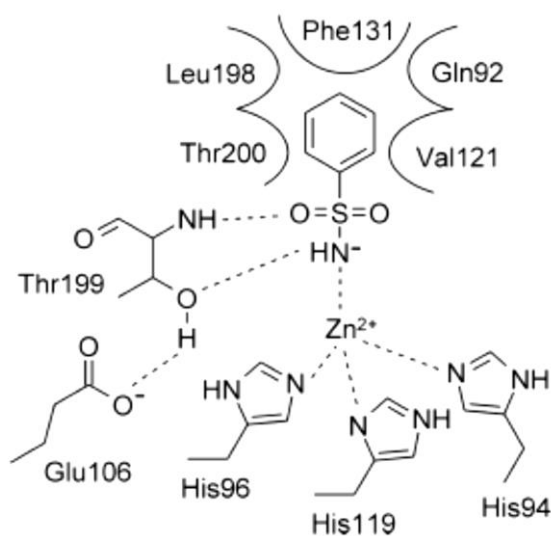
Phe131
Leu198   Gln92
Thr200   Val121

NH----O=S=O
HN⁻
Thr199
O
H
Zn²⁺
O
O⁻
HN   N   N   NH
N   NH
Glu106   His96
His119   His94

Figure 4.5: Benzenesulfonamide interactions in the active site.

Targeting slight differences in active site topology and structure of CAs, has become a relevant challenge in this research field, since it would allow to selectively inhibit/activate the CAs of interest, depending on the therapeutic application.

4.2 The *sugar approach* and MVE in CAs modulation

In recent years, a promising new strategy to differentiate transmembrane hCA IX from the physiologically dominant cytosolic isozymes hCA I and II has emerged. It consists

in the development of inhibitors with polar or charged tails, thus impairing them the ability to diffuse through lipid membranes. The site active of the hCA IX indeed, is outside the cell membrane and by binding polar tails to the sulfonamide group makes these inhibitors selective for this isoform. This is defined by Winum et al. as the "tail approach".[142]

Sugars represent the best candidates for this function. The innovation of *sugar approach* relies in carbohydrates natural occurrence, that is often a prerequisite for biological activity and can influence the pharmacokinetics and the mechanism of action and also their good solubility in water. Moreover, the variety in the stereochemistry of those compounds can be exploited to improve the selectivity and affinity towards a particular isozyme of CA.

Once understood the importance of the sugar tail, the anomeric sulfonamides, a class of glycosides where the sulfonamide function is directly linked to the anomeric carbon of the carbohydrate, have been studied. In the figure below (figure 4.6) the different interactions of the "tail" with the various amino acid residues of the active site of the hCA II are visible.[146]
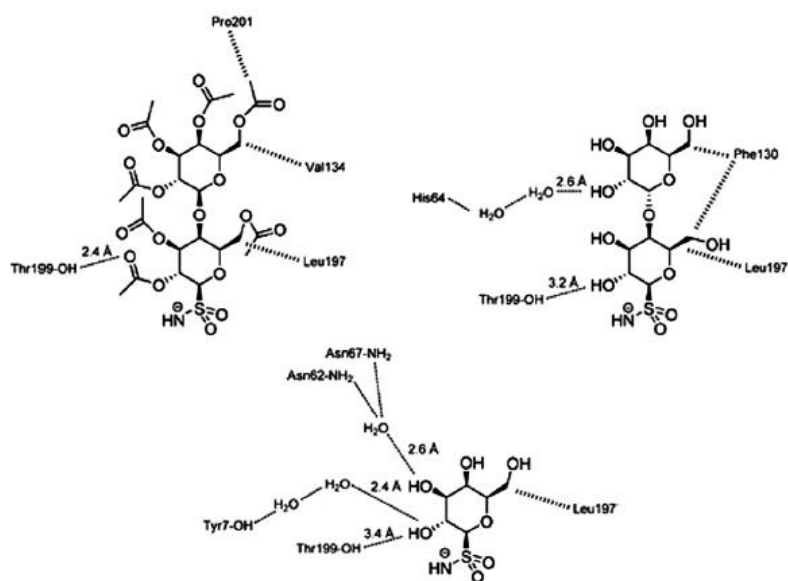

Figure 4.6: Interactions of the sugar fraction in the active site of hCA II.

Another relevant example concerns the synthesis of a class of glycosides where the sulfonamide moiety is anchored to sugar by a triazole ring obtained by reaction of CuAAC (Copper catalyzed Azide-Alkyne Cycloaddition). In particular Wilkinson and collaborators report the formation of a class of glycoconjugate benzenesulfonamides by

---

[146] Winum J. Y., Colinas P. A., Supuran C. T., *Bioorg. Med. Chem.* **2013**, *21*, 1419–1426.

reaction between a benzenesulfonamide with an alkyne and an *O*-glycoside with an azido group (figure 4.7).[147]
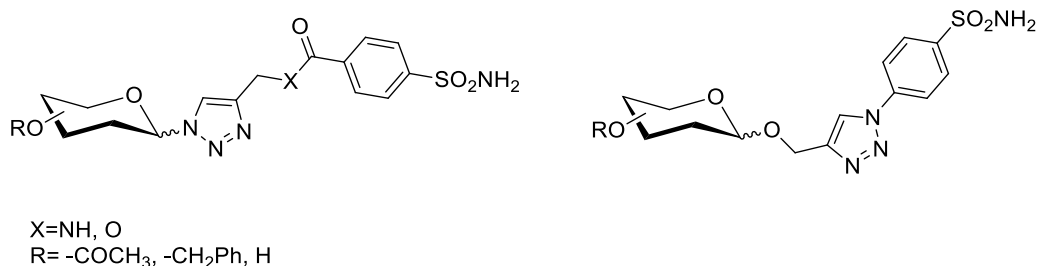

X=NH, O
R= -COCH$_3$, -CH$_2$Ph, H

Figure 4.7: Class of glycoconjugate benzenesulfonamides.

Among the different approaches reported in literature to obtain more potent and selective CAs inhibitors/activators, it has been recently reported those based on the synthesis of multivalent structures.[148] Indeed, crystallographic studies performed on the CAII isoform have shown that more than one molecule can bind in the enzymatic cavity, paving the way for a new generation of multivalent inhibitors/activators.[142] The first studies in this sense date back to 2012, the year in which Whiteside et al. for the first time they used a bivalent benzenesulfonamide in the interaction with CA.[149]

Among the platforms/ scaffolds that have been explored for the synthesis of new multivalent inhibitors/ activators of CA enzymes, there are systems based on gold nanoparticles,[150] silica,[151] dendrimers,[152] and peptides (figure 4.8).[153]

[147] Wilkinson B. L., Innocenti A., Vullo D., Supuran C. T., Poulsen S.-A., *J. Med. Chem.* **2008,** *51,* 1945–1953.

[148] Kanfar N., Bartolami E., Zelli R., Marra A., Winum J.-Y., Ulrich S., Dumy P., *Org. Biomol. Chem.* **2015**, *13*, 9894.

[149] Mack E. T., Snyder P. W., Perez-Castillejos R. P., Bilgicer B. B., Moustakas D. T., Butte M. J., Whiteside G.*, J. Am. Chem. Soc.*, **2012**, 134, 333-345.

[150] M. Stiti, A. Cecchi, M. Rami, M. Abdaoui, V. Barragan-Montero, A. Scozzafava, Y. Guari, J.-Y. Winum, C. T. Supuran, *J. Am. Chem. Soc.* **2008**, *130*, 16130.

[151] Touisni N., Kanfar N., Ulrich S., Dumy P., Supuran C. T., Mehdi A., Winum J.-Y., *Chem. Eur. J.* **2015**, *21*, 10306.

[152] Carta F., Osman S. M., Vullo D., AlOthman Z., Supuran C. T., *Org. Biomol. Chem.* **2015**, *13*, 6453

[153] Kanfar N., Tanç M., Dumy P., Supuran C. T., Ulrich S., Winum J.-Y., *Chem. Eur. J.* **2017**, *23*, 6788.
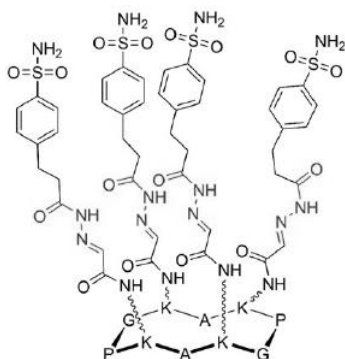
Figure 4.8: Peptide scaffold with ArSO$_2$NH$_2$ moieties.

Furthermore, the research groups of Prof Supuran and Dr Ratto have reported the formulation of hybrid nanoparticle gold and sulfonamide constructs for the recognition and inhibition of the CAIX and CAXII isoforms expressed in hypoxic cells.[154]

While the importance of the sugar component has been already investigated, the effect of an iminosugar-sulfonamide conjugated on CAs has never been studied. Moreover, until now, the multivalent effect against the enzyme carbonic anhydrase has been investigated exclusively with reference to the sulfonamide function.

Our project inserts in this context. Our first aim was to examine the effects of inhibitors/activators based on iminosugars (in whom synthesis we are expertise) on carbonic anhydrases modulation, by synthesizing a small library of monovalent compounds containing sugar and iminosugars and to compare their activity in order to identify a new class of modulators with a new selectivity profile with respect to the different isozymes of CAs. Secondly, we also aimed to design multivalent structures, containing both sugars and iminosugars, to evaluate the multivalent effect (MVE) on CAs inhibition.

This part of PhD project was achieved in collaboration with the group of Prof. Supuran of the NEUROFARBA Department of the University of Florence, and, as previously announced, aims to synthesize monovalent and multivalent systems based on sugars and iminosugars, in order to identify a new class of inhibitors activators with selectivity towards different isozymes of CAs. First, we had to synthesize the iminosugar/sugar unities to conjugate with the benzene sulfonamide scaffold, that we then linked exploiting the CuAAC click reaction, a versatile and very efficient strategy in the construction of multivalent iminosugars (see section 3.1). In particular, we performed the reaction on benzenesulfonamides with the terminal alkyne-end and a linker amino or thiourea,

---

[154] Ratto F., Witort E., Tatini F., Centi S., Lazzeri L., Carta F., Lulli M., Vullo D., Fusi F., Supuran C.T., Scozzafava A., Capaccioli S., Pini R., *Adv. Funct. Mater.* **2015**, *25*, 316.

synthesized in the group of Prof. Supuran and the appropriate sugar/iminosugar derivatives bearing a terminal azido moiety (scheme 4.1).
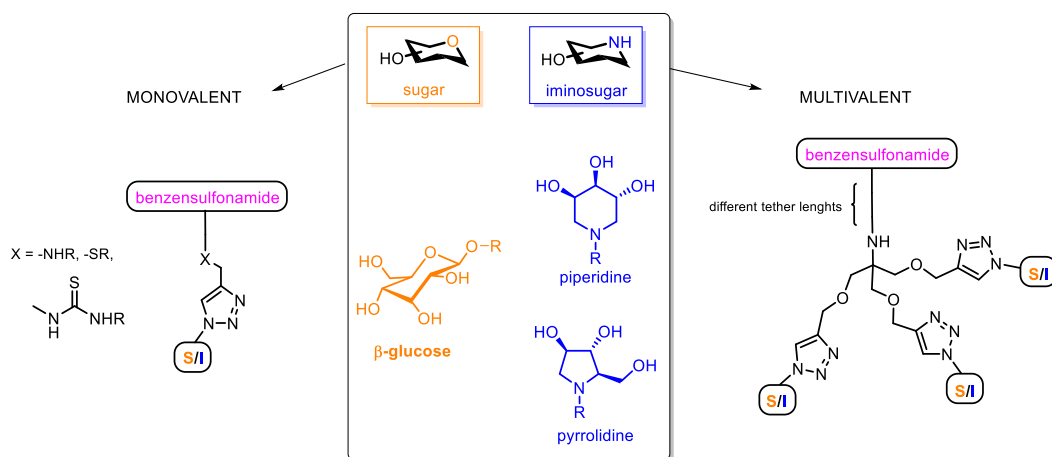
Scheme 4.1: Schematic representation of aim of the project.

In this way we initially built a small library of monovalent compounds containing the iminosugar function and the benzene sulfonamide (in addition to the triazole group which is formed in the Click Chemistry reaction). In this phase, the aim was to study the role of chain length between triazole and iminosugar in order to obtain the best biological response in terms of activity / selectivity. Then, for the design of the multivalent architectures, we wanted first of all to understand if the multimerization of the sugar unit of the whole glycosulfonamide conjugate was possible and then if it would carry some advantages in the biological response towards CAs. To do that, we selected as first attempt a β-glucose properly functionalized, that is compound **182** (scheme 4.2).

182
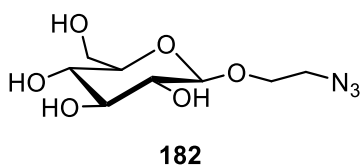
**Scheme 4.2:** β-glucose unit to conjugate with sulfonamide scaffold.

Once defined the better synthetic pathway, and once verified if effectively exists a positive MVE, the further aim was to multimerize onto dendrimeric scaffold and to link to benzenesulfonamide our iminosugars.

4.3 Results and discussion

First of all, we dealt with the synthesis of the monovalent 'glycosylsulfonamide' derivatives containing sugar and iminosugar tails, to have, in the case of the sugar a monovalent refence compound to compare with the multivalent structure that we aimed to synthesize in a second step of the project. Secondly, by conjugating iminosugars to benzenesulfonamide scaffolds, we wanted to evaluate the role of a sugar mimetic on the selectivity of the inhibitor towards the different isoforms of hCAs.

Synthesis of monovalent sugar-benzenesulfonamide adduct:
We started with the synthesis of the sugar derivative, choosing as sugar unit a β-glucose derivative properly functionalized with a two carbon atoms chain bearing an azido moiety in the terminal position to allow the performing of CuAAC reaction with the benzenesulfonamide scaffold (**182**, scheme 4.4). Starting from *O*-acetyl protected 1-α-trichloroacetimidate **57** (see chapter 2, scheme 4.3), obtained from tetraacylated D-glucopyranose, we obtained the azido derivative **183** after a glucosylation reaction performed in dry dichloromethane at -76°C in the presence of a Lewis acid to favor the formation of the β-anomer, and a substitution of the chlorine using sodium azide.[155]
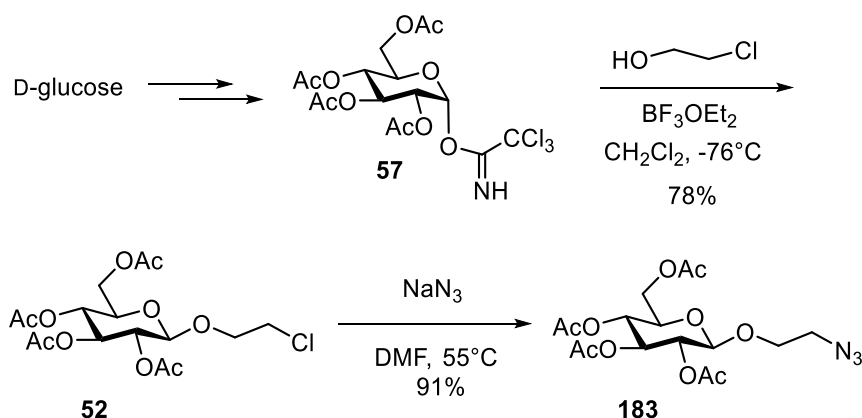
Scheme 4.3: Synthesis of azido derivative **183**.

The subsequent CuAAC reaction was carried out with the azido sugar derivative to form the monovalent compound with the benzenesulfonamide scaffold **184**. The development of the conditions took a long time and several attempts; indeed it was necessary to adapt the procedures found in the literature to our specific substrate to efficiently afford compound

_____

[155] Chong P. Y., Petillo P. A., *Org. Let.* **2000**, 2, 1093-1096.

185. The first attempt to obtain compound **185** was effectuated by performing the CuAAC between azide **183** and the thiourea scaffold **184** (scheme 4.4).
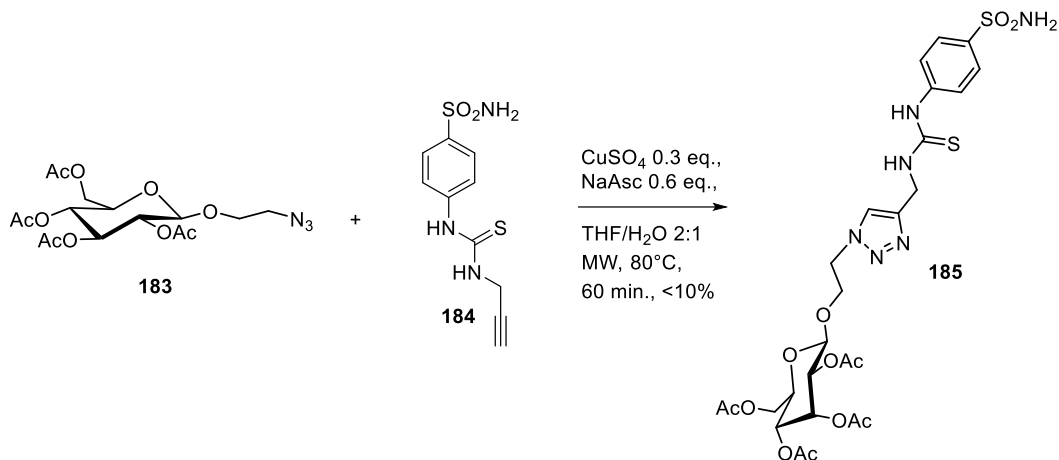
Scheme 4.4: Scheme of CuAAC to afford compound **185**.

Unfortunately, the yield was lower than 10%, and for this reason we tried different conditions reported in table 4.1, in which we made gradual changes on all the parameters to try to identify the problem that prevented the reaction from proceeding.

	Sodium Ascorbate (eq.)	CuSO$_4$ (eq.)	THF (ml)	H$_2$O (ml)	t-BuOH (ml)	time	T (°C)	yield
a)						65 min	80 (MW)	<10%
b)	0.6	0.3	2	1	-	22 h	r.t.	<10%
c)	0.5	0.1	3	1	1	44 h	50	<10%
d)	0.1	0.001	-	0.35	0.35	18 h	r.t.	<10%

Table 4.1: CuAAC conditions used to afford compound **185**.

In all the cases we did not recovered the product in amounts higher than 10% yield. The difficulties encountered led us to hypothesize that the problem could derive from the particular reagents used, in particular from the use of alkyne **184**. Since, despite various attempts, none of these changes led to the desired result, we formulated the hypothesis that the thiourea function contained in **184** was responsible for these failures. Probably, the presence of such copper-coordinating groups hampered the catalytic role of the copper

by sequestrating it from the reaction environment. This hypothesis was also confirmed by the bad results obtained with other two substrates: the pyrrolidine iminosugar that will be illustrate later, and with the deprotected sugar derivative **182** (scheme 4.5).
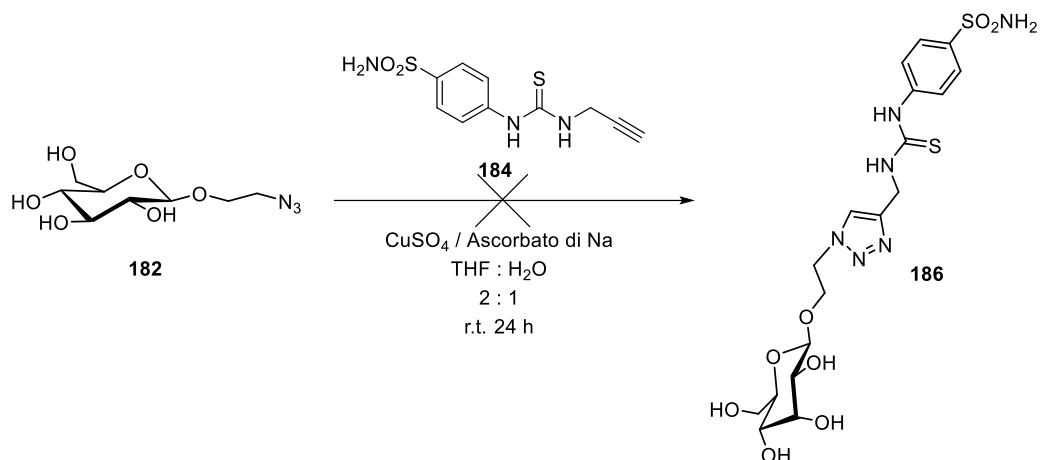
Scheme 4.5: Attempt with deprotected sugar **182**.

Again, performing the reaction without heating, we did not afford the desired product. Based on these results, we then chose to change the synthetic strategy (scheme 4.6). According to this new strategy (Strategy B and B'), the thiourea bond is formed in the last synthetic step, while the CuAAC reaction is performed on the propargyl amine.
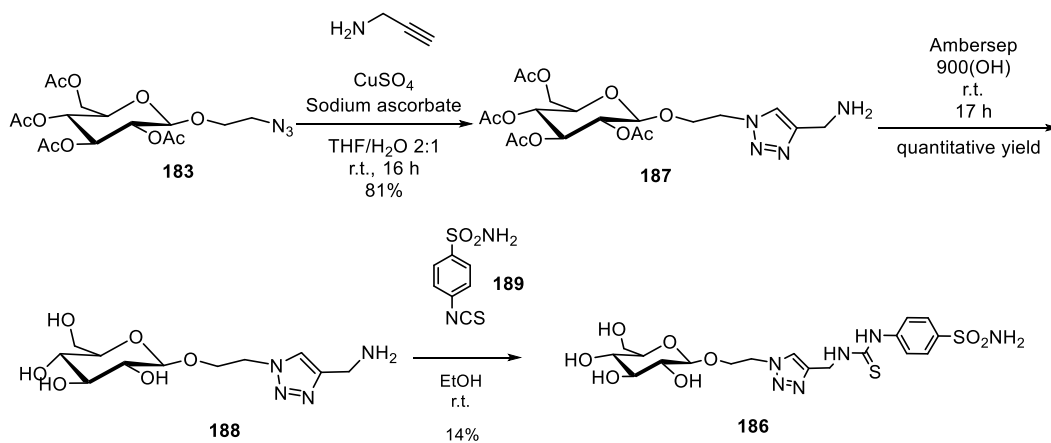
Scheme 4.6: Alternative strategy to afford compound **186**.

With this new procedure the problem related to the presence of thiourea in the click step has been eliminated since this is only subsequently formed by reaction between amine and isocyanate; we then chose to perform the click reaction first and finally the coupling. In this case, the best yield could be obtained by performing the CuAAC reaction at room temperature overnight (scheme 4.6). Moreover, before the purification step with FCC, the

use of the copper scavenger resin Quadrasil MP® results necessary to efficiently reach the desired purity degree.

Synthesis of multivalent sugar-benzenesulfonamide adduct:

Once the best conditions have been defined for the monovalent adduct, we were able to apply this synthetic protocol to our multivalent derivative. We decided to start the study of MVE applied to CAs inhibitors with the trimeric scaffold already exploited in other works (see section 3.1), the tris-propargylated amine TRIS **81** (scheme 4.7). In this case, we performed the reaction using the microwaves heating, and we afforded trivalent adduct in 45% yield.
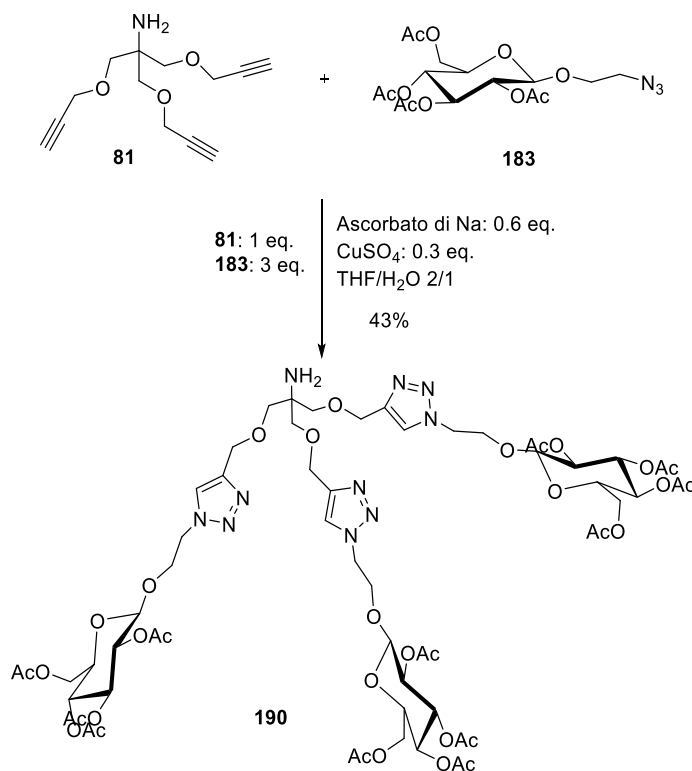
Scheme 4.7: Synthesis of trivalent glycosulfonamide **190**.

As final step, we treated compound **190** with strongly basic resin Ambersep 900-OH to afford deprotected **191** in quantitative yield (scheme 4.8).

_____
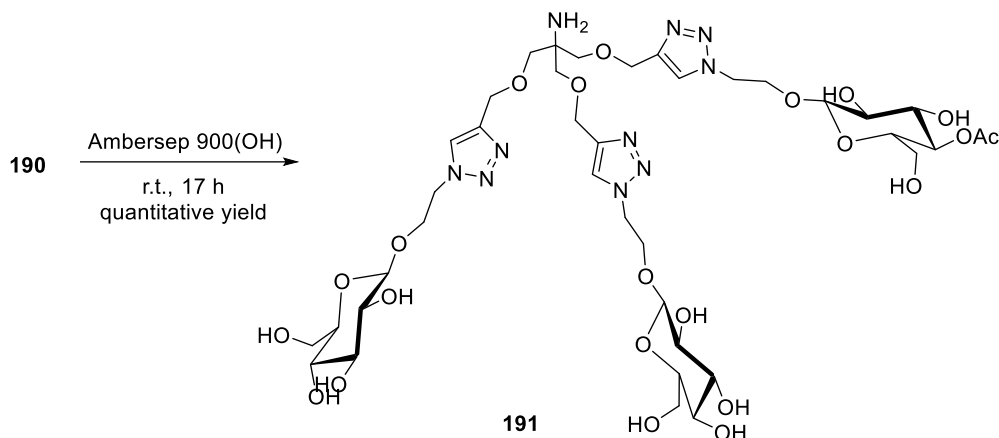
**Scheme 4.8:** Deprotection of trivalent **190** to afford final product **191**.

With **191** trivalent compound in hand and following the procedure used in the case of monovalent adduct, we performed the coupling reaction with isothiocyanate **189** (scheme 4.9), but obtaining the final product **192** with a yield lower than 20%. Anyway, we recovered it in a sufficient amount to perform the biological assays.
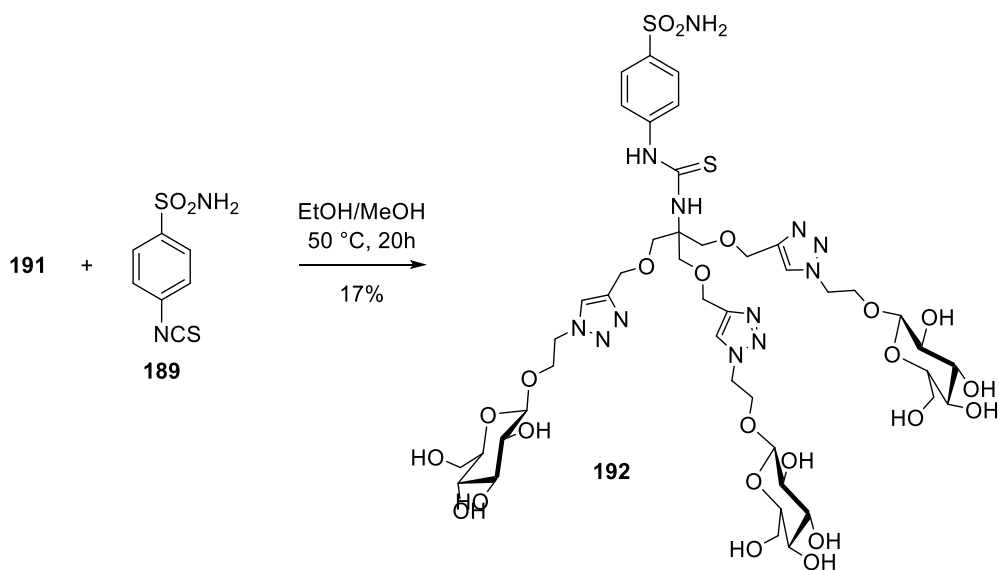
Scheme 4.9: Coupling with isothiocyanate.

Synthesis of monovalent piperidine iminosugar-benzenesulfonamide adducts:
The first iminosugar that we decide to conjugate to sulfonamide is a trihydroxypiperidine iminosugar (**192**, scheme 4.9). It is synthesized starting from D-mannose derived intermediate **80**, that was subjected to a double reductive amination with an azido-amino chain of proper length.
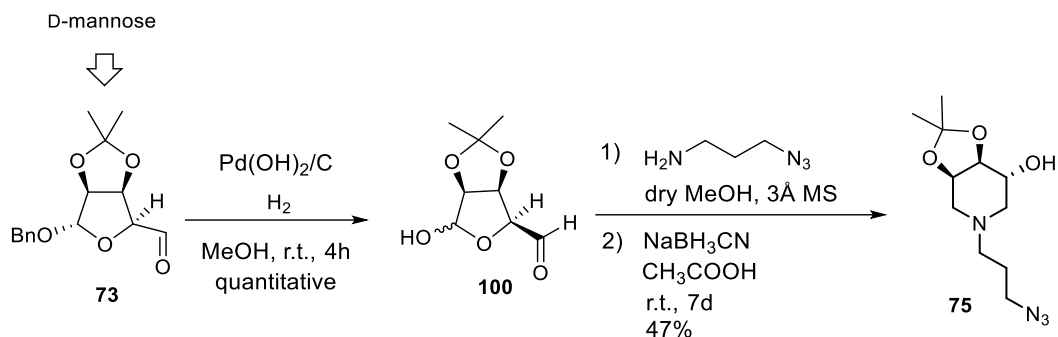
Scheme 4.11: Piperidine iminosugar **75** to conjugate with benzenesulfonamide scaffolds.

Product **75** was obtained with an overall yield of 47%. With the azido derivative in hands, in analogy with the sugar monovalent adduct **185**, we performed the click reaction with propargylamine to afford amino derivative **193** (85% yield), that was first deprotected with strongly basic resin Ambersep 900-OH with a quantitative yield, then coupled with isothiocyante **189** to afford final benzenesulfonamide conjugate **195** (scheme 4.10). In this case the yield of reaction was lower than 20%, but we recovered a sufficient amount of product to perform biological inhibition tests.
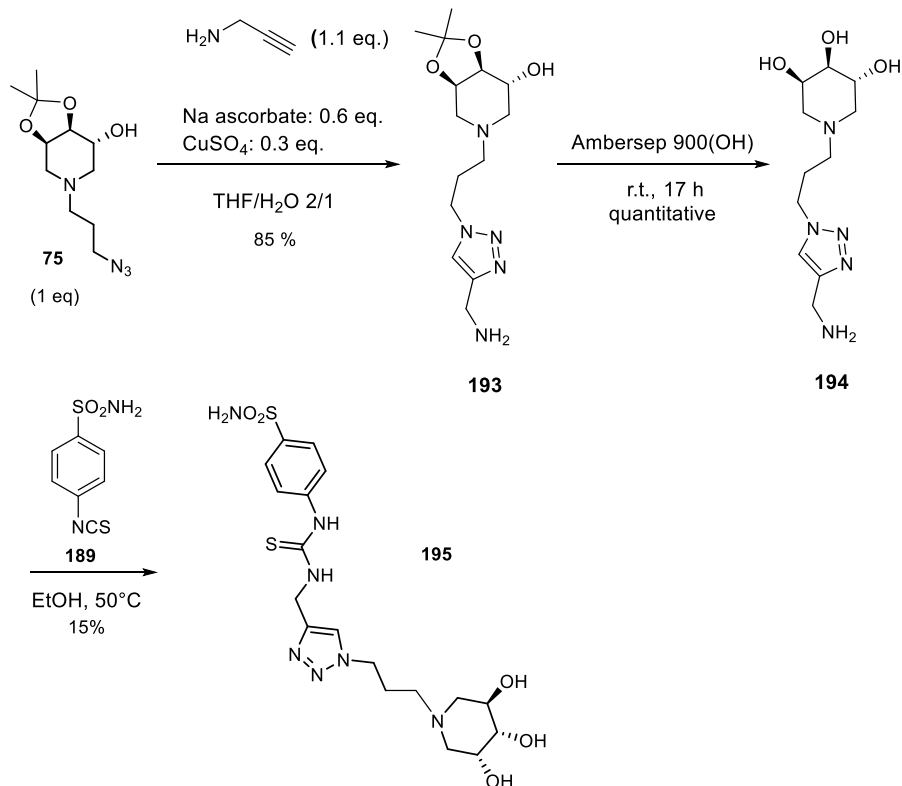
Scheme 4.10: Synthesis of compound **195**.

_____

Synthesis of monovalent pyrrolidine iminosugar-benzenesulfonamide adducts:

Since our initial project was to compare the biological activity of pyrrolidine and piperidine iminosugar, another part of this thesis was dedicated to the synthesis of the pyrrolidine-benzenesulfonamide glycoconjugates. To do that, we initially chose to use a pyrrolidine iminosugar derivative with a comparable chain length of the piperidine compound.

The iminosugar that we decide to conjugate to sulfonamide is the pyrrolidine **108**, whose synthesis has already been developed in our group (see chapter 3, scheme 4.11).
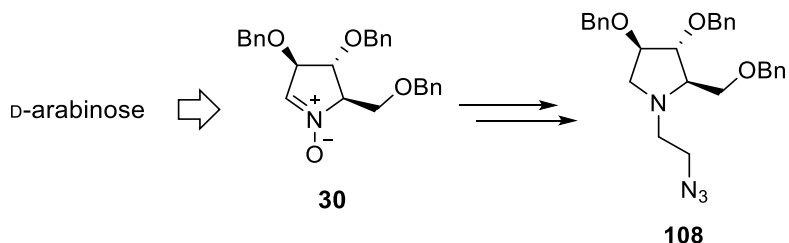
Scheme 4.11: Synthetic strategy to obtain pyrrolidine derivative **108**.

Starting from commercially available D-arabinose and passing through nitrone key intermediate **30**, we afforded azido pyrrolidine derivative **108**, as already described in section 3.2.3. We planned to 'click' this azido derivative through CuAAC reaction to the three different sulfonamide scaffolds **196**, **197** and **184** in order to afford the 'glycosulfonamides' **198**, **199** and **200** (scheme 4.12).
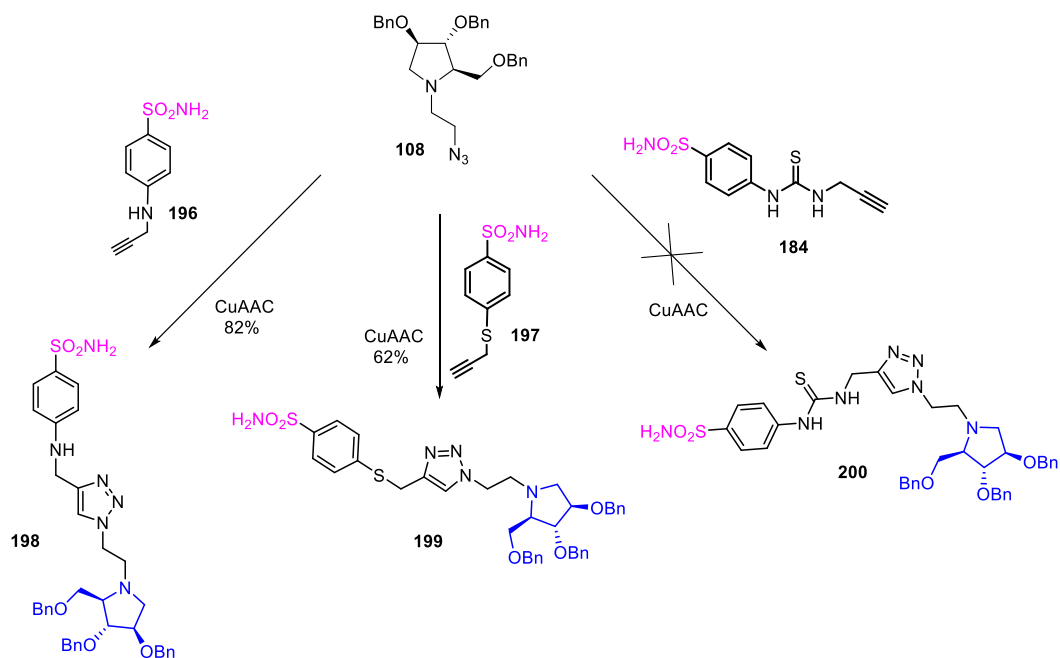
Scheme 4.12: Click reaction of pyrrolidine **108** with the three sulfonamide scaffolds.

While the synthesis of amino derivative **198** and **199** proceeded without any problems by using the click conditions applied in the synthesis of multimeric iminosugars (see section 3.1), even if the yield of **199** could be improved, the synthesis of thiourea adduct **200** was not a trivial task. Indeed, as expected from the results obtained with the sugar adducts, performing the cycloaddition in the 'standard' conditions used in previous cases (80°C heating with microwaves for 45' minutes and room temperature for 16 hours), we did not recover the desired product. Moreover, we tried to change strategy by effectuating the click reaction to form the triazole linker, before the formation of thiourea linkage, using propargylamine as alkyne to click with pyrrolidine **108** in analogy of strategy used for sugar adduct **185** and piperidine iminosugar **201** (scheme 4.13).
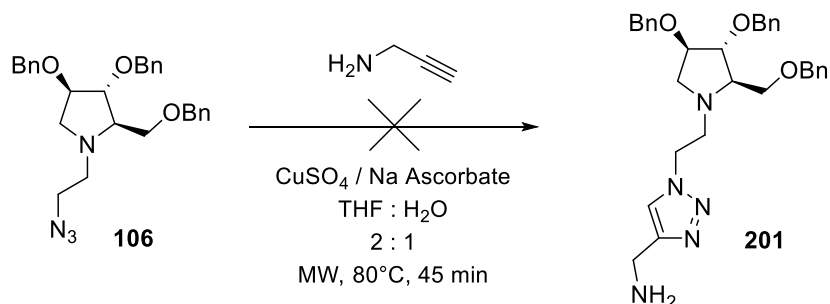
**Scheme 4.13:** Click reaction with propargylamine.

Although, after purification by FCC in this case, it was impossible to recover the desired product **201**. For this reason, we could not afford the final thiourea adduct **200**.

It was no possible to remove the benzyl protecting groups of derivatives 198 and 199 by means of catalytic hydrogenation (H$_2$, Pd(OH)$_2$/C). Again, we suspected that the problem is related to the presence of the sulfonamide group. We therefore decided to test those compounds with benzyl protected hydroxy groups.

In order to evaluate the effect of a pyrrolidine iminosugar linked to the benzenesulfonamide scaffold avoiding the problems related to the deprotection step, we decide to elongate the carbon chain on the endocyclic nitrogen of pyrrolidine, as previously done in the case of resorcinarene adducts (section 3.2.3). In this case we could efficiently perform the deprotection of iminosugar moiety before to conjugate it to the scaffolds. The first attempt was effectuated with scaffold **196**, since in the previous case gave the best yield (scheme 4.14).
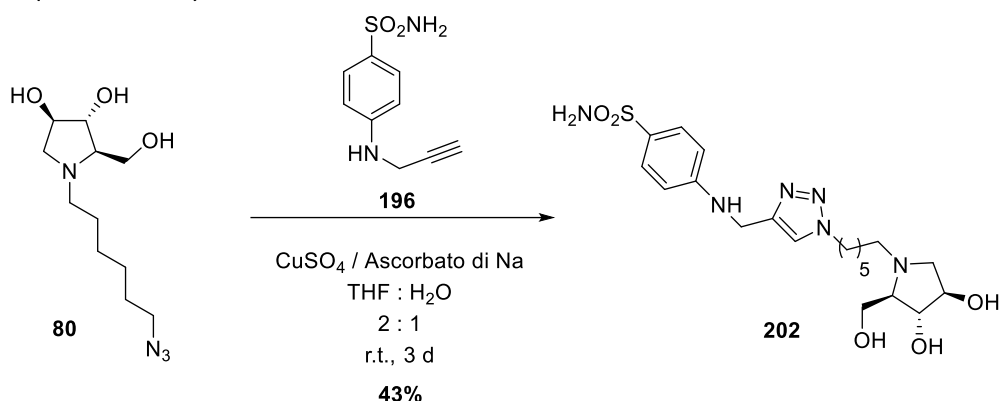
Scheme 4.14: Conjugation of pyrrolidine **80** to benzenesulfonamide scaffold **202**.

In this case we were able to afford adduct **202** (in a percentage yield that could be improve in the future) that we finally tested. Applying the same strategy to obtain the adduct with scaffold bearing the sulphur atom (**197**, scheme 4.12), we did not observe the formation of any product, from the FCC we recovered all the starting material. Further investigation to better understand those problematics related to CuAAC with benzenesulfonamide scaffolds, are now ongoing in our laboratories.

Aiming to synthesize also the thiourea derivative bearing the longer spacer (**203**, scheme 4.15), we tried to apply the same strategy used in the case of sugar adducts, and to perform the coupling amine-isothiocyanate. To do that, we first needed to reduce the azido moiety to afford the amine necessary in the subsequent coupling step.
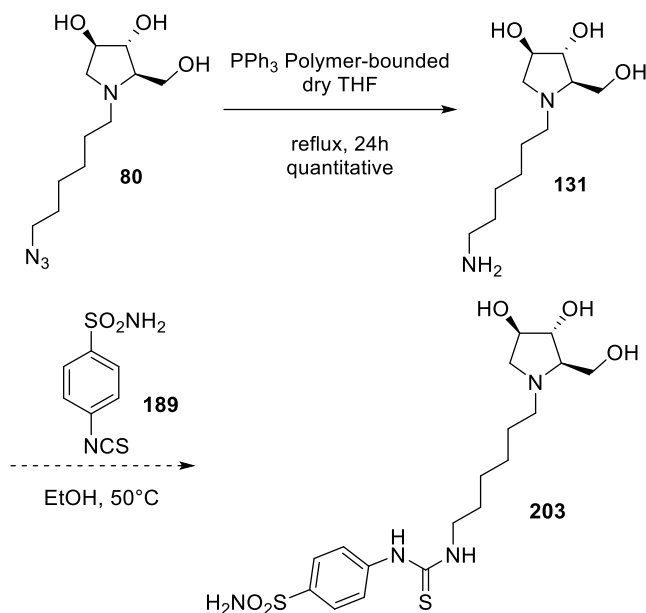
Scheme 4.15: Synthesis of thiourea adduct **203**.

In the preliminary attempt the product **203** was obtained with excellent yield (higher than 90%), and the purification step is now ongoing.

4.4 Biological evaluation

All the synthesized compounds were tested thanks to the collaboration with Prof. Supuran of the department of NEUROFARBA (University of Florence). Compounds **186**, **192**, **195**, **198**, **199** and **202** were investigated for their inhibitory effects against four physiological relevant isoforms, (hCA I, II, IX and XII) by means of a stopped flow CO_2 hydrase assay.[156] The data are shown in table 4.2 with the AAZ (acetazolamide) as reference compound, that is the compound sulfonamide based used in the market in the treatment of some forms of glaucoma.[157]
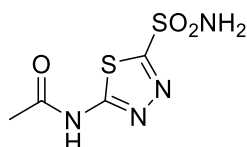

Figure 4.9: AAZ, acetazolamide, the reference compound.

[156] Khalifah RG., *J. Biol. Chem.*, **1971**, *246*, 2561–73.

[157] Supuran CT., *Expert Rev. Neurother.*, **2015**, *15*, 851–6.

	K_i (nM)*			
Inhibitors	hCA I	hCAII	hCA IX	hCA XII
186	64.1	148.2	2.3	4.8
192	759.7	579.3	143.3	207.2
195	322.2	427.3	135.6	21.7
198	>10000	>10000	>10000	>10000
199	>10000	9755	3135	906.0
202	3228	89.1	2202	438.0
AAZ	250.0	12.1	25.8	5.7

*Mean from 3 different assays, by a stopped flow technique (errors were in the range of $\pm$ 5-10 % of the reported values).

The monovalent sugar adduct **186** resulted a good inhibitor towards all the human CAs, showing inhibition percentages comparable to those of the reference compound, that results even less potent in the case of hCA IX, one of the isoforms involved in tumoral growth. Comparing it with the inhibitory activity of the trivalent compound **192**, we can notice no enhancement in inhibition percentage, and no selectivity profile towards any isoforms. Trying to rationalize those results, we thought that the reason of the lower activity with respect to the monovalent analogue may rely in the scaffold structure, also considering the excellent inhibitory value obtained with the monovalent sugar derivative **186**. Probably the distance between the sulfonamide moiety and the polar tail, which is necessary to impart the selectivity towards the transmembrane forms (IX and XII), is too short, hampering in this way the sulfonamide to reach the catalytic site. For this reason, we are planning to elongate the tether's length to obtain a more flexible adduct (see section 4.4). The activity of the piperidine iminosugar **195** was better than the trivalent sugar glycoconjugate, but lower than the monovalent sugar adduct. Indeed, it is a quite good inhibitor (remaining in the nanomolar range) but, more interestingly, selective towards isoform XII, again important for anticancer applications. It would be interest, once improved the reaction conditions and the design of the multimeric scaffold, to evaluate the potentiality of the piperidine iminosugar compound when presented in a multimeric fashion. Moving to the pyrrolidine derivatives, for those separated from the benzenesulfonamide moiety by a two carbon atoms chain, we did not observe encouraging

biological activities. In particular, compound **198** did not show inhibition towards any CA isoform, while a partial activity was shown by pyrrolidine adduct **199**, which resulted even quite selective, partially inhibiting isoform XII. Probably those results can be ascribed to the benzyl protecting groups that impart hydrophobicity to the whole system. By elongating the tether's length between the tail and the scaffold, an increment of the inhibitory potency was observed. Indeed, adduct **202** resulted in a better inhibition with respect to the adducts **198** and **199** with the shorter linker. In particular, derivative **202** showed some selectivity towards hCAII enzyme, which is involved in some forms of glaucoma.

4.5 Conclusions

In conclusion, in order to identify a class of inhibitors/activators with a new selectivity profile towards different isozymes of CAs, we synthesized mono- and multivalent systems based on sugar (a β-glucose derivative) and iminosugars (piperidine and pyrrolidine derivatives), thanks to the collaboration with Prof. Supuran (NEUROFARBA department, University of Florence). All new derivatives were tested against four different isoforms of human carbonic anhydrases (hCAs I, II, IX and IXX) involved in some forms of glaucoma (I and II) and in the processes of tumoral growth (IX and XII), respectively. The adducts showed interesting inhibitory potentiality in the cases of monovalent sugar glycosulfonamide conjugate **186**, the monovalent piperidine adduct **192** and the pyrroline derivative bearing a longer tether length **202** (6-C atoms chain). The inactivity (for compound **198**) and the low inhibition values (for compound **199**) of the pyrrolidine conjugates with the 2-carbon atom chain linker can be ascribed to the protection of the iminosugar hydroxyl groups. Indeed, the presence of free hydroxyl groups seems necessary to impart a good solubility in water and to favour the interactions of the inhibitor with the enzymatic active site of the carbonic anhydrases. As a matter of fact, pyrrolidine-based adduct **202** resulted a quite good inhibitor and, most importantly, was selective towards only one isoform, hCAII showing a K_i= 89.1 nM. An unexpected result is that one related to the multivalent derivative **192**, that lost the inhibitory activity showed by its monovalent counterpart against all of the carbonic anhydrase isoforms. Indeed, while monovalent sugar derivative **186** showed a remarkably inhibitory potency towards all the four CAs, the trivalent analogue **192** resulted to be less potent and selective. Our hypothesis is related to the linker's length between the sulfonamide moiety and the trivalent scaffold, that probably is too short resulting in a higher steric hindrance. This feature, indeed, could influence the multivalent selective recognition of the sugar tails. For this reason, we

designed a new trivalent inhibitor in which the benzenesulfonamide is more distant from the TRIS scaffold, and its synthesis is now ongoing in our laboratories (scheme 4.15).
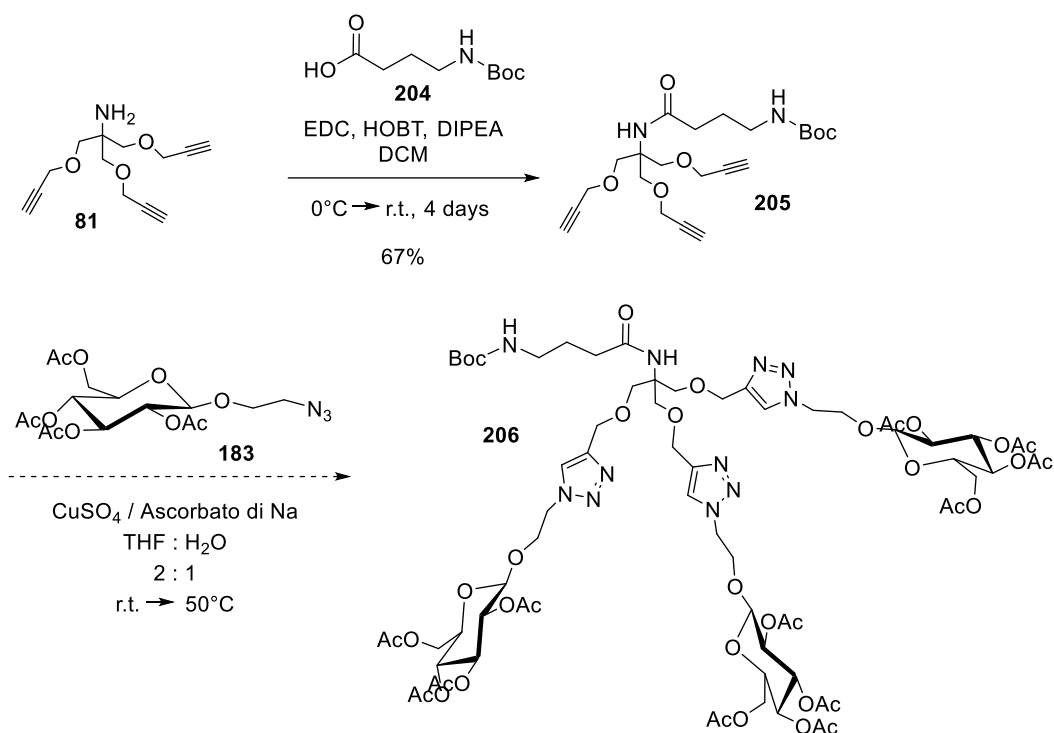
Scheme 4.15: Synthetic pathway to obtain compound **206** with a longer spacer.

Starting from trivalent alkyne scaffold **81**, we introduced a 4-carbon atoms acid linker exploiting the free amino moiety of the TRIS with a coupling reaction, affording compound **205** (67% yield), that we will click to **183**, and deprotect to obtain final compound **207**. If the biological data will be promising, we will apply the same strategy to the iminosugar-based derivatives to test their activity and evaluate their selectivity profile.
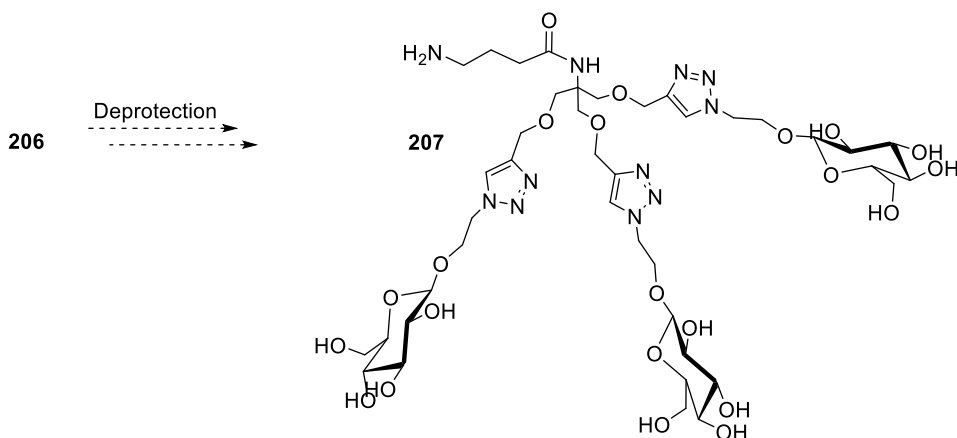
Scheme 4.16: Deprotection of **206** to afford final **207**.

4.6 Experimental section

For the general details see paragraph 2.4. Additionally, the biological inhibition tests were performed as it follows:

An Applied Photophysics stopped-flow instrument has been used for assaying the CA catalyzed CO_2 hydration activity. Phenol red (at a concentration of 0.2 mM) has been used as indicator, working at the absorbance maximum of 557 nm, with 20mM Hepes (pH 7.5) as buffer, and 20mM Na_2SO_4 (for maintaining constant the ionic strength), following the initial rates of the CA-catalyzed CO_2 hydration reaction for a period of 10–100 s. Stock solutions of inhibitor (0.1 mM) were prepared in distilled–deionized water and dilutions up to 0.01 nM were done thereafter with the assay buffer. Inhibitor and enzyme solutions were preincubated together at room temperature (15 min) prior to assay, in order to allow for the formation of the E–I complex. Data from Table 1 were obtained after 15 min incubation of enzyme and inhibitor, as usual protocol for all sulfonamides.[158] The inhibition constants were obtained by non-linear least-squares methods using PRISM 3 and the Cheng–Prusoff equation, as reported earlier[159] and represent the mean from at least three different determinations.

---

[158] Mishra C.B., Kumari S., Angeli A., Monti S.M., Buonanno M., Prakash A., Tiwari M., Supuran C.T., *J. Enzyme Inhib. Med. Chem.*, **2016**, *31*, 174–9.

[159] Chohan Z.H., Scozzafava A., Supuran C.T., *J. Enzyme Inhib. Med. Chem.*, **2002**, *17*, 261–6.

Synthesis of monovalent sugar derivative 186: To a suspension of **188** (62 mg, 0.20 mmol) in EtOH (3 mL) **189** (86 mg, 0.40 mmol) was added, and the reaction mixture was stirred at room temperature for 20 hours. Then, the crude was evaporated under reduced pressure and purified by FCC (CH_2Cl_2:MeOH from 10:1 to 5:1) affording pure **186** (*R*f = 0.32, 15 mg, 0.03 mmol, 14% yield) as a yellow oil. **^{1}H-NMR** (400 MHz, CD_3OD): δ= 8.12 (s, 1H, H-triazoleo), 7.83 (AB system, *J* = 7.0 Hz, 2H, H-Ar), 7.67 (AB system, *J* = 7.1 Hz, 2H, H-Ar), 4.87 (s, 2H, H-9), 4.63 (t, *J* = 4.9 Hz, 2H, H-8), 4.29 (dd, *J* = 7.8; 1.1 Hz, 1H, H-1), 4.23 (q, *J* = 5.6 Hz, 1H, Ha-7), 4.00 (q, *J* = 6.4, 5.2 Hz, 1H, Hb-7), 3.85 (d, *J* = 11.9 Hz, 1H, Ha-6), 3.64 (dd, *J* = 11.6 Hz; 4.3, 1H, Hb-6), 3.31-3.25 (m, 3H, H-3, H-4, H-5), 3.17 (t, *J* = 7.8 Hz, 1H, H-2) ppm; **^{13}C-NMR** (100 MHz, CD_3OD): δ= 181.6 (s, 1C, C=S), 144.0 (s, 1C, triazole), 142.7 (s, 1C, NH-C-Ar), 126.6 (d, 1C, triazole), 124.3 (s, 1C, SO_2NH_2-C-Ar), 122.0 (d, 4C, C-Ar), 103.1 (d, 1C, C-1), 76.5 (d, 1C, C-2), 73.4 (d, 2C, C-3, C-5), 70.1 (t, 1C, C-6), 67.6 (d, 1C, C-4), 61.2 (t, 1C, C-7), 50.2 (t, 1C, C-8), 39.1 (t, 1C, C-9) ppm; **MS (ESI)**: *m/z* calcd (%) for $C_{18}H_{26}N_6O_8S_2$ 518.13; found: 541.05 (100%, [M+ Na]$^+$).

Synthesis of monovalent sugar derivative 190: To a solution of **183** (313 mg, 0.75 mmol) in 3 ml of a 2:1 THF:H_2O mixture were added $CuSO_4$ (30 mol%), sodium ascorbate (60 mol%) and TRIS-alkyne **81** (1 equiv.). The reaction mixture was stirred at 80°C (MW irradiation) for 45 min until TLC analysis (DCM: MeOH 10:1) showed the disappearance of the starting material (*R*f = 0.59) and formation of a new product (*R*f = 0.00). After filtration through Celite®, the solvent was removed under reduced pressure and the crude was first treated with Quadrasil® MP resin then purified by FCC (CH_2Cl_2:MeOH:NH_3 from 20:1 to 10:1:0.1) affording pure **190** (*R*f = 0.39, 161 mg, 0.11 mmol, 43% yield) as an orange waxy solid. **^{1}H-NMR** (400 MHz, $CDCl_3$): δ= 7.63 (s, 3H, H-triazole), 5.16 (t, *J* = 9.5 Hz, 3H, H-2), 5.05 (t, *J* = 9.6 Hz, 3H, H-3), 4.97 (t, *J* = 9.1 Hz, 3H, H-4), 4.57-4.48 (m, 15H, H-7, H-β, H-1), 4.26-4.22 (m, 6H, H1-8, Ha-6), 4.11 (d, *J* = 12.2 Hz, 3H, Hb-6), 3.94-3.90 (m, 3H, Hb-8), 3.71-3.68 (m, 3H, H-5), 3.45 (ps, 6H, Hα), 2.08 (s, 12H, OAc), 2.01 (s, 12H, OAc), 1.98 (s, 12H, OAc), 1.93 (s, 12H, OAc) ppm; **^{13}C-NMR** (50 MHz, $CDCl_3$): δ= 170.5, 170.1, 169.4, 169.3 (s, 12C, C=O), 144.8 (s, 3C, triazolo), 123.9 (d, 3C, triazolo),100.6 (d, 3C, C-1), 77.7 (s, 3C, C-2), 77.0 (d, 3C; C-3), 76.4 (s, 3C, C-4), 72.5 (t, 3C; Cα), 72.1 (d, 3C, C-5) 71.0 (t, 3C,C-7) 68.4 (t, 3C, Cβ), 67.7 (t, 3C, C-6), 61.8 (s, 1C, HN*C*($CH_2O)_3$-), 50.0 (t, 3C, C-8), 20.7, 20.6 (q, 12C, CH_3) ppm; **IR** ($CDCl_3$): ν = 3684, 2954, 2875, 2360, 2254, 1751, 1431, 1373, 1224, 1043, 931 cm^{-1}. **MS (ESI)**: *m/z* calcd (%) for $C_{61}H_{86}N_{10}O_{33}$ 1486.54; found: 755.50 (100%, [(M+ Na)/2]$^+$).

Synthesis of trivalent sugar derivative 191: Compound **190** was dissolved in MeOH (20 mL) and left stirring overnight at room temperature with the strongly basic resin Ambersep 900-OH. The reaction mixture was filtered and evaporated under reduced pressure to afford the final product **191** without any further purification (88 mg, 0.09 mmol,

90% yield) as a waxy white solid. **^{1}H-NMR** (400 MHz, CD_3OD): δ= 8.10 (s, 3H, H-triazole), 4.63 (t, *J* = 4.5 Hz, 6H, H-8), 4.55 (s, 6H, Hβ), 4.30 (dd, *J* = 7.8 Hz; 0.8, 3H, H-1), 4.26-4.20 (m, 3H, Ha-7), 4.00-3.95 (m, 3H, Hb-7), 3.85 (d, *J* = 11.9 Hz, 3H, Ha-6), 3.66-3.62 (m, 3H, Hb-6), 3.40 (s, 6H, Hα), 3.31-3.30 (m, 3H, H-3), 3.27-3.26 (m, 6H, H-4, H-5), 3.19 (t, *J* = 8.2 Hz, 3H, H-2) ppm; **^{13}C-NMR** (100 MHz, CD_3OD): δ= 144.3 (s, 3C, C-triazole), 124.8 (s, 3C, C-triazole), 103.1 (s, 3C, C-1), 76.6 (d, 6C, C-3, C-4), 76.5 (t, 3C, Cα), 73.5 (d, 2C, C-2), 71.1 (t, 3C, HN*C*(CH$_2$O)$_3$-), 70.1 (d, 3C, C-5), 67.6 (d, 3C, C7), 63.9 (s, 3C, Cβ), 61.3 (s, 1C, C-6), 50.1 (t, 3C, C-8) ppm; **MS (ESI)**: *m/z* calcd (%) for $C_{37}H_{62}N_{10}O_{21}$ 982.41; found: 1005.23 (100%, [(M+ Na)]$^+$), 983.21 (76%, [(M+ Na)]$^+$).

Synthesis of trivalent sugar derivative 192: To a suspension of **191** (59 mg, 0.06 mmol) in EtOH (1 mL) **189** (13 mg, 0.06 mmol) was added, and the reaction mixture was stirred at 50°C for 20 hours. Then, the crude was evaporated under reduced pressure and purified by FCC (CH$_2$Cl$_2$:MeOH from 10:1 to 1:2) affording pure **192** (*R*f = 0.27, 12 mg, 0.01 mmol, 17% yield) as coulorless oil. **^{1}H-NMR** (400 MHz, CD_3OD): δ= 8.11 (s, 3H, H-triazole), 7.75 (AB system, *J* = 8.8 Hz, 2H, H-Ar), 7.49 (AB system, *J* = 8.4 Hz, 2H, H-Ar), 4.62 (ps, 12H, H-β, H-8), 4.29 (d, *J* = 7.8 Hz; 1.1, 3H, H-1), 4.25-4.19 (m, 3H, Ha-7), 4.00-3.96 (m, 3-H, Hb-7), 3.85 (pd, *J* = 11.8 Hz, 3H, Ha-6), 3.67-3.62 (m, 3H, Hb-6), 3.03 (q, *J* = 1.6 Hz, 9H, H-3, H-4, H-5), 3.27-3.26 (m, 6H, Hα), 3.20-3.16 (m,3H, H-2) ppm; **^{13}C-NMR** (100 MHz, CD_3OD): δ= 143.9 (s, 3C, C-triazole), 126.4 (s, 3C, C-triazole), 125.1 (s, 1C, SO$_2$NH$_2$-C-Ar), 122.5 (d, 4C, C-aromatic), 103.1 (s, 3C, C-1), 76.6 (t, 6C, C-3, C-4), 76.5 (d, 3C, Cα), 73.5 (s, 3C, C-2), 70.1 (s, 6C, C-5), 67.6 (s, 3C, C-7), 63.8 (t, 3C, Cβ), 61.3 (s, 1C, C-6), 50.2 (t, 3C, C-8) ppm; **MS (ESI)**: *m/z* calcd (%) for $C_{44}H_{68}N_{12}O_{23}S_2$ 1196.40; found: 1194.96 (100%, [M-H]$^+$).

Synthesis of monovalent piperidine iminosugar derivative 195: To a suspension of **194** (23 mg, 0.08 mmol) in EtOH (1 mL) **189** (17 mg, 0.08 mmol) was added, and the reaction mixture was stirred at 50°C for 20 hours. Then, the crude was evaporated under reduced pressure and purified by FCC (CH$_2$Cl$_2$:MeOH from 10:1 to 5:1) affording pure **195** (*R*f = 0.33, 6 mg, 0.01 mmol, 15% yield) as yellow waxy solid. **^{1}H-NMR** (400 MHz, CD_3OD): δ= 8.03 (s, 1H, H-triazole), 7.83 (AB system, *J* = 8.9 Hz, 2H, H-Ar), 7.68 (AB system, *J* = 8.8 Hz, 2H, H-Ar), 4.72 (t, *J* = 6.8 Hz, 2H, H-3'), 3.89-3.86 (m, 1H, H-3), 3.75 (dt, *J* = 8.0 Hz; 4.1, 1H, H-4), 3.40-3.30 (m, 3H, H-5, C*H$_2$*NH$_2$), 2.79-2.69 (m, 2H, Ha-2, Ha-6), 2.36-2.24 (m, 3H, Hb-2, H-1'), 2.11-2.01 (m, 3H, Hb-6, H-2') ppm; **^{13}C-NMR** (50 MHz, CD_3OD): δ= 144.3 (s, 1C, triazole), 126.6 (s, 1C, triazole), 123.8 (s, 2C, aromatic), 122.3 (s, 2C, aromatic), 74.0 (t?, 1C, C-4), 68.3 (s, 1C, C-5), 67.9 (s, 1C, C-3), 56.7 (s, 1C, C-6), 56.3 (s, 1C, C-2), 53.8 (s, 1C, C-1'), 39.1 (s, 1C, C-3'), 29.4 (s, 1C, C*H$_2$*NH$_2$), 27.0(s, 1C, C-2') ppm; **MS (ESI)**: *m/z* calcd (%) for $C_{18}H_{27}N_7O_5S_2$ 485.15; found: 508.12 (100%, [M+Na]$^+$).

_____

Synthesis of monovalent pyrrolidine iminosugar derivative 198: To a solution of **108** (103 mg, 0.22 mmol) in 3 ml of a 2:1 THF:H_2O mixture were added $CuSO_4$ (30 mol%), sodium ascorbate (60 mol%) and alkyne **196** (1 equiv.). The reaction mixture was stirred at 80°C (MW irradiation) for 45 min until TLC analysis (DCM: MeOH 10:1) showed the disappearance of the starting material (*R*f = 0.59) and formation of a new product (*R*f = 0.00). After filtration through Celite®, the solvent was removed under reduced pressure and the crude was first treated with Quadrasil® MP resin then purified by FCC (AcOEt: Hexane = 1:1) affording pure **198** (*R*f = 0.10, 125 mg, 0.18 mmol, 82% yield) as a yellow oil. **[α]$^D_{20}$** = -5.96 (c= 0.57 in $CHCl_3$); **^{1}H-NMR** (400 MHz, $CDCl_3$): δ= 7.60 (d, *J* = 6.7 Hz, 3H, AB system, H-triazole), 7.35-7.21 (m, 15H, H-Ar), 6.48 (d, *J* = 8.6 Hz, 2H, A'B' system), 4.80 (d, *J* = 6.3 Hz, 1H, Ha-3'), 4.54-4.29 (m, 8H, H-2', CH$_2$-OBn), 4.26 (d, *J* = 5.6 Hz, 1H, Hb-3'), 3.95 (d, *J* = 5.0 Hz, 1H, H-3), 3.79 (d, *J* = 3.7 Hz, 1H, H-4), 3.43 (dd, *J* = 9.9, 5.2 Hz, 1H, Ha-1'), 3.36 (dd, *J* = 9.9, 6.0 Hz, 1H, Ha-6), 3.29 (dd, *J* = 13.4, 8.0 Hz, 1H, Hb-6), 3.13 (d, *J* = 10.3 Hz, 1H, Ha-2), 2.83 (dq, *J* = 10.1, 5.1 Hz, 2H, H-5, Hb-1'), 2.66 (dd, *J* = 10.3, 5.1 Hz, 1H, Hb-2) ppm; **^{13}C-NMR** (100 MHz, $CDCl_3$): δ= 151.0 (s, NH-CAr), 144.4 (s, C-SO_2NH_2), 138.1 (s, C-triazole), 129.5-127.8 (d, 16C, C-Ar), 123.1 (d, C-triazole), 112.1 (s, 6C, C-Ar), 85.1 (d, C-4), 81.7 (d, C-3) 71.7-71.2 (t, 3C, C-Ar), 71.6 (t, C-6), 69.1 (d, C-5), 57.3 (t, C-2), 54.0 (t, C-1'), 49.0 (t, C-2'), 39.9 (t, C-3') ppm; **IR** ($CDCl_3$): ν = 3424, 3273, 3032, 2864, 2249, 1954, 1890, 1811, 1730, 1599, 1516, 1454, 1335, 1055 cm^{-1}. **MS (ESI):** *m/z* calcd (%) for $C_{37}H_{42}N_6O_5S$ 682.29; found: 705.28 (100%, [M+ Na]$^+$).

Synthesis of monovalent pyrrolidine iminosugar derivative 199: To a solution of **108** (57 mg, 0.12 mmol) in 3 ml of a 2:1 THF:H_2O mixture were added $CuSO_4$ (30 mol%), sodium ascorbate (60 mol%) and alkyne **197** (1 equiv.). The reaction mixture was stirred at 80°C (MW irradiation) for 45 min until TLC analysis (DCM: MeOH 10:1) showed the disappearance of the starting material (*R*f = 0.59) and formation of a new product (*R*f = 0.00). After filtration through Celite®, the solvent was removed under reduced pressure and the crude was first treated with Quadrasil® MP resin then purified by FCC (AcOEt: Hexane = from 1:5 to 2:1) affording pure **199** (*R*f = 0.26, 48 mg, 0.07 mmol, 62% yield) as a yellow oil. **[α]$^D_{22}$** = -9.93 (c= 0.87 in $CHCl_3$); **^{1}H-NMR** (400 MHz, $CDCl_3$): δ= 7.68 (d, *J* = 8.4 Hz, 2H, AB system), 7.58 (s, 1H, H-triazole), 7.35-7.20 (m, 17H, H-Ar, A'B' system), 4.52-4.26 (m, 8H, H-2', CH$_2$-OBn), 4.13 (s, 2H, H-3'), 3.92 (d, *J* = 4.1 Hz, 1H, H-3), 3.74 (d, *J* = 4.0 Hz, 1H, H-4), 3.39 (dd, *J* = 9.8, 5.3 Hz, 1H, Ha-1'), 3.33-2.78 (m, 2H, H-6), 3.10 (d, *J* = 10.0 Hz, 1H, Ha-2), 2.83-2.78 (m, 2H, H-5, Hb-1'), 2.60 (dd, *J* = 10.3, 5.1 Hz, 1H, Hb-2) ppm; **^{13}C-NMR** (50 MHz, $CDCl_3$): δ= 143.6 (s, C-SO_2NH_2), 143.1 (s, C-triazole), 139.1 (s, S-CAr), 138.2-138.1 (s, 6C, C-Ar), 128.6-127.0 (d, 16C, C-Ar), 123.4 (d, C-triazole), 85.2 (d, C-4), 81.8 (d, C-3) 73.4-71.3 (t, 3C, C-Ar), 71.1 (t, C-6), 69.1 (d, C-5), 57.3 (t, C-2), 54.2 (t, C-1'), 49.2 (t, C-2'), 27.4 (t, C-3') ppm; **IR** ($CDCl_3$): ν = 3433, 3345, 3032, 2920, 2864, 2247, 1584, 1454, 1344, 1167, 1103 cm^{-1}. **MS (ESI):** *m/z* calcd (%) for $C_{37}H_{41}N_5O_2S_2$ 699.45; found: 722.40 (100%, [M+ Na]$^+$).

Synthesis of monovalent pyrrolidine iminosugar derivative 202: To a solution of **81** (35 mg, 0.14 mmol) in 3 ml of a 2:1 THF:H_2O mixture were added $CuSO_4$ (30 mol%), sodium ascorbate (60 mol%) and alkyne **196** (1 equiv.). The reaction mixture was stirred at room temperature for 3 days until TLC analysis (DCM: MeOH 10:1) showed the disappearance of the starting material (*R*f = 0.63) and formation of a new product (*R*f = 0.00). After filtration through Celite®, the solvent was removed under reduced pressure and the crude was first treated with Quadrasil® MP resin then purified by FCC (CH_2Cl_2:MeOH:NH_3 from 10:1:0.1 to 7:1:0.1) affording pure **202** (*R*f = 0.60, 25 mg, 0.06 mmol, 43% yield) as a white waxy solid. **[α]$^D_{23}$** = -6.25 (c= 0.87 in $CHCl_3$); **^{1}H-NMR** (400 MHz, CD_3OD): δ= 7.82 (s, 1H, H-triazole), 7.57 (d, *J* = 8.8 Hz, 2H, AB system), 6.65 (d, *J* = 8.9 Hz, 2H, A'B' system), 4.41 (s, 2H, H-7'), 4.32 (t, *J* = 7.0 Hz, 2H, H-6'), 3.99 (d, *J* = 4.6 Hz, 1H, H-3), 3.87 (d, *J* = 2.4 Hz, 1H, H-4), 3.75-3.67 (m, 2H, H-6), 3.18 (d, *J* = 10.9 Hz, 1H, Ha-2), 3.02-2.95 (m, 1H, Ha-1'), 2.92-2.88 (m, 1H, Hb-2), 2.76 (bs, 1H, H-5), 2.60-2.53 (m, 1H, Hb-1'), 1.87-1.79 (m, 2H, H-5'), 1.51 (t, *J* = 15.0 Hz, 2H, H-2'), 1.32-1.23 (m, 4H, H-3', H-4') ppm; **^{13}C-NMR** (50 MHz, CD_3OD): δ= 152.8 (s, NH-CAr), 147.1 (s, C-SO_2NH_2), 131.5 (s, C-triazole), 128.9 (d, 2C, AB system), 124.0 (d, C-triazole), 112.8 (s, 2C, A'B' system), 79.7 (d, C-4), 76.7 (d, C-3), 76.0 (d, C-5), 61.8 (t, C-6), 60.6 (t, C-2), 57.2 (t, C-1'), 51.2 (t, C-6'), 39.5 (t, C-7'), 31.0 (t, C-5'), 27.7-27.1 (t, 3C, from C-2' to C-4') ppm; **MS (ESI)**: *m/z* calcd (%) for $C_{20}H_{32}N_6O_5S$ 468.22; found: 491.36 (100%, [(M+ Na]$^+$), 469.37 (94%, [(M+ Na]$^+$).

Synthesis of trivalent scaffold 205: A solution of EDC·HCl (1-Ethyl-3-(3-dimethylaminopropyl) carbodimide hydrochloride (56 μL, 0.31 mmol), 1–hydroxybenzotriazole (HOBt, 42 mg, 0.31 mmol) and **204** (58 mg, 0.29 mmol) in DCM (29 mL) was left stirring for 1 hour. and then added to a solution of **81** (67 mg, 0.29 mmol) and *N*,*N*-diisopropylethylamine (55 μL, 0.31 mmol). The reaction mixture was left stirring at room temperature, for 4 days, then diluted with DCM (7 mL) and washed with $KHSO_4$ (2 x 15 mL), with a satured solution of $NaHCO_3$ (2 x 15 mL) and brine (2 x 15 mL), dried over anhydrous Na_2SO_4 and concentrated under vacuum. The crude was purified by column chromatography (DCM: Et_2O 2:1) affording pure **205** (*R*f = 0.48, 80 mg, 0.19, 67% yield). **^{1}H-NMR** (400 MHz, $CDCl_3$): δ = 5.94 (s, 1H, H-NC=O), 4.78 (s, 1H, Boc-NH), 4.12 (d, *J* = 2.4 Hz, 6H, H-α), 3.82 (s, 6H, H-β), 3.17-3.12 (m, 2H, H-4), 2.43 (t, *J* = 2.3 Hz, 3H, H-alkyne), 2.7 (t, *J* = 7.1 Hz, 2H, H-2), 1.76 (p, *J* = 6.9 Hz, 2H, H-3), 1.41 (s, 9H, CH_3 Boc) ppm; **^{13}C-NMR** (50 MHz, $CDCl_3$): δ = 172.8 (s, HN-$\underline{C}$=O), 156.3 (s, HN-$\underline{C}$=O Boc), 79.7 (s, $\underline{C}$-CH_3 Boc), 79.3 (s, 3C, $\underline{C}$-CH), 74.7 (d, 3C, C-alkyne), 68.7 (t, 3C, C-β), 59.4 (s, $\underline{C}$-C-β), 58.8 (t, 3C, C-α), 40.0 (t, C-4), 34.5 (t, C-2), 28.6 (q, 3C, C-$\underline{C}H_3$ Boc), 26.2 (d, C-3) ppm; **MS (ESI)**: *m/z* calcd (%) for $C_{22}H_{32}N_2O_6$ 420.23; found: 443.20 (100%, [M+ Na]$^+$).**IR** ($CDCl_3$): $\tilde{v}$ = 2429, 3306, 2936, 2253, 1703, 1508, 1470, 1364, 1256, 1219, 1167, 1098, 945 cm^{-1}.